LIQUEFIED NATURAL GAS PORTFOLIO OPTIMISATION UNDER IMO SHORT TERM MEASURES FOR ANNUAL DELIVERY PLANNING

PARISA MOSTAFAZADEH

A thesis submitted in partial fulfilment of the requirements of Liverpool John Moores University for the degree of Doctor of Philosophy

June 2026

Abstract

The global effort to mitigate climate change and transition towards net-zero emissions has intensified the need for cleaner energy carriers. Low-carbon fuels such as liquefied natural gas (LNG), hydrogen, ammonia, and methanol have emerged as viable alternatives to conventional fossil fuels due to their lower greenhouse gas emissions. They are crucial for decarbonising shipping and transport. However, the production of these fuels is often geographically concentrated, necessitating long-distance transportation, primarily via maritime shipping, to meet international demand. The shipping of cryogenic fuels presents considerable logistical and environmental challenges, particularly in the context of tightening international regulations and the growing emphasis on decarbonisation across the maritime sector.

This thesis investigates the optimisation of maritime logistics for low-carbon cryogenic fuels, focusing on both operational efficiency and environmental compliance. Special attention is given to LNG, which is currently the most commercially mature and widely transported low-carbon fuel. The work is presented through the development and application of advanced optimisation models that consider a wide range of technical and economic constraints. These include routing, vessel scheduling, speed optimisation, cargo pairing between suppliers and customers, time-varying fuel prices, and operational costs. Moreover, cryogenic shipping constraints such as fuel boil-off rates, the management of heel (minimum retained fuel for tank cooling), fuel consumption rate, and compatibility of the vessel and port are explicitly modelled to reflect real-world operational conditions.

To address these multifaceted challenges, the research introduces a novel two-pronged optimisation framework. A Mixed-Integer Linear Programming (MILP) model is developed for high-fidelity, small- to medium-scale scenarios, enabling precise scheduling and resource allocation. For larger, industrial-scale applications involving a heterogeneous fleet and hundreds of cargo movements, a genetic-based metaheuristic algorithm (GBMHA) is proposed. This hybrid framework offers both exact and heuristic solutions, balancing computational feasibility with solution quality.

The applicability of this framework is demonstrated using real operational data provided by a global LNG supplier. The findings indicate that while the MILP model efficiently handles small- to medium-scale deliveries, the metaheuristic approach successfully scales to manage over 130 transactions and 60 vessels, encompassing a delivery planning horizon of more than 18 months. These outcomes validate the robustness and scalability of the proposed approach in supporting strategic decision-making for Annual Delivery Planning (ADP).

In parallel, the thesis examines the impact of emerging environmental regulations introduced by the International Maritime Organization (IMO), particularly the Carbon Intensity Indicator (CII). Using the same modelling framework, scenarios are tested to understand how CII compliance affects LNG portfolio optimisation. The analysis indicates that ensuring compliance generally results in a reduction in overall profitability of between 0.3% and 10%, depending on the extent to which fleets transition towards greener configurations. However, strategic adjustments in vessel selection, such as favouring smaller ships with better emissions profiles and route optimisation can help offset these losses while improving environmental performance.

The analysis conducted in this study further reveals that greener fleet strategies do not automatically result in reduced CO_2 emissions, underscoring the complex interplay between regulatory compliance, environmental performance, and economic viability.

This research highlights the importance of integrated, data-driven planning in balancing operational, economic, and regulatory pressures. It underscores that achieving environmental targets in the maritime sector is not solely a matter of compliance, but one that requires strategic innovation and optimisation. By contributing novel modelling tools and empirical insights, this thesis advances the field of sustainable maritime logistics and provides actionable guidance for industry stakeholders navigating the transition to low-carbon fuel transport.

Acknowledgements

I extend my heartfelt gratitude to the many individuals and for their invaluable support throughout my PhD journey. Without their help, completing this thesis would have been impossible.

First, I would like to express my heartfelt gratitude to my primary academic supervisor, Dr. Ben Matellini, for his unwavering support, belief in me, and consistent guidance throughout this journey. Dr. Matellini was always there when I needed direction, encouragement, or simply reassurance. His insightful advice, patience, and dedication helped me navigate both the challenges and milestones of this research. I am truly thankful for the trust he placed in me and for the invaluable role he played in shaping not only my project but also my development as a researcher.

I am also deeply grateful to Professor Thanh Trung Nguyen, whose continuous support made a significant difference in my work. He always ensured that I had everything necessary to carry out my research, whether it was resources, tools, or institutional support. His willingness to help in every situation and his responsiveness were deeply appreciated and made my project smoother and more manageable.

Special thanks to Dr. Shayan Kavakeb, my industrial supervisor, whose practical insights and real-world perspective added tremendous value to this project. Through our collaboration, I gained a much clearer understanding of how research translates into industry applications. His guidance gave me a broader view of the relevance and impact of my work beyond the academic setting, which I will carry forward in my future career.

It has been an honour to work with such committed and inspiring mentors. Each of you has contributed uniquely and meaningfully to this thesis, and for that, I am sincerely grateful.

I would like to thank my wonderful friends, Fatemeh and Zahra. They are the best; they always supported me and brought joy and laughter to my life, and I really missed them during my PhD. I also want to thank my colleagues at LOOM, School of Technology, Engineering and Maritime Operations, for their support and encouragement in particular, Massoud, Cihad, and my lovely friends Cherene and Hande.

Last, but certainly not least, I am deeply grateful to my family.

To my dad, Ajdar, and my siblings, Parvaneh, Dariush, Shabnam, Ahmad and Sara, your constant encouragement has been a source of strength throughout my journey. During this PhD, I have missed you all immensely. The memory of my mother, whose unwavering support and belief in me continue to inspire, remains a guiding light in my life. To Hojat, my loving husband, you are the greatest love of my life. Your patience and steadfast support during this research have been truly admirable. With you, this PhD journey became not only possible but also joyful and fulfilling.

This thesis is dedicated to my family.

Table of Contents

List of Figures

List of Tables

List of Algorithms

List of Abbreviations

AEE	Auxiliary Engine Economiser
APS	Advanced Planning and Scheduling
BPSO	Binary Particle Swarm Optimisation
CH_4	Methane
CII	Carbon Intensity Indicator
CO_2	Carbon Dioxide
DCS	Data Collection System
DRL	Deep Reinforcement Learning
DWT	Dead Weight Tonnage
EEDI	Efficiency Design Index
EEOI	Energy Efficiency Operational Indicator
EPL	Engine Power Limitation
EEXI	Energy Efficiency Existing Ship Index
GA	Genetic Algorithm
GBMHA	Genetic-Based Metaheuristic Algorithm
GHG	Greenhouse Gas
GT	Gross Tonnage
HFO	Heavy Fuel Oil
IMO	International Maritime Organisation
IRP	Inventory Routing Problem
LF	Load Factor
LNG	Liquefied Natural Gas
LTC	Long-Term Contracts
MDO	Marine Diesel Oil
MILP	Mixed-Integer Linear Programming
MINLP	Mixed Integer Nonlinear Programming
MIP	Mixed-Integer Programming
MMBTU	Million British Thermal Units

N_2O	Nitrogen Oxides
NTW	Normal Time Window
SA	Sensitivity Analyses
SAS	Sensitivity Analysis Scenario
SC	Supply Chain
SEEMP	Ship Energy Efficiency Management Plan
TCCO	Turbocharger Cut-Outs
TSS	Two-Stage Stochastic
TW+1D	Time Window plus one day
VFD	Variable Frequency Drive
VRP	LNG Vehicle Routing Problem
WHRS	Waste Heat Recovery Systems

CHAPTER 1 INTRODUCTION

Summary

This chapter introduces the research background, providing an overview of the LNG supply chain alongside its key technical and practical requirements. The research aims and objectives are then outlined, followed by the research questions, novelties and the scope and structure of the thesis.

1.1 Research Background

The global energy landscape is undergoing a profound transformation, driven by increasing demand for cleaner fuels and a rapidly intensifying focus on environmental sustainability. As international pressure mounts to reduce greenhouse gas (GHG) emissions, low-carbon fuels have emerged as key enablers in the transition towards a net-zero carbon future (de Oliveira, et al., 2022). Among these, liquefied natural gas (LNG), hydrogen, ammonia, and methanol are considered particularly promising due to their relatively low emissions profiles in comparison to traditional fossil fuels (Bilgili, 2023; Law, et al., 2022).

Nevertheless, the production of these fuels is often geographically concentrated, necessitating long- distance transportation to energy- consuming regions (Mokhatab, et al., 2013). Maritime shipping, due to its scalability and economic viability, has become the predominant mode of transport for low-carbon fuels (IMO, 2011); however, the logistical planning of such operations is highly complex, especially when considering long-term scheduling over several months or even years. Factors such as route optimisation, vessel deployment, scheduling, speed variation, fleet fuel consumption, time-varying fuel price, contractual constraints, and alignment of global supply and demand must be meticulously managed to achieve cost efficiency and regulatory compliance.

The complexity of transporting low-carbon fuels is further intensified by their physical properties. With most of these fuels existing in gaseous form at ambient conditions, transportation necessitates liquefaction and cryogenic storage. Cryogenic fuels introduce specific technical challenges including boil-off rates (natural

evaporation during voyage), onboard fuel retention (heel), and the usage of cargo fuel for vessel propulsion. These operational considerations fundamentally impact the economic and environmental efficiency of maritime transport and therefore must be carefully integrated into any optimisation framework (Grønhaug & Christiansen, 2009).

Although hydrogen, ammonia, and methanol are expected to feature prominently in future shipping supply chains, only LNG currently benefits from a fully developed global infrastructure. The assumption is that the optimisation framework developed for LNG shipping can be suitably adapted to other low-carbon cryogenic fuels as their global supply chains mature, given the operational and technical similarities that exist between them (Ghafri, et al., 2023; Al-Breiki & Bicer, 2020). Also, natural gas is widely regarded as a transitional fuel, offering substantial environmental advantages over coal and oil (Ejder, et al., 2024; Lindstad, et al., 2020). Its adaptability for transport in either gaseous or liquefied form, and the ability to reduce volumetric footprint by a factor of 600 when liquefied, make LNG particularly well-suited for global maritime distribution (Mokhatab, et al., 2013). Furthermore, geopolitical shifts have underscored the strategic value of LNG. For example, in 2022, LNG imports into Europe rose by 60% compared to the previous year, reaching 121 million tonnes, largely to offset the decline in Russian pipeline gas (Shell, 2023; Chen, et al., 2024). Industry forecasts project LNG demand to reach between 650 and 700 million tonnes annually by 2040, necessitating significant enhancements in supply chain optimisation and delivery planning (Shell, 2023). The explicit focus on Liquefied Natural Gas (LNG) in this model is driven by its critical role as the primary transition fuel in the maritime decarbonisation agenda.

To address these demands, substantial academic and industrial efforts have focused on the development of mathematical models and algorithmic approaches for LNG shipping optimisation. The literature has explored diverse problems such as vessel routing (Yazdi, et al., 2020; Ghiami, et al., 2015; Halvorsen-Weare & Fagerholt, 2013), the LNG Inventory Routing Problem (IRP) (Eriksen, et al., 2022), and Annual Delivery Plan (ADP) optimisation (Deshpande, et al., 2022; Andersson, et al., 2017). However, the increasing emphasis on environmental compliance has introduced new dimensions to the optimisation problem, particularly considering evolving regulatory requirements from the International Maritime Organization (IMO) (Hua, et al., 2024; Tran, et al., 2023; Lu, et al., 2023).

Maritime transport currently accounts for approximately 90% of global trade by volume (IMO, 2011), and while it remains the most carbon-efficient form of freight transport, its total GHG emissions are significant. Between 2012 and 2018, emissions from international shipping rose by nearly 10%, and without intervention, emissions could increase by up to 130% of 2008 levels by 2050 (Faber, et al., 2020). The shipping sector emitted approximately 858 million tonnes of CO_2 in 2022 alone, placing it among the top global emitters, higher than entire industrialised economies such as Brazil and Germany (Balcombe, et al., 2019; Clark, et al., 2023).

To curb emissions, the IMO has introduced a progressive regulatory framework, including the Energy Efficiency Design Index (EEDI), the Energy Efficiency Existing Ship Index (EEXI), and the Carbon Intensity Indicator (CII). The CII represents a pivotal shift towards operational emission metrics. It quantifies a vessel's carbon efficiency by evaluating CO_2 emissions per unit of transport work, thereby linking environmental performance with logistical operations. From 2023 onwards, compliance with CII has become mandatory for all vessels above 5,000 gross tonnes, requiring annual improvements in carbon intensity and impacting strategic fleet management, voyage planning, and fuel consumption (IMO, 2021b; ClassNK, 2023).

Given these developments, there is a critical need for optimisation models that not only address both economic performance but also ensure strict regulatory compliance. While some studies have begun to incorporate environmental parameters into shipping models (Zarrinkolah & Hosseini, 2023; Kim, et al., 2023; Bouman, et al., 2017), a comprehensive integration of CII-based regulatory constraints into LNG delivery planning remains underdeveloped.

This thesis seeks to bridge this gap by developing a robust, regulation-compliant optimisation framework for LNG portfolio planning. The concept of portfolio delivery planning must be explicitly defined as the integrated optimisation of supply procurement, cargo matching, and maritime routing. In this study, the framework models the LNG portfolio as a multi-criteria system, accounting for supplier heterogeneity, contractual flexibility, vessel-specific characteristics, time-varying market prices, and emissions performance metrics. Furthermore, this study explicitly accounts for operational constraints commonly encountered in industrial practice, including delivery time windows, time-varying fuel prices, vessel capacity limitations, contractual obligations, bunker fuel consumption, and cargo boil-off.

This real-world problem is formulated explicitly from the perspective of a central decision-maker: a commercial LNG distributor or portfolio manager. From this commercial perspective, the model optimises the profitability of a single global energy enterprise. This enterprise acts as the central integrating node—procuring LNG from multiple suppliers to fulfil the demands of diverse customers across a complex, multi-source to multi-destination routing network. The maritime transport component is strictly executed by a heterogeneous fleet of multiple specialised LNG carriers (liquid tankers), as opposed to standard containerised maritime freight. This scale and vessel specificity introduce unique operational and environmental complexities that the central decision-maker must mathematically balance.

The novelty of this research is multi-faceted. It centres on a scalable methodology, a Mixed-Integer Linear Programming (MILP) model is proposed to optimise LNG shipping operations under commercial and environmental constraints. To address the scalability and complexity of real-world industrial scenarios, the MILP model is complemented with a genetic-based metaheuristic algorithm designed for complex industrial applications. Furthermore, it distinguishes itself by investigating the specific impact of CII regulations on LNG optimisation, establishing a foundation for decision-makers to effectively balance commercial and environmental objectives.

1.2 Research Aim and Objectives

The overarching aim of this doctoral research is to develop a novel advanced decision-support framework that enables optimal LNG delivery planning under emerging decarbonisation regulations, particularly the IMO's Carbon Intensity Indicator short-term measures. The proposed framework incorporates the majority of real-world constraints encountered in annual delivery planning, such as delivery time windows, loading and unloading capacity limitations, vessel capacity restrictions, time-varying fuel price, calorific values of energy suppliers, vessel contractual obligations, cargo boil-off, and heel quantities.

To achieve this, the thesis pursues the following objectives:

1) To conduct a comprehensive review of the state-of-the-art literature concerning maritime logistics, LNG portfolio planning, and environmental regulatory frameworks (such as Carbone Intensity Indicator), thereby identifying critical gaps in current mathematical optimisation methodologies. (Chapter 2)
2) To develop a comprehensive mixed integer linear program model for annual LNG portfolio optimisation from the perspective of an integrated commercial LNG portfolio operator, capturing key operational decisions such as supplier–customer matching, vessel allocation, vessel routing and scheduling, fuel consumption of vessels, and inventory management of LNG carriers. (Chapter 3)
3) To design and implement a metaheuristic algorithm solution approach capable of efficiently solving large-scale LNG delivery planning problems and addressing the computational challenges associated with real-world industrial data. (Chapter 3)
4) To validate the performance and robustness of the proposed MILP model and metaheuristic algorithm using empirical data from an industrial partner, including sensitivity analyses and comparative benchmarking against exact optimisation method. (Chapter 3)
5) To extend the base optimisation model to incorporate the CII, in accordance with IMO's short-term measures, by integrating environmental constraints related to fuel consumption, sailing distance, vessel capacity, and emissions ratings. (Chapter 4)
6) To analyse the operational and economic impact of CII compliance on LNG portfolio planning, exploring the trade-offs between regulatory compliance and profit maximisation, to assess how CII-related constraints influence optimal fleet deployment. (Chapter 4)
7) To enhance the developed metaheuristic algorithm to handle CII-compliant optimisation, ensuring it can generate near-optimal solutions under complex environmental and operational constraints in a computationally efficient manner. (Chapter 4)
8) To apply the developed optimisation framework to evaluate the complex trade-offs between regulatory compliance, environmental impact, and economic profitability, specifically analysing the effects of CII ratings on profit, CO_2 emission and fleet management. (Chapter 4 and 5)

1.3 **Research Questions**

To fulfil the predominant aim of this thesis, a set of clearly defined research objectives has been established. These objectives give rise to a corresponding set of research questions that guide the methodological development, model formulation. Algorithm design, and empirical analysis undertaken in this study. Addressing these research questions ensures that each objective is systematically examined and that the research contributions are rigorously substantiated. To this end, the study seeks to answer the following research questions:

Q1: How does a Mixed-Integer Linear Programming (MILP) framework compare mathematically and operationally to alternative methodologies for annual LNG portfolio planning? (Chapter 2 and 3)

Q2: How can a MILP model be formulated to optimise LNG portfolio delivery planning while jointly capturing supplier–customer matching, vessel allocation, routing and scheduling, fuel consumption, onboard inventory management under real-world operational and economic constraints? (Chapter 3)

Q3: How do metaheuristic frameworks perform computationally and operationally when compared to exact optimisation and alternative decision-making methods for large-scale LNG delivery planning? (Chapter 2 and 3)

Q4: What heuristic or metaheuristic solution approach can be designed to efficiently solve large-scale LNG delivery planning problems, and how can it address the computational limitations of exact optimisation methods when applied to real-world industrial data? (Chapter 3)

Q5: How robust and effective are the proposed solutions found as optimal tools for the proposed framework when evaluated using empirical industrial data, and how their performances vary under different operational conditions?

Q6: How can the IMO carbon intensity indicator short-term measures be systematically incorporated into LNG portfolio optimisation models through environmental and operational constraints in relation to fuel consumption, sailing distance, vessel capacity and emissions ratings? (Chapters 3 and 4)

Q7: How can the existing LNG delivery planning model be extended to integrate CII-related constraints, and how do CII-related constraints influence the trade-offs between profit maximisation and regulatory compliance in fleet deployment decisions? (Chapter 4)

Q8: How can the proposed metaheuristic algorithm be enhanced to efficiently generate high-quality solutions for CII-compliant LNG delivery planning problems under increased environmental and operational complexity? (Chapter 5)

Q9: What strategic and operational insights can be derived from the optimisation results to support shipping companies and supply chain stakeholders in adapting planning, routing, and fleet management decisions in response to maritime decarbonisation regulations? (Chapter 5)

1.4 Original Contributions

To directly address the methodological and practical gaps identified in the current literature and the growing need for regulation-compliant decision-support tools in maritime logistics, this thesis introduces a new paradigm for LNG portfolio planning. The original contributions of this research are summarised as follows:

- Advancement of Maritime Logistics Modelling: By establishing a methodologically rigorous optimisation framework, this research successfully integrates complex operational, technical, and economic variables within global LNG supply chain planning. This comprehensive synthesis significantly advances the state-of-the-art in maritime operations research, providing a robust mathematical foundation for solving previously intractable, multi-layered scheduling challenges.

- Pioneering Integration of Environmental Regulations: This thesis introduces the first explicitly integrated modelling approach that directly couples the International Maritime Organization's (IMO) Carbon Intensity Indicator (CII) mandates with dynamic, portfolio-level LNG delivery planning. This novel formulation mathematically bridges commercial and environmental objectives, empowering stakeholders to definitively evaluate and navigate the critical trade-offs between fleet profitability and strict regulatory compliance.

- Quantitative Evaluation of Regulatory Impacts: The research delivers a comprehensive quantitative assessment detailing the cascading operational and economic impacts of modern emissions constraints. It explicitly maps how the enforcement of CII compliance fundamentally alters established industry logic, driving necessary and measurable shifts in vessel routing pathways, fleet allocation strategies, time-window scheduling, and overarching cost structures within the LNG supply chain.
- Development of a Practical Decision-Support Tool: Beyond its theoretical and algorithmic contributions, the developed framework functions as a practical, strategic decision-support tool for the maritime industry. It bridges the gap between academic operations research and commercial practice by generating actionable managerial insights for fleet operators, charterers, and portfolio managers. This explicitly supports more informed, data-driven decision-making under the dual pressures of increasing market uncertainty and stringent IMO environmental regulations.

Collectively, this research contributes to the advancement of system-level optimisation approaches in maritime decarbonisation and offers a deeper understanding of how environmental regulations reshape operational and economic decision-making in LNG logistics networks.

1.5 Scope and Structure of the Thesis

This section outlines the scope and structure of the thesis. It first delineates the boundaries of the research by clarifying the aspects of LNG portfolio optimisation, vessel operations, and regulatory considerations that are explicitly addressed, as well as those that fall outside the scope of this study. It then provides an overview of the organisation of the thesis, describing the purpose and content of each chapter and highlighting how the chapters collectively contribute to addressing the research.

While the maritime industry is exploring various decarbonisation pathways including ammonia, hydrogen, and methanol marine fuels. The scope of this research focuses exclusively on Liquefied Natural Gas (LNG). LNG currently represents the most technically mature and commercially deployable low-carbon transition fuel. Unlike zero-carbon alternatives that still face prohibitive barriers regarding energy density, safety, and lack of bunkering facilities, LNG benefits from an established global shipping infrastructure and a commercially viable

supply chain (dos Santos, et al., 2022). Because of this immediate operational readiness, focusing the optimisation framework on LNG provides immediate, actionable value to an industry actively navigating the energy transition (Ejder, et al., 2024). Therefore, this thesis is focused on the optimisation of annual LNG delivery planning within a portfolio context, considering the integrated decision of supplier-customer matching, vessel assignment, routing and scheduling, and on-board inventory management of LNG carriers. This study explicitly accounts for operational constraints commonly encountered in industrial practice. Other environmental regulations, long-term decarbonisation pathways, and alternative fuel technologies are therefore beyond the scope of this research and are not explicitly modelled.

From a regulatory perspective and following the IMO's announcement of short-term decarbonisation measures, the thesis concentrates on the CII short-term measures introduced under MARPOL Annex VI and examines its implications for LNG portfolio planning and fleet deployment. As the CII is directly determined by a vessel's annual fuel use and voyage distance (IMO, 2021a), both of which play a central role in LNG supply-chain portfolio optimisation, this research extends the original mathematical formulation to explicitly integrate CII-related constraints. Other environmental regulations, long-term decarbonisation pathways, and alternative fuel technologies are beyond the scope of this research and are not explicitly modelled.

The framework models the LNG portfolio as a complex, multi-criteria system, accounting for supplier heterogeneity, contractual flexibility, vessel-specific characteristics, time-varying market prices, and emissions performance metrics. By formulating the problem as a MILP model, the study enables the joint optimisation of cargo pairing, vessel allocation, fleet scheduling, and routing within a unified framework, providing a decision-support tool aligned with both regulatory and commercial objectives.

The choice of MILP is motivated by the structural characteristics of the problem. The key decision variables such as vessel assignment, routing decisions, and supplier–customer pairing are inherently discrete, while the majority of operational constraints can be represented in linear form. This makes MILP a natural and efficient modelling approach, allowing the use of well-established solvers that provide exact optimal solutions for tractable instances.

Alternative approaches, such as stochastic programming, could capture uncertainty in parameters such as demand or prices; however, incorporating stochastic elements would significantly increase model complexity and computational burden, particularly given the already large-scale combinatorial structure of the problem. Similarly, Mixed Integer Nonlinear Programming (MINLP) could represent nonlinear relationships more explicitly, but such formulations are generally more difficult to solve and may not guarantee global optimality in large-scale applications. It is also noted that MILP is a subclass of Mixed Integer Programming (MIP), where the linear structure ensures computational tractability and solution reliability. Therefore, adopting a MILP formulation provides a practical balance between model realism, computational efficiency, and solution optimality, making it particularly suitable for large-scale LNG portfolio optimisation problems.

In summary, methodologically, the scope of this research is strictly confined to MILP and metaheuristic algorithms. This boundary is set because the dual nature of LNG portfolio planning (requiring both precise, discrete decision-making and the ability to process massive, complex datasets) cannot be adequately solved by a single standard approach. While MILP provides the necessary rigorous mathematical foundation for exact optimisation, a complementary metaheuristic algorithm is developed to ensure computational tractability for large-scale, real-world industrial scenarios.

The extended model evaluates the implications of the CII regulation on operational planning, asset utilisation, and overall profitability. By embedding CII, the study offers an advanced decision-support system for industry stakeholders. This system enables them to optimise asset deployment and maintaining compliance with IMO regulations while aligning environmental and economic objectives.

The structure of the thesis is organised into five chapters which are outlined below, and visually summarised in Figure 1.1.

- **Chapter 1: Introduction**

  This chapter introduces the research motivation, background, aim and objectives, scope, and contributions. It establishes the context of LNG supply chain optimisation and the regulatory landscape and sets out the structure of the thesis.

- **Chapter 2: Literature Review**

  A comprehensive review of existing literature is conducted in this chapter, first establishing the critical role of the sector to justify the specific focus on LNG logistics. The review then systematically evaluates maritime portfolio optimisation, environmental regulations, and CII compliance. Crucially, the chapter critically compares various mathematical and heuristic approaches, providing clear evidence as to why the chosen solution methods (MILP and metaheuristics) are the most suitable for this problem domain. Finally, it identifies the primary research gaps that motivate the proposed framework, particularly the lack of integrated models that jointly address operational efficiency and regulatory adherence within LNG portfolio planning.

- **Chapter 3: MILP Model Development and Metaheuristic Solution Approach**

  This chapter presents the formulation of the base MILP model for LNG portfolio optimisation. It details all operational assumptions, parameters, and constraints relevant to real-world LNG logistics. In parallel, a genetic-based metaheuristic algorithm is developed to solve the problem efficiently for larger instances. The model is validated using real operational data provided by an industrial partner. Extensive sensitivity analyses and comparative experiments are conducted to evaluate the performance and robustness of both the exact and metaheuristic methods.

- **Chapter 4: Integration of CII Regulation into Portfolio Optimisation**

  In this chapter, the MILP and metaheuristic models developed in Chapter 3 are extended to include the IMO's CII as an operational constraint. The revised model incorporates emission performance into routing, scheduling, and vessel allocation decisions. The impact of CII on portfolio optimisation is analysed through realistic simulation scenarios based on actual industrial data. This chapter also discusses how the model supports strategic decision-making for regulatory compliance while maximising economic returns.

- **Chapter 5: Conclusions and Future Work**

  The final chapter summarises the key findings, theoretical and practical contributions, and implications of the research. It also highlights limitations and outlines possible directions for future work, including

the incorporation of other environmental metrics or regulatory instruments, such as the Energy Efficiency Existing Ship Index (EEXI) or Emission Trading Schemes (ETS).

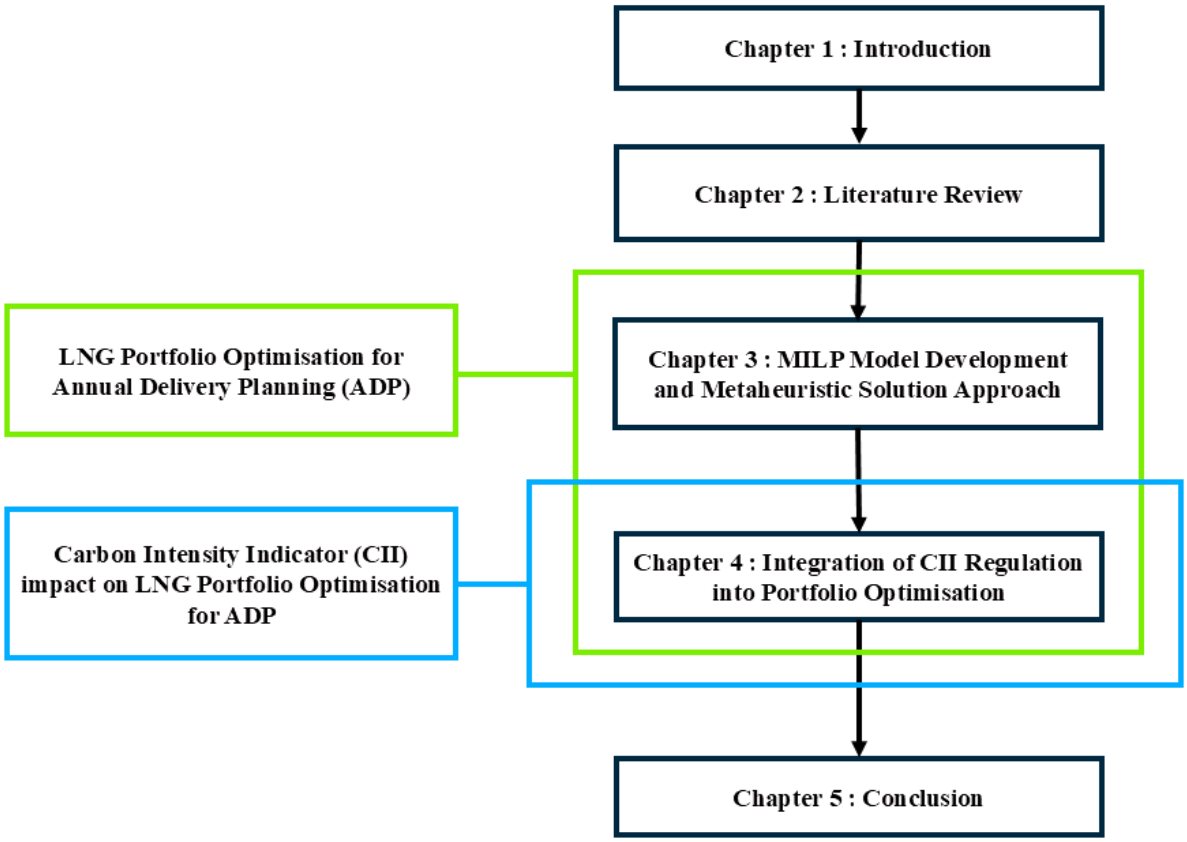

Figure 1.1: Structure of the Thesis

1.6 Conclusion

In summary, this introductory chapter has provided the essential background for the research, highlighting the growing intersection between commercial LNG portfolio management and emerging maritime decarbonisation regulations. Having defined the research objectives, the boundaries of the study, and the proposed structural roadmap, the overarching trajectory of the thesis is now clear. However, to fully justify the development of the intended optimisation framework, a deeper dive into the current academic and industrial consensus is required. Chapter 2 will therefore systematically review the state-of-the-art literature to formally identify the methodological and practical gaps that necessitate this research.

CHAPTER 2 LITERATURE REVIEW

Summary

This chapter presents a literature review divided into five subsections, with the final section highlighting the research gap. As LNG currently represents the only low-carbon fuel with an established global shipping infrastructure and a commercially viable supply chain, most of the research on low-carbon fuel shipping optimisation has focused exclusively on LNG. Consequently, the LNG supply chain has been extensively examined from a range of operational and logistical perspectives, leading to the development of diverse modelling approaches and solution methodologies tailored to various industrial contexts.

This literature review is organised thematically, with sections classified according to key research domains within operations research. Each section critically evaluates existing studies, identifies methodological advances, and highlights gaps that inform the development of the models and approaches presented in this thesis.

2.1 Literature Search Methodology

To systematically review the existing literature and identify methodological gaps in LNG operations research, a comprehensive search was conducted primarily using Google Scholar, cross-referenced with standard academic databases including Scopus and Web of Science.

To ensure a focused and unbiased selection of literature, the search was executed using combinations of the following keywords:

- Operational Keywords: "LNG supply chain," "LNG annual delivery plan," "LNG portfolio," "LNG inventory management," and "LNG carriers routing and scheduling."
- Regulatory & Environmental Keywords: "Carbon intensity indicator and LNG carriers," "CII and LNG supply chain," "IMO short-term measures and maritime shipping," "GHG emissions and CII," and "Alternative marine fuels and CII."

To capture the evolution of optimisation techniques in this field, the search timeframe was set to encompass publications from 2009 to the present. From the initial search results, references were explicitly selected for detailed analysis based on four rigorous inclusion criteria:

1. A primary focus on quantitative Operations Research (OR) models, intentionally excluding purely qualitative policy reviews.
2. The explicit inclusion of multi-vessel routing and scheduling dynamics.
3. The application of algorithmic or mathematical solution methods (e.g., exact methods, heuristics, or metaheuristics) to solve the Annual Delivery Program (ADP) or the Inventory Routing Problem (IRP).
4. Their approach to integrating environmental regulations, specifically examining how the Carbon Intensity Indicator (CII) has been implemented within mathematical models, and at what level of decision-making (e.g., isolated ship-level compliance versus integrated, fleet-wide portfolio planning).

The search was scoped to prioritise contemporary research reflecting modern algorithmic advancements and recent regulatory shifts. This structured approach ensures that the subsequent review is both comprehensively broad and acutely focused on the specific gaps this thesis aims to bridge.

2.2 LNG Annual Delivery Planning

In the liquefied natural gas sector, contractual arrangements underpin the majority of commercial transactions and logistics planning. Among these, Long-Term Contracts (LTCs) typically ranging from 20 to 25 years are the most prevalent (Rakke, et al., 2011). These contracts provide supply security for buyers while ensuring long-term revenue streams for producers. As part of fulfilling such contracts, LNG suppliers are required to deliver variable volumes of LNG across multiple destinations and time windows, often under stringent operational and commercial constraints. To manage these complex delivery obligations over an annual horizon, producers frequently rely on the development of an Annual Delivery Plan (ADP) (Deshpande, et al., 2022). This strategic planning tool involves determining optimal vessel allocations, cargo quantities, unloading schedules, and

voyage routes. The ADP thus plays a crucial role in ensuring contractual compliance, optimising operational efficiency, and managing supply-demand alignment over extended periods.

The foundational operational research on ADP generation was introduced by Rakke et al. (2011), who formulated a Mixed-Integer Programming (MIP) model that integrated the option to divert surplus LNG to the spot market. However, a critical limitation of this early exact formulation was its NP-hard nature, rendering it computationally intractable for large-scale, real-world instances**.** Recognising this computational bottleneck, subsequent research fundamentally shifted towards heuristic and decomposition methodologies. For example, Stålhane et al. (2012) advanced the field by applying first-descent neighbourhood search and branch-and-bound hybrids. By comparatively evaluating these techniques against standard MIPs, Stålhane et al. demonstrated that acceptable, near-optimal solution quality could be obtained without the crippling computational burden of exact methods, justifying the use of heuristic frameworks in dynamic supply chain environments. While early heuristic models improved computation times, they often relied on oversimplified logistical assumptions. To bridge the gap between mathematical theory and commercial reality, later studies progressively critiqued earlier limitations by integrating complex physical constraints. For instance, whereas early models assumed unconstrained port capacities, Al-Haidous et al. (2016) and later Deshpande et al. (2022) argued that ignoring receiving terminal infrastructure leads to infeasible schedules, successfully expanding ADP formulations to strictly encompass berth availability and inventory holding limits.

Several recent studies have extended the foundational ADP modelling framework by introducing novel operational features and advanced solution methodologies and focused on expanding the flexibility of the routing network itself (Werner, et al., 2014; Moraes & Faria, 2016; Venkataramanan & Srinivasan, 2024). For example, Li et al. (2011) expanded routing flexibility by incorporating transshipment ports, addressing the unique geographic constraints of remote projects like Yamal LNG. This addition expanded the logistical network and allowed for greater route flexibility and vessel utilisation. By integrating transshipment capabilities, the model addressed geographic and operational challenges that arise in Arctic or remote LNG projects, offering a valuable framework for planning under extreme environmental or infrastructural constraints Similarly, Mutlu et al. (2016) challenged the traditional point-to-point delivery assumption by introducing split

deliveries, proving that allowing a single cargo to be divided across multiple destinations substantially lowers overall delivery costs. This operational flexibility not only reflected real-world LNG logistics practices but also contributed to cost efficiency. The authors introduced a tailored heuristic algorithm which, in comparative evaluations, outperformed commercial optimisation software, delivering substantially lower-cost solutions within reasonable computational times. Building upon strategic LNG scheduling, Andersson et al. (2017) explicitly critiqued pure cost-minimisation approaches, proving through a bi-objective branch-and-cut model that opportunistic spot-market sales must be jointly optimised alongside LTC obligations to truly maximise portfolio revenues.

Despite these significant advancements in operational realism, the vast majority of existing ADP literature treats critical voyage parameters such as vessel speed as static and focuses entirely on economic objectives. A notable recent exception is Haug et al. (2023), who identified that assuming a standard cruising speed severely limits operational flexibility. Their MIP model revealed that treating vessel speed as a dynamic decision variable dramatically improves both schedule feasibility and profitability.

Critically, however Haug et al. (2023) and the aforementioned literature have successfully mastered the operational mechanics of LNG scheduling, they evaluate routing, speed, and scheduling exclusively through an economic and logistical lens. This reveals a fundamental gap in the current state-of-the-art: existing ADP frameworks remain entirely blind to emerging, cumulative environmental constraints. As global maritime regulations shift towards mandatory decarbonisation, ADP models that optimise purely for profit without integrating metrics like the IMO's Carbon Intensity Indicator (CII) risk generating commercially unviable or non-compliant portfolios.

2.3 LNG Routing and Scheduling Planning

Ensuring a sustainable and uninterrupted supply of LNG is critical for global energy security. Accordingly, the routing and scheduling of LNG carriers serves as the operational backbone of the supply chain, physically linking production facilities with terminal distribution. Efficient coordination of these maritime elements is

paramount for reducing operational costs and maintaining supply resilience, prompting extensive operations research into advanced routing methodologies.

Early approaches to the LNG routing problem frequently struggled with the immense computational complexity of integrating voyage routes with port-level constraints. To address this, Halvorsen-Weare and Fagerholt (2013) proposed a decomposition-based heuristic, separating the core routing problem from the feasibility of berth scheduling and inventory. While this approach successfully generated mathematically optimal routes, it relied on deterministic assumptions. Recognising the inherent fragility of deterministic plans in volatile maritime environments, Halvorsen-Weare et al. (2013) immediately critiqued their own prior work, developing a robust optimisation strategy that internalised uncertainty in sailing times and production rates. This necessary transition towards uncertainty management was further advanced by.

Cho et al. (2014) who evolved the standard Vehicle Routing Problem (VRP) into a two-stage stochastic model using Monte Carlo optimisation. By doing so, they successfully demonstrated that accounting for demand volatility is a strict requirement for generating resilient, real-world delivery schedules. More recently, Sangaiah et al. (2020) reinforced this consensus by applying a robust MILP model and a novel metaheuristic to shield vendor costs from operational unpredictability.

As models became better equipped to handle uncertainty, researchers began critiquing the rigid, point-to-point logistical assumptions of earlier frameworks. Bittante et al. (2018) challenged traditional routing topologies by introducing a MIP model that explicitly supported load-splitting operations, multiple depots, and repeat voyages, proving that structural routing flexibility is essential for minimising fuel procurement costs. Simultaneously, the literature experienced a paradigm shift from pure cost-minimisation to dynamic profit-maximisation.

Msakni and Haouari (2018) addressed this by developing a hybrid mathematical and variable neighbourhood search approach. Crucially, they integrated mandatory LTC deliveries with spot market cargoes and heterogeneous, variable-speed fleets—proving that routing decisions cannot be isolated from dynamic market opportunities. Recognizing the computational burden of these highly flexible, profit-driven models, Yazdi et al. (2020), demonstrated the necessity of advanced algorithms, successfully applying Binary Particle Swarm Optimisation (BPSO) to generate highly profitable routing solutions within condensed planning horizons.

Furthermore, recent studies have argued that maritime routing cannot be viewed in a vacuum; researchers such as Utku (2023) and Zhang et al. (2024) have expanded the routing boundary entirely, developing nonlinear MIP frameworks that integrate maritime carrier allocation with inland multimodal transport and port-based reward mechanisms.

In summary, the operations research domain concerning LNG routing and scheduling has matured significantly, progressing from basic deterministic cost-minimisation to highly sophisticated, stochastic, and profit-driven frameworks. Modern algorithms successfully capture complex realities such as load-splitting, spot-market integration, variable speeds, and multimodal constraints.

However, a critical methodological void remains. Despite these algorithmic leaps, the aforementioned literature evaluates routing efficiency almost exclusively through logistical and economic lenses. Consequently, there is a severe lack of research addressing carbon efficiency within these advanced routing models. By treating fuel consumption purely as a financial cost rather than a strictly regulated environmental constraint, the current state-of-the-art fails to internalise the IMO's short-term greenhouse gas regulations. This highlights an urgent need for an integrated routing framework capable of balancing profit-maximising cargo pairing and variable speed scheduling against the cumulative, non-negotiable boundaries of CII.

2.4 LNG Inventory and Routing Problems

Within the context of LNG supply chains, transport schedules and terminal storage capacities are tightly coupled. The Maritime Inventory Routing Problem (MIRP) provides a strategic framework to manage this coupling, decomposing complex logistical systems to identify optimal delivery schedules, routing paths, and inventory holding levels. The adaptation of the IRP to the LNG sector was pioneered by Grønhaug and Christiansen (2009) and Grønhaug et al. (2010), who introduced arc-flow and path-flow models utilizing branch-and-price algorithms to enable multi-unloading operations. While foundational, these early exact formulations struggled with the immense computational complexity inherent to large-scale LNG networks. Subsequent research focused heavily on refining these mathematical structures to improve tractability.

In a separate line of research, Goel et al. (2012) focused on minimising the penalty costs associated with lost production and stockouts. Their approach employed an arc-flow MIP formulation for scheduling LNG deliveries while optimising vessel assignments. To address computational complexity, the authors proposed an improved local neighbourhood search heuristic, which demonstrated effective performance on real-world-scale problems. In another study Biresselioglu, et al. (2012) modelled the Turky's future LNG supply chain; they formulated and solved a mixed integer programming model that determines the optimal sourcing strategy for Turkey's increasing LNG demand.

Expanding on their earlier work, Goel et al. (2015) later introduced a constraint programming-based formulation with an iterative search heuristic. Despite its novelty, this approach was soon outperformed by subsequent studies. To overcome the limitations in scalability, researchers introduced the rolling horizon heuristic approach, which decomposes long-term planning horizons into shorter, manageable sub-periods, enhancing computational feasibility without significantly compromising solution quality.

Subsequent research focused heavily on refining these mathematical structures to improve tractability. For example, Ghiami et al. (2015) explicitly compared arc-flow and path-flow formulations, proving that path-flow models yielded vastly superior computational efficiency when handled by commercial solvers like CPLEX. Furthermore, Ghiami et al. advanced the physical realism of the IRP by integrating natural gas evaporation (boil-off), a critical operational constraint frequently omitted in broader strategic models such as (Bittante, et al., 2018). Or in the other research Jokinen et al. (2015) proposed a MILP framework tailored to small-scale LNG coastal delivery systems. Their model optimised both supply chain design and fuel procurement costs, incorporating key factors such as satellite port placement, optimal vessel sizing and utilisation, and customer allocation strategies.

Despite improvements in exact formulations such as the exact branch-price-and-cut algorithm developed by Rakke et al. (2015) which yielded significantly tighter lower bounds, the literature ultimately recognised that exact solvers face insurmountable scalability limits for global, annual portfolios. Consequently, researchers pivoted towards advanced heuristics. Shao et al. (2015) successfully addressed this computational bottleneck by replacing traditional solvers with a hybrid heuristic method. By integrating diverse construction heuristics

with sequential singleton search techniques, they reduced CPU times by a factor of nearly four, proving that heuristic frameworks are practically essential for real-world industrial IRP applications. In the other study conducted by Zhang et al., (2017) three stage stochastic programming method for inventory routing in demanding countries has been developed. A more localised application was explored by Budiyanto et al. (2019) in a case study of LNG distribution to a gas-fired power plant in Sumatra, Indonesia. The focus was on optimising distribution routes for small-scale LNG carriers, underscoring the flexibility and adaptability of IRP frameworks to regional energy contexts

Concurrently, the literature critiqued the deterministic nature of early IRP models, recognising that LNG logistics are highly vulnerable to external volatility. This led to a surge in stochastic programming. To combat environmental disruptions, Cho et al. (2018) and Xiaozhi (2020) developed two-stage stochastic models utilizing historical weather data, allowing vessels to proactively adjust speeds or bypass severe weather routes to protect expected profits. Similarly, Sheikhtajian et al. (2020) introduced stochastic tactical planning to minimize contractual penalties caused by uncertain travel times.

Beyond physical disruptions, researchers also tackled commercial and demand-side uncertainty. Utku and Soyöz (2020) highlighted how demand fluctuations destabilise supply-storage balances, proving that integrating offshore floating storage provides necessary operational buffers. Eriksson et al. (2022) expanded this by modelling contractual uncertainty via multi-stage stochastic programming, demonstrating that indeterminacy regarding future customers fundamentally dictates economies of scale and infrastructure investments. Furthermore, Yazdi et al. (2021) and Khalilpour and Karimi (2012) argued that deterministic long-term contracts must be mathematically integrated with dynamic spot market opportunities and incremental discount schemes to truly capture commercial reality. Taken together, this body of work establishes that treating parameters as fixed is fundamentally inadequate; modern IRPs must integrate demand volatility and contractual flexibility to generate robust portfolios.

Taken The literature on LNG IRPs has undeniably progressed from basic arc-flow formulations to highly sophisticated, stochastic, and heuristically driven models capable of handling multi-terminal deliveries, weather

disruptions, and evaporation. However, a critical synthesis of this domain reveals two glaring methodological gaps.

First, across the primary subdomains of routing, scheduling, and inventory management, existing studies predominantly optimize these elements sequentially or isolate specific commercial factors. Notably absent is the joint optimisation of these logistical dimensions alongside dynamic supplier-customer cargo pairing. Given the extreme volatility of global LNG prices, dynamic cargo matching is a primary driver of portfolio profitability. Treating routing as a separate mathematical problem from dynamic procurement and cargo pairing yields inherently suboptimal commercial portfolios.

Second, and most critically, despite the advanced inclusion of stochastic weather and demand parameters, there is an absolute void regarding greenhouse gas accounting and regulatory adaptation. None of the aforementioned state-of-the-art IRP frameworks explicitly internalise the IMO's short-term decarbonisation measures, such as the CII. Optimising vessel speeds, and inventory holding to maximise profit without applying the cumulative boundaries of the CII risks generating delivery plans that are legally non-compliant or subject to severe regulatory penalties. Therefore, a comprehensive framework that simultaneously pairs cargoes, routes vessels, and manages inventory all while strictly bounded by environmental carbon metrics represents an urgent and unresolved frontier in maritime operations research.

2.5 IMO Short-Term GHG Regulations and Their Impact on LNG Portfolio

In response to the growing environmental concerns and the rise of GHG emissions from international shipping, academic attention has also turned toward the regulatory frameworks set by the International Maritime Organization (IMO). These regulations particularly the Energy Efficiency Existing Ship Index (EEXI) and the Carbon Intensity Indicator (CII) not only influence shipping operations but also shape the research agenda for maritime logistics, including delivery planning and inventory routing (IMO, 2021b; Hua, et al., 2024). Understanding how these measures affect routing efficiency, scheduling flexibility, and compliance costs is essential for advancing sustainable LNG transportation models.

Maritime shipping remains the backbone of global trade, accounting for approximately 90% of international goods transport by volume (IMO, 2011). The global fleet has expanded significantly in recent years, growing from 116,000 vessels in 2009 to over 130,000 by 2021, accompanied by a 46% increase in deadweight tonnage (DNV, 2022). This growth, coupled with increased trade volumes, has contributed to a notable rise in greenhouse gas (GHG) emissions. According to The United Nations Conference on Trade and Development (UNCTAD), emissions from international shipping have risen by 20% over the past decade, now representing nearly 3% of global GHG emissions, placing the maritime sector among the top six largest national-equivalent emitters globally (Balcombe, et al., 2019; de Oliveira, et al., 2022; Clark, et al., 2023).

Between 2012 and 2018 alone, GHG emissions from shipping rose from 977 to 1,076 million tonnes, with CO_2 emissions increasing by 9.3% over the same period (Lu, et al., 2023). According to IMO's fourth greenhouse gas study, without decisive regulatory intervention, shipping emissions could increase to 90 – 130% of 2008 levels by 2050 (Faber, et al., 2020). In this context, the decarbonisation of maritime transport has become an urgent global priority.

In response, the IMO adopted its Initial GHG Strategy in 2018, targeting a 40% reduction in carbon intensity by 2030 and at least 50% in absolute GHG emissions by 2050, relative to 2008 levels (IMO, 2018). This ambition was significantly increased under the 2023 Revised GHG Strategy, which aims to reach net-zero emissions from international shipping by or around 2050, with intermediate checkpoints for 2030 and 2040 (IMO, 2023).

To operationalise these goals, the IMO introduced a series of technical and operational measures, including:

- Energy Efficiency Design Index (EEDI): Mandatory for new ships since 2013.
- Ship Energy Efficiency Management Plan (SEEMP) and Energy Efficiency Operational Indicator (EEOI): Introduced as operational guidelines encouraging the optimisation of fuel use and emissions. Notably, the EEOI served as an early, voluntary precursor to the mandatory CII framework (de Oliveira, et al., 2022)

- Energy Efficiency Existing Ship Index (EEXI) and Carbon Intensity Indicator (CII): Mandatory from 2023, applying to existing fleets to enforce year-on-year improvements in carbon performance (IMO, 2021a; IMO, 2022b; Ten, et al., 2023)

Among these, the CII regulation is particularly relevant to shipping operations research. It evaluates carbon intensity based on cargo mass and distance travelled and assigns vessels a rating from A to E. Ships rated D for three consecutive years or E for one year must submit corrective action plans (ClassNK, 2023). For LNG vessels, which often operate on tight long-term contracts and fixed schedules, compliance with CII may require significant adjustments to routing, scheduling, and speed often at the cost of operational efficiency.

The urgent need for effective decarbonisation measures within maritime transport is not deniable. Reducing air pollutants from shipping is not only essential for mitigating climate change, but also for improving air quality and addressing associated public health risks, particularly for communities located near ports and along coastlines. Greenhouse gas emissions from ships can come from various sources such as ship engines, cooling systems, and combustion systems. The most common greenhouse gas emissions are carbon dioxide (CO_2), methane (CH_4), and nitrogen oxides (N_2O). Management of greenhouse gas emissions in international shipping is important to reduce the negative impact on the environment (Prasetyo, et al., 2023).

Recent studies have begun to address the impact of such regulations on vessel speed, emission amount and loading cargo amount. Operational strategies such as slow steaming, optimised port calls, and multimodal transport integration are increasingly evaluated not only for cost-effectiveness but also for compliance with CII and EEXI metrics (Zhang, et al., 2024).

The introduction of these regulations has also spurred modelling innovations in optimisation, where emission-related constraints are now embedded in mixed-integer programming (MIP) and stochastic optimisation models (Tran, et al., 2023; Hua, et al., 2024). As such, emissions compliance is becoming a key dimension in delivery planning problems, making regulatory constraints a critical component of current operations research literature in maritime logistics. On the other hand, the implications of this regulation extend far beyond routine operational adjustments. As highlighted by Hua et al. (2024), the CII has significant economic repercussions, influencing vessel valuation, second-hand sales and purchases, financial leasing agreements, and charterers' selection

criteria. Consequently, enhancing the operational CII rating has become both an environmental necessity and a commercial imperative.

2.5.1 **Operationalisation and Metrics of the CII**

The CII is calculated based on the amount of CO_2 emitted per unit of deadweight tonnage and nautical mile travelled vessel, benchmarked against a required CII derived from a reference line adjusted by an annual reduction factor (IMO, 2021a). These factors are progressively tightened, starting from 5% in 2023 to 11% by 2026 (IMO, 2022b). This trajectory compels ship operators to continuously improve their vessels' operational efficiency (Yuan, et al., 2023).

A significant methodological limitation arises from the CII's reliance on deadweight tonnage (DWT) rather than actual cargo mass. Due to the lack of comprehensive data on real cargo weight, the IMO adopted a supply-based approach, potentially overestimating efficiency by up to 30% (Kim, et al., 2023). Wang et al. (2021) emphasise the importance of integrating real-time data to enhance the accuracy of CII measures. Consequently, the validity of CII as a true reflection of carbon performance remains questionable. This concern is echoed in Sardar et al. (2024) study, who found that 63% of oil tankers assessed were rated E primarily due to outdated engines and inefficient operational behaviours such as excessive idling and poor route planning.

Tran et al. (2023) explored the implications of CII compliance for vessels operating in ice-covered waters. Given that the CII regulatory framework permits the exclusion of time spent navigating ice (IMO, 2022d) and the associated emissions from annual efficiency reporting, their study investigated how this exemption might influence routing strategies. By proposing a shift from an annualised CII metric to a distance-based calculation, the authors aimed to offer more granular operational control. While the regulation is intended to incentivise lower sailing speeds and reduced emissions, the findings suggest that the ice navigation exemption may, in certain contexts, counteract these intended benefits. The potential for this provision to distort routing incentives raises questions about the overall effectiveness and consistency of the CII framework in promoting emissions reductions across varying operational environments.

2.5.2 **Compliance Mechanisms and Economic Implications**

Under the current CII regulation, ships over 5,000 gross tonnage (GT) are rated annually on a five-point scale (A to E), where ‘A’ denotes major superior performance and ‘E’ indicates inferior performance (IMO, 2022c). When a vessel receiving a D rating for three consecutive years, or an E in any single year, must submit a corrective action plan via the Ship Energy Efficiency Management Plan (SEEMP). This plan must outline concrete steps for improving performance to at least a C rating in subsequent years. Non-compliant ships must adjust their operations before resuming service (Qi, et al., 2021). According to Clarksons research 30% of ships expected to be rated D or E in CII assessments (Bartlett, 2023).

Economically, compliance carries tangible consequences. Schroer et al. (2022) observed that retrofitting older vessels often yields negative returns due to their limited remaining service life. While replacing these ships with larger, newer models could reduce emissions by up to 30%, this transition is projected to span up to 25 years (Bouman, et al., 2017). Barreiro et al. (2022) and Zarrinkolah and Hosseini (2023) suggest that maintaining or improving a vessel's rating will necessitate measures such as speed optimisation, adoption of fuel-efficient technologies, or a transition to low-carbon fuels. While the CII system penalises underperforming vessels, it simultaneously introduces potential incentives for higher-performing ones. Port authorities and regulatory agencies are encouraged to offer operational or financial benefits to ships rated A or B, thereby fostering the early adoption of low-emission technologies and practices (IMO, 2022a). However, the increasing stringency of the rating thresholds presents a significant challenge. A vessel rated C in one year may be reclassified as D in the subsequent year, even without any decline in performance, if proactive efficiency measures are not implemented. This dynamic nature of the grading system necessitates continuous operational improvements to avoid penalisation and to remain eligible for any incentive-based advantages.

2.5.3 **Alternative Fuels and Technological Innovation**

According to DNV (2022), 94.5% of the existing global fleet operates on fossil fuels, with 66.8% of newbuilds projected to follow this trend indicating a slow but emerging transition. The literature converges on a shared recognition that LNG, while a useful bridging solution, cannot deliver the emissions reductions necessary to

meet long-term targets set by the IMO (Lindstad, et al., 2020). Studies by Ejder et al. (2024); Al-Haidous, et al. (2022) and Balcombe et al. (2019) confirm that while LNG reduces carbon dioxide emissions by approximately 30%, its net climate benefits are significantly undermined by methane slip, resulting in total GHG reductions of only 8–20%. This limitation is compounded by upstream emissions associated with fuel extraction and processing, which can erode the perceived environmental advantages of alternative fuels if sustainability is not embedded in their production (Balcombe, et al., 2019; IRENA, 2019).

Despite these constraints, alternative fuels such as hydrogen, ammonia, and methanol are expected to dominate future maritime energy mixes (Xing, et al., 2020; Bilgili, 2021; Bilgili, 2023). However, their commercial viability, infrastructure readiness, and full life-cycle impacts remain uncertain. Potential of alternative fuels in decarbonization have been assessed in the study by Law et al. (2022). Recent innovations, such as the hydrogen proton exchange membrane fuel cells tested by Inal et al. (2024), suggest that such technologies may offer radical reductions in emissions up to 38% and provide sustained compliance with CII performance standards. Furthermore, in other study, cold ironing also known as shore power has been highlighted as one of the viable short-term measures for reducing maritime emissions and enhancing CII compliance, emphasizing the need for optimised economic models (Sevgili, et al., 2025). The widespread adoption of such solutions depends not only on technical feasibility but also on integrated policy frameworks, supply chain reconfiguration, and stakeholder coordination. These dynamics underscore the need for optimisation models that can assess trade-offs between economic, operational, and environmental objectives under regulatory constraints.

2.5.4 **Operational Strategies for Efficiency Improvement**

Operational interventions offer some of the most immediate and cost-effective pathways for improving energy efficiency and complying with the CII. Among these, speed-related strategies particularly slow steaming and speed optimisation have attracted significant attention for their dual benefits of emission reduction and economic viability. The effects of slow steaming on the environmental performance in liner shipping have been assessed by Woo & Moon, (2014). Slow steaming involves deliberate operation below design speed, whereas speed optimisation adjusts vessel speed dynamically to minimise fuel consumption within logistical and

environmental constraints (Psaraftis, 2019). In the other study conducted by Sheng, et al. (2019) vessel speed and fleet size have been optimised for industrial services for under emission control area regulation.

Recent modelling studies reinforce the value of these strategies. Hua et al. (2024) demonstrated that a genetic algorithm-based schedule adjustment could yield a 5–8% increase in annual full-load distance while maintaining at least a C rating. Similarly, Yuan et al. (2023) proposed a short-term fleet upgrade strategy that required an average speed reduction of 7%, with some vessels necessitating cuts of over 20% to remain within acceptable CII thresholds. Empirical analyses corroborate these findings. Zincir (2023) showed that slow steaming alone enabled general cargo vessels to achieve an 'A' rating under CII without retrofitting especially valuable for ageing fleets with limited upgrade potential.

The hydrodynamic and environmental impacts of speed reduction have also been quantified. Degiuli et al. (2024) found that speed reductions of 10 –30% yielded corresponding emissions reductions of 16.89–25.74% while maintaining constant transport work. However, the authors caution that any potential regulation mandating uniform speed limits must consider vessel-specific profiles to avoid unintended inefficiencies.

Expanding on this operational perspective, Taskar et al. (2023) investigated speed optimisation; their model formulated a single-objective optimisation problem that maintained fixed voyage routes and timeframes. While the expected emission reductions from speed optimisation are modest relative to the IMO's broader decarbonisation targets, the approach remains attractive due to its ease of implementation. They incorporated key physical considerations such as calm water resistance, added wave resistance, and wind resistance into their model. Simulation results for two container vessels demonstrated fuel savings of up to 6%, with higher savings achieved at lower speeds and during seasons prone to adverse weather. The study also found that combining slow steaming with speed optimisation led to further fuel savings while preserving schedule reliability, highlighting the potential of integrated operational strategies for simultaneously enhancing efficiency and regulatory compliance.

While operational adjustments are effective in the short term, many vessels particularly older, conventionally fuelled ships face technical limitations that necessitate retrofits for EEXI and CII compliance. According to ClassNK (2022), over 80% of NK-classed ships have already adopted additional measures to meet EEXI

requirements. A leading approach is Engine Power Limitation (EPL), which deliberately caps engine output to lower emissions (Tadros, et al., 2023; Chuah, et al., 2023). Bayraktar and Yüksel (2023) evaluated EPL across five ship types and found it essential for compliance when vessels rely on Heavy Fuel Oil (HFO) or Marine Diesel Oil (MDO). Their study also highlighted the role of alternative fuels such as LNG and methanol in improving both EEXI and CII ratings, especially in dual-fuel configurations.

From a techno-economic standpoint, Schroer et al. (2022) compared EPL with other retrofit options including turbocharger cut-outs (TCCO), waste heat recovery systems (WHRS), variable frequency drives (VFDs), and auxiliary engine economisers (AEEs). Analysing six representative container ships, they identified EPL as the most cost-effective solution. However, they also observed that EPL can result in significant increases in voyage duration up to 794 hours annually in some cases, raising concerns about feasibility in certain trade routes. Their analysis also pointed to diminishing returns when multiple retrofits are layered onto a single vessel.

Ersoy et al. (2025) applied a machine learning model (M5 Rules) to engine room data from an oceangoing tanker to assess the combined effects of slow steaming and EPL. They found that slow steaming alone failed to meet EEXI thresholds, whereas a 32% EPL ratio enabled compliance. Moreover, while slow steaming improved the vessel's CII rating to B, adding EPL elevated it to A valid through 2026. These findings reinforce the importance of integrating operational and technical strategies rather than relying on any single measure in isolation.

Collectively, the literature affirms that while slow steaming and speed optimisation offer valuable short-term compliance tools, they alone may not suffice to meet the IMO's long-term decarbonisation targets, they provide a viable interim strategy. More importantly, their low capital requirements, scalability, and compatibility with existing infrastructure make them a compelling foundation for broader regulatory and commercial responses to carbon intensity reduction. Technical interventions such as EPL are increasingly critical particularly for older or heavily utilised vessels. Effective regulatory alignment will likely depend on ship-specific combinations of operational, technical, and fuel-switching strategies, calibrated to vessel design, trade route, and economic viability.

2.5.5 **Integrated Approaches and Emerging Computational Tools**

The need for integrated and adaptive strategies is increasingly evident. Zhang et al. (2024) demonstrate that while CII-driven optimisation reduces emissions, it necessitates larger fleets to preserve service levels. Similarly, Cheng et al. (2025) reveal that stricter CII enforcement in tramp shipping encourages shorter ballast distances and higher onboard loads, though with economic trade-offs.

To anticipate and manage compliance, novel data-driven tools have been developed. Mühmer et al. (2024) propose a forecasting model using real-time voyage and environmental data to predict CII performance. On the algorithmic front, Alshareef and Alghanmi (2024) demonstrate that deep reinforcement learning (DRL) surpasses traditional optimisation techniques in improving vessel efficiency dynamically. From a technological standpoint, newer electronically controlled engines are expected to fare better under CII/EEXI regimes due to their efficiency at low-speed operations (Polemis, et al., 2023). Despite its methodological shortcomings, the CII framework has been instrumental in catalysing a shift toward decarbonisation (Cheng, et al., 2025). However, questions remain regarding its fairness, data reliability, and long-term efficacy. Literature increasingly calls for an evolution from capacity-based to cargo-specific metrics and from annual averages to more dynamic, per-distance calculations.

The research landscape now shifts towards holistic compliance models that integrate operational, technical, and computational strategies. A significant research gap persists in quantifying real-world outcomes across diverse ship types and trading routes, particularly under increasingly stringent regulatory environments. The increasing role of LNG in global energy markets has intensified the need for efficient and sustainable delivery planning. Portfolio optimisation for annual LNG delivery, balancing supply, and demand across a network of geographically dispersed suppliers and consumers has attracted considerable academic and industrial attention due to its economic and logistical complexities. At the same time, the LNG sector is undergoing a significant transformation. According to the Shell LNG Outlook 2025, global LNG demand is projected to increase by approximately 60 per cent by 2040, driven by industrial decarbonisation efforts, economic expansion in Asia, and the energy requirements of emerging technologies. Nevertheless, despite this strong long-term growth

potential. With over 170 million tonnes of new LNG capacity anticipated by 2030, the task of designing efficient and sustainable delivery portfolios is becoming increasingly complex (Shell, 2025).

2.6 **Research Gaps**

A review of existing scholarship reveals two key limitations in the modelling of LNG supply chain operations. Firstly, the operational and logistical complexity of LNG supply chains is rarely captured in its full practical richness. Existing studies have typically addressed individual components of the supply chain such as routing, scheduling, or inventory management in isolation, without fully representing the multifaceted interactions that characterise real-world delivery planning.

However, both industry practice and the literature indicate that LNG logistics decisions are inherently interconnected. Factors such as supplier heterogeneity, time-varying market prices, contractual flexibility, and delivery coordination across multiple customers play a critical role in determining operational efficiency and cost performance (Cheng, et al., 2025; Budiyanto, et al., 2019; Andersson, et al., 2017). Despite this, few models explicitly capture the dynamic interactions between multiple suppliers and customers, including simultaneous optimisation of cargo pairing, vessel allocation, and routing decisions.

In addition, several technical and economic characteristics such as fuel boil-off, chartering costs, port compatibility constraints, minimum delivery commitments, and variations in calorific value are widely recognised as key drivers of operational feasibility and economic performance in LNG transportation (Deshpande, et al., 2022; Grønhaug, et al., 2010; Cho, et al., 2014). These factors directly influence fuel consumption, cargo value, and scheduling efficiency, yet they are often simplified or excluded in existing optimisation frameworks.

Furthermore, important operational features, including the distinction between laden and ballast legs and the use of variable sailing speeds, have a direct impact on both emissions and fuel consumption profiles (Qi, et al., 2021; Psaraftis, 2019). Nevertheless, these elements are rarely incorporated in an integrated manner within existing models. As a result, there remains a clear gap in the literature for a comprehensive optimisation

framework that integrates operational, technical, and economic factors within a unified LNG portfolio decision-making context.

The second limitation relates to the integration of environmental regulations, particularly the Carbon Intensity Indicator (CII), into LNG logistics optimisation. While a growing body of research has examined ship-level CII compliance (Zhang, et al., 2024; Degiuli, et al., 2024; Chuah, et al., 2023) strategies such as speed optimisation, fuel switching, and engine retrofitting very few studies have extended this analysis to the portfolio level of delivery planning. In practice, LNG suppliers and fleet operators face a dual objective: fulfilling contractual and market commitments while complying with increasingly stringent environmental regulations.

The introduction of CII introduces a new class of operational constraints that fundamentally alter the economic logic of fleet management and scheduling decisions. Traditional optimisation models, which primarily focus on cost minimisation or utilisation maximisation, are not designed to incorporate carbon intensity limits as binding constraints. Consequently, portfolio managers lack systematic tools to support decision-making that simultaneously ensures regulatory compliance, operational efficiency, and profitability.

Moreover, operational inefficiencies such as extended idling and suboptimal routing not only reduce commercial performance but also negatively impact CII ratings (Sardar, et al., 2024). For example, prolonged port waiting times generate emissions without corresponding transport work, while increased boil-off during idle periods results in cargo loss and reduced efficiency. Despite these practical implications, no integrated optimisation framework currently exists to quantify and mitigate these effects within LNG supply chain planning.

From the methodology perspective, a critical synthesis of the existing literature reveals a distinct evolutionary trajectory in the operational modelling of LNG supply chains. Early research successfully established the foundational mathematics of routing and scheduling, progressing from basic deterministic formulations to complex frameworks capable of handling load-splitting, transshipment, and spot-market integrations. However, this review identifies two critical, unresolved methodological gaps that the present study seeks to address:

First, as demonstrated by early studies such as Rakke et al (2011) exact mathematical formulations, such as standard MIP provide necessary rigorous baselines and guarantee global optimality. However, the literature

universally acknowledges that maritime routing and scheduling problems are strongly NP-hard. As researchers have attempted to add real-world operational realism (such as variable speeds, heterogeneous fleets, and time-varying LNG market price) into these exact models, the computational burden has become insurmountable for large-scale, industrial datasets. While some studies have attempted to resolve this using Mixed-Integer Nonlinear Programming (MINLP) to handle non-linear fuel curves, these formulations are notoriously difficult to solve and frequently fail to guarantee optimality at a global portfolio scale. Therefore, while a Mixed-Integer Linear Programming (MILP) model is strictly necessary to mathematically define the problem and establish an exact baseline, relying on it as the sole solution method for an annual, global delivery program is methodologically insufficient. Therefore, to bypass the computational limits of exact methods, the literature has increasingly turned to heuristics and decomposition methods (Stålhane, et al., 2012; Rakke, et al., 2011). While these approaches run efficiently, they were designed primarily for pure cost-minimisation or profit-maximisation. As identified in Section 2.5, the current state-of-the-art is fundamentally unequipped to handle the IMO's Carbon Intensity Indicator (CII). The CII is not a simple, point-to-point constraint; it is a cumulative, year-long environmental metric. Standard heuristics and local search algorithms struggle with cumulative constraints because an apparently optimal local decision made in January (e.g., sailing at maximum speed to capture a high spot price) can fatally degrade the vessel's CII rating by December.

Based on these identified shortcomings, this thesis proposes a hybrid methodological approach. First, a comprehensive MILP framework is developed to establish a rigorous, mathematically exact baseline capable of linearising complex physical and environmental constraints. Second, to address the computational intractability of the MILP on real-world industrial data, a Genetic-Based Metaheuristic Algorithm (GBMHA) is developed. The choice of a genetic-based metaheuristic is directly justified by the literature's demand for algorithms capable of escaping local optima when evaluating massive, combinatorial search spaces. Unlike basic descent heuristics, a well-calibrated Genetic Algorithm is uniquely suited to evaluate the long-term, cumulative trade-offs required by CII compliance, successfully balancing the dual mandate of annual profit-maximisation and strict environmental regulation within viable computational timeframes.

By addressing the identified gaps, this research contributes to the development of a comprehensive LNG portfolio optimisation framework that integrates operational complexity with environmental performance

considerations. In doing so, it provides a decision-support tool capable of assisting LNG suppliers and fleet operators in navigating the combined challenges of market dynamics, logistical constraints, and regulatory compliance.

2.7 Conclusion

This chapter has systematically reviewed the expanding body of literature concerning maritime logistics, environmental regulations, and LNG supply chain operations. Based on this review, what is notably absent in the current scholarship is a unified, system-level modelling approach that combines the operational complexity of LNG and low-carbon fuel supply chains with the environmental and regulatory considerations introduced by the IMO's CII. There is a pressing need to examine how regulatory constraints affect decision-making at the portfolio level, to evaluate trade-offs between emissions compliance and cost efficiency, and to identify optimisation strategies that are both commercially viable and environmentally sustainable. This research therefore addresses a critical and timely gap by proposing an integrated optimisation framework for annual LNG delivery planning that explicitly incorporates CII constraints. The framework models the supply chain as a complex, multi-criteria system, accounting for supplier heterogeneity, contractual flexibility and obligations, vessel-specific characteristics, and time-varying market price, while also embedding emissions performance metrics. To operationalise this framework and overcome the computational limitations of exact optimisation on large-scale industrial datasets identified in the literature, the following chapter (Chapter 3) will detail the development of this MILP model alongside a complementary metaheuristic solution approach.

CHAPTER 3 A NOVEL MIXED INTEGER LINEAR PROGRAMME FOR LNG PORTFOLIO OPTIMISATION FOR ANNUAL DELIVERY PLANNING

Summary

This chapter details the methodological framework developed to optimise the complex routing and scheduling challenges inherent in global cryogenic fuel supply chains. It begins by introducing a novel mathematical formulation (Section 3.1) that integrates a comprehensive suite of real-world operational and economic factors (such as time-varying market prices, variable vessel speeds, calorific heterogeneity, and idle-time management) which have previously been treated in isolation. To overcome the computational limitations of this exact formulation when applied to large-scale networks, the chapter then details the development of a customised evolutionary metaheuristic algorithm equipped with novel encoding and constraint-handling mechanisms. Finally, the proposed framework is validated using real-world benchmarking data provided by a commercial partner, establishing a robust computational foundation for the remainder of the thesis.

3.1 Introduction

The objective of this chapter is to present a mathematical model that addresses a set of interrelated and complex challenges encountered in the global cryogenic fuel shipping supply chain. Building upon the research gaps outlined in the second chapter, this model is the first to provide a comprehensive and integrated formulation that brings together various realistic operational and economic factors in a unified optimisation framework.

Existing literature has often approached such challenges in a fragmented manner, focusing either on simplified representations of supply-demand relationships or treating routing and scheduling problems in isolation. In contrast, the model proposed in this chapter is characterised by its ability to simultaneously capture several critical dimensions of real-world operations. These include, but are not limited to, the temporal and spatial variability of fuel prices among different suppliers, constraints on the quantity of fuel that each supplier can provide, and the requirements to fulfil time-sensitive and geographically dispersed customer demands.

A distinctive feature of the model lies in its treatment of supplier-customer cargo pairing. This aspect is addressed by evaluating geographical proximity, vessel deployment based on live location data, and route optimisation through selectable voyage speeds. These elements are crucial in reducing fuel consumption and voyage time, thereby enhancing overall profitability. Additionally, the model incorporates the timing of vessel arrivals, cargo loading schedules, and idle periods at sea or port, all of which are managed in a manner that seeks to optimise operational efficiency.

Furthermore, the model introduces the concept of calorific value variation across suppliers as a decision-making criterion. By including fuel quality (expressed in Million British Thermal Units), the model enhances the precision with which economic outcomes can be estimated. This is particularly relevant given the time-dependent nature of fuel prices, which introduces a level of complexity not previously addressed in mathematical formulations within this domain.

A further novel aspect of the model is its handling of vessel idle periods, both in the ballast (empty) and laden (cargo-carrying) phases of a voyage. Idle periods contribute significantly to cost inefficiencies due to chartering expenses, unnecessary fuel consumption, and fuel losses from boil-off. The model explicitly aims to minimise such inefficiencies, thereby providing a more sustainable and cost-effective approach to voyage planning.

To enable the application of the proposed model to realistic and large-scale scenarios, a dedicated evolutionary algorithm has been developed, the details of which are provided in the following section. This algorithm has been tailored to capture the complexity of the model by introducing a novel solution representation, specialised initialisation routines, and robust constraint-handling mechanisms.

The validation of the model is undertaken using empirical data from an industrial partner, allowing for the construction of test cases that replicate actual operational conditions. These test cases not only provide a foundation for evaluating the effectiveness of the proposed methodology but also serve as a benchmarking platform for future research in the field.

In summary, the mathematical model introduced in this chapter provides a significant and original contribution to the literature on maritime logistics and fuel supply chains. By integrating a wide array of realistic factors into

a coherent analytical framework, the model offers a powerful tool for enhancing operational decision-making in global low-carbon shipping environments.

3.2 Baseline MILP for LNG Portfolio Optimisation for ADP

This section presents the core mathematical formulation developed to optimise the global shipping of cryogenic fuels, with a particular focus on Liquefied Natural Gas (LNG). The model has been constructed with the primary objective of maximising overall profit across an annual delivery programme of a single global energy enterprise. To achieve this, the formulation simultaneously addresses several critical operational decisions, including the optimal allocation of vessels to specific cargoes, the strategic pairing of suppliers with customers, and the efficient routing and scheduling of voyages.

The model captures the economic intricacies of the fuel supply chain by seeking to minimise total operational costs, comprising chartering, fuel consumption, boil-off losses, and port charges, while ensuring that delivery commitments are met. By integrating these elements into a cohesive optimisation framework, the model provides data-driven decision support that reflects both the scale and complexity of real-world LNG logistics. The goal is to enable the companies to enhance operational efficiency and profitability through intelligent planning and resource deployment.

3.2.1 Problem Description

The global supply chain for LNG, and more broadly for future low-carbon cryogenic fuels, represents a highly complex logistical and operational system. It involves a wide network of geographically dispersed suppliers and customers, each operating under dynamic market conditions and physical constraints. In this study, the real-world problem is formulated explicitly from the perspective of a central decision-maker: a commercial LNG distributor or portfolio manager.

Operating as the crucial intermediary, the distributor purchases LNG from various global suppliers and sells it to multiple customers to fulfil strict contractual demands. To execute these trades, the distributor must efficiently allocate and manage a heterogeneous fleet of vessels. The overarching objective of the decision-maker is to

maximise overall portfolio profitability by strategically pairing suppliers with customers, allocating the most appropriate vessels, and determining optimal sailing speeds, all while navigating fluctuating market prices and complex physical constraints.

To depict the fundamental structure of this optimisation challenge before introducing the mathematical notation, Figure 3.1 provides a static conceptual overview of the network topology. As illustrated, the operational

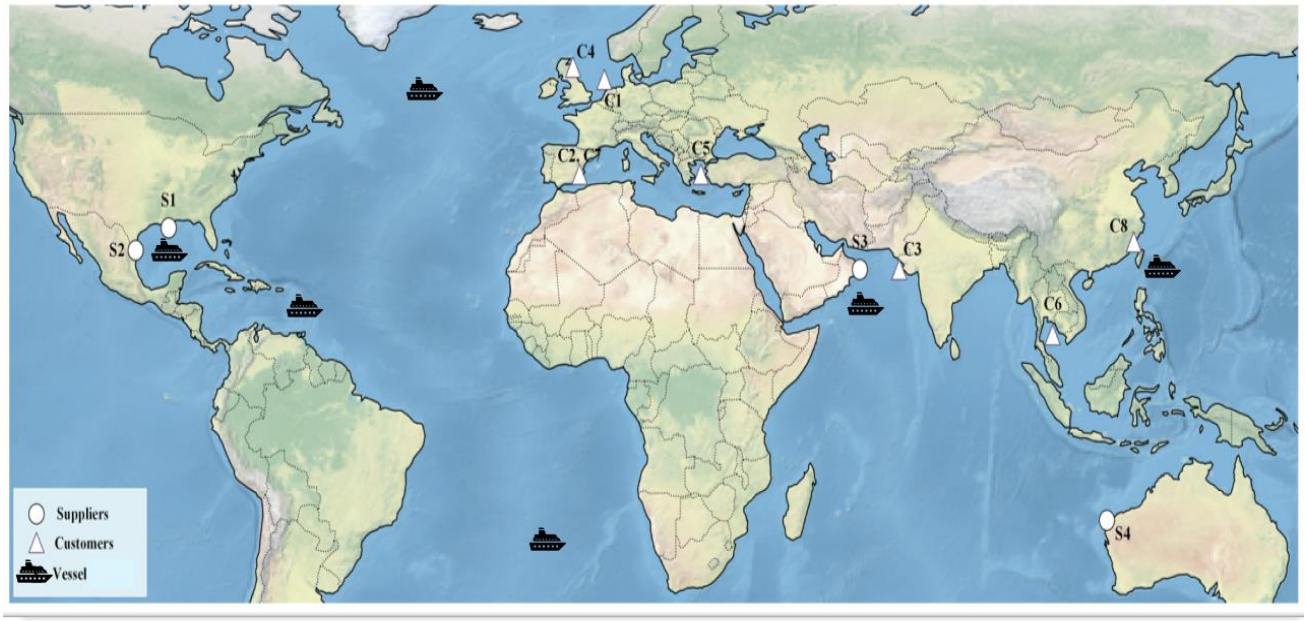

Figure 3.1: Conceptual representation of the LNG supply chain network from the distributor's perspective, illustrating the available fleet, heterogeneous suppliers, and final customer demand nodes.

framework encompasses the heterogeneous fleet (initial live locations), the fixed supply nodes where dynamic procurement occurs, and the geographically dispersed customer demand nodes. The core challenge for the distributor is not merely moving between these fixed points, but determining the optimal, simultaneous combinations of supply, demand, vessel selection, and variable speed across this global network.

To ensure this formulation accurately captures the operational realities of the industry, the selection of the following key characteristics is rigorously grounded in established Maritime Inventory Routing Problem (MIRP) and cryogenic logistics literature:

- **Diverse and dynamic supplier market**: The model considers a wide range of suppliers, each offering fuel at prices which vary dynamically over time. These suppliers also operate under capacity limitations

and individual contractual constraints regarding loading schedules and fuel amount availability, reflecting the shift toward dynamic spot-market procurement highlighted in recent energy trade studies (Zhang, et al., 2021; Al-Haidous, et al., 2016).

- **Customer demand fulfilment**: The model allows for the distribution of loaded fuel among multiple customers in order to maximise overall profitability by buying LNG in its cheapest price. The necessity of partial deliveries for optimising complex MIRPs has been widely validated in the literature (Utku, 2023; Utku & Soyöz, 2020).
- **Strategic cargo pairing and vessel allocation**: The assignment of vessels to specific supplier-customer routes is informed by a range of operational and economic criteria (including chartering costs, boil-off, live locations, and port compatibility). Integrating these physical and economic constraints into vessel allocation is universally recognised as essential for robust maritime operations (Chen, et al., 2024; Eriksen, et al., 2022; Cho, et al., 2018; Cho, et al., 2014).
- **Modelling of variable vessel speeds**: Voyage speeds are not fixed but instead are treated as decision variables. Variable speed optimisation is a heavily cited mechanism in modern or literature for balancing voyage time against nonlinear fuel consumption and scheduling constraints (Hua, et al., 2024; Sheng, et al., 2019).
- **Vessel idleness as an explicit cost factor**: The model seeks to manage vessel idle time, which incurs multiple penalties including chartering costs, unnecessary fuel usage, and boil-off losses. The management of idle time is extensively documented as a primary driver of cost inefficiency in maritime logistics (Al-Haidous, et al., 2022; Al-Haidous, et al., 2016).
- **Operational constraints on port compatibility and berth scheduling**: Not all vessels are compatible with all ports, and berth availability is strictly time constrained. Precise berth scheduling and port compatibility are standard, non-negotiable constraints in applied MIRP formulations (Yazdi, et al., 2020).
- **Dynamic supplier-customer pairing under price volatility**: The supplier-customer pairing is treated as a dynamic process based on real-time market conditions. This aligns with contemporary research

emphasizing the need for supply chain models to react to volatile global energy markets rather than relying on static contracts (Haug, et al., 2023; Zhang, et al., 2021; Khalilpour & Karimi, 2012).

In addressing these challenges, the model provides an integrated and practical framework capable of guiding strategic and operational decisions specifically for the commercial LNG distributor. It reflects the realities faced by commercial operators and accommodates the simultaneous consideration of physical constraints, economic objectives, and environmental parameters. The resulting problem structure is therefore representative of a truly global and highly dynamic supply chain environment.

3.2.2 **Model Assumptions**

In order to ensure the feasibility, tractability, and real-world relevance of the mathematical model developed for this study, a number of carefully considered assumptions have been made. These assumptions serve to define the operational context of the global LNG (and future low-carbon cryogenic fuel) supply chain under investigation. While grounded in real-world logistics, they also aim to strike a balance between model complexity and solvability.

The modelling assumptions adopted in this study are based on a combination of industry practice, data availability, and the need to ensure computational tractability. Where possible, assumptions are aligned with established approaches in the literature on maritime logistics and LNG transportation.

It is acknowledged that the LNG supply chain is influenced by a wide range of operational, technical, and environmental factors. However, not all variables can be incorporated without significantly increasing model complexity and computational burden. Therefore, the assumptions focus on the most influential factors affecting routing, allocation, fuel consumption, and emissions performance, while less critical or highly uncertain parameters are simplified. While these assumptions provide a realistic and tractable representation of the system, it is recognised that certain aspects such as real-time operational disruptions, detailed thermodynamic behaviour, or continuous operational variability are not explicitly modelled. These limitations are not expected to alter the overall structural insights of the study but represent potential areas for future research and model refinement.

Fleet and Vessel Characteristics

In this study, vessel speed is represented using discrete levels (e.g., low, medium, and high) to balance modelling realism with computational tractability. While vessel speed is inherently a continuous variable, modelling it as continuous would introduce severe non-linear relationships between speed, fuel consumption, and emissions. This would lead to a significantly more complex optimisation problem that is exceedingly difficult to solve efficiently at an industrial scale. The selected discrete speed levels correspond directly to typical operational regimes in maritime practice such as slow steaming, standard cruising, and higher-speed operations and therefore accurately capture the key trade-offs between fuel consumption, voyage duration, and emissions performance. This discretisation may slightly limit the precision of speed-related decisions, particularly in identifying marginal improvements between intermediate speed values. However, it is not expected to significantly affect optimal routing or overarching emissions outcomes, as the model still robustly captures the dominant relationships influencing these decisions (Sheng, et al., 2019).

Furthermore,, all vessels are assumed to start their operations from a predefined initial location, corresponding to the main supplier port managed by the company and it ensures that vessels return to the primary operational hub to await their next planning cycle or remain idle which is a standard "closed-loop" or "depot-return" assumption widely utilised in Vehicle Routing Problems (VRP) (Cho, et al., 2014). This assumption simplifies the initial conditions of the scheduling problem while reflecting the operational reality of centralised LNG sourcing.

Additionally, a minimum heel quantity of LNG is assumed to be maintained onboard at all times. This reflects operational requirements in LNG shipping, where a residual cargo is necessary to maintain cryogenic tank conditions and avoid costly and time-consuming re-cooling procedures. Consequently, vessels are not allowed to be completely emptied during operations.

Fuel and Cargo Management

The fuel and cargo management framework in this study is designed to reflect real-world LNG trading and operational practices. Based on industry data and transaction records, all fuel-related quantities including LNG

loading and unloading volumes are measured in MMBtu. This standardised unit allows for consistent comparison and aggregation of LNG supplied from different sources, despite variations in calorific value across suppliers.

In practice, LNG suppliers offer cargoes with differing calorific values, which introduces variability into the supply chain. This study incorporates such heterogeneity to better represent real market conditions, where cargo quality and energy content are not uniform.

Operationally, loading and discharging activities are subject to supplier and customer-specific contractual constraints. These include minimum and maximum cargo quantity thresholds, as well as predefined time windows within which loading and unloading must be completed. These constraints are derived from industry data and reflect typical contractual and logistical limitations in LNG operations.

The scope of the LNG supply chain model in this study is focused on the core operational stages of loading, transportation, and discharge. Other aspects of the broader LNG value chain, such as upstream production or downstream regasification, are not explicitly modelled, allowing the analysis to concentrate on the optimisation of maritime logistics and portfolio decisions.

Price, Demand, and Market Dynamics

The LNG market in this study is characterised by temporal price variability, reflecting the dynamic nature of global energy markets. As a result, prices cannot be assumed constant over the planning horizon. Buying and selling prices are exogenous, time-varying input parameters, both suppliers and customers are modelled with time-dependent price. Suppliers offer LNG at varying selling prices, while customers exhibit differing willingness to pay, with both evolving over time in response to market conditions. This representation captures the inherent volatility and competitiveness of LNG trading environments.

In terms of demand, all customer requirements are assumed to be fully satisfied within the planning horizon. Unmet demand is not permitted in this case study and to do so the portfolio's total available supply and the cumulative carrying capacity of the fleet strictly exceed the aggregate customer demand to ensure the

mathematical feasibility of the "no unmet demand", reflecting contractual obligations and service-level expectations in LNG markets and a single customer's discrete demand request must be fulfilled by exactly one supplier and transported by exactly one assigned vessel. Additionally, it is assumed that sufficient LNG supply is available from the set of suppliers to meet total demand, allowing the optimisation to focus on allocation and logistics decisions rather than supply scarcity.

Within this market setting, the objective function is designed to maximise overall portfolio profitability. It incorporates revenue from LNG sales alongside key cost components, including vessel chartering costs, port charges, fuel consumption, boil-off losses, and vessel idleness. This ensures that both economic performance and operational efficiency are captured within the optimisation framework.

Routing, Scheduling, and Operational Timing

Routing, scheduling, and operational timing in this study is modelled to reflect practical maritime logistics while maintaining computational efficiency and discretised into uniform weekly intervals throughout the planning horizon. While the overarching planning horizon and time-varying market parameters are discretised into uniform weekly intervals, specific operational durations that typically require less than one week—such as vessel waiting, loading, unloading, and short voyage times—are modelled as continuous fractional units of a week (e.g., a duration of 3.5 days is mathematically represented as 0.5 weeks). This preserves the precise chronology of short-term logistical activities while maintaining alignment with weekly market fluctuations. Furthermore, Operational timing is governed by port-specific loading and discharging windows. When a vessel arrives before the start of a scheduled operation, it is assumed to remain idle until its time window starts. During such periods, vessels incur idle costs, which are modelled using a stepwise structure and assumed to be equivalent to their active operational cost, reflecting the economic impact of underutilisation.

Vessel routing is determined based on the shortest available nautical distances between ports, providing a simplified yet realistic representation of voyage planning and fuel consumption estimation.

Furthermore, vessel availability is treated as time-dependent, meaning that scheduling decisions account for each vessel's current location and the completion of prior assignments. This ensures that routing and allocation

decisions remain operationally feasible and consistent with real-world constraints on vessel movement and turnaround times.

3.2.3 **Mathematical Modelling**

To facilitate the mathematical formulation of the model, the following notation is introduced. The decision variables, sets, and parameters are defined as follows:

- *Sets* represent the structural elements of the problem, such as vessels, suppliers, customers, and time periods.
- *Parameters* capture the fixed inputs to the model, including vessel specifications, port capacities, prices, and time windows.
- *Decision variables* denote the values to be optimised, such as vessel assignments, fuel quantities, routing choices, and inventory levels.

A detailed list of these components in separate tables is presented below. The following Table 3.1 notations are used in the model:

Table 3.1: LNG Portfolio Optimisation Notation Sets

Sets	***Description***
$\boldsymbol{i, j}$	*Demand/cargo (1 to N) where i=1 indicates the dummy depot*
$\boldsymbol{p}$	*Suppliers (1 to P)*
$\boldsymbol{v}$	*Vessels (1 to V)*
$\boldsymbol{t}$	*Time step (1 to T)*
$\boldsymbol{s}$	*Speed level (1 to S)*

All Parameters that have been used in the model are summarised in Table 3.2 and the decision variables that would be the outcomes of the model are presented in Table 3.3.

Table 3.2: LNG Portfolio Optimisation Parameters

D_{pi}	*Distance between demand i and supplier p (nautical mile)*
$D_{vp}^{live\_location}$	*Distance between live location of vessel v and supplier p (nautical mile)*
$T_{vs}^{ballast/laden}$	*Required time for vessel v to travel 1 nautical mile in a ballast / laden leg at speed level s (based on week)*
ST_{vi}^{unload}	*Time taken for unloading for vessel v at demand i*
$cost_{vi}^{unload}$	*Unload cost for cargo i and vessel v*
ST_{vp}^{load}	*Time taken for loading for vessel v at supplier p*
$cost_{vp}^{load}$	*Load cost for vessel v at supplier p*
$C_{vs}^{ballast/laden}$	*Fuel consumption rate per nautical mile for vessel v in ballast / laden leg at speed level s*
$Ci_{v}^{ballast/laden}$	*Fuel consumption rate for vessel v in ballast/laden idle time*
$Cap_{p}^{min/max}$	*Load range for supplier p*
LF_{v}	*Load Factor of vessel v*
$Cap_{v}^{heelout}$	*Minimum allowed inventory level for vessel v to avoid heel out*
Dem_{it}^{total}	*Maximum LNG amount to be delivered through cargo i at time t where* $\sum_{t=1}^{T} Dem_{1t}^{total} = 0$

$\boldsymbol{Dem_i^{committed}}$	*LNG amount committed to be delivered through cargo* i *where* $Dem_{it}^{total} \geq Dem_i^{comitted} \quad \forall i, t$
$\boldsymbol{PS_{it}}$	*Forecasted LNG selling price for cargo* i *at time* t
$\boldsymbol{PB_{pt}}$	*Forecasted LNG purchase price for supplier* p *at time* t
$\boldsymbol{cap_v^{heelout} \leq inv_v^{initial}}$	*Initial LNG inventory level in vessel v*
$\boldsymbol{S_v}$	*Size of Vessel v* (m^3)
$\boldsymbol{CV_p}$	*Calorific value of LNG in supplier p*
$\boldsymbol{vt_j^{early/tardy}}$	*Earliest/latest allowed time for the delivery of cargo j where* $vt_1^{early/tardy} = 0$
$\boldsymbol{st_{pj}^{min/max}}$	*Earliest/latest allowed time for the loading of cargo j at supplier p where* $\sum_{p=1}^{P} st_{p1} = 0$
$\boldsymbol{B_{vp}^{compat-sup}} \begin{cases} \mathbf{1} \\ \mathbf{0} \end{cases}$	*If vessel v can berth along supplier p* *otherwise*
$\boldsymbol{B_{vi}^{compat-dem}} \begin{cases} \mathbf{1} \\ \mathbf{0} \end{cases}$	*If vessel v can berth along demand* i *otherwise*
$\boldsymbol{Vavail_v^{start/end}}$	*Start date and end dates limiting availability of vessel v*
$\boldsymbol{\lambda_v^{ballast/laden}}$	*Boil-off rate for vessel v at ballast/laden leg*
$\boldsymbol{cost_v^{shipping}}$	*Shipping (fixed) cost for vessel v upon utilization*

$\boldsymbol{VCost_v}$	*Variable cost for using vessel v per week*
$\boldsymbol{FC}$	*Vessel Fuel Cost*
$\boldsymbol{BigM}$	*A very large positive number*

Table 3.3: LNG Portfolio Optimisation Decision Variables

$\boldsymbol{x_{ijv}} \begin{cases} \mathbf{1} \\ \mathbf{0} \end{cases}$	*if vessel v travels from demand i to j* *otherwise*
$\boldsymbol{z_{js}} \begin{cases} \mathbf{1} \\ \mathbf{0} \end{cases}$	*if speed level s is applied to travel from/to demand j* *otherwise*
$\boldsymbol{y_{it}^{load/unload}} \begin{cases} \mathbf{1} \\ \mathbf{0} \end{cases}$	*If load/unloading of cargo i occurs at time t* *otherwise*
$\boldsymbol{u_v} \begin{cases} \mathbf{1} \\ \mathbf{0} \end{cases}$	*if vessel v is used* *otherwise*
$\boldsymbol{g_{ip}} \begin{cases} \mathbf{1} \\ \mathbf{0} \end{cases}$	*if cargo i is allocated to supplier p* *otherwise*
$\boldsymbol{ut_i}$	*Unloading time for cargo i*
$\boldsymbol{lt_i}$	*Loading time for cargo i*
$\boldsymbol{atl_i}$	*Arrival time of cargo i for loading*
$\boldsymbol{atul_i}$	*Arrival time of cargo i for unloading*

$\boldsymbol{IT_{vi}^{Ballast/Laden}}$	*Vessel v's idle time in ballast/laden leg upon receiving service in location i*
$\boldsymbol{fuel_i^{consumption}}$	*Fuel consumption of transporting cargo i*
$\boldsymbol{V_{vi}^{Time}}$	*Duration of the voyage for vessel v transporting cargo i*
$\boldsymbol{Load_i}$	*Loaded LNG amount for cargo i*
$\boldsymbol{Unload_i}$	*Unloaded LNG amount for cargo i*
$\boldsymbol{Inv_{iv}^{ballast/laden}}$	*LNG inventory level in vessel v while going on voyage on ballast/laden leg of cargo i*
$\boldsymbol{Rev_i}$	*Revenue amount generated through selling LNG at demand i*
$\boldsymbol{Exp_i}$	*Cost of buying LNG for demand i*

The objective function and model developed is presented as follows.

$$\begin{aligned} MaxZ = & \sum_{i=1}^{N}(Rev_i - Exp_i) - \sum_{i=1}^{N}\left(FC \times fuel_i^{consumption}\right) \\ & - \sum_{v=1}^{V}\left(cost_v^{shipping} \times u_v\right) \\ & - \sum_{i=1}^{N}\sum_{v=1}^{V}\left(V_{vi}^{Time} + IT_{vi}^{Ballast} + IT_{vi}^{Laden}\right) \times VCost_v \\ & - \sum_{i=2}^{N}(cost_i^{unload} + \sum_{p=1}^{P}(cost_p^{load} \times g_{pi})) \\ & - \sum_{i=1}^{N}\sum_{v=1}^{V}\left(IT_{vi}^{Laden} \times Ci_v^{Laden} + IT_{vi}^{Ballast} \times Ci_v^{ballast}\right) \times FC \end{aligned} \quad (1)$$

The objective function is maximising the profit of each deal by covering the following earning and expense items.

$\boldsymbol{Rev_i - Exp_i}$	*Profit of delivering per cargo i*
$\boldsymbol{FC \times fuel_i^{consumption}}$	*Fuel consumption fee on voyages*
$(\boldsymbol{IT_{vi}^{Laden} \times Ci_v^{Laden} + IT_{vi}^{Ballast} \times Ci_v^{ballast}) \times FC}$	*Fuel consumption fee on idle time*
$(\boldsymbol{cost_v^{shipping} \times u_v) + (V_{vi}^{Time} \times VCost_v)}$	*Fixed and variable cost vessel v per cargo i*
$(\boldsymbol{IT_{vi}^{Ballast} + IT_{vi}^{Laden}) \times VCost_v}$	*Idle cost of the vessel v per cargo i*
$\boldsymbol{cost_i^{unload} + (cost_p^{load} \times g_{pi})}$	*Associated port cost of cargo i*

3.2.3.1 **Constraints**

The mathematical model developed in this study is structured to address the operational and economic complexities of global cryogenic fuel logistics, specifically within the context of LNG shipping. The model incorporates a comprehensive set of constraints, each serving to capture real-world restrictions, logistical rules, and commercial conditions that govern vessel movement, cargo allocation, timing, and resource utilisation. The following provides a detailed explanation of the constraints embedded in the MILP formulation:

$$\sum_{v=1}^{V}\sum_{j=1}^{N} x_{ijv} = 1 \qquad \forall i > 1 \tag{1}$$

$$\sum_{j=1}^{N} x_{1jv} = u_v \qquad \forall v \tag{2}$$

$$\sum_{i=1}^{N} x_{ijv} = \sum_{i=1}^{N} x_{jiv} \qquad \forall v, j \tag{3}$$

$$\sum_{p=1}^{P} g_{pi} = 1 \qquad \forall i > 1 \tag{4}$$

$$\sum_{s=1}^{S} z_{js} = 1 \qquad \forall j \tag{5}$$

$$lt_i \geq Vavail_v^{start} \times \sum_{j=1}^{N} x_{ijv} \qquad \forall i, v \tag{6}$$

$$ut_i \leq Vavail_v^{end} + BigM \times (1 - \sum_{j=1}^{N} x_{ijv}) \qquad \forall i, v \tag{7}$$

$$\sum_{j=1}^{N} x_{ijv} + g_{pi} \leq B_{vp}^{compat-sup} + 1 \qquad \forall v, p, i > 1 \qquad (8)$$

$$\sum_{j=1}^{N} x_{ijv} \leq B_{vi}^{comapt-dem} \qquad \forall v, i > 1 \qquad (9)$$

$$\sum_{p=1}^{P} \left(st_{pi}^{max} * g_{pi}\right) \geq lt_i \qquad \forall i > 1 \qquad (10)$$

$$lt_i \geq \sum_{p=1}^{P} (st_{pi}^{min} * g_{pi}) \qquad \forall i > 1 \qquad (11)$$

$$ut_j \leq vt_j^{tardy} \qquad \forall j \qquad (12)$$

$$ut_j \geq vt_j^{early} \qquad \forall j \qquad (13)$$

$$ut_j + BigM \times \left(2 - g_{pj} - \sum_{i=1}^{N} x_{ijv}\right) \geq lt_j + \sum_{s=1}^{S} \left(D_{pj} \times T_{vs}^{laden} \times z_{js}\right) + ST_{vp}^{load} \qquad \forall v, p, j > 1 \qquad (14)$$

$$atul_j \leq lt_j + BigM \times \left(2 - g_{pj} - \sum_{i=1}^{N} x_{ijv}\right) + \sum_{s=1}^{S} \left(D_{pj} \times T_{vs}^{laden} \times z_{js}\right) + ST_{vp}^{load} \qquad \forall v, p, j > 1 \qquad (15)$$

$$atul_j + BigM \times \left(2 - g_{pj} - \sum_{i=1}^{N} x_{ijv}\right) \geq lt_j + \sum_{s=1}^{S} \left(D_{pj} \times T_{vs}^{laden} \times z_{js}\right) + ST_{vp}^{load} \qquad \forall v, p, j > 1 \qquad (16)$$

$$lt_j + BigM \times (2 - x_{ijv} - g_{pj}) \geq ut_i + \sum_{s=1}^{S} (D_{pi} \times T_{vs}^{ballast} \times z_{is}) + ST_{vi}^{unload} \qquad \forall i > 1, v, p, j > 1 \qquad (17)$$

$$lt_j + BigM \times (2 - x_{1jv} - g_{pj}) \geq ut_1 + \sum_{s=1}^{S} (D_{vp}^{livelocation} \times T_{vs}^{ballast} \times z_{is}) \qquad \forall v, p, j > 1 \qquad (18)$$

$$atl_j + BigM \times (2 - x_{ijv} - g_{pj}) \geq ut_i + \sum_{s=1}^{S} (D_{pi} \times T_{vs}^{ballast} \times z_{is}) + ST_{vi}^{unload} \qquad \forall i > 1, v, p, j > 1 \qquad (19)$$

$$atl_j \leq ut_i + \sum_{s=1}^{S} (D_{pi} \times T_{vs}^{ballast} \times z_{is}) + ST_{vi}^{unload} + BigM \times (2 - x_{ijv} - g_{pj}) \qquad \forall i > 1, v, p, j > 1 \qquad (20)$$

$$atl_j + BigM \times (2 - x_{1jv} - g_{pj}) \geq Vavail_v^{start} + \sum_{s=1}^{S} (D_{vp}^{livelocation} \times T_{vs}^{ballast} \times z_{js}) \qquad \forall v, p, j > 1 \qquad (21)$$

$$atl_j \leq Vavail_v^{start} + \sum_{s=1}^{S} (D_{vp}^{livelocation} \times T_{vs}^{ballast} \times z_{js}) + BigM \times (2 - x_{1jv} - g_{pj}) \qquad \forall v, p, j > 1 \qquad (22)$$

$$IT_{vj}^{Laden} + BigM \times \left(1 - \sum_{i=1}^{N} x_{ijv}\right) \geq ut_j - atul_j \qquad \forall v, j \qquad (23)$$

$$IT_{vi}^{Balalst} + BigM \times \left(1 - x_{ijv}\right) \geq lt_j - atl_j \qquad \forall v, i, j \qquad (24)$$

$$fuel_j^{consumption} + BigM \times \left(2 - x_{ijv} - g_{pj}\right) \geq \sum_{s=1}^{S} [(D_{pi} \times T_{vs}^{ballast} \times C_{vs}^{ballast} \times z_{is}) + (D_{pj} \times T_{vs}^{laden} \times C_{vs}^{laden} \times z_{js})] \qquad \forall i > 1, v, j > 1, p \qquad (25)$$

$$fuel_j^{consumption} + BigM \times \left(2 - x_{1jv} - g_{pj}\right) \geq \sum_{s=1}^{S} [(D_{vp}^{livelocation} \times T_{vs}^{ballast} \times C_{vs}^{ballast} \times z_{1s}) + (D_{pj} \times T_{vs}^{laden} \times C_{vs}^{laden} \times z_{js})] \qquad \forall v, j > 1, p \qquad (26)$$

$$V_{vj}^{Time} + BigM \times \left(2 - x_{ijv} - g_{pj}\right) \geq \sum_{s=1}^{S}[(D_{pi} \times T_{vs}^{ballast} \times z_{is}) + (D_{pj} \times T_{vs}^{laden} \times z_{js})] \quad \forall i > 1, v, j > 1, p \quad (27)$$

$$V_{vj}^{Time} + BigM \times \left(2 - x_{1jv} - g_{pj}\right) \geq \sum_{s=1}^{S}[(D_{vp}^{livelocation} \times T_{vs}^{ballast} \times z_{1s}) + (D_{pj} \times T_{vs}^{laden} \times z_{js})] \quad \forall v, j > 1, p \quad (28)$$

$$ut_i + BigM \times \left(1 - y_{it}^{unload}\right) \geq t - 0.5 \quad \forall i, t \quad (29)$$

$$t + 0.5 + BigM \times \left(1 - y_{it}^{unload}\right) \geq ut_i \quad \forall i, t \quad (30)$$

$$lt_i + BigM \times \left(1 - y_{it}^{load}\right) \geq t - 0.5 \quad \forall i, t \quad (31)$$

$$t + 0.5 + BigM \times \left(1 - y_{it}^{load}\right) \geq lt_i \quad \forall i, t \quad (32)$$

$$Load_i \leq cap_p^{max} + BigM(1 - g_{pi}) \quad \forall i, p \quad (33)$$

$$Load_i \geq \sum_{p=1}^{P}(cap_p^{min} * g_{pi}) \quad \forall i \quad (34)$$

$$Unload_i \leq \sum_{t=1}^{T} Dem_{it}^{total} \times y_{it}^{unload} \quad \forall i \quad (35)$$

$$Unload_i \geq Dem_i^{committed} \quad \forall i \quad (36)$$

$$Inv_{jv}^{laden} \leq Inv_{iv}^{ballast} - ((D_{pi} \times T_{vs}^{ballast} + IT_{vi}^{Balalst}) \times \lambda_v^{ballast} \times S_v \times CV_p) + Load_j + BigM \times \left(3 - x_{ijv} - z_{is} - g_{pj}\right) \quad \forall i > 1, j > 1, v, s, p \quad (37)$$

$$Inv_{jv}^{laden} \leq Inv_{1v}^{ballast} - (D_{pi} \times T_{vs}^{ballast} \times \lambda_v^{ballast} \times S_v \times CV_p) + Load_j + BigM \times \left(3 - x_{1jv} - z_{1s} - g_{pj}\right) \quad \forall j > 1, v, s, p \quad (38)$$

$$Inv_{jv}^{ballast} \leq Inv_{jv}^{laden} - ((D_{pj} \times T_{vs}^{laden} + IT_{vj}^{Laden}) \times \lambda_v^{laden} \times S_v \times CV_p) - Unload_j + BigM \times \left(3 - \sum_{i=1}^{N} x_{ijv} - z_{js} - g_{pj}\right) \quad \forall j > 1, v, s, p \quad (39)$$

$$Inv_{1v}^{ballast} = inv_v^{initial} \quad \forall v \quad (40)$$

$$Inv_{iv}^{laden} \leq (S_v \times LF_v \times CV_p) + BigM(1 - g_{pi}) \quad \forall i, v, p \quad (41)$$

$$Inv_{iv}^{laden} - Load_i + BigM \times (1 - \sum_{j=1}^{N} x_{ijv}) \geq Cap_v^{heelout} \quad \forall i, v \quad (42)$$

$$Exp_i + BigM \times \left(2 - y_{it}^{load} - g_{pi}\right) \geq PB_{pt} \times Load_i \quad \forall i, p, t \quad (43)$$

$$(PS_{it} \times Unload_i) + BigM \times \left(1 - y_{it}^{unload}\right) \geq Rev_i \quad \forall i, t \quad (44)$$

$$\sum_{t=1}^{T} y_{it}^{unload} = 1 \qquad \forall i > 1 \qquad (45)$$

$$\sum_{t=1}^{T} y_{it}^{load} = 1 \qquad \forall i > 1 \qquad (46)$$

Routing and Movement Constraints:

- **Constraint (1)** ensures that each physical location whether a supplier or a customer is visited exactly once. This prevents redundant routing and eliminates the possibility of idle or unnecessary vessel movements. It enforces exclusivity in port visitation, thereby preserving resource efficiency.
- **Constraint (2)** mandates that if a vessel is activated for any operation, it must depart from a designated dummy depot, representing the initial location. This constraint is essential for initiating any route and for establishing a structured sequence of operations.
- **Constraint (3)** enforces routing continuity by requiring that vessels must return from the same node through which they entered. This bidirectional consistency ensures that vessel movement is both logical and traceable and avoids routing ambiguities.

Cargo Allocation and Vessel-Customer Pairing Constraints:

- **Constraint (4)** guarantees that every cargo is linked to a unique supplier. This reflects contractual or logistical realities in the LNG market, where each consignment must be traceable to its source.
- **Constraint (5)** defines the speed level assigned to each cargo voyage. As vessel speed directly impacts fuel consumption and timing, this constraint ensures that the model appropriately captures speed-dependent cost variations and delivery windows.

Temporal Scheduling and Port Compatibility Constraints:

- **Constraints (6) and (7)** govern the scheduling of loading and unloading operations, respectively. These constraints ensure that the commencement of such operations falls within the permissible time windows assigned to each vessel and port.

- **Constraint (8)** enforces compatibility between vessels and loading ports, while **Constraint (9)** applies the same check for unloading ports. These constraints reflect operational limitations such as berth dimensions, vessel draught, and port handling capabilities.
- **Constraints (10) and (11)** impose temporal bounds on loading operations, ensuring they do not exceed the time allotted by the port's schedule both for the earliest and latest time of loading.
- **Constraints (12) and (13)** mirror this logic for unloading operations, ensuring punctuality and being in threshold (early and tardy) of the availability time of the allocated vessel.

Operational Timing and Synchronisation Constraints:

- **Constraint (14)** computes the unloading start time for cargo j, incorporating voyage duration, the loading duration, and port service times.
- **Constraints (15) and (16)** define the arrival time for unloading by using a linearised Big-M approach to handle logical dependencies without introducing non-linearity, thereby preserving computational tractability.
- **Constraints (17) and (18)** calculate the start time for loading cargo j as a function of the previous unloading activity, associated service times, and sailing durations to the new port with considering the live location of the vessel at the start of the journey in constraint (18) as well.
- **Constraints (19) through (22)** establish the arrival time for loading activities by tracing the vessel's journey from its prior operation and synchronising with time window requirements of the loading port which vessel arrival time should be in this allowed threshold.

Idle Time, Fuel Use, and Voyage Duration Constraints:

- **Constraints (23) and (24)** quantify idle periods during both laden (cargo-laden) and ballast (empty return) legs of each voyage. This is critical for estimating time-related costs, such as charter hire, fuel consumption, and operational delays.
- **Constraints (25) and (26)** calculate fuel consumption for each voyage based on vessel characteristics, route length, and selected speed, accounting for both active transit and idle operations.

- **Constraints (27) and (28)** estimate the voyage duration of each cargo when assigned to a particular vessel. This duration is crucial for computing weekly operating costs and aligning vessel schedules with the ADP.

Time Window Satisfaction Constraints:

- **Constraints (29) and (30)** enforce strict adherence to time windows by ensuring that unloading may only occur within a defined weekly interval, represented by the time slot $(t - 0.5, t + 0.5)$.
- **Constraints (31) and (32)** introduce binary auxiliary variable y_{it}^{load}, which take the value of 1 if the loading of cargo i occurs within the prescribed time window $(t - 0.5, t + 0.5)$. This binary encoding facilitates time-based decision-making and simplifies scheduling logic.

Supply, Demand, and Inventory Constraints:

- **Constraints (33) through (36)** ensure that the quantity of LNG loaded and discharged respects both the minimum and maximum operational thresholds. These thresholds reflect the port's supply limits, customer demand capacities, and minimum contractual obligations.
- **Constraint (37)** tracks the evolution of vessel inventory across voyages by updating the remaining quantity after boil-off losses and consumption. **Constraint (38)** addresses the initial inventory in the vessel's first laden leg, taking into account its departure from a live location.
- **Constraint (39)** calculates the boil-off loss during voyage and idle periods based on the vessel's boil-off coefficient and fuel capacity in MMBTU, enabling accurate estimation of fuel losses over time.
- **Constraint (40)** assigns the initial inventory of fuel onboard each vessel, which has been standardised at 4,000 MMBTU at the start of the planning horizon.
- **Constraint (41)** ensures that the total fuel inventory onboard never exceeds the vessel's capacity, which is determined by its load factor and the calorific value of the fuel from the assigned supplier.
- **Constraint (42)** introduces a lower bound on fuel inventory, ensuring that vessels always carry a minimum heel amount to prevent tank warm-up and preserve operational integrity.

Economic and Time-Varying Market Price Constraints:

- **Constraints (43) and (44)** calculate the cost incurred for fuel purchases from suppliers and the revenue earned from sales to customers. These values are adjusted to reflect temporal variations in LNG market prices throughout the planning horizon.

Loading and Unloading Duration Constraints:

- **Constraints (45) and (46)** explicitly define the time durations within which loading and unloading operations must be executed. These constraints are vital for preventing delays and coordinating berth schedules efficiently.

3.2.3.2 Model Summary

The mathematical model developed in this study captures the operational and commercial complexities of a real-world, global cryogenic fuel shipping supply chain. It has been formulated as a MILP model with the primary objective of maximising the company's annual profit under realistic operational constraints.

To ensure that the model accurately reflects the most critical aspects of the industry, the selection of its core parameters was rigorously informed by the foundational Maritime Inventory Routing Problem (MIRP) literature and recent studies on cryogenic logistics. Based on this scholarly consensus, the model integrates the following essential components of the supply chain:

- **Routing and Scheduling:** The model determines the optimal routing and scheduling of a heterogeneous fleet of vessels, considering live locations, vessel speeds, port time windows, and journey durations. As established in maritime logistics literature, integrated routing and scheduling is the primary driver of both cost minimisation and regulatory compliance (Hua, et al., 2024; Budiyanto, et al., 2019; Jokinen, et al., 2015) .

- **Supplier-Customer Pairing:** Each cargo delivery is optimally matched between suppliers and customers, considering factors such as geographical proximity, price volatility, availability, loading and

unloading capacities, and time-sensitive demand requirements. This time-varying market price addresses the shift from rigid, point-to-point LNG contracts to flexible, portfolio-level trading highlighted by recent market analyses (Zhang, et al., 2024; Deshpande, et al., 2022; Rakke, et al., 2015).

- **Fleet Management:** Operational characteristics of each vessel such as fuel consumption, boil-off rates, loading factors, and port compatibility are captured. Vessels operate under realistic contractual and capacity constraints, with provisions for idle time and initial inventories, reflecting the severe operational impacts of fleet heterogeneity widely recognised in the literature (Zhang, et al., 2024; Prasetyo, et al., 2023) .
- **Inventory and Fuel Management:** The model tracks on-board inventory levels throughout the voyage, accounts for boil-off during laden and ballast legs and ensures that a minimum heel level is maintained to avoid re-cooling costs. Managing BOG and heel is universally acknowledged by scholars as the defining, non-negotiable constraint that separates cryogenic shipping from standard bulk routing (Cho, et al., 2018; Mutlu, et al., 2016)
- **Price Considerations:** Fuel prices vary over time, and the model includes idle costs, chartering fees, port charges, and revenue from fuel sales. Constraints have been formulated to capture the economic cost of each operational decision, grounding the optimisation in the realities of market price volatility (Cheng, et al., 2025; Bittante, et al., 2018; Khalilpour & Karimi, 2012)

Overall, the model provides a comprehensive and integrated decision-support tool that captures the real-world interactions and trade-offs inherent in the global LNG and low-carbon fuel shipping context. It can generate optimal or near-optimal plans for routing, scheduling, allocation, and fuel management under high levels of uncertainty and complexity.

3.3 Experimental Results of the MILP Model

This section evaluates the validity and computational performance of the developed MILP model in addressing real-world LNG portfolio optimisation problems. A series of test cases based on empirical data provided by an

industrial partner in the LNG supply chain is analysed, and the resulting outcomes are discussed in the subsequent sections.

3.3.1 **MILP Model Validation**

To validate the proposed MILP model, a series of test cases were designed and implemented using data provided by the industrial partner. These instances reflect operational conditions typically encountered in global cryogenic fuel shipping, particularly within the LNG sector.

The test cases vary in terms of the number of suppliers and customers, vessel speed levels, fleet size, and planning horizon. Each instance focuses on optimising the delivery of LNG from multiple suppliers to customer ports worldwide, through the strategic pairing of cargoes and efficient vessel allocation. The model accounts for procurement from suppliers, each with unique calorific values, limited loading capacities, and specific time windows for loading operations. Once the LNG is loaded, it is transported to designated customers, subject to unloading constraints and port-specific time windows, as summarised in Table 3.4.

Computational experiments were executed on a high-performance workstation equipped with dual Intel Xeon E5-2650 processors and 128 GB of RAM. The CPLEX commercial solver (version 22.1.1) was employed with default settings. Each instance was solved either to optimality (a zero-optimality gap) or until the 9-hour computational time limit was reached, whichever occurred first. This validation process served to demonstrate the model's robustness, practical applicability, and computational tractability under diverse and realistic operating conditions.

3.3.2 **Exact Method Approach-Data**

A range of test instances has been solved using data provided by our industrial partners. However, it should be noted that the parameters and inputs presented in this section represent a scaled, representative subset of the actual data. Due to strict commercial confidentiality constraints regarding the industrial partner's proprietary operations, the full comprehensive dataset cannot be published in its entirety. Nevertheless, the provided subset accurately reflects the complexity of the operational reality. As detailed in Table 3.4, each delivery scenario

specifies strict unloading time windows, with no allowance for delays or missed slots. Furthermore, minimum and maximum LNG discharge limits are defined for each customer, reflecting rigorous contractual obligations and physical operational constraints.

The technical specifications of selected vessels are presented in Table 3.5**,** including each vessel's boil-off rate**,** fuel consumption during idle periods**,** load factor**,** and vessel capacity (in cubic metres)**.** These parameters are critical in modelling both the operational performance and the environmental efficiency of the fleet.

In addition, the shortest distances between all relevant loading and discharging ports are outlined in Table 3.6 and are used as the basis for routing decisions and voyage time estimations.

Table 3.4: Cargo Characteristics

Cargo No.	Destination (Customers)	Unloading Window Start	Unloading Window End	Unloading Volume Min (MMBTU)	Unloading Volume Max (MMBTU)
1	Netherlands	15-Jul 00:00	17-Jul 23:59	3,600,000	3,800,000
2	Spain	20-Jul 00:00	22-Jul 23:59	3,500,000	3,800,000
3	India	13-Jul 00:00	15-Jul 23:59	3,800,000	4,000,000
4	United Kingdom	27-Jul 00:00	29-Jul 23:59	2,800,000	3,000,000
5	Turkey	5-Aug 00:00	7-Aug 23:59	3,600,000	3,800,000
6	Thailand	30-Jul 00:00	1-Aug 23:59	3,600,000	3,800,000
7	Spain	8-Aug 00:00	10-Aug 23:59	3,800,000	4,100,000
8	Taiwan	27-Aug 00:00	29-Aug 23:59	2,800,000	3,000,000
9	Taiwan*	31-Aug 00:00	2-Sep 23:59	3,600,000	3,800,000
10	Italy	20-Aug 00:00	22-Aug 23:59	3,600,000	3,800,000
11	Netherlands	24-Aug 00:00	26-Aug 23:59	2,800,000	3,000,000
12	Netherlands	28-Aug 00:00	30-Aug 23:59	2,800,000	3,000,000
13	Turkey	1-Sep 00:00	3-Sep 23:59	3,600,000	3,800,000
14	Thailand	20-Sep 00:00	22-Sep 23:59	3,600,000	3,800,000
15	United Kingdom	9-Sep 00:00	11-Sep 23:59	3,500,000	3,800,000
16	Kuwait	3-Sep 00:00	5-Sep 23:59	3,500,000	3,800,000
17	Netherlands	17-Sep 00:00	19-Sep 23:59	2,800,000	4,000,000
18	Spain	21-Sep 00:00	23-Sep 23:59	3,500,000	3,800,000
19	Netherlands	25-Sep 00:00	27-Sep 23:59	3,500,000	3,800,000
20	United Kingdom	29-Sep 00:00	1-Oct 23:59	3,500,000	3,800,000
21	Taiwan	28-Sep 00:00	30-Sep 23:59	2,800,000	3,000,000
22	Netherlands	7-Oct 00:00	9-Oct 23:59	3,800,000	4,000,000

23	Spain	11-Oct 00:00	13-Oct 23:59	3,600,000	3,800,000
24	India	10-Oct 00:00	12-Oct 23:59	3,800,000	4,000,000
25	United Kingdom	19-Oct 00:00	21-Oct 23:59	3,600,000	3,800,000
26	India	13-Oct 00:00	15-Oct 23:59	3,600,000	3,800,000
27	Netherlands	27-Oct 00:00	29-Oct 23:59	3,600,000	3,800,000
28	Netherlands	31-Oct 00:00	2-Nov 23:59	3,600,000	3,800,000
29	Turkey	9-Nov 00:00	11-Nov 23:59	3,600,000	3,800,000
30	United Kingdom	13-Nov 00:00	15-Nov 23:59	2,800,000	4,000,000

*Another port in Taiwan

Table 3.5: Vessel Characteristics

Vessel No.	Idle Fuel Consumption (MT/day)	Boil-off Laden (%)	Boil-off Ballast (%)	Capacity(m^3)	Load factor (%)	DWT(MT)
1	15.00	0.085%	0.040%	174,041	99.35	81,898
2	12.60	0.085%	0.041%	174,001	98.50	82,286
3	12.00	0.085%	0.041%	174,253	98.50	82,064
4	17.00	0.080%	0.040%	173,989	98.50	82,064
5	15.00	0.085%	0.040%	174,019	99.35	81,956
6	14.29	0.080%	0.040%	173,900	98.50	78,794
7	15.00	0.065%	0.065%	199,830	98.00	95,039
8	14.29	0.080%	0.040%	174,004	98.50	82,064
9	22.00	0.130%	0.110%	147,895	98.50	71,835
10	30.00	0.150%	0.110%	145,958	98.50	74,535
11	7.80	0.080%	0.080%	177,377	98.50	78,578
12	15.00	0.085%	0.040%	174,041	99.35	82,286
13	15.00	0.085%	0.040%	174,041	99.35	81,898
14	12.60	0.085%	0.041%	174,001	98.50	82,286
15	12.00	0.085%	0.041%	174,253	98.50	82,064

Table 3.6: Distance between ports (nautical mile)

Distance (nautical mile)	1st Supplier	2nd Supplier	3rd Supplier	4th Supplier	5th Supplier
Netherlands	4,958	5,104	5,822	9,330	4,411
Spain	5,232	5,378	4,127	7,635	3,832
India	9,703	9,850	789	3,749	7,116
United Kingdom	4,880	5,026	5,739	9,247	4,333

Turkey	6,340	6,486	3,121	6,629	4,940
Thailand	12044	12,123	3,835	2,365	8,714
Taiwan	10,353	10,432	4,792	2,829	9,528
Taiwan*	10,454	10,533	4,707	2,739	9,446
Italy	6,369	6,516	3,825	7,333	4,969
Kuwait	9,914	10,061	776	4,969	7,552

3.3.3 **Real World Case Studies**

To demonstrate the practical applicability of the proposed model, the primary case study investigates the annual delivery program of one of the world's largest integrated commercial LNG distributors. The scale of this operation encompasses the global transportation of approximately 480 million MMBTU of LNG, representing a total portfolio revenue approaching 4 billion USD. Geographically, the logistical network spans a highly complex multi-continental routing system, linking major LNG supplier terminals across four continents to a diverse customer base distributed throughout European and Asian markets. The size and complexity of each test instance, along with the corresponding number of variables and constraints, are summarised in Table 3.7. Although the mathematical model is structured around 46 core categories of constraints, the application of these constraints across multiple indexed dimensions leads to a substantial increase in the total number of constraints and variables. This combinatorial expansion highlights the intricate and high-resolution nature of the problem formulation.

As the number of cargoes or other key parameters increases, such as the number of vessels, suppliers, or planning periods, the model scales non-linearly resulting in an exponential growth in both variables and constraints (see Table 3.7). In this context, S, D, V, SL, and T represent the number of suppliers, customers, vessels, speed levels, and time periods (weeks), respectively. It is worth mentioning that, to assess the impact of speed on portfolio optimisation and vessel rating under the CII regulation, vessel speed was discretised into three representative levels: 14 knots (slow steaming, SL = 1), 16 knots (medium speed, SL = 2), and 18 knots (higher speed, SL = 3). While vessel speed is physically a continuous variable with a non-linear relationship to fuel consumption, incorporating continuous speed directly into the routing formulation would create a Mixed-Integer Non-Linear

Programming (MINLP) problem, rendering the model computationally intractable for large-scale operations. By discretising speed, the model successfully captures the macro-level trade-offs between voyage duration, fuel consumption, and emissions without compromising computational efficiency. While this simplification restricts the solution space to bounded speed profiles rather than infinite continuous variations, it provides a sufficiently granular and realistic approximation of standard maritime operating profiles, ensuring that optimal routing and strategic emissions outcomes remain robust.

The exact optimisation approach developed in this study successfully handled problem instances involving up to 30 cargoes, 5 suppliers, and 15 vessels, over a 35-week planning horizon, incorporating all three speed levels. The results for the first 20 solvable instances are reported in Table 3.8, with the problem size given in the second column. The subsequent columns present the disaggregated costs and resulting profit, while the final columns indicate the total CPU time required and the optimality gap attained at termination.

Table 3.7: Size of instances

Example No.	Example Size (S, C, V, SL, T)	No of Binary Variables	No of Continuous Variables	No of Constraints
1	(1,2,20,1-2-3,6)	313	826	2,059
2	(3,5,6,2,20)	527	658	5,318
3	(3,5,6,2-3,20)	533	658	5,648
4	(4,8,9,2,25)	1,319	1,657	20,806
5	(4,8,9,3,25)	1,319	1,657	20,806
6	(3,9,10,1-2-3,22)	1,615	2,130	27,450
7	(4,9,10,2,26)	1,685	2,130	28,039
8	(4,10,9,3,25)	1,807	2,221	30,432
9	(4,11,10,2,26)	2,259	2,794	39,699
10	(4,12,10,2,26)	2,576	3,156	46,279
11	(5,12,10,2,26)	2,589	3,156	56,709
12	(5,13,10,2,26)	2,927	3,538	65,436
13	(5,14,10,2,26)	3,285	3,940	74,783
14	(5,15,10,2,26)	3,663	4,362	84,750
15	(5,20,12,2,30)	6,947	8,074	172,341
16	(5,25,15,2,35)	12,526	14,362	326,525

Example No.	Example Size (S, C, V, SL, T)	No of Binary Variables	No of Continuous Variables	No of Constraints
17	(5,25,15,2-3,35)	12,552	14,362	377,150
18	(5,25,20,3,30)	15,781	19,042	430,890
19	(5,30,15,2,35)	17,256	19,447	461,485
20	(5,30,15,1-2-3,35)	17,318	19,447	605,485

All instances were solved either within a 9-hour time limit or until a zero-optimality gap was reached, using the CPLEX commercial solver (version 22.1.1) under its default settings. The results of these computational experiments are summarised in Table 3.8, which presents a detailed breakdown of the financial and operational performance of each example.

The "Revenue minus Expenditure" column reflects the profit obtained from selling LNG, taking into account the associated costs of buying it from suppliers. The shipping cost category includes both the fixed cost of chartering a vessel and the weekly operational costs incurred throughout the voyage. The fuel cost accounts for the fuel consumed both during sailing and while the vessel is idle. Correspondingly, the idle cost captures the expense incurred during periods when vessels are not in operation but remain available within the planning horizon.

The port cost reflects the expenditure linked to loading and unloading activities at respective ports. The net profit column indicates the overall profit after deducting all associated costs. The number of active vessels represents how many from the available fleet were utilised in the solution of the corresponding instance, as indicated by the fleet size in the "Example Size" column.

The CPU time column reports the total computational time required to reach a solution. If the optimality gap reaches zero before the 9-hour time limit, the reported time is the actual solving time. Otherwise, the CPU time is capped at 9 hours, and a non-zero optimality gap is reported.

In total, 20 problem instances were solved, and the results detailing cost components, profit, and computational performance are presented in Table 3.8.

Table 3.8: Experimental Result of Exact Method

No.	Example Size (S, C, V, SL, T)	Revenue – Expenditure ($)	Shipping Cost ($)	Fuel Cost ($)	Idle Cost ($)	Port Cost ($)	Net Profit ($)	Active Vessels	CPU time	GAP%
1	(1,2,20,1-2-3,6)	58,778,476	13,396,991	874,815	1,603,009	649,157	42,254,504	2	1.57s	0
2	(3,5,6,2,20)	162,398,255	33,868,449	2,577,008	6,567,728	1,876,727	117,508,344	4	2.5s	0
3	(3,5,6,2-3,20)	162,528,480	32,111,900	2,750,948	8,138,100	1,876,727	117,650,805	4	2.9s	0
4	(4,8,9,2,25)	237,021,534	64,342,726	6,256,895	21,492,643	2,854,055	142,075,215	7	5.6s	0
5	(4,8,9,3,25)	243,666,910	56,119,367	6,039,676	25,592,911	2,917,973	152,996,982	7	14s	0
6	(3,9,10,1-2-3,22)	277,241,592	64,818,873	6,418,272	26,643,406	3,223,210	176,137,830	7	9h	28.41
7	(4,9,10,2,26)	270,716,097	70,094,016	7,923,623	25,460,111	3,159,292	165,019,115	7	23s	0
8	(4,10,9,3,25)	303,497,920	66,814,391	7,660,976	32,897,888	3,639,353	192,485,312	7	261s	0
9	(4,11,10,2,26)	332,714,993	82,779,535	8,590,710	27,326,668	3,904,715	210,113,365	7	281s	0
10	(4,12,10,2,26)	354,604,775	89,757,393	9,266,910	38,222,515	4,233,996	213,123,961	8	3h 40 m	0
11	(5,12,10,2,26)	354,604,775	89,757,393	9,266,910	38,222,515	4,233,996	213,123,961	8	9h	17.40
12	(5,13,10,2,26)	380,627,807	99,246,476	11,292,701	31,602,302	5,265,814	233,220,514	8	9h	29.08
13	(5,14,10,2,26)	411,056,835	99,004,768	10,669,301	44,798,050	4,874,280	251,710,437	8	9h	31.39
14	(5,15,10,2,26)	444,941,337	105,397,984	11,499,932	47,540,915	5,513,565	274,988,941	8	9h	36.14
15	(5,20,12,2,30)	603,612,900	130,343,901	14,516,523	64,781,841	8,633,692	385,336,943	9	9h	52.42
16	(5,25,15,2,35)	742,902,897	185,226,813	24,631,938	35,860,371	12,538,348	484,645,426	9	9h	60.91
17	(5,25,15,2-3,35)	755,951,291	155,679,400	18,168,152	47,697,224	11,661,783	522,744,731	8	9h	64.39
18	(5,25,20,3,30)	758,640,501	148,869,794	20,065,278	77,131,830	9,232,789	503,340,810	9	9h	71.41
19	(5,30,15,2,35)	910,182,821	193,883,956	22,836,935	77,738,886	12,765,840	602,957,205	9	9h	64.35
20	(5,30,15,1-2-3,35)	909,612,703	216,778,729	29,407,753	94,398,318	15,102,158	553,925,745	12	9h	91.31

As illustrated in Table 3.8, an increase in the number of cargoes correlates directly with an extended computational time for solving the problem. In smaller instances such as those involving up to 12 cargoes and four suppliers the model demonstrates a high level of computational efficiency, reaching a zero-optimality gap in a relatively short period. However, as the problem size expands through the inclusion of more cargoes,

suppliers, or vessels, the solver is required to handle a substantially larger set of constraints and decision variables, leading to an exponential increase in computational complexity.

Furthermore, the complexity of the model is significantly amplified with the introduction of multiple speed levels. This is clear in Example 6, where despite a modest number of cargoes, the solver required the full 9-hour time allowance to reach a better solution, ultimately achieving a gap of 28.41%. This highlights the computational burden introduced by additional speed configurations, which expand the decision space and create more routing and scheduling permutations.

The influence of speed levels is also apparent when comparing second and third Examples, which are structurally identical except for the inclusion of a second speed level. In second Example, the model is restricted to a single speed of 16 knots, whereas in third Example, an additional speed of 18 knots is permitted. The outcome demonstrates that the inclusion of the second speed option leads to a higher overall profit, thereby confirming the model's ability to optimise routing and scheduling more effectively when allowed greater flexibility in operational speeds.

Interestingly, although the third example shows increased idle time for vessels, the total shipping and idle costs are lower than in scenarios constrained to a single speed level (2^{nd} example). This is because the model leverages higher speeds to reduce overall voyage durations and enhance cargo pairing strategies. The effect of these changes is also visible in the fuel consumption and boil-off rates, which vary depending on whether the vessel is operating on a laden or ballast leg. These dynamics contribute to reduced operational costs and ultimately enhanced profitability, despite the increased computational effort required.

This analysis reinforces the importance of balancing model flexibility with computational tractability, particularly when incorporating real-world operational complexities such as multiple speed levels and heterogeneous fleet characteristics.

3.3.4 **Optimality Progress of the MILP Model**

The optimality progress graph was generated for the 30-cargo instance with a single speed level (Example 19). As illustrated in Figure 3.3, a clear trend emerges in which an increasing number of iterations corresponds to a

decreasing optimality gap and an overall enhancement in solution quality. Although convergence is gradual, the model achieves a substantial reduction in the optimality gap, reaching approximately 64% after around 42 million iterations.

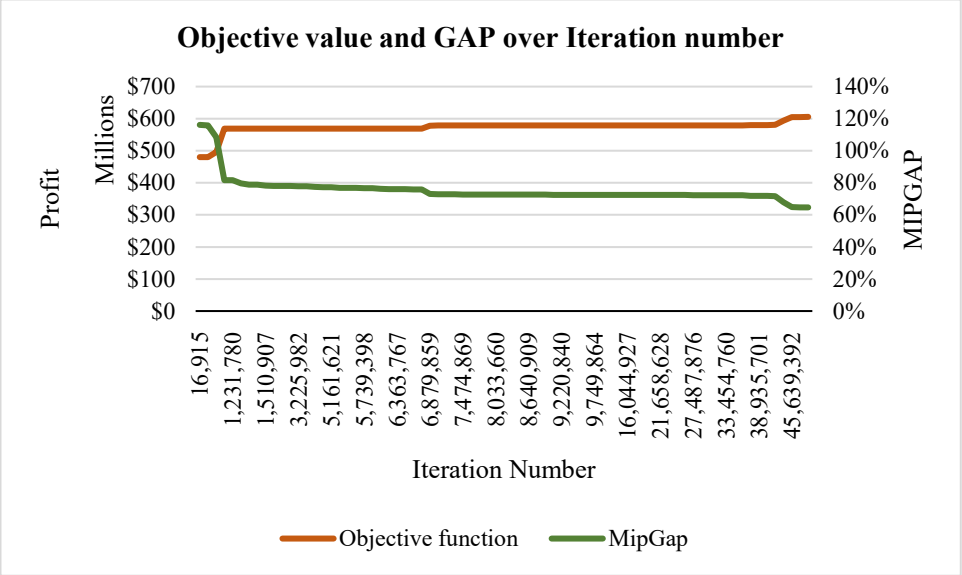

Figure 3.2:Optimality graph over Iteration No for example (5, 30, 15, 2, 35)

A comparable pattern is observed when progress is examined with respect to computational time, as shown in Figure 3.3. After the designated nine-hour runtime, the model obtains a solution yielding an estimated profit of approximately $605 million. This represents an improvement of around $129 million in comparison to the first feasible solution, which stood at $476 million. While the final solution retains a non-zero gap, these results underscore the model's capacity to generate significantly improved outcomes over time, even in complex, large-scale scenarios, within practical computational limits.

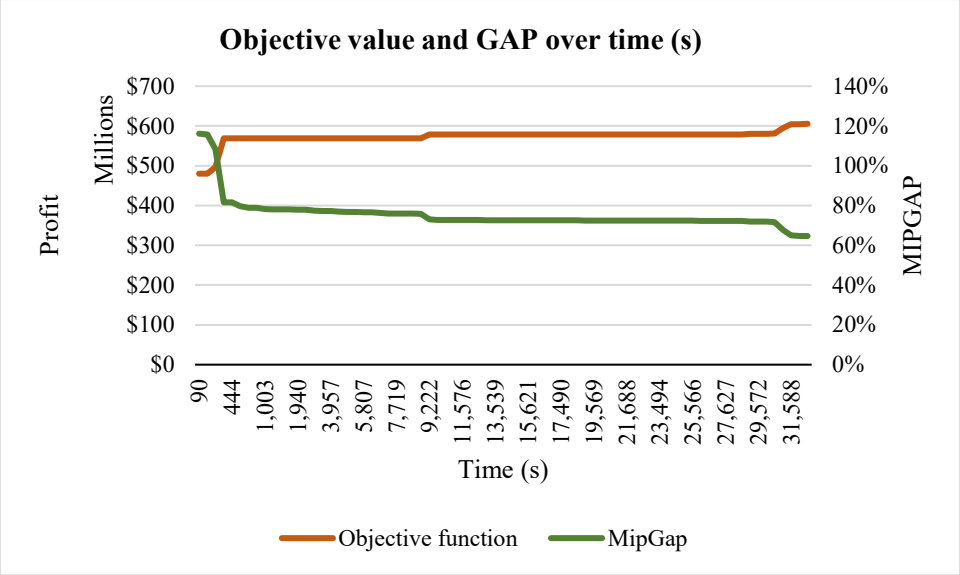

Figure 3.3: Optimality graph over time for example (5, 30, 15, 2, 35)

3.4 Genetic-Based Metaheuristic Algorithm (GBMHA)

The optimisation problem under investigation has been formulated as a MILP model. Despite substantial effort to linearise the numerous initial non-linear expressions, the problem remains inherently complex and is classified as NP-hard (Zhang, et al., 2021). In combinatorial optimisation, an NP-hard classification indicates that no known algorithm can guarantee an exact optimal solution in polynomial time. Consequently, as the size of the problem increases (such as adding more vessels, delivery nodes, or discrete speed) the computational time required to solve the MILP grows exponentially, rendering exact methods impractical for large-scale, real-world delivery scenarios. As such, obtaining an exact global optimum within a practical timeframe is often infeasible, particularly for large-scale, real-world industrial cases where time and computational resources are limited.

In this context, the pursuit of high-quality approximate solutions becomes both necessary and justifiable. Even the attainment of a locally optimal solution holds significant value in industrial settings, where real-world constraints and uncertainties exist. To this end, a metaheuristic algorithm tailored to the specific characteristics of the problem has been developed.

The most prominent and widely adopted metaheuristic techniques in the optimisation domain is the Genetic Algorithm (GA). Rooted in the principles of natural selection, GA belongs to the broader class of Evolutionary Algorithms (EAs) and is particularly effective for solving complex optimisation and search problems. Its core operators are selection, crossover, and mutation which inspired by biological evolution and are used to iteratively improve solution quality over successive generations (Mitchell, 1998).

In this research, a genetic-based solution methodology is proposed due to the structural characteristics and complexity of the LNG portfolio optimisation problem. The key decision variables such as supplier–customer pairing, vessel routing, fleet allocation, and discrete speed levels are inherently discrete and combinatorial in nature. Genetic Algorithms (GA) are particularly well suited to such problems, as they allow these decision variables to be naturally encoded within a chromosome structure, preserving the integrity of the solution throughout the optimisation process.

In addition, the problem involves a large and complex search space with multiple interacting constraints, making exact optimisation approaches computationally challenging for large-scale instances. The GA provides an efficient way to explore this search space and identify high-quality near-optimal solutions within a reasonable computational time.

While alternative metaheuristic approaches, such as Particle Swarm Optimisation (PSO), could also be considered, they are generally more suited to continuous optimisation problems and require additional adaptations to handle discrete decision structures. In contrast, the GA offers a more direct and flexible framework for representing and solving the combinatorial aspects of the problem.

Therefore, the genetic-based approach provides a suitable balance between solution quality, computational efficiency, and the ability to handle the structural complexity of the LNG portfolio optimisation problem.

large-scale scenarios.

3.4.1 **Solution Structure**

As previously discussed, a feasible solution to the proposed MILP model must integrate cargo pairing, vessel scheduling, and routing, while strictly adhering to all operational and temporal constraints to avoid any form of violation. To effectively capture the complexity of this integrated problem within the metaheuristic framework, the chromosome structure which encodes a complete solution has been partitioned into three distinct sub-chromosomes, each corresponding to a critical component of the problem.

To initialise potential solutions within the GA, a permutation-based encoding approach is employed, whereby random permutations of integers are generated to represent structured solutions. This encoding ensures flexibility in capturing the combinatorial nature of the problem while preserving feasibility in early generations.

The first sub-chromosome, referred to as the pairing string, encodes the supplier–customer pairing scheme. This sub-chromosome consists of a permutation of the integers from 1 to N+M, where N and M denote the total number of customers and suppliers, respectively. Within this representation, integers from 1 to N correspond to customer nodes, while integers from N+1 to N+M represent supplier nodes. For enhanced visual clarity and interpretability, customer genes are graphically depicted in white, whereas supplier genes are shown in grey.

Pairing:	1	2	N+1	…	N-2	N+M-1	N-1	N	N+M

The example provided above illustrates the structure of the pairing sub-chromosome. In this illustration, the first two genes represent customers 1 and 2, while the third gene correspond to supplier 1, i.e. customer index N+1, where N is the number of customers. The interpretation rule for this sub-chromosome is that each customer is paired with the next immediate supplier that follows it in the sequence. Thus, in the given example, customers 1 and 2 are paired with first supplier. Similarly, customer N−2 is paired with supplier M−1, and customers N−1 and N are both paired with supplier M. This pairing strategy allows for flexibility while maintaining the structural integrity of supplier–customer matching. As noted earlier, for visual clarity, customer genes are represented in white, and supplier genes in grey.

The second sub-chromosome, referred to as the routing string, follows a similar encoding principle but serves a different functional purpose. Whereas the first sub-chromosome determines supplier–customer pairings, the routing string specifies the cargo-to-vessel routing assignments. This string comprises a permutation of integers from 1 to N+ V, where N represents the number of cargoes and V denotes the number of vessels. In this representation, the first N integers correspond to cargoes, and the integers greater than N denote vessels.

The interpretation rules here mirrors that of the pairing string: each cargo is assigned to the next immediate vessel in the sequence. For instance, if cargo 3 is followed by vessel 12 in the chromosome, then cargo 3 is routed using vessel 12. This structure not only simplifies the routing logic but also enhances the computational efficiency of the Genetic Algorithm during crossover and mutation operations. Again, for clarity, cargo genes are visually encoded in white, while vessel genes appear in grey.

Routing:	1	2	N+1	…	N-3	N-2	N-1	N	N+V

The example presented above illustrates the structure of the routing sub-chromosome. In this instance, cargoes numbered 1 and 2 are served by the first vessel (represented by gene N+1) based on their position in the sequence. Likewise, cargoes N-3, N-2, N-1, and N are served by the vessel identified in gene N+V, again maintaining the precise order in which they appear within the sub-chromosome. This ordering ensures that vessel assignment respects the sequence defined by the permutation, thus facilitating a feasible and interpretable cargo–vessel routing scheme.

The final sub-chromosome, referred to as the speed string, completes the chromosome structure by encoding the vessel-speed allocation. This sub-chromosome consists of a permutation of integers where values from 1 to N represent the cargoes, and values from N+1 to N+S correspond to the speed levels assigned to the vessels, with S denoting the number of distinct speed levels available. The purpose of this sub-chromosome is to assign an operational speed level to each vessel for each cargo delivery leg, thereby influencing fuel consumption, boil-off rates, and ultimately, the overall profitability of the delivery programme.

For clarity and visual interpretation, cargo genes in this sub-chromosome are depicted in white, while speed genes are shown in grey.

Speed:	1	2	N+1	…	N-2	N+S-1	N-1	N	N+S

The example illustrated in the row above demonstrates the structure of the speed sub-chromosome. In this case, cargoes 1 and 2 are transported using the vessel speed indicated by gene N+1, whereas cargoes N−1 and N are transported at the speed specified by gene N+S. Each speed gene thereby governs the operational velocity for the associated set of cargoes, affecting voyage duration, fuel consumption, and boil-off rate, key factors in overall cost and profit calculations.

This chromosome structure encapsulates the three fundamental components of the proposed solution: cargo pairing**,** vessel routing, and speed allocation. Collectively, these elements establish the framework for an integrated, feasible solution to the problem. The interdependencies among these sub-chromosomes are crucial for generating high-quality solutions, as will be demonstrated in the integrated example provided below.

Pairing:	1	2	N+1	…	N-2	N+M-1	N-1	N	N+M
Routing:	1	2	N+1	…	N-3	N-2	N-1	N	N+V
Speed:	1	2	N+1	…	N-2	N+S-1	N-1	N	N+S

An integrated solution inherently contains sufficient information to determine the pairing between customers and suppliers, the allocation and routing of vessels across the fleet, as well as the speed levels at which each cargo is to be transported. However, the direct application of standard permutation-based operators from GAs on such integrated chromosomes does not ensure the feasibility of the resulting solutions. This is primarily due to the complex operational constraints, such as limitations on loading and unloading quantities and strict adherence to time window boundaries.

To address this challenge and to improve the overall quality of the population, rather than relying solely on purely random chromosomes which are highly unlikely to satisfy feasibility requirements, several compatibility checks and guiding mechanisms have been embedded within the algorithm. These tailored methods serve both to filter infeasible solutions and to steer the evolutionary process towards the feasible region of the solution space. The specific details of these mechanisms are presented in the following sections.

3.4.2 Three-Dimensional Compatibility Check and Intelligent Initialisation

To prevent the algorithm from being burdened with excessive complexity and to reduce the need for extensive feasibility checks during the early stages, the initial population is not generated in a purely random manner. Instead, a set of well-defined rules and compatibility criteria are introduced and applied from the outset to construct a more intelligent and structured initial population. These preliminary mechanisms aim to guide the algorithm towards promising regions of the solution space while preserving a manageable computational effort. The specific conditions and criteria used for generating feasible initial solutions, in accordance with the predefined chromosome structure, are outlined below. Only if all these conditions are satisfied is an initial solution admitted into the population pool. The pseudocode of the first algorithm is provided in Algorithm 3.1. The algorithm consists of eight sequential steps that must be evaluated initially in order to generate a feasible supplier–customer–vessel compatibility matrix. Each step of the algorithm is described in detail below.

Step 1 and 2: Vessel compatibility assessment ensures that the selected vessel is operable at both the loading and unloading ports, preventing infeasible port assignments.

Step 3 and 4: Capacity Evaluation checks that the vessel can carry the required amount of LNG, accounting for:

- The minimum demand committed from the customer.
- The boil-off loss was incurred during transit.
- The heel amount, which is the minimum retained fuel to maintain safe vessel operations during the ballast leg.

Step 5: Timing Considerations verify that the planned loading and delivery fall within the prescribed time windows, considering the earliest supplier loading time and travel duration.

Step 6: Initial Journey Availability assesses whether the vessel is available early enough to complete the journey to the supplier within the loading window.

Step 7: Unloading Verification ensures the unloading operation is feasible within the vessel's operational schedule, considering both the unloading time and vessel availability.

Step 8: return feasible compatibility matrix

Algorithm 3.1: Pseudocode of Three-Dimensional Compatibility-Check algorithm

Input:

$S = \{s_1, s_2, \ldots, s_m\}$: set of suppliers $V = \{v_1, v_2, \ldots, v_n\}$: set of vessels $C = \{c_1, c_2, \ldots, c_p\}$: set of customers

Output:

Filtered 3D compatibility matrix $M'_{svc} \subseteq M_{svc}$, where only feasible(s, v, c) combinations remain.

Step1: Construct initial compatibility matrix

$$M_{svc} = \begin{cases} 1 & \text{if } s \in S, v \in V, c \in C \text{are mutually compatible} \\ 0 & \text{otherwise} \end{cases}$$

Step2: Identify compatible supplier-customer pairs

$$P_{sc} = \{(s, c) | \exists v \in V \rightarrow M_{svc} = 1\}$$

Step3: Compute minimum required transportation capacity

For each compatible cargo (compatible supplier-customer) $(s, c) \in P_{sc}$:

$$Q_{min}(s, c) = Dem_c^{committed} + B_{ballast}(s, c) + B_{Laden}(s, c) + Cap_v^{heel}$$

Where: $B_{ballast\,/Laden}$: boil- off gas loss (ballast & laden legs)

Step4: Prune supplier-customer incompatibilities

Remove any (s, c) where supplier capacity $Q_s < Q_{min}(s, c)$:

$$P_{sc} := P_{sc} \backslash \{(s, c) | Q_s < Q_{min}(s, c)\}$$

Step5: Prune vessel-cargo incompatibilities

For each vessel $v \in V$:

If $Q_v < Q_{min}(s, c)$, set $M_{svc} = 0$

Step6: Apply temporal feasibility filters

For each feasible cargo (s, c):

- Compute earliest arrival time: $atul_{(s-c)} = st^{min}(s) + T_{(s-c)}^{laden}$
- If $atul_{(s-c)} \notin [vt_c^{early}, vt_c^{tardy}]$

  Remove (s, c) from P_{sc}& set $M_{svc} = 0$

Step7: Vessel availability constraints:

If $Vavail_v^{start} > st^{min}(s)$ or $Vavail_v^{end} < atul_{(s-c)}$

Remove vessel v from M_{svc}

Step8: Return feasible compatibility matrix:

$$M'_{svc} = \{(s, v, c) | M_{svc} = 1\}$$

By implementing these eight steps in advance, the likelihood of generating infeasible solutions is significantly reduced, thereby improving both the quality of the initial population and the overall computational efficiency of the algorithm. This is primarily achieved by replacing the purely random initialisation strategy with a more intelligent, compatibility-informed weighted initialisation. In this approach, feasible pairings and assignments are not only verified against the core constraints but also ranked based on their relative desirability or fitness.

The compatibility checks outlined in Algorithm 3.1 serve as a pre-filtering mechanism, and the solutions that pass these checks will go through second method (Algorithm 3.2). In this algorithm scores are subsequently used to calculate probabilistic weights that guide the selection process during chromosome generation. As a

result, higher-ranking (i.e., more promising or cost-effective) combinations are given a greater probability of being selected, while still maintaining a degree of diversity in the initial population. The Algorithm 3.2 details the ranking criteria and how these weights are incorporated into the chromosome construction process.

Algorithm 3.2: Intelligent Initialisation

Input: P_{sc}: set of viable unallocated pairings (supplier, customer), V (set of vessels),
$A_{i,v} = 1 \Leftrightarrow$ vessel v compatible with cargo$i$ (s_i, c_i),
For cargo$i$, the number of compatible vessels: $v_i = \sum_{v=1}^{n} A_{i,v}$
Output: Initial population of (pairing, routing, speed) chromosomes

While there exist, unallocated customers do ($\sum_{j \in P} w_j = 0$):

Step1: cargo weight and cargo selection probabilities

For each cargo $i \in P_{sc}$calculate: $w_i = \frac{1}{v_i}$ $(v_i \geq 1)$ and $p_i = \frac{w_i}{\sum_{j \in P} w_j}$

Pick i^* with probability p_{i^*} : $i^* \sim Categorial(p_i)_{i \in P}$

Step2: vessel weights and conditional vessel selection

Given a selected cargo i^*, let the set of vessels compatible with it be: $V_{i^*} = \{v: A_{i^*,v} = 1\}$

Define each vessel's weight (based on the current cargo weight it can serve):

$$W_v = \sum_{j \in P} A_{j,v} w_j \quad \text{for } v \in V_{i^*}$$

Conditional probability of choosing vessel $v$given cargoi^*:$Pr(V = v|i^*) = \frac{W_v}{\sum_{v \in V_{i^*}} W_v}$ $v \in V_{i^*}$

Select vessel:

$$v^* \sim Categorical(Pr(V = v|i^*))_{v \in V_{i^*}}$$

Step 3: Allocation and update rules (Zero-out customers)

Suppose the chosen cargo i^*has customer c^*, zero the weight of all cargos with customer c^*.

$$j \in P_{c^*}: \text{set } w_j \leftarrow 0$$

Remove allocated customers from P_{sc}

Recompute any dependent quantities: $W_v \leftarrow \sum_{j \in P} A_{j,v} w_j, p_j \leftarrow \frac{w_j}{\sum_{k \in P} w_k}$

For $v \in V$: sort allocated cargoes by customer time window $\Rightarrow O_v = (i_1, i_2, \ldots, i_{k_v})$

So far, both routing and pairing sub-chromosomes are populated. Randomly generated speed levels are used next to construct the speed sub-chromosome.

With this developed algorithm (Algorithm 3.2), Vessels with higher weights are deprioritised in the early stages of selection in order to reserve them for later assignments where flexibility is more constrained and their compatibility is critical.

3.4.3 **Feasibility Steps**

The design of the solution structure must prioritise the generation of feasible solutions. Due to the inherent complexity of the problem and the multitude of interdependent constraints, purely random initial solutions are highly unlikely to satisfy all requirements, even when guided by the predefined compatibility and weighted

initialisation via ranking algorithms. Therefore, to more effectively steer the algorithm towards the feasible regions of the solution space, we propose a series of feasibility enforcement steps. These steps are intended to strengthen the feasibility of the generated solutions by enforcing two principal categories of constraints:

A) Supply, Demand, and Vessel Availability Time Windows

- Ensuring synchronisation between supplier loading schedules, customer unloading windows, and vessel availability periods.
- The alignment of these time windows is critical to guarantee that vessels can perform operations within the permitted timeframes without incurring delays or violations.

Algorithm 3.3: Pseudocode of the Re-Scheduling algorithm

Input: Vessel tour $O_v = (i_1, i_2, \ldots, i_{k_v})$ and Permissible time window of cargo$i$ $[a_i, b_i]$
Output: Improved schedule or infeasible flag
For $v \in V$:
    Compute arrival time ⇒ t_i=$ArrivalTime(i, O_v)$
    Compute tardiness⇒ $tardi_i = max(0, t_i - b_i)$
Compute $TTF = \sum_i tardi_i$
Sort cargos in descending order of $tardi_i$
While ∃cargo i with $tardi_i > 0$ do:
    Select cargo with highest tardiness: Let $i^* = argmax_i(tardi_i)$
    Let v^* be the vessel currently serving i^*
    Let O_{v^*}be the current tour of v^*
    For each feasible position k in O_{v^*}:
        Recompute t_{i^*}if moved to position k
        Attempt intra-vessel shift
        If $t_{i^*} \in [a_{i^*}, b_{i^*}]$:
            Evaluate TTF_{new}
            If $TTF_{new} < TTF$
                Perform move
                $TTF = TTF_{new}$
                Go to the beginning of the while loop
        Elif
            Attempt inter-vessel reassignment
            Let $V_{comp_{i*}} = \{v \in V: v \neq v^*\}$and $v$is compatible with cargo i^*
            For $v \in V_{comp_{i*}}$:
                Append $i^*$to O_v
                Recompute arrival times on v, and TTF_{new}
                If $TTF_{new} < TTF$
                Remove i^* from O_{v^*}& assign to v
                $TTF = TTF_{new}$
                Go to the beginning of the while loop
        Else
            Undo assignment
            Mark solution infeasible

Exit Algorithm
End while
Return final Schedule

B) Inventory Balancing

- Considering supplier and vessel capacities, minimum and maximum customer demand, and additional operational considerations such as boil-off during transit and heel-on-board requirements post-discharge.
- This ensures that the amount of LNG loaded is not only sufficient to meet demand but also feasible in terms of what each vessel and supplier can handle.

Algorithm 3.4: Pseudocode of the Inventory Balancing algorithm

Input:
For $v \in V$: $O_v$of allocated cargos ; For v: Q_v, $Cap_v^{heelout}$, $B_{i_{O_v}}^{ballast}$, $B_{i_{O_v}}^{laden}$
Output: Updated load quantities for each cargo i in O_v
For $v \in V$:
Compute inventory &surplus variables as per the following:
$inv_{iv}^{laden-end} = inv_{iv}^{start-laden} - B_{iv}^{laden}$
$inv_{iv}^{start-ballast} = inv_{iv}^{laden-end} - unload_{iv}$
$inv_{iv}^{ballast-end} = inv_{iv}^{start-ballast} - B_{iv}^{ballast}$
$inv_{jv}^{start-laden} = inv_{iv}^{ballast-end} + load_{jv} \mid j$ comes right after i in O_v
$Surplus_{iv} = inv_{iv}^{ballast-end} - Cap_v^{heelout}$
Determine all viable subtours of O_v:
A subtour S is viable if:
a) S ends where $O_v$ends, and
b) $MS_v > 0$ (Minimum surplus amount of LNG in subtour$S$among cargos)
Identify the Longest Viable Subtour (LVS_v)
While $LVS_v \neq \emptyset$:⇒ (There is no cargo left in in the LVS_v)
Identify the most expensive customer $j \in LVS_v$&
Increase cargo$j$'s loaded amount by MS_v
Update:
Impacted inventory variables, $Surplus_{iv}$, S, LVS_v
End while
End For
Return Updated load plan for all vessels.

Together, these feasibility steps contribute to an intelligent initialisation process designed to enhance the quality of the initial population. They play a key role in handling the complexity of loading and unloading

schedules, as well as the corresponding fuel quantities, thereby significantly improving the likelihood of generating feasible solutions from the outset.

Algorithm 3.3 and Algorithm 3.4 outlines the steps undertaken to guide the GA solution toward feasibility by addressing critical operational constraints, including time windows, inventory balancing, and cost-effective fuel allocation. By following these steps, the algorithm computes all relevant costs and revenues, thereby deriving the objective function value for each chromosome in the population. These include:

- Revenue from selling LNG,
- Cost of buying LNG,
- Shipping costs (fixed and daily),
- Fuel consumption during sailing and idle periods,
- Port handling charges,
- Penalties from unallocated cargoes (if any).

This computed objective function serves as the fitness value of the chromosome.

3.4.4 **Fitness Evaluation**

During the fitness evaluation phase, each member of the generated population is assessed in accordance with the objective function defined in previous section. This function encapsulates the total profitability of each solution by incorporating revenues, operational costs, and penalties associated with infeasibility. The population size represents a critical parameter, as it directly influences both the diversity of the search space and the algorithm's capacity to explore and exploit potential solutions effectively.

Following the evaluation, individuals are ranked in descending order based on their fitness values, thereby prioritising solutions that yield higher profitability. This ordered ranking serves as the foundation for the subsequent selection procedures, ensuring that superior individuals are more likely to be retained and propagated in the evolutionary process. The emphasis on maximisation aligns with the overarching objective of enhancing the economic performance of the proposed LNG scheduling and routing framework.

3.4.4.1 **Individuals Selection Methods**

To preserve high-quality solutions across generations, an elitism strategy is incorporated within the genetic algorithm. This mechanism applies a retention ratio, whereby a proportion of the top-performing individuals which are calculated as the product of the population size and the predefined keeping ratio are directly carried forward into the subsequent generation. This approach ensures that the algorithm safeguards the most promising solutions identified thus far, thereby maintaining a steady trajectory of optimisation progress. Moreover, it mitigates the risk of quality deterioration arising from the stochastic nature of crossover and mutation operations, which might otherwise lead to the loss of valuable genetic material.

3.4.4.2 **Cross Over Function**

For the remainder of the population by excluding elite individuals, genetic operators are employed to generate offspring and promote genetic diversity. Among these, crossover serves as the principal mechanism, facilitation the combination of genetic material from selected parent solutions to create new individuals. A predefined crossover ration determines the proportion of the population involved in this recombination process. In this study, a single-point crossover method is adopted, with the crossover point set at 0.5 (see Table 3.9 and Algorithm 3.5).

Accordingly, each parent is divided into two equal segments: the first half from one parent is combined with the second half from the other to generate offspring. This approach enables the effective exchange of solution characteristics while striving to preserve feasibility in the resulting population.

Algorithm 3.5: The "Cross-over" function algorithm

1. Randomly select one elite chromosome (P_1) along with one out of the general population (P_2). Consider the following two parents as an example.
2. Repeat the following for all the three sub-chromosomes.
   2.1. Break both from the user-defined breaking point. For example, applying a break point of 0.5 results in splitting in halves. Consider the following example.

P_1	2	1	10	3	7	5	4	9	6	8
P_2	5	7	10	9	1	8	4	3	6	2

   2.2. Make the following two offsprings through pasting halves of different parents together

1^{st} offspring = 1^{st} half of P1 + 2^{nd} half of P_2

2^{nd} offspring = 1^{st} half of P2 + 2^{nd} half of P_1

Offspring 1	2	1	10	3	7	8	4	3	6	2
Offspring 2	5	7	10	9	1	5	4	9	6	8

   2.3. It is very likely at this stage for both offsprings to have repetitive genes. In the above example for instance, the 1^{st} offspring has two genes containing number 2 and two genes containing number 3 with no gene containing neither number 5 nor 9. Where the situation for the 2^{nd} offspring is vice versa.
   2.4. Find repetitive genes in both offsprings and keep replacing them ending up having two offsprings with no repetitive genes. In this case, the result for the above example would be as follows.

Offspring 1	2	1	10	3	7	8	4	9	6	5
Offspring 2	5	7	10	9	1	2	4	3	6	8

3.4.4.3 **Mutation Function**

Subsequent to the crossover operation, the algorithm employs a mutation mechanism to introduce stochastic alterations to the offspring, thereby enhancing diversity within the search space (Algorithm 3.6). A mutation ratio of 0.2 is applied (see Table 3.9), indicating that 20% of the genes within each genome are randomly selected for modification.

This operator plays a critical role in preventing premature convergence by enabling the algorithm to explore previously unvisited regions of the solution space and escape from local optima. All mutated solutions are subjected to a feasibility assessment (Algorithm 3.3 & Algorithm 3.4). In cases where infeasibility is detected,

corrective measures are taken either by repairing the infeasible components or by replacing them with newly generated feasible elements.

Algorithm 3.6: The "Mutation" function algorithm

1- Randomly select one out of the population and repeat the following across all three of its sub-chromosomes. For instance, following is an example sub-chromosome that is about to be mutated through the next steps.

The initial chromosome	10	2	7	8	5	9	3	4	1	6

2- Calculate the number of swaps using the user-defined mutation ratio. In the case of applying a mutation ratio of 0.2 on the above example the number of swaps would be 2.
Number of swaps = number of genes multiplied by the mutation ratio rounded to the next integer

3- Pick and swap two genes randomly as required many times to match the number of swaps calculated in the previous step.

Round 1	Randomly selected genes	10	2	7	8	5	9	3	4	1	6
	First swap	10	2	3	8	5	9	7	4	1	6
Round 2	Randomly selected genes	10	2	3	8	5	9	7	4	1	6
	Second swap	10	2	3	8	5	7	9	4	1	6

The algorithm then re-applies both the feasibility procedures and fitness evaluation to the updated population. This cyclical process ensures continuous improvement of solution quality by identifying high-performing individuals while maintaining a balance between exploration (diversifying the search space) and exploitation (refining promising solutions). The iterative progression enables the algorithm to converge towards an optimal or near-optimal solution within a computationally acceptable timeframe.

3.4.4.4 **Algorithm's Parameter Tuning**

Parameters play a pivotal role in the performance of heuristic and meta-heuristic algorithms (Ali Pitchay & Shorman, 2015; Mosayebi & Sodhi, 2020). These parameters bring essential flexibility to the algorithm, helping the optimiser orchestrate modules aimed at putting developed functionalities to their best use. For instance, allocating greater computational time to crossover operations result in a better and more efficient performance when navigating a smooth objective surface. However, as the search space becomes more complex and multi-modal, there is an increased need to utilize escape and exploration techniques, such as mutation. Adjusting

parameters such as crossover and mutation percentages enables the optimiser to balance the algorithm's exploration-exploitation trade-off without requiring major structural reconfigurations.

To maximise computational efficiency, this study employs a dynamic, parametric programming approach. This entails the live assessment of the algorithm's convergence, followed by recurrent switching between exploitative and explorative configurations:

- Explorative Configuration: This setting guides the algorithm to focus primarily on global search. This configuration is deployed when there is a lack of tangible progress on a global optimality scale, while the general population continues to converge towards local optimality. The coexistence of these two observations is a strong indicator that the algorithm is "stuck" in a local optimum. Therefore, the algorithm is programmed to automatically switch to an explorative configuration whenever it experiences this predefined stuck mode.
- Exploitative Configuration: Conversely, this setting is automatically applied once the algorithm successfully escapes the stuck mode. Under these circumstances, concentrating on further exploitation of the current local optimums helps improve the overall efficiency and convergence speed of the algorithm.

As discussed, two criteria have been applied to define the real-time optimisation mode whether it is evaluated to be normal, stuck or terminal. In the following formulas, f_n^{avg} and f_n^* represent the average fitness value across the general population and the global optimum value of the latest generation respectively where f_{n-1}^* indicates the global optimum value for the previous generation.

Global Optimality Progress Indicator (*GOPI*): $\frac{f_n^* - f_{n-1}^*}{f_{n-1}^*}$

Local Optimality Convergence Indicator (*LOCI*): $\frac{f_n^* - f_n^{avg}}{f_n^*}$

Both *GOPI* and *LOCI* fall below their pre-defined "stuck-indicative" thresholds, it signals that the algorithm has entered a stuck mode. If at least one indicator rises above the threshold, it gives the algorithm the green light to

switch back to the normal exploitative configuration for efficiency purposes. This dynamic toggle enables the algorithm to efficiently balance its exploration and exploitation efforts while converging toward a near-optimal solution within a reasonable computational time. The evolution process terminates either when both *GOPI* and *LOCI* hit their corresponding terminal thresholds, the algorithm exhausts its maximum allowed execution time, or it reaches the maximum iteration limit.

While the stage-altering mechanism dynamically controls parameter shifting, the foundational operational thresholds and percentage ranges required rigorous calibration. Parameter tuning in this study was conducted through an extensive preliminary experimentation phase. A subset of representative problem instances was executed across a grid of parameter settings to establish the optimal boundaries that govern both the explorative and exploitative modes. This calibration ensured that the selected values optimally served their specific configuration purposes without causing premature convergence or excessive computational overhead.

A summary of the proposed algorithm is presented as pseudocode in Algorithm 3.7. The empirically calibrated parameters for both the explorative and exploitative configurations, along with the core static parameters used to drive the algorithm, are detailed in Table 3.9.

Algorithm 3.7: The Pseudocode for the devised GBMHA

1. Import input data
2. Read Table 1
3. Run Algorithm 3.1
4. Run Algorithm 3.2
5. Run below feasibility steps
   5.1. Run Algorithm 3.3
   5.2. Run Algorithm 3.4
6. For the infeasible solution, calculate their total unmet committed demand amount that happens due to their timing obligations or capacity shortage.
7. Calculate the following components required to measure a solution's overall fitness:
   7.1. Total revenue (Selling LNG)
   7.2. Total cost of supply of LNG (Buying LNG)
   7.3. Total cost of operation covering fuel, shipping, port and vessel idle costs
   7.4. The total penalty of unmet committed demand
8. Sort the population on descending order
9. Simulate the natural selection and evolution processes through the following steps util running out of time or hitting the maximum allowed number of iterations.
   9.1. Select and leave the top elite chromosomes unchanged
   9.2. Apply cross-over function (Algorithm 3.5)
   9.3. Apply mutation function (Algorithm 3.6)

9.4. Run Algorithm 3 and 4 on the new generation
9.5. Evaluate new population's fitness
9.6. Calculate GOPI and LOCI and compare them against used-defined thresholds $GOPI < T_{stuck}^{GOPI}$ means that the Global Optimality Progress indicator is showing signs of getting stuck; while $GOPI < T_{ter\,min\,al}^{GOPI}$ is a signal to terminate the evolution loop. The same logic applies to LOCI using its own "stuck indicative" and "terminal" threshold.
    9.6.1. Terminate the evolution loop, if both GOPI and LOCI are implying it.
    9.6.2. Otherwise, if both show signs of getting stuck then go ahead and load explorative configuration.
    9.6.3. Otherwise, continue with the application of exploitative configuration.

Table 3.9: GA Parameters

Parameters	Value	Description
Population size	100	Total number of individuals in the population.
Keep percentage	10%	Fraction of elite individuals retained in each generation.
Crossover percentage	40%-75%	Fraction of the population subject to crossover.
Breaking point	50%	Location in the genome where crossover occurs.
Mutation ratio	15% - 40%	Fraction of genes in each individual subject to mutation.
GOPI threshold range	< 0.5% - 2%	Global Optimality Progress Indicator
LOCI threshold range	< 15% - 30%	Local Optimality Convergence Indicator
Maximum allowed execution time	35,000 seconds	Maximum allowed execution time
Maximum allowed number of iterations	100	Maximum allowed number of iterations
	Explorative setting	
GOPI threshold	< 2%	Global Optimality Progress Indicator
LOCI threshold	< 30%	Local Optimality Convergence Indicator
Crossover percentage	40%	Fraction of the population subject to crossover.
Mutation ratio	50%	Fraction of genes in each individual subject to mutation.
	Exploitative setting	
GOPI threshold	> 2%	Global Optimality Progress Indicator
LOCI threshold	> 30%	Local Optimality Convergence Indicator
Crossover percentage	75%	Fraction of the population subject to crossover.
Mutation ratio	15%	Fraction of genes in each individual subject to mutation.

3.5 Experimental Result of GBMHA

To validate the performance and effectiveness of the developed metaheuristic algorithm, the same set of problem instances previously solved using the exact mathematical approach were re-evaluated using the GA-based metaheuristic method. The complete results for all instances are provided in the Table 3.10.

It is important to note that, due to the inherent stochastic nature of metaheuristic algorithms, each experiment was conducted 15 times. The results presented in the table represent the average values obtained across these runs. Furthermore, the standard deviation across these experiments remained consistently below 0.6%, thereby demonstrating the stability and reliability of the proposed solution method.

All computational times are reported in seconds. Additionally, the final column in the results table illustrates the optimality percentage, indicating the proportion of the exact method's solution quality achieved by the metaheuristic approach. This metric highlights the ability of the GBMHA method to approximate high-quality solutions within significantly reduced computational time relative to the exact method.

Table 3.10: Result of GBMHA Examples

No.	Size (S, C, V, SL, T)	Revenue – Expenditure ($)	Shipping cost ($)	Fuel cost ($)	Idle cost ($)	port cost ($)	Net Profit ($)	active vessels	CPU time (s)	(GBMHA/ MILP) optimality %
1	(1,2,20,1-2-3,6)	58,483,334	13,771,492	855,200	1,274,074	649,157	41,933,412	2	33	99.24
2	(3,5,6,2,20)	162,296,512	33,868,449	2,605,903	6,567,728	1,876,727	117,377,705	4	40	99.89
3	(3,5,6,2-3,20)	162,304,681	32,829,676	2,723,381	7,436,986	1,876,727	117,437,910	4	44	99.82
4	(4,8,9,2,25)	235,983,306	66,877,924	6,551,053	18,769,950	2,811,351	140,973,028	7	76	99.22
5	(4,8,9,3,25)	242,619,636	59,247,454	6,469,813	22,464,825	2,856,967	151,580,578	7	73	99.07
6	(3,9,10,1-2-3,22)	276,011,582	69,918,866	7,647,380	21,617,467	3,119,501	173,708,368	7	92	98.62
7	(4,9,10,2,26)	269,189,369	72,002,729	7,585,588	23,518,638	3,140,990	162,941,424	7	145	98.74
8	(4,10,9,3,25)	302,024,502	72,790,569	8,642,879	28,521,710	3,556,566	188,512,779	7	247	97.94
9	(4,11,10,2,26)	329,675,477	85,514,688	9,852,016	24,509,683	3,893,416	205,905,673	7	173	98.00
10	(4,12,10,2,26)	352,174,251	96,876,141	10,912,377	30,993,017	4,193,912	209,198,803	8	246	98.16
11	(5,12,10,2,26)	352,839,829	100,299,811	11,501,836	27,973,149	5,256,789	207,808,244	8	240	97.51
12	(5,13,10,2,26)	378,426,062	103,371,246	11,568,138	30,773,660	5,664,648	227,048,369	8	277	97.35
13	(5,14,10,2,26)	407,501,978	108,570,584	12,739,575	35,790,284	5,973,802	244,427,732	8	341	97.11
14	(5,15,10,2,26)	442,185,492	116,583,210	13,762,731	36,804,144	6,713,181	268,322,226	8	377	97.58
15	(5,20,12,2,30)	596,861,877	155,810,741	18,800,237	57,630,130	10,480,317	354,140,452	10	831	91.90

16	(5,25,15,2,35)	740,019,600	191,630,333	23,815,659	74,659,831	12,441,227	437,472,552	11	1,377	90.27
17	(5,25,15,2-3,35)	749,215,993	181,452,617	24,089,729	82,057,664	12,275,932	449,340,051	11	1,271	85.96
18	(5,25,20,3,30)	746,813,314	172,702,921	25,434,805	95,480,594	12,640,998	440,553,996	11	1,090	87.53
19	(5,30,15,2,35)	901,426,693	223,972,665	29,015,695	110,779,649	14,575,300	523,083,383	12	2,113	86.75
20	(5,30,15,1-2-3,35)	916,876,902	217,153,882	30,638,760	122,766,195	14,228,207	532,089,857	13	1,653	96.06

As evidenced by the results presented in the metaheuristic results table, the developed GBMHA demonstrates a strong performance across all tested instances. On average, the algorithm achieves approximately 95% of the optimality of the exact solutions obtained via the mathematical approach. This level of solution quality is particularly noteworthy given the significant computational efficiency of the metaheuristic method.

More specifically, while the exact approach may require up to nine hours of computation to reach an optimal solution or an acceptable MIP gap, the metaheuristic algorithm is capable of producing high-quality solutions in just one-twentieth of the computational time, often within minutes. This substantial reduction in runtime highlights the practical applicability of the proposed method, especially for large-scale or real-time industrial problems where timely decision-making is crucial.

The relatively minor trade-off in solution optimality is more than compensated by the dramatic gain in computational speed, making the proposed approach highly suitable for scenarios where near-optimal solutions are sufficient and computational resources or time are constrained. Furthermore, the low standard deviation (less than 0.6%) across multiple independent runs affirms the robustness and consistency of the algorithm's performance.

In summary, the results confirm that the metaheuristic algorithm is not only computationally efficient but also capable of reliably approximating optimal solutions with a high degree of accuracy, thereby offering a compelling alternative to exact optimisation methods for complex real-world LNG scheduling problems.

3.5.1 **Comparison of Metaheuristic and Exact method Approaches**

To provide a clearer understanding of the comparative performance between the exact and metaheuristic approaches, a detailed analysis was conducted. Specifically, the execution time gap was computed as the difference between the execution time of the mathematical model and that of the metaheuristic algorithm. This metric was used exclusively for instances that were successfully solved by both methods, and the results of this comparison are illustrated in Figure 3.5.

The findings reveal a distinct trend. For small-sized problem instances, the exact approach is able to generate optimal solutions within a reasonable computational timeframe, thereby outperforming the metaheuristic method in terms of solution quality. However, as the problem size increases, the execution time gap widens significantly. This reflects the scaling limitations of the exact method, which becomes increasingly computationally intensive and, at times, infeasible for large instances.

In contrast, the metaheuristic algorithm consistently offers high-quality solutions with remarkable computational efficiency. For larger instances, the algorithm achieves approximately 90% optimality relative to the exact solutions obtained via CPLEX, while reducing the computational time by several orders of magnitude.

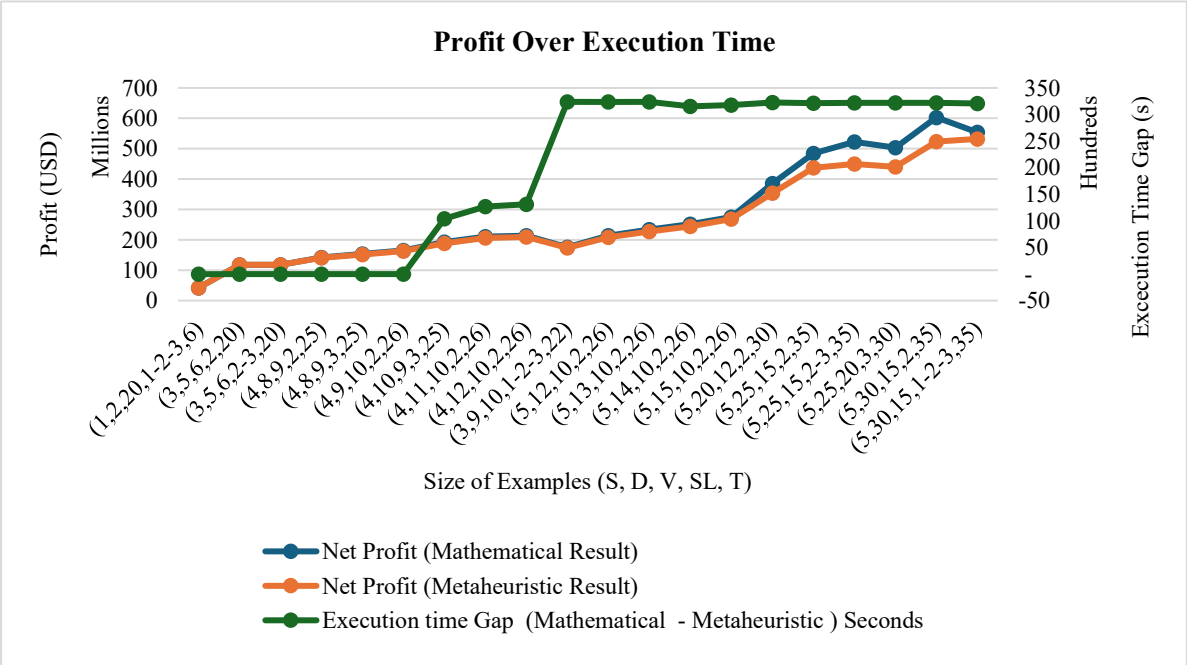

Figure 3.4: Comparison between Exact and GBMHA approaches

This trade-off underscores the practical value of the proposed method in real-world industrial settings where timely decision-making is often prioritised over exact optimality.

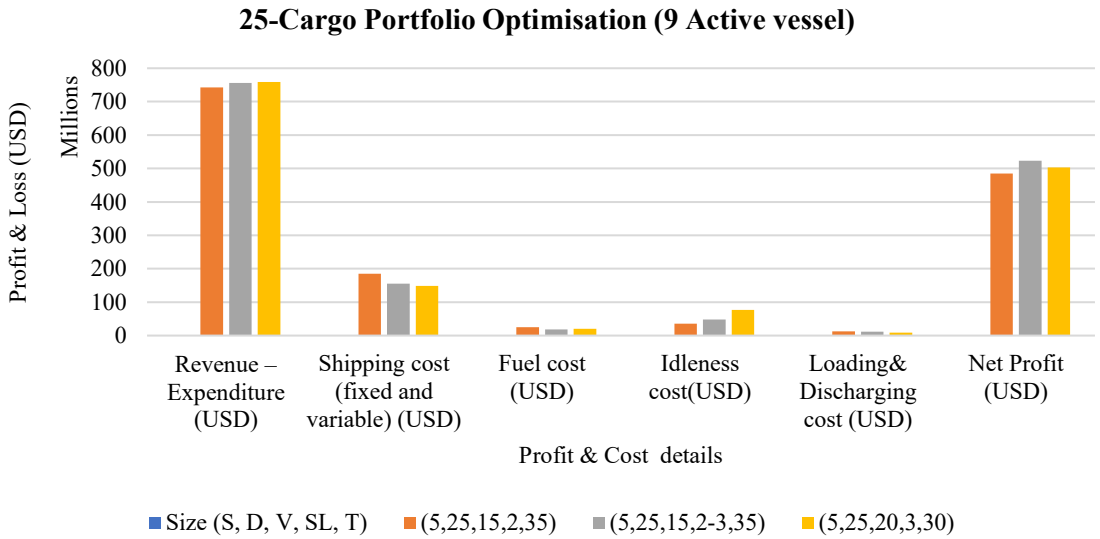

Figure 3.5:Exact Method Result for 25 cargo at speed of 16, 16-18 and 18 knots

An additional observation concerns the notable variation in vessel idle costs between the two solution approaches. To better illustrate this difference, the graphical output of a representative example is provided in Figure 3.6 and Figure 3.7, respectively. The most significant divergence between the two approaches lies in their treatment of idle time costs, which results from distinct fleet utilisation strategies. Furthermore, another insight drawn from Figure 3.6 and Figure 3.7 is the impact of vessel speed allocation on overall portfolio performance and profitability. Speed selection significantly influences both travel duration and fuel efficiency, thereby playing a pivotal role in operational planning. This relationship between vessel speed and economic outcome will be examined in greater detail in the sensitivity analysis section that follows.

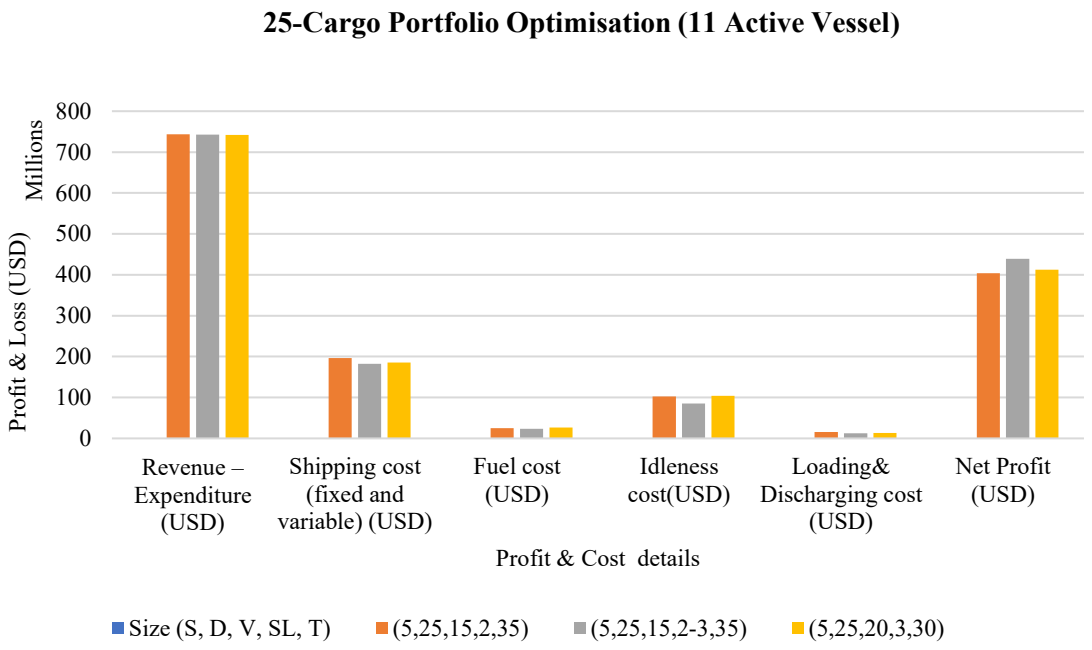

Figure 3.6:Metaheuristic Algorithm Result for 25 cargo at speed of 16, 16-18 and 18 knots

In particular, the metaheuristic algorithm tends to activate a greater number of vessels (11 out of the total fleet), even if some of these vessels are not immediately required for cargo transport. Since all vessels are considered available from the beginning of the planning horizon, the early activation of vessels incurs idle costs that are subsequently captured in the objective function. In contrast, the exact optimisation model adopts a more conservative allocation strategy, employing only 9 of the 15 available vessels. This more efficient scheduling reduces idle costs but may limit flexibility and, in certain scenarios, constrain the solution space, potentially compromising optimality.

This contrast underscores the trade-off between resource utilisation and profit maximisation, a critical consideration in maritime logistics planning. It reinforces the importance of selecting an appropriate solution method depending on the operational context, particularly in terms of the scale and time-sensitivity of the problem instance.

3.5.2 **Large scale Case studies for Real World Problems**

The primary motivation for developing the proposed metaheuristic algorithm lies in its capacity to address large-scale, real-world instances of the portfolio optimisation problem in delivery planning. In this section, 20

industrial-scale case studies, based on realistic operational data, are solved using the metaheuristic approach. This serves to demonstrate the algorithm's scalability and practical applicability in complex logistics environments.

Table 3.11 outlines the scope and dimensionality of the problem instances considered. Notably, the largest case study involves 2 suppliers, 137 cargoes, and a heterogeneous fleet of 67 vessels, operating over a 72-week planning horizon with three discrete vessel speed levels. This industrial-scale instance results in an extremely complex mathematical structure, comprising 21,835,420 constraints**,** 1,370,074 continuous variables, and 1,305,828 binary variables**,** as detailed in Table 3.11.

Table 3.11: Size of GBMHA Case Studies

No.	Size (S, C, V, SL, T)	No of binary variables	No of continuous variables	No of constraints
21	(2,40,30,1-2-3,30)	54,360	63,232	875,815
22	(2,45,32,1-2-3,30)	72,211	82,994	1,172,631
23	(2,50,35,1-2-3,35)	96,685	109,507	1,574,480
24	(2,55,35,1-2-3,35)	115,960	130,042	1,895,500
25	(2,60,35,1-2-3,40)	137,595	152,327	2,248,405
26	(2,65,40,1-2-3,40)	182,535	201,442	3,001,915
27	(2,70,40,1-2-3,42)	210,844	230,902	3,471,779
28	(2,75,40,1-2-3,42)	240,889	262,362	3,974,719
29	(2,80,45,1-2-3,45)	306,635	332,677	5,074,200
30	(2,85,45,1-2-3,45)	344,910	372,562	5,716,420
31	(2,90,45,1-2-3,52)	386,709	414,697	6,401,349
32	(2,95,50,1-2-3,55)	476,695	509,962	7,909,445
33	(2,100,50,1-2-3,60)	527,780	561,772	8,754,225
34	(2,105,50,1-2-3,60)	580,405	616,082	9,638,145
35	(2,110,55,1-2-3,63)	698,361	740,047	11,618,536
36	(2,115,55,1-2-3,63)	761,716	805,282	12,684,236
37	(2,120,60,1-2-3,69)	903,088	952,522	15,051,008
38	(2,125,60,1-2-3,69)	978,203	1,029,682	16,315,593
39	(2,130,65,1-2-3,70)	1,143,045	1,202,197	19,095,935
40	(2,137,67,1-2-3,72)	1,305,828	1,370,074	21,835,420

Despite the high dimensionality and complexity of these cases, the metaheuristic algorithm is able to solve all instances efficiently. The corresponding results for the large-scale examples are summarised in Table 3.12,

providing a comprehensive view of the algorithm's performance in managing large delivery portfolios under realistic operational settings.

Table 3.12: Result of metaheuristic algorithm for large examples

No.	Size (S, C, V, SL, T)	Revenue – Expenditure ($)	Shipping cost ($)	Fuel cost ($)	Idle cost ($)	Port cost ($)	Net Profit ($)	active vessels	CPU time (s)
21	(2,40,30,1-2-3,30)	1,218,325,145	341,663,359	47,117,465	424,059,999	16,248,471	389,235,850	19	2,640
22	(2,45,32,1-2-3,30)	1,367,386,566	382,979,792	57,013,235	483,804,633	18,487,550	425,101,357	21	3,127
23	(2,50,35,1-2-3,35)	1,489,161,662	431,859,559	63,411,022	543,133,784	20,650,519	430,106,778	21	4,600
24	(2,55,35,1-2-3,35)	1,641,642,283	470,462,020	70,368,486	600,751,326	22,600,469	477,459,981	23	6,100
25	(2,60,35,1-2-3,40)	1,781,762,698	516,952,731	80,326,546	666,828,850	24,803,272	492,851,299	24	5,440
26	(2,65,40,1-2-3,40)	1,969,090,708	558,307,300	94,140,310	789,412,659	26,925,913	500,304,526	24	4,050
27	(2,70,40,1-2-3,42)	2,068,221,626	599,263,652	99,849,786	825,891,980	28,714,314	514,501,894	27	5,100
28	(2,75,40,1-2-3,42)	2,136,749,743	639,472,651	104,325,848	836,994,108	31,464,426	524,492,710	25	10,000
29	(2,80,45,1-2-3,45)	2,389,803,380	711,432,081	117,181,841	985,022,949	33,016,776	543,149,733	27	7,800
30	(2,85,45,1-2-3,45)	2,475,601,054	729,801,807	126,470,024	1,041,432,948	35,092,519	542,803,754	27	10,000
31	(2,90,45,1-2-3,52)	2,643,148,845	800,170,465	131,728,565	1,137,877,225	37,161,667	536,210,923	32	10,000
32	(2,95,50,1-2-3,55)	2,809,009,844	836,538,607	138,258,888	1,248,854,093	39,339,342	546,018,913	30	11,000
33	(2,100,50,1-2-3,60)	2,907,411,661	887,870,607	146,091,417	1,266,663,582	41,108,089	565,677,966	29	15,000
34	(2,105,50,1-2-3,60)	3,065,029,100	928,209,227	146,501,255	1,376,233,898	43,524,063	570,560,658	32	20,000
35	(2,110,55,1-2-3,63)	3,117,000,532	945,607,313	154,680,965	1,392,993,787	45,430,205	578,288,262	31	12,500
36	(2,115,55,1-2-3,63)	3,358,887,979	1,019,682,284	175,504,500	1,562,985,975	47,505,948	553,209,272	32	30,000
37	(2,120,60,1-2-3,69)	3,491,508,622	1,091,282,346	182,055,168	1,601,548,872	49,653,718	566,968,521	33	17,500
38	(2,125,60,1-2-3,69)	3,685,142,112	1,100,153,969	188,469,765	1,762,209,454	51,674,151	582,634,773	34	25,000
39	(2,130,65,1-2-3,70)	3,739,429,796	1,168,606,530	196,387,221	1,736,180,365	53,600,139	584,655,542	33	35,000
40	(2,137,67,1-2-3,72)	4,008,346,094	1,197,313,734	218,256,180	1,938,777,247	56,240,710	597,758,224	36	35,000

3.6 Comparative Evaluation and Commercial Benchmarking

To rigorously validate the performance of the proposed GBMHA and quantify its value to industry stakeholders, a comparative evaluation was conducted against current commercial practices.

In the absence of a universally standardised benchmark for LNG portfolio optimisation, a Business-As-Usual (BAU) Baseline was reconstructed to represent the existing commercial approach. This baseline simulates the company's historical, manual planning process, which typically relies on a "greedy" nearest-neighbour assignment heuristic. In this baseline, vessels are dispatched to the nearest available compatible port at standard fixed cruising speeds, and cargoes are matched sequentially without the capacity for simultaneous portfolio-level profit maximisation or dynamic CII tracking.

The proposed algorithm and the BAU Baseline were evaluated across a selection of ten large-scale industrial instances, varying in size and complexity (from 40 to 137 customers). To ensure clarity in the commercial comparison, the financial results are presented in millions of US Dollars ($M). The comparative results, detailing annual portfolio profit, computational execution time are summarised in Table 3.13.

Table 3.13: Comparative Evaluation of AGA vs. Company Baseline (BAU)

No.	Size (S, C, V, SL, T)	Company Baseline (Greedy BAU)		Proposed Approach (GBMHA)		GBMHA Improvement over Baseline	
		Total Profit ($M)	Execution Time (s)	Total Profit ($M)	Execution Time (s)	ΔProfit (%)	Time (+/-)
21	(2,40,30,1-2-3,30)	330.8	120	389.2	2,640	+ 17.6%	-2,520
23	(2,50,35,1-2-3,35)	361.3	188	430.1	4,600	+ 19.0%	-4,412
25	(2,60,35,1-2-3,40)	409.0	200	492.8	5,440	+ 20.4%	-5,240
27	(2,70,40,1-2-3,42)	421.9	360	514.5	5,100	+ 21.9%	-4,740
29	(2,80,45,1-2-3,45)	439.9	400	543.1	7,800	+ 23.4%	-7,400
31	(2,90,45,1-2-3,52)	428.9	465	536.2	10,000	+ 25.0%	-9,535
33	(2,100,50,1-2-3,60)	446.8	654	565.6	15,000	+ 26.5%	-14,346
35	(2,110,55,1-2-3,63)	456.8	1,250	578.2	12,500	+ 26.5%	-11,250
37	(2,120,60,1-2-3,69)	442.2	1,800	566.9	17,500	+ 28.1%	-15,700
40	(2,137,67,1-2-3,72)	466.2	2,300	597.7	35,000	+ 28.2%	-32,700

The comparative analysis reveals significant commercial advantages of the proposed Adaptive GA approach, explicitly demonstrating the severe limitations of current industry planning methods. The Company Baseline (BAU) consistently yielded significantly lower profitability across all tested scales. More importantly, as the complexity of the delivery network scaled (from 40 customers in Instance 21 to 137 customers in Instance 40), the financial performance gap widened dramatically. While a manual greedy heuristic only lost 17.6% of potential profit on the smallest instance, it left over 28% of the potential profit uncaptured on the largest instance. This mathematically proves that as LNG portfolios become more complex, manual sequential planning fails to recognise global optimisation opportunities, such as spot market capitalisation. Although the greedy BAU baseline calculates faster than proposed algorithm (< 2300 seconds), this speed comes at a fatal operational cost. In an industrial context, an execution time of several hours is perfectly acceptable for generating an ADP. Therefore, the computational time required by the proposed algorithm is vastly outweighed by the generation of millions of dollars in additional revenue and the guarantee of strict environmental compliance.

3.7 **Sensitivity Analysis**

In the preceding sections, it was observed that vessel speed selection and LNG procurement prices play a significant role in influencing the profitability and operational feasibility of delivery plans. Specifically, the same optimisation problem, when solved under different vessel speed allocations, yielded noticeably distinct profit outcomes (for instance experiment No 16,17 and 18 in Table 3.8). This observation underscores the importance of vessel speed as a key decision variable in fleet routing and portfolio optimisation.

Furthermore, given that LNG is a tradable commodity, its procurement price at the supplier side is subject to market variability. These price differentials have a direct impact on the supplier–customer pairing strategy and influence the overall cost-effectiveness of the delivery portfolio. Since pairing decisions are highly sensitive to cost parameters, understanding how changes in LNG prices affect the optimisation outcome is essential for robust planning.

This section, therefore, presents a structured sensitivity analysis aimed at two major factors:

1. The effect of varying vessel speeds on route planning, fuel consumption, and resulting profitability.
2. The impact of LNG price variations across suppliers on supply allocation decisions and overall portfolio configuration.

By systematically varying these parameters, the analysis seeks to reveal underlying trade-offs, guide operational policy, and provide deeper insights into the responsiveness of the developed mathematical model and metaheuristic algorithm under different economic and operational scenarios.

3.7.1 **Sensitivity Analyses on Vessel Speed**

To systematically evaluate the impact of vessel speed on the operational planning of the LNG supply chain, a detailed sensitivity analysis was conducted. This analysis focuses on how speed variations influence key model outcomes, including cargo pairing combination, fleet utilisation (the number of active vessels), and accumulated idle time.

The analysis was performed on a 10-cargo test instance, formally parameterized by the 5-tuple (4, 10, 9, SL, 25). To measure the sensitivity of the supply chain's economic performance against transit speeds, six distinct scenarios were defined and solved:

- **Scenario 1**: Vessels are restricted to operating at 16 knots ($SL \in \{2\}$).
- **Scenario 2**: Vessels are restricted to operating at 18 knots ($SL \in \{3\}$).
- **Scenario 3**: Vessels may operate at either 14 or 16 knots ($SL \in \{1, 2\}$).
- **Scenario 4**: Vessels may operate at either 16 or 18 knots ($SL \in \{2, 3\}$).
- **Scenario 5**: Vessels may operate at either 14 or 18 knots ($SL \in \{1, 3\}$).
- **Scenario 6**: Vessels may operate dynamically across all three speed levels ($SL \in \{1, 2, 3\}$).

While increasing vessel speed naturally affords greater logistical flexibility, the primary trade-offs lie in the thermodynamic and economic consequences. Specifically, higher speeds drastically increase fuel consumption costs while simultaneously reducing transit times, which consequently minimises the volume of LNG lost to boil-off. These interconnected factors result in highly variable overall revenues and operational costs across the

different speed configurations. The detailed economic and operational outcomes of these six scenarios are presented in Table 3.14.

Table 3.14: Experimental results of conducted Sensitivity Analysis on Vessel Speed

Scenario	Speed (knots)	Revenue – Expenditure ($)	Shipping cost ($)	Fuel cost ($)	Idle cost ($)	Port cost ($)	Shipping + Idle cost ($)	Net Profit ($)	Active vessel	Gap (%)
1	16	296,904,582	76,374,602	7,869,771	27,326,668	3,575,434	103,701,269	181,758,107	7	0
2	18	303,497,920	66,814,391	7,660,976	32,897,888	3,639,353	99,712,279	192,485,312	7	0
3	14, 16	296,888,686	77,818,697	7,720,774	25,882,572	3,575,435	103,701,269	181,891,209	7	0
4	16, 18	303,341,129	70,876,150	7,202,470	28,836,129	3,639,353	99,712,279	192,787,027	7	21.99
5	14, 18	303,487,607	68,481,838	7,507,071	31,230,440	3,639,353	99,712,279	192,628,904	7	10.18
6	14,16,18	303,335,333	71,812,275	7,115,777	27,900,004	3,639,353	99,712,279	192,867,925	7	24.49

A deeper analysis of the financial metrics in Table 3.8 reveals several critical operational insights regarding fleet management and speed optimisation. First, the data highlights a distinct profitability threshold tied to the highest speed tier. Scenario constrained to lower speeds (Scenario 1 and 3) plateau at a net profit of approximately $181.8 million. Conversely, introducing the 18-knot capability (Scenarios 2, 4, 5, and 6) instantly generates an approximate $11 million premium, as the increased speed allows vessels to capture highly lucrative supplier with lower LNG purchase price.

However, operating exclusively at maximum speed (Scenario 2) incurs the highest idleness cost across all configurations, reaching nearly $32.9 million. This mathematically illustrates the classic maritime "hurry up and wait" dilemma: vessels arrive too early and incur massive idle penalties while waiting for strict port time windows to open.

Scenario 6 definitively proves the value of dynamic speed optimisation. By allowing the algorithm to seamlessly transition between all three speed tiers, Scenario 6 achieves the highest overall net profit ($192.86 million) while keeping fuel costs remarkably low ($7.11 million). The MILP model acts intelligently sprinting at 18 knots to hit profitable suppliers, but actively slow steaming at 14 or 16 knots when there is schedule slack, effectively

mitigating both excessive fuel burn and idle penalties. Finally, the active fleet utilisation remains constant at 7 vessels across every scenario. This indicates that for this specific ADP, increasing vessel speed does not allow the company to reduce the physical size of the required fleet. Therefore, the true economic value of speed flexibility does not lie in capital reduction, but entirely in optimising the thermodynamic efficiency (BOG) and dynamic financial margins of the existing vessels.

Beyond the raw financial metrics, the optimal cargo pairing strategy is highly sensitive to the availability of the highest speed tier. As illustrated in Figure 3.8, the United States (S1) and Oman (S3) emerge as the dominant suppliers in the majority of optimised scenarios. This preference is primarily driven by their advantageous geographic proximity to dense customer clusters and being the profitable suppliers among other available suppliers.

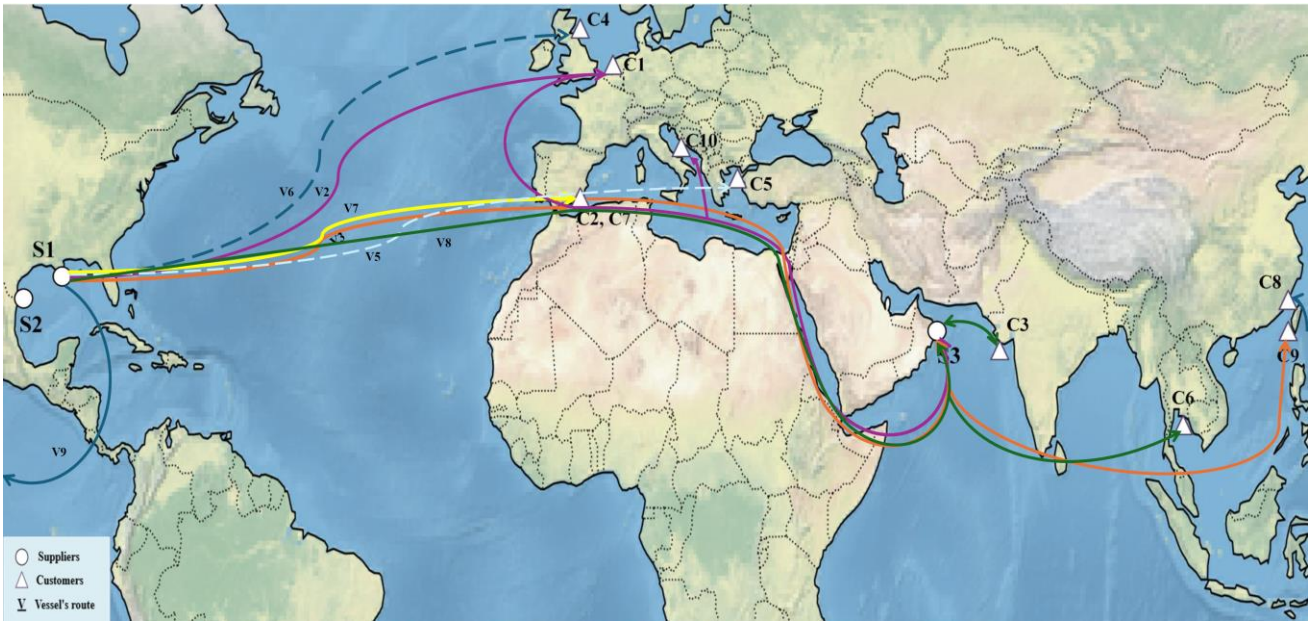

Figure 3.7: Optimal vessel routing & Supplier-customer matching in scenarios 2,4,5 and 6

However, transiting from either of these two suppliers to geographically distant customers such as those in Thailand (C6) and Turkey (C5) at restricted speeds of 14 or 16 knots frequently results in time-window violations. Consequently, in scenarios where the maximum allowable speed cannot exceed 16 knots, the model dynamically reconfigures the supplier-customer pairings to maintain strict temporal feasibility.

As shown in Figure 3.9, under these low-speed constraints, the model adapts by pairing Thailand (C6) with the much closer Australian supplier(S4), while Turkey (C5) is reallocated to Oman (S3). Conversely, when the 18-

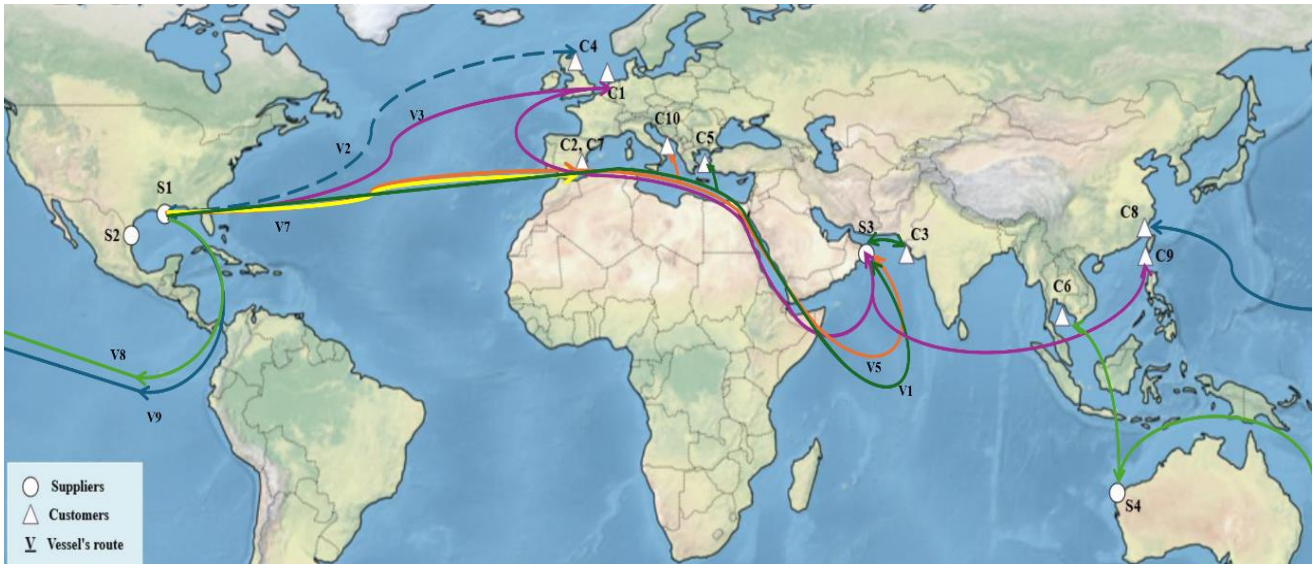

Figure 3.8: Optimal vessel routing & Supplier-Customer matching in first and third scenarios

knot speed level is enabled within the optimisation framework, the solver successfully capitalises on this faster transit time to improve global optimality (reverting Thailand to Oman and Turkey to the United States (S1)). Ultimately, these geographical shifts underscore that the fundamental structural decisions of the LNG supply chain are intrinsically dependent on available vessel transit speeds.

3.7.2 **Sensitivity Analyses on LNG Price**

Another critical factor considered by the optimisation model in determining supplier-customer pairings is the variation in LNG purchase prices at the supplier side. To assess the model's sensitivity to fluctuations in purchase prices and to evaluate the impact of differing supplier price levels on the overall solution, a comprehensive sensitivity analysis has been undertaken. This analysis specifically investigates the relationship between boil-off quantities, inter-port distances, and resulting supplier-customer pairings in the context of profit maximisation.

Under the assumption that all vessels are initially located at the port in the United States (i.e., the location of the first supplier), the analysis captures the inherent trade-offs between transportation-related boil-off losses,

shipping costs, fuel consumption, and resultant profitability. The central objective is to determine the most economically advantageous supplier selections under varied price conditions.

For this analysis, 2nd scenario from the previous section has been selected as the reference case. This scenario involves four suppliers, ten cargoes, nine vessels, and a uniform vessel speed of 18 knots (4, 10, 9, 3, 25). The focus here is on the sensitivity of the optimisation results to the LNG purchase prices at supplier ports. It is assumed that LNG prices vary across suppliers and are expressed on a per MMBTU basis, denoted as X. The specific price values used in this analysis are summarised in Table 3.15.

Table 3.15: LNG purchase price at different suppliers per scenario

Scenarios	**1st Supplier**	**2nd Supplier**	**3rd Supplier**	**4th Supplier**
1	X	X	X	X
2	1.75X	X	1.5X	1.25X
3	1.5X	1.25X	X	1.75X
4	1.25X	1.5X	1.75X	X
5	X	1.75X	1.25X	1.5X

In the first scenario, LNG prices are assumed to be uniform across all suppliers. Under these conditions, the model determines the supplier-customer pairings solely based on logistical considerations, such as distance, boil-off losses, and operational constraints, to maximise overall profitability. In subsequent scenarios, this uniformity is relaxed, and price differentials are introduced, whereby certain suppliers offer LNG at lower prices relative to others. This allows for a more comprehensive examination of how price variations influence the optimisation process. By incorporating both economic and logistical factors, this refined approach provides deeper insight into the trade-offs underpinning supplier selection and customer pairing, thereby enhancing our understanding of profitability drivers in LNG portfolio planning.

A detailed review of these results emphasises that while the model is highly responsive to price fluctuations, raw commodity cost does not strictly dictate the final supply chain design. Several critical insights emerge from this analysis:

First, geographic proximity and temporal constraints frequently override purchase price advantages. For example, the proximity between the third supplier and customers in India and Italy dictates that these two customers are consistently paired with the third supplier across all five scenarios. This pairing remains mathematically optimal even when the third supplier does not offer the lowest relative market price, proving that the logistical cost of rerouting outweighs the potential commodity savings (see Table 3.16).

Second, the outcomes of Scenario 4 serve as a stark indicator of the optimality trade-off between purchase price and distance-related expenses. In this scenario, the fourth supplier (Australia) offers the absolute lowest market price (X). Despite this economic advantage, its significant geographic distance from the primary customer clusters restricts it to fulfilling only three specific cargoes (Thailand and two Taiwan deliveries).

Furthermore, to capitalise on this cheap Australian LNG and bridge the geographic gap, the optimisation model is forced to charter an additional LNG carrier, increasing the active fleet from 7 to 8 vessels (Table 3.17). The deployment of this extra vessel drastically inflates the combined shipping and idleness costs to nearly $111 million. Consequently, despite purchasing the cheapest available LNG, Scenario 4 yields the lowest overall net profit of the entire analysis, plunging to $151.06 million.

Ultimately, this sensitivity analysis underscores the critical importance of holistic portfolio optimisation. It mathematically demonstrates that relying solely on the cheapest FOB (Free on Board) LNG provider is a flawed procurement strategy. Instead, true profit maximisation in the LNG supply chain requires the simultaneous, integrated evaluation of commodity prices, fleet utilisation, thermodynamic losses, and routing logistics.

Table 3.16: Price Sensitivity Analyses result on Cargo Pairing

Scenarios	1st Supplier	2nd Supplier	3rd Supplier	4th Supplier
1	Netherland, Spain, United Kingdom, Turkey, Spain, Taiwan	-	India, Thailand, Taiwan*, Italy	-
2	-	Netherland, Spain, United Kingdom, Turkey, Spain, Taiwan, Taiwan*	India, Thailand, Italy	-
3	-	Netherland, Spain, United Kingdom, Turkey	India, Thailand, Italy, Spain, Taiwan, Taiwan*	-
4	Netherland, Spain, United Kingdom, Turkey, Spain	-	India, Italy	Thailand, Taiwan, Taiwan*
5	Netherland, Spain, United Kingdom, Turkey, Spain, Taiwan, Taiwan*	-	India, Thailand, Italy	-

Table 3.17: Price Scenario Detailed Profit Cost Results of Example (4, 10, 9, 3, 25)

Scenario	Revenue – Expenditure ($)	Shipping cost ($)	Fuel cost ($)	Idle cost ($)	Port cost ($)	Shipping + Idle cost ($)	Net Profit ($)	Active vessel	Gap (%)
1	303,497,920	66,814,391	7,660,976	32,897,888	3,639,353	99,712,279	192,485,312	7	0
2	285,560,386	71,019,760	8,164,712	28,692,519	4,006,033	99,712,279	173,677,362	7	0
3	293,211,177	74,477,897	8,780,467	25,234,382	3,613,577	99,712,279	181,104,855	7	0
4	274,686,515	75,972,015	8,996,568	35,020,935	3,630,615	110,992,950	151,066,382	8	0
5	294,130,208	69,640,201	7,979,974	30,072,078	3,730,861	99,712,279	182,707,094	7	0

This sensitivity analysis reinforces the necessity of adopting a holistic approach to portfolio optimisation. It becomes evident that selecting the supplier offering the lowest LNG price does not inherently lead to maximum profitability. Rather, effective optimisation requires the integrated consideration of all relevant factors, including logistics, operational constraints, and market dynamics, to achieve a truly optimal outcome.

3.8 Conclusion

This chapter presented a novel MILP model, and a new GBMHA specifically designed to optimise the annual delivery planning of the global shipping supply chains for low-carbon cryogenic fuels with the application to LNG supply chain.

3.8.1 Strengths of the Proposed Methodological Framework

The proposed model and metaheuristic algorithm were evaluated using a set of real-world LNG case studies derived from industrial data. The mathematical model demonstrated commendable performance, yielding a notable improvement in profit and offering a valuable benchmark for strategic planning. Nevertheless, when addressing long-term planning scenarios involving a larger number of cargoes, the developed metaheuristic algorithm proved highly effective. On average, it achieved 95% of the exact solution's optimality while requiring only one-twentieth of the execution time (20 times faster). This efficiency makes it particularly suitable for large-scale, time-sensitive operational planning.

The experimental findings also provide significant operational insights. The inventory levels on board the vessels, coupled with the amount of fuel lost to boil-off during transit, emerged as key factors influencing overall profitability. Furthermore, vessel speed was shown to be a critical parameter; the adoption of variable or dynamic speeds notably enhanced profit margins by reducing voyage times in both laden and ballast legs. The results suggest that a speed strategy incorporating multiple levels is more advantageous than a fixed-speed policy. In parallel, the fluctuating prices of LNG across different suppliers played a decisive role. Choosing a more cost-effective supplier despite a longer sailing distance proved profitable, provided that vessel inventory was efficiently managed to meet demand within the required time windows. These findings emphasise the complexity of LNG delivery planning, where interdependent variables must be carefully balanced to maximise profitability.

What sets the proposed framework apart is its operational realism. It is one of the closest models available in the literature that reflects the complexities encountered in real-world LNG shipping. Both the mathematical

model and the metaheuristic algorithm demonstrated robustness in addressing practical constraints and operational limitations. This dual-method approach allows companies to tailor their delivery planning based on their specific operational horizons whether short-term scheduling or long-term strategic deployment making the model adaptable to diverse industrial contexts.

Furthermore, the value of this approach lies not only in its optimisation capability but also in its support for detailed operational insight. In this context, the model's adaptability becomes particularly valuable. Although originally developed for LNG as a transitional, low-carbon fuel currently dominant in the maritime sector, the framework can be modified to support supply chains involving alternative clean fuels such as ammonia, hydrogen, or methanol (Al-Breiki & Bicer, 2020; Ghafri, et al., 2023). Each of these fuels introduces specific logistical challenges, including storage requirements, handling procedures, infrastructure limitations, and cost structures. Nonetheless, they represent crucial pathways toward achieving a decarbonised shipping industry. By extending the model to accommodate these alternative fuels, it could serve as a robust optimisation tool to support the efficient and sustainable operation of future maritime fuel supply chains.

3.8.2 Transition to Environmentally Constrained Optimisation

While the proposed model successfully addresses the operational complexities of LNG supply chain portfolio optimisation, it was deliberately formulated as an economically driven baseline. Having established a robust computational framework for profit maximisation, the critical next step is to expand this formulation to address the pressing industry mandate of environmental sustainability. Given the significant role of maritime transport in the global logistics of LNG and the increasing international regulatory pressure to reduce greenhouse gas emissions, modern decision-support tools must evolve beyond purely economic objectives to incorporate strict environmental indicators.

In particular, recent short-term regulations introduced by the IMO notably the Energy Efficiency Existing Ship Index (EEXI) and the Carbon Intensity Indicator (CII), which came into force in 2023 highlight the urgent need for models that integrate environmental compliance. While the EEXI addresses the technical energy efficiency

of ship engines, the CII focuses on operational efficiency, quantified by annual fuel consumption and the total distance sailed. Because the CII has a direct, rigid link to voyage planning, speed selection, and operational idle times, it represents a fundamental shift in how fleets must be managed.

Therefore, rather than treating environmental compliance as separate from logistical efficiency, the following chapter (Chapter 4) will directly extend the mathematical model and metaheuristic algorithm developed here. By integrating CII constraints into the established framework, the thesis will assess exactly how emission-related thresholds alter portfolio optimisation and delivery planning. In doing so, the research transitions this economically powerful baseline model into a comprehensive, regulation-compliant decision-support tool for the modern maritime industry.

CHAPTER 4 OPERATONAL TRADE-OFFS IN LNG SHIPPING UNDER CARBON INTENSITY REGULATION: A DATA-DRIVEN EVALUATION OF PORTFOLIO AND ROUTING STRATEGIES

Summary

In response to global climate objectives, the IMO has introduced a series of short-term regulatory measures aimed at decarbonising maritime transport. Among these, the EEXI and the CII represent key initiatives. While the EEXI pertains to the technical efficiency of a vessel's propulsion system, the CII addresses operational efficiency and is calculated based on the total fuel consumed and the distance sailed over a calendar year. Although alternative environmental and economic metrics were considered such as EEOI and AER, they often serve as voluntary guidelines, historical precursors, or regional financial mechanisms.

Given CII's mandatory global enforcement, strong operational relevance and direct impact on voyage planning and scheduling decisions, the CII is selected for integration into the extended version of the optimisation model, as introduced in the previous chapter. This chapter builds upon that foundation by investigating the implications of CII implementation on LNG portfolio optimisation within the framework of ADP.

To this end, a MILP model is applied to realistic data provided by a commercial partner. This allows for the evaluation of trade-offs between economic performance and environmental compliance. Furthermore, the previously developed metaheuristic algorithm has been enhanced to incorporate CII constraints, thereby enabling large-scale instances to be solved more efficiently while ensuring adherence to emerging environmental standards. The results presented in this chapter provide insights into how CII regulations influence supply chain decisions, fleet deployment, and overall profitability in the LNG shipping context.

4.1 Introduction

The primary aim of this chapter is to extend the previously developed MILP model to present a more comprehensive approach to LNG portfolio optimisation by integrating environmental considerations,

specifically the CII. To complement the MILP model and address the computational challenges of large-scale, real-world instances, the previously developed metaheuristic algorithm is also enhanced to incorporate the CII framework. This ensures that the proposed approach remains scalable, robust, and practically applicable within the operational complexities of the LNG supply chain. To the best of the author's knowledge, no existing research has yet incorporated the CII metric within a portfolio optimisation framework for LNG delivery planning, nor evaluated its implications for profitability and operational feasibility. The importance of incorporating the CII into portfolio optimisation lies in the critical role maritime shipping plays in global trade, accounting for approximately 90% of international merchandise transport by volume (IMO, 2011).

The IMO has introduced a series of regulatory measures to mitigate greenhouse gas emissions from maritime transport, encompassing both technical and operational frameworks. While technical indices such as the Energy Efficiency Design Index (EEDI) and the Energy Efficiency Existing Ship Index (EEXI) are fundamental to the global decarbonisation agenda, they are static, design-based metrics that relate strictly to a vessel's physical specifications. In contrast, the CII stands out as a dynamic, operational metric that assesses the annual carbon intensity of vessels based on actual deployment. Because the core focus of this thesis is on operational decision-making, the CII is explicitly integrated into the framework. Given its direct, mathematical relationship with voyage planning, fuel consumption, and dynamic vessel scheduling, the CII is the only IMO metric directly influenced by the model's decision variables. Therefore, its integration into the extended delivery planning and portfolio optimisation model is both highly relevant and practically necessary. This chapter evaluates the implications and constraints that CII introduces to the portfolio optimisation problem. The aim is to provide a comprehensive understanding of how environmental regulations impact operational and economic decisions, ultimately supporting decision-makers in aligning profitability with sustainability objectives.

The remainder of this chapter is structured as follows. Section 4.2 briefly go through the complexity of integrating CII in the LNG Portfolio Framework, section 4.3 introduces the extended MILP model developed for LNG portfolio optimisation within the context of ADP, incorporating the CII. Section 4.4 presents the model validation results using a range of problem instances. The improved metaheuristic algorithm, adapted to account for CII constraints, is detailed in Section 4.5. Section 4.6 offers a comprehensive discussion of the analytical results. Finally, Section 4.7 concludes the chapter with key findings and implications.

4.2 The Complexity of Integrating CII Constraints

Transitioning from the economically driven baseline model (Chapter 3) to a regulation-compliant framework introduces significant mathematical and operational complexities. Firstly, the introduction of the Carbon Intensity Indicator (CII) shifts the optimisation from independent voyage routing to highly interdependent annual scheduling. Because the CII is an annual, cumulative metric, the model must now evaluate the cascading impact of individual voyage decisions on the fleet's year-end compliance rating. Secondly, integrating these stringent environmental thresholds drastically reduces the feasible solution space. The metaheuristic algorithm must navigate a much tighter set of constraints, as many highly profitable routing combinations are rendered infeasible due to emissions violations. Finally, the CII framework introduces a severe penalty for vessel idleness; while the baseline model could leverage idle time for economic advantage, under CII, idling generates emissions without accumulating distance, thereby severely degrading the vessel's rating. Consequently, incorporating the CII requires a fundamentally more sophisticated balancing of conflicting economic and environmental objectives.

4.3 Extended MILP Formulation Incorporating the Carbon Intensity Indicator (CII)

This chapter is dedicated to the integration of the CII regulation into the previously developed MILP model. It explores how this short-term regulatory measure, introduced by the IMO, can be effectively embedded within a portfolio optimisation framework for the global delivery of cryogenic fuels specifically LNG. The following sections detail the rationale for incorporating the CII into delivery planning and outline the implications of its inclusion on operational and strategic decision-making. The extended model retains its primary objective of maximising overall profit across an annual delivery programme, while simultaneously addressing the additional constraint imposed by the CII metric. In doing so, it continues to optimise key operational elements such as vessel-to-cargo allocation, supplier-customer pairings, and voyage routing and scheduling. However, with the CII constraint now in place, the model is required to deliver an optimal portfolio that not only meets economic goals but also remains compliant with emerging environmental regulations.

The extended model captures the economic intricacies of the LNG supply chain by aiming to minimise total operational costs, which include chartering expenses, fuel consumption, boil-off losses, port charges, and the additional costs associated with vessel ratings under the CII regulation. Simultaneously, it ensures that all delivery commitments are fulfilled within the defined time windows. By integrating these operational and regulatory elements into a unified optimisation framework, the model offers robust, data-driven decision support that mirrors the scale and complexity of real-world LNG logistics. The overarching objective is to equip shipping companies with the tools to improve operational efficiency and profitability through strategic planning and optimised resource allocation now further aligned with the IMO's newly enforced short-term decarbonisation measures.

4.3.1 **Problem Statement and Contributions**

The CII is an operational metric introduced by the IMO for vessels over 5,000 Gross Tonnage (GT). Developed from the earlier Energy Efficiency Operational Indicator (EEOI), the CII has become mandatory for existing ships from 2023 onwards (Ten, et al., 2023). It functions as a regulatory mechanism aimed at limiting CO_2 emissions from maritime transport. The CII quantifies a vessel's emissions performance by measuring the mass of CO_2 emitted per unit of transport work typically defined as either the cargo mass or deadweight tonnage transported over a given distance (IMO, 2021a; ClassNK, 2022).

The performance of each vessel is then benchmarked against a required CII value, derived from a reference line adjusted annually by a reduction coefficient. This reduction factor is designed to tighten progressively, increasing from 5% in 2023 to 11% by 2026, with an annual increment of 2% (IMO, 2022b). As such, shipowners are required to continuously improve the operational efficiency of their fleets to remain compliant with these evolving targets (Yuan, et al., 2023).

Vessels are rated annually on a five-point scale from A to E, where 'A' indicates superior performance and 'E' represents the lowest rating (IMO, 2022a). A vessel that receives a D rating for three consecutive years, or an E rating in a single year, is mandated to submit a corrective action plan as part of its Ship Energy Efficiency Management Plan (SEEMP). This plan must outline the steps to improve performance to at least a C rating in

subsequent years. Vessels that remain non-compliant are expected to revise their operations accordingly before they can continue service (Qi, et al., 2021).

Despite increasing attention to decarbonisation in maritime logistics, current portfolio management models particularly those focused on LNG largely neglect the integration of newly introduced short-term regulatory measures such as the CII. Given that the CII is calculated based on both the annual sailing distance and fuel consumption (including time spent sailing or idle), its inclusion in delivery and fleet planning may impose significant constraints and alter operational decisions.

To address this gap in the literature, the previously developed MILP model is extended to incorporate CII constraints directly into the portfolio optimisation process. This extension aims to equip decision-makers with a more comprehensive view of how fleet performance under CII influences delivery strategies, customer fulfilment, and overall profitability.

Achieving optimal performance under the CII framework necessitates the simultaneous consideration of several interdependent variables within the LNG supply chain, including:

- Vessel-specific attributes (e.g., contractual status, capacity, boil-off rates in laden and ballast legs, fuel consumption rate in different modes, loading factor, capacity, and DWT).
- Operational constraints (e.g., loading/discharging time window, port charges).
- LNG market dynamics (e.g., supplier-specific price and calorific values).
- Port–vessel compatibility.
- Minimum and maximum delivery thresholds per shipment.

To this end, CII performance thresholds are explicitly embedded within the extended optimisation framework. This enables more responsive, regulation-compliant planning while maintaining economic efficiency. The enhanced model thus serves as a robust decision-support tool, helping stakeholders navigate regulatory impacts, adjust delivery schedules, and manage operational costs.

By incorporating environmental constraints directly into portfolio optimisation, this research offers a novel, systems-level approach that aligns LNG shipping logistics with global decarbonisation mandates facilitating sustainable planning and improved regulatory compliance across the maritime sector.

4.3.2 **MILP – Incorporating CII in Portfolio Optimisation**

This extended model builds upon the mathematical framework developed in Chapter 3. The original model was designed to optimise an annual delivery plan for LNG by determining optimal supplier–customer pairings (cargo matching), vessel allocation, voyage scheduling, and routing while operating under a comprehensive set of operational and economic constraints. The objective was to maximise overall profit within the context of LNG portfolio optimisation for ADP.

In its initial formulation, the model made decisions concerning cargo pairing, the quantity of LNG to be loaded and discharged, the timing of loading and unloading operations, and the allocation of vessels to each supplier–customer pair. It also monitored inventory levels at all stages of the vessel's journey from arrival at the port, through the loading phase, to the completion of the return ballast leg. However, a key limitation of the original model was its omission of environmental considerations, specifically the CII ratings of the vessels participating in the delivery plan.

To address this gap, the current work extends the model through a series of modifications, with particular emphasis on the integration of the CII regulatory framework as defined by the IMO. In this study CII regulation are implemented as soft constraints linked to rating assignments rather than hard feasibility cuts. This enhancement enables the model to reflect not only economic and operational efficiency but also environmental compliance thereby offering a more holistic and regulation-aware approach to LNG delivery planning. These enhancements are introduced to embed environmental considerations directly into the optimisation framework, thereby enabling more informed decision-making that effectively balances economic performance with regulatory compliance. Selected constraints are revised, or new ones are developed, and the objective function is adapted to reflect CII-related criteria. The objective of these modifications is to enhance the environmental sustainability of the model's outcomes, without compromising its foundational operational goals.

To incorporate the CII into the mathematical formulation, it is essential to account for both the total distance travelled by each vessel and the corresponding fuel consumption. These variables are internally determined by the model and are crucial for identifying optimal supplier–customer pairings, selecting vessels that deliver superior CII ratings, or simultaneously coordinating these decisions in a manner that yields optimal environmental and economic performance.

The key goal of this study is to achieve improved CII ratings for the vessels deployed, while also maximising portfolio profitability by jointly optimising operational and environmental constraints. The following section outlines the necessary parameters, decision variables, and constraints required to compute the CII rating of each vessel within the extended optimisation model.

4.3.3 **Carbone Intensity Indicator (CII) Compliance**

The motivation for extending the original model stems from the imperative to comply with the IMO's CII regulations, introduced under MARPOL Annex VI (IMO, 2021a). These regulations mandate a progressive reduction in the operational carbon intensity of ships between 2023 and 2030, with annual performance ratings assigned on a five-point scale from A (most efficient) to E (least efficient). Incorporating CII compliance into LNG delivery planning is therefore essential not only to ensure regulatory conformity but also to mitigate the operational and financial risks associated with poor carbon ratings (categories D or E), such as mandatory corrective actions or potential limitations on commercial activity (IMO, 2022c).

The inclusion of CII constraints introduces a pivotal change to the model's objective function, which in its earlier formulation was solely focused on maximising profit. In the extended model, the objective must now strike a balance between economic gains (e.g., voyage profitability and cargo throughput) and environmental performance, as quantified by each vessel's attained CII rating. This dual objective is operationalised through the integration of new constraints and objective function components, ensuring that vessel selection, routing, and scheduling decisions not only support profitability but also contribute to maintaining favourable CII ratings ideally within categories A to C.

This shift reflects a multi-objective approach, aligned with the evolving regulatory landscape in maritime logistics, where operational efficiency and environmental responsibility are increasingly interdependent priorities.

To incorporate CII compliance into the existing optimisation framework, several new parameters and decision variables are introduced. These additions capture key attributes including voyage-specific fuel consumption, sailing distance, vessel capacity, and regulatory benchmarks. Together, these elements enable the model to compute each vessel's attained CII, compare it against the required CII, and assign an annual performance rating accordingly.

The newly introduced model components include:

Parameters:

$\boldsymbol{CF}$	*Conversion factor between fuel consumption and CO_2 emission*
$\boldsymbol{EC_{(A-E)}}$	*Estimated environmental cost per rating*
$\boldsymbol{CII^{v}_{(A-D)}}$	*CII thresholds to label vessel v according to their CO_2 emission performance*
$\boldsymbol{DWT_v}$	*Dead weight tonnage of vessel v*
$\boldsymbol{fuel_v^{consumption\ idle}}$	*Fuel consumption rate of vessel v while it is idle*
$\boldsymbol{fuel_{vi}^{consumption}}$	*Fuel consumption rate of vessel v while transporting cargo i*
$\boldsymbol{fuel_v^{consumption\ operation}}$	*Fuel consumption rate of vessel v in loading/discharging duration*

Variables:

$\boldsymbol{etA_v}\begin{cases}\mathbf{1}\\\mathbf{0}\end{cases}$	*if vessel $\boldsymbol{v}$ is environmentally recognised to fall into category A* *otherwise*
$\boldsymbol{etB_v}\begin{cases}\mathbf{1}\\\mathbf{0}\end{cases}$	*if vessel v is environmentally recognised to fall into category B* *otherwise*
$\boldsymbol{etC_v}\begin{cases}\mathbf{1}\\\mathbf{0}\end{cases}$	*if vessel v is environmentally recognised to fall into category C* *otherwise*
$\boldsymbol{etD_v}\begin{cases}\mathbf{1}\\\mathbf{0}\end{cases}$	*if vessel v is environmentally recognised to fall into category D* *otherwise*

$\boldsymbol{etE_v}\begin{cases}\mathbf{1}\\\mathbf{0}\end{cases}$	*if vessel v is environmentally recognised to fall into category E* *otherwise*
$\boldsymbol{em_{iv}}$	*Produced emission for vessel v after departing from location i*
$\boldsymbol{Distance_{vi}}$	*Distance travelled by vessel v for cargo i in nautical miles*

4.3.3.1 Operational Carbon Intensity Indicator (CII) for Individual Ships

In accordance with the IMO Guidelines on the Operational Carbon Intensity Indicator of Individual Ships for the implementation of Regulation 28 of MARPOL Annex VI (2021a), the attained annual operational CII of a ship is calculated in its simplest form as the ratio between the total mass of carbon dioxide (M) emitted and the total transport work (W) performed during a given calendar year:

$$Attained\ CII_{ship} = \frac{M}{W}$$

The mass of CO_2 emissions (M) represents the total amount of CO_2, in grams, generated from all fuel oil consumed on board a vessel over a given calendar year. It is calculated as the sum of CO_2 emissions from each type of fuel used, as follows:

$$M = FC_f \times CF_f$$

where:

f is the fuel oil type.
FC_f is the total mass (in grams) of consumed fuel oil of type in the calendar year, as reported under IMO DCS; and
CF_f represents the fuel oil mass to CO_2 mass conversion factor for fuel oil type

To calculate the transport work (W), in the absence of data on actual transport work, the supply-based transport work (W_s) may be used as a proxy. It is defined as the product of a ship's capacity and the total distance travelled over a given calendar year, as follows:

$$W_s = C \times D_t$$

where:

C represents the ship's capacity:

For bulk carriers, tankers, container ships, gas carriers, LNG carriers, general cargo ships, refrigerated cargo carrier and combination carriers, deadweight tonnage (DWT) should be used as Capacity (IMO, 2022a).

D_t represents the total distance travelled (in nautical miles), as reported under IMO DCS.

In alignment with these IMO guidelines, this study integrates the calculation of each vessel's CII into the broader portfolio optimisation framework. The total fuel consumption used to compute M encompasses all operational modes, including periods of sailing, berthing, and idling. By incorporating the full operational fuel profile, the model ensures accurate representation of each vessel's environmental performance within the optimisation process.

For the purposes of this study, Light Fuel Oil (LFO) is assumed to be the primary fuel type utilised by all vessels within the fleet. Fuel consumption is estimated as a function of the duration of vessel activity across distinct operational phases, including idling (during both laden and ballast legs), port operations (at loading and discharging terminals), and transit during the sailing phase. The aggregate fuel consumption (in grams), which serves as the basis for calculating the CII, is determined as follows:

$$\sum_{j=1}^{J} \begin{pmatrix} fuel_{vj}^{consumption} + \left(IT_{vj}^{Balalst} + IT_{vj}^{Laden}\right) \times fuel_{v}^{consumption\ idle} \\ + \left(ST_{vj}^{load} + ST_{vj}^{unload}\right) \times fuel_{v}^{consumption\ operation} \end{pmatrix} \times 10^{6}$$

Transport work is calculated based on the carrying capacity of each vessel. In the context of this study, which focuses on LNG portfolio optimisation, capacity is represented by the DWT of each vessel, denoted as (C). The total distance travelled, measured in nautical miles for each vessel, is determined through Constraints (18) – (20) outlined in section 4.2.3.3. Accordingly, the total transport work is expressed as follows:

$$D_t = \sum_{j=1}^{J} Distance_{vj}$$

The final expression for the $Attained\ CII_{ship}$ per vessel is given by the following formula:

$$\frac{\sum_{j=1}^{J}\left(\begin{matrix} fuel_{vj}^{consumption} + \left(IT_{vj}^{Balalst} + IT_{vj}^{Laden}\right) \times fuel_{v}^{consumption\ idle} \\ + \left(ST_{vj}^{load} + ST_{vj}^{unload}\right) \times fuel_{v}^{consumption\ operation} \end{matrix}\right) \times CF \times 10^{6}}{DWT_{v} \times \left(\sum_{j=1}^{N} Distance_{vj}\right)}$$

4.3.3.2 **Operational CII Reference Line**

Having established the attained CII for each vessel in the fleet, it is essential to benchmark these values against a standard reference to evaluate their relative environmental performance. To this end, the IMO defines an operational CII reference line, denoted as:

$$CII_{ref} = \alpha\ Capacity^{-c}$$

This reference line represents the median operational carbon intensity performance of a specified group of ships, expressed as a function of vessel capacity, using data from the year 2019 as the baseline. In the context of this study, the reference line serves as a benchmark against which the attained CII of each LNG vessel is compared. By contrasting the attained CII with the corresponding CII_{ref}, we can assess whether a vessel's emissions performance exceeds, matches, or falls short of the industry standard. This comparison is critical not only for compliance evaluation but also for guiding vessel allocation and routing decisions within the optimisation model to enhance both environmental and operational outcomes. Here, CII_{ref} denotes the reference value for the year 2019. The variable *Capacity* corresponds to the same measure defined in the specific CII for the relevant ship type (DWT in the case of LNG carriers) as summarised in Table 4.1. The parameters $\boldsymbol{a}$ and $\boldsymbol{c}$ are estimated using median regression analysis, based on the attained CII values and capacities of individual ships as reported in the IMO Data Collection System (DCS) for the year 2019. This regression yields a reference curve against which the carbon performance of contemporary vessels can be evaluated.

Table 4.1: Parameters for determining the 2019 ship type specific reference lines

	Ship Type	***Capacity***	***a***	***c***
LNG Carrier	100,000 DWT and above	DWT	9.827	0.000
	65,000 DWT and above, but less than 100,000 DWT	DWT	14479E10	2.673

	less than 65,000 DWT	65,000	14779E10	2.673

4.3.3.3 **CII Reduction Factor**

To ensure continuous improvement in environmental performance, the required annual operational CII for each ship type incorporates a progressive reduction factor, as mandated under Regulation 28 of MARPOL Annex VI. This requirement establishes a trajectory of increasing stringency between 2023 and 2030. The required CII is calculated using the following expression:

$$Required\ annual\ Operational\ CII\ = \left(1 - \frac{z}{100}\right) \times CII_{ref} \quad (1)$$

In this formula, CII_{ref} refers to the 2019 reference value, as defined in the IMO Guidelines on the Reference Lines for Use with Operational Carbon Intensity Indicators (IMO, 2022a). The variable z represents the reduction factor, which reflects the percentage reduction in carbon intensity required for a given year. These reduction factors are specified for different ship types and years in Table 4.2, with values gradually increasing from 2023 to 2030. This mechanism encourages ship operators to progressively lower their carbon intensity over time, thereby aligning operational practices with broader decarbonisation objectives set by the IMO.

Table 4.2: Reduction factor (Z%) for the CII relative to the 2019 reference line

Year	Reduction Factor relative to 2019 (%)
2023	5
2024	7
2025	9
2026	11
2027	- **
2028	- **
2029	- **
2029	- **

** Z factors for the years of 2027 to 2030 to be further strengthened and developed considering the review of the short-term measure.

4.3.3.4 **CII Rating**

In accordance with Regulation 28 of MARPOL Annex VI, an operational energy efficiency performance rating must be assigned annually to each ship subject to the regulation (IMO, 2021a). This rating is determined in a transparent and robust manner, based on the deviation of a ship's attained annual operational CII from its required annual CII value. To facilitate this rating process, the IMO has defined a five-grade scale (A to E), applied for each year from 2023 to 2030 (IMO, 2022c). This system is based on four boundaries: the superior boundary, lower boundary, upper boundary, and inferior boundary. By comparing the attained CII of a vessel against these boundary values, a corresponding rating can be assigned.

These boundaries are derived from the distribution of attained CIIs of individual ships in the baseline year of 2019. The intention is to ensure that the ratings reflect relative performance across the global fleet. Specifically:

- The middle 30% of vessels (in terms of attained CII) are assigned a C rating.
- The upper 20% and the next upper 15% receive D and E ratings, respectively.
- The lower 20% and next lower 15% are assigned B and A ratings, respectively.

This distribution-based structure is illustrated in Figure 4.1.

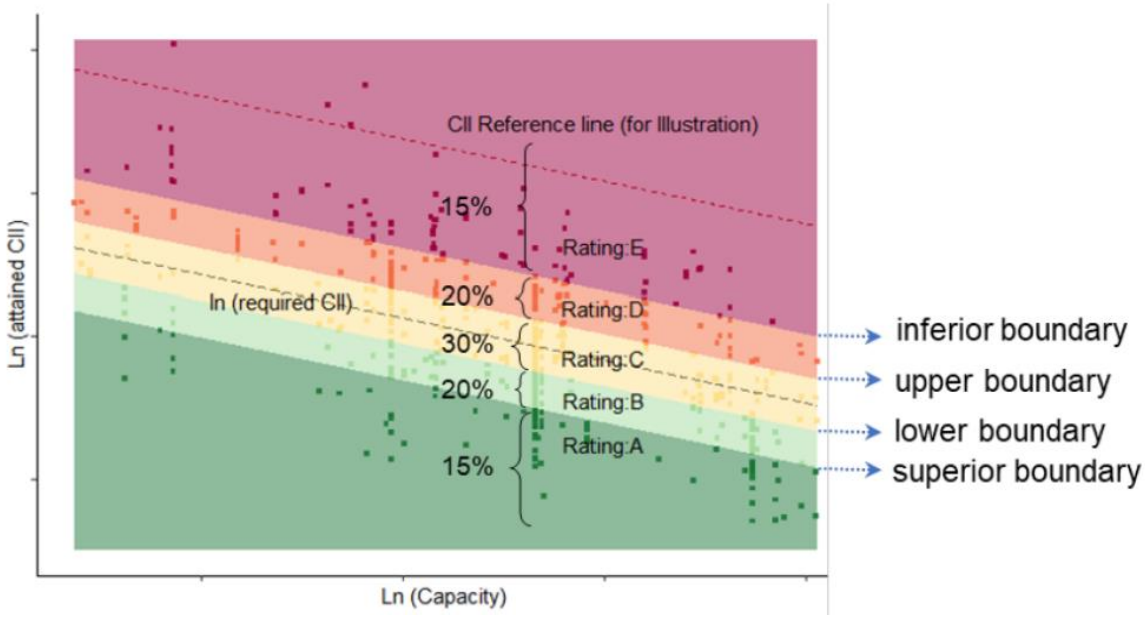

Figure 4.1: Operational energy efficiency performance rating scale (IMO, 2022c)

The four boundary values are formulated as exponential adjustments to the $Required\ CII$, as follows:

$$\text{superior boundary} = \exp(d_1) \times Required\ CII$$

$$\text{lower boundary} = \exp(d_2) \times Required\ CII$$

$$\text{upper boundary} = \exp(d_3) \times Required\ CII$$

$$\text{inferior boundary} = \exp(d_4) \times Required\ CII$$

Here, d_1 , d_2 , d_3, d_4 are empirically determined parameters derived from the 2019 CII distribution data, ensuring consistency in rating thresholds across years. The estimated vectors after exponential transformation for determining the rating boundaries of LNG carriers are as follows:

Table 4.3 : dd vector value for LNG ships

Ship type		**Capacity in CII calculation**	***dd* vectors (after exponential transformation)**			
			$\exp(d_1)$	$\exp(d_2)$	$\exp(d_3)$	$\exp(d_4)$
LNG carriers	100,000 DWT and above	DWT	0.89	0.98	1.06	1.13
	less than 100,000 DWT		0.78	0.92	1.10	1.37

4.3.3.5 **Attained CII**

Consequently, if the objective is to ensure that all vessels within the fleet operate at or above a designated performance threshold such as maintaining a rating of C or higher the required annual operational CII must be appropriately adjusted. This adjustment ensures that each vessel's attained CII remains below the acceptable upper boundary associated with the selected rating. Incorporating this regulatory constraint into the optimisation framework allows the model to enforce compliance with IMO decarbonisation targets, while simultaneously pursuing operational and economic objectives. In doing so, the model ensures that environmental performance is not treated as an isolated evaluation metric but is instead embedded directly into the core decision-making process of LNG portfolio optimisation.

$$\frac{\Sigma_{j=1}^{J}\begin{pmatrix} fuel_{vj}^{consumption} + \left(IT_{vj}^{Balalst} + IT_{vj}^{Laden}\right) \times fuel_{v}^{consumption\ idle} \\ + \left(ST_{vj}^{load} + ST_{vj}^{unload}\right) \times fuel_{v}^{consumption\ operation} \end{pmatrix} \times CF \times 10^{6}}{DWT_{v} \times \left(\sum_{j=1}^{N} Distance_{vj}\right)} < Required\ CII_{year} \times exp(d_{1-4}) \quad (2)$$

By replacing the required CII reference and the boundary limits to the above equation for the 2025 CII calculation, we will have:

$$\frac{\Sigma_{j=1}^{J}\begin{pmatrix} fuel_{vj}^{consumption}+\left(IT_{vj}^{Balalst}+IT_{vj}^{Laden}\right)\times fuel_{v}^{consumption\ idle} \\ +\left(ST_{vj}^{load}+ST_{vj}^{unload}\right)\times fuel_{v}^{consumption\ operation} \end{pmatrix}\times CF\times 10^{6}}{DWT_{v}\times\left(\sum_{j=1}^{N} Distance_{vj}\right)} < \left(1-\frac{z}{100}\right)\times CII_{ref}\times\ exp(d_{1-4}) \quad (3)$$

For the year 2025, the reduction factor z , as specified in Table 4.2, is equal to 9%. Given that all vessels considered in this study have a DWT between 65,000 and 100,000 (Table 4.3), the corresponding reference line for the CII applies to this specific DWT range. Accordingly, the required annual operational CII for 2025 is calculated using the following formulation:

$$\frac{\Sigma_{j=1}^{J}\begin{pmatrix} fuel_{vj}^{consumption}+\left(IT_{vj}^{Balalst}+IT_{vj}^{Laden}\right)\times fuel_{v}^{consumption\ idle} \\ +\left(ST_{vj}^{load}+ST_{vj}^{unload}\right)\times fuel_{v}^{consumption\ operation} \end{pmatrix}\times CF\times 10^{6}}{DWT_{v}\times\left(\sum_{j=1}^{N} Distance_{vj}\right)} < 0.91\ \times \alpha_{V}\ DWT^{-C_V}\times\ exp(d_{1-4}) \quad (4)$$

According to the Table 4.1, the α and c is equal to 14479E10 and 2.673 respectively, so the final equation would be:

$$\frac{\Sigma_{j=1}^{J}\begin{pmatrix} fuel_{vj}^{consumption}+\left(IT_{vj}^{Balalst}+IT_{vj}^{Laden}\right)\times fuel_{v}^{consumption\ idle} \\ +\left(ST_{vj}^{load}+ST_{vj}^{unload}\right)\times fuel_{v}^{consumption\ operation} \end{pmatrix}\times CF\times 10^{6}}{DWT_{v}\times\left(\sum_{j=1}^{N} Distance_{vj}\right)} < 0.91\times 14479E10\times DWT_{v}{}^{-2.673}\times\ exp(d_{1-4}) \quad (5)$$

The numerator of the fraction represents the total amount of fuel consumed. When multiplied by the fuel-specific conversion factor (CF) and 10^6, it yields the total mass of CO_2 emissions, expressed in grams. This expression can be replaced by $\sum_{i=1}^{N} em_{jv}$ which denotes the total emissions produced by vessel v across all delivery activities and by replacing the other side of the equation with $CII_{(A-D)}^{v}$, the final formulation, tailored for integration into our optimisation model, becomes:

$$Attained\ CII_{year} = \frac{\sum_{j=1}^{N} em_{jv}}{\left(\sum_{j=1}^{N} DWT_{v}\times Distance_{vj}\right)} < CII_{(A-D)}^{v} \quad (6)$$

4.3.3.6 **Model Extensions for CII Compliance**

To reflect the trade-off between economic performance and environmental responsibility, the original objective function designed solely to maximise the profit of the LNG delivery plan has been extended by introducing an

environmental cost component. This new term accounts for the carbon intensity of each vessel, expressed through its fuel consumption, and penalises high-emission operational plans accordingly.

Specifically:

Environmental cost has been introduced as a function of Vessel Ratings, which contributes directly to the attained CII.

The fuel consumption index has been reformulated from a general aggregate to a per cargo–vessel basis, allowing for finer granularity and more accurate tracking of emissions per shipment.

The modified objective function is expressed as:

$$MaxZ = Total\ Profit - \sum_{i=1}^{N}\sum_{v=1}^{V}\left(FC \times fuel_{vi}^{consumption}\right) - \sum_{v=1}^{V}(EC_A \times etA_v + EC_B \times etB_v + EC_C \times etC_v + EC_D \times etD_v + EC_E \times etE_v) \quad (7)$$

Where:

$Total\ Profit$ represents the revenue from delivered LNG cargoes minus operational costs except fuel consumption of the vessel on its journey (Chapter1)

$fuel_{vi}^{consumption}$ is the total fuel consumption of the vessel on her journey for delivering a cargo

$EC_{(A-E)}$ is a penalty factor that allows calibration of the importance of environmental costs relative to profit (e.g., sensitivity analysis can vary $EC_{(A-E)}$ to test different environmental priorities).

By indexing fuel consumption to individual cargo–vessel pairs, the model now captures the environmental performance of each routing and allocation decision, enabling the optimisation process to favour more carbon-efficient vessel deployment without compromising profitability.

Subjected to:

$$fuel_{vj}^{consumption} + BigM \times \left(2 - x_{ijv} - g_{pj}\right) \geq \sum_{s=1}^{S}[(D_{pi} \times C_{vs}^{ballast} \times z_{is}) + (D_{pj} \times C_{vs}^{laden} \times z_{js})] \qquad \forall i > 1, v, j > 1, p \quad (8)$$

$$fuel_{vj}^{consumption} + BigM \times (2 - x_{1jv} - g_{pj}) \geq \sum_{s=1}^{S}\left[\left(D_{vp}^{livelocation} \times C_{vs}^{ballast} \times z_{1s}\right) + \left(D_{pj} \times C_{vs}^{laden} \times z_{js}\right)\right] \quad \forall v, j > 1, p \quad (9)$$

$$em_{jv} + BigM(1 - U_v) \geq \left[fuel_{vj}^{consumption} + \left(IT_{vj}^{Balalst} + IT_{vj}^{Laden}\right) \times fuel_{v}^{consumption\ idle} + \left(ST_{vj}^{load} + ST_{vj}^{unload}\right) \times fuel_{v}^{consumption\ operation}\right] \times CF \times 10^{6} \quad \forall v, j \quad (10)$$

$$Distance_{vj} \leq BigM \times \left(\sum_{i=1}^{I} x_{ijv}\right) \quad \forall j > 1, p \quad (11)$$

$$Distance_{vj} \leq \sum_{p=1}^{P}\left(D_{pi} + D_{pj}\right) \times g_{pj} + BigM \times \left(1 - x_{ijv}\right) \quad \forall i > 1, v, j > 1 \quad (12)$$

$$Distance_{vj} \leq \sum_{p=1}^{P}\left(D_{vp}^{livelocation} + D_{pj}\right) \times g_{pj} + BigM \times \left(1 - x_{1jv}\right) \quad \forall v, j > 1 \quad (13)$$

$$CII_A^v \times DWP_v \times \left(\sum_{j=1}^{N} Distance_{vj}\right) + BigM \times (1 - etA_v) \geq \sum_{i=1}^{N} em_{jv} \quad \forall v = 1, \ldots, V \quad (14)$$

$$CII_B^v \times DWP_v \times \left(\sum_{j=1}^{N} Distance_{vj}\right) + BigM \times (1 - etB_v) \geq \sum_{i=1}^{N} em_{jv} \quad \forall v = 1, \ldots, V \quad (15)$$

$$CII_C^v \times DWP_v \times \left(\sum_{j=1}^{N} Distance_{vj}\right) + BigM \times (1 - etC_v) \geq \sum_{i=1}^{N} em_{jv} \quad \forall v = 1, \ldots, V \quad (16)$$

$$CII_D^v \times DWP_v \times \left(\sum_{j=1}^{N} Distance_{vj}\right) + BigM \times (1 - etD_v) \geq \sum_{i=1}^{N} em_{jv} \quad \forall v = 1, \ldots, V \quad (17)$$

$$etA_v + etB_v + etC_v + etD_v + etE_v = u_v \quad \forall v = 1, \ldots, V \quad (18)$$

In the extended optimisation model, Constraints (8) and (9) are formulated to estimate the total fuel consumption for each vessel assigned to cargo delivery operations. These constraints account for both laden and ballast legs, capturing fuel used during active transportation and repositioning voyages, respectively. Constraint (10) aggregates the total emissions generated from fuel consumption, incorporating not only the emissions from sailing but also from port operations and idle periods, provided that a vessel is allocated to a delivery task. This holistic view ensures that the model captures all operational phases contributing to annual CO_2 emissions. To support the calculation of transport work, which is required for determining the CII. Constraints (11) through (13) compute the total distance travelled by each vessel across its voyages. This distance is then multiplied by

the vessel's deadweight tonnage (used as a proxy for capacity in the case of LNG carriers) to estimate the supply-based transport work.

Following the estimation of fuel consumption and distance travelled, the model assigns a CII rating to each vessel based on its annual operational carbon performance. Constraints (14) to (17) govern this classification process by comparing each vessel's attained CII against IMO-defined thresholds for performance bands A through D (denoted as $CII^{v}_{(A-D)}$). These constraints ensure that only one appropriate rating is applied per vessel, reflecting its emission efficiency over the planning horizon.

To enforce rating exclusivity, Constraint (18) mandates that each operational vessel must receive exactly one CII rating, thereby prevent dual classification and ensure consistency in regulatory reporting and planning.

In this study, all vessels are assumed to operate exclusively on LFO also referred to as marine gasoil. This assumption directly impacts the CO_2 emission calculations, as the fuel-specific carbon conversion factor ($\boldsymbol{CF}$) for LFO is applied across all vessels in the model. The use of a consistent fuel type ensures comparability of CII ratings across the fleet and allows for an accurate reflection of operational inefficiencies stemming from both voyage planning and vessel allocation decisions. Thus, the model not only evaluates economic viability but also supports regulatory compliance by quantifying and constraining environmental impact within the decision-making process.

4.4 Experimental Result of Extended MILP model (CII included)

To evaluate the operational and environmental implications of incorporating the CII rating into fleet optimisation, a set of representative problem instances is selected. These instances are specifically chosen based on their ability to reach an optimality gap of zero using an exact solution method, ensuring that observed variations in outputs could be attributed solely to the presence or absence of CII-related constraints rather than computational limitations. This methodological consistency provides a robust foundation for comparative analysis against baseline scenarios where environmental considerations are excluded.

Each instance is evaluated under ten distinct experimental scenarios. Scenario 0 served as the baseline, wherein the optimisation model operates without any CII constraints. In Scenarios 1 through 9, a progressive penalty

structure is introduced for vessels failing to attain an 'A' rating, representing increasing regulatory pressure or internal sustainability targets. This staged penalty structure allows a controlled observation of the model's adaptive behaviour under escalating environmental requirements, thereby simulating a reasonable regulatory tightening in future policy trajectories. The penalty amount is provided in Table 4.4. there is no penalty associated to rating A, while for other rating the penalty amount is increasing scenario by scenario to see how model reacts to these costs.

Table 4.4: Associated Penalty Cost ($) of CII rating of each Scenario

Scenario No.	Rating A	Rating B	Rating C	Rating D	Rating E
0	0	0	0	0	0
1	0	550,000	1,650,000	2,750,000	3,850,000
2	0	700,000	2,100,000	3,500,000	4,900,000
3	0	950,000	2,850,000	4,750,000	6,650,000
4	0	1,300,000	3,900,000	6,500,000	9,100,000
5	0	1,750,000	5,250,000	8,750,000	12,250,000
6	0	2,300,000	6,900,000	11,500,000	16,100,000
7	0	2,950,000	8,850,000	14,750,000	20,650,000
8	0	3,700,000	11,100,000	18,500,000	25,900,000
9	0	4,550,000	13,650,000	22,750,000	31,850,000

The Size of each example that has been solved with exact method solution is provided in Table 4.5. All instances are solved until a zero-optimality gap was reached, using the CPLEX commercial solver (version 22.1.1) under its default settings.

Table 4.5: Size of Exact method examples solved by CPLEX

No.	Size (S, C, V, SL, T)	No of Binary Variables	No of Continuous Variables	No of Constraints
1	(3, 5, 6, 2, 20)	558	724	6,979
2	(3, 5, 6, 3, 20)	558	724	6,979
3	(3, 5, 6, 1-2, 20)	564	724	7,819

No.	Size (S, C, V, SL, T)	No of Binary Variables	No of Continuous Variables	No of Constraints
4	(3, 5, 6, 1-3, 20)	564	724	7,819
5	(3, 5, 6, 2-3, 20)	564	724	7,819
6	(3, 5, 6, 1-2-3, 20)	570	724	8,659
7	(4, 8, 9, 2, 25)	1,359	1,810	21,652
8	(4, 8, 9, 3, 25)	1,359	1,810	21,652
9	(4, 8, 9, 1-2, 25)	1,368	1,810	24,532
10	(4, 8, 9, 1-3, 25)	1,368	1,810	24,532
11	(4, 8, 9, 2-3, 25)	1,368	1,810	24,532
12	(4, 8, 9, 1-2-3, 25)	1,377	1,810	27,412
13	(4, 9, 10, 2, 26)	1,730	2,320	29,179
14	(4, 9, 10, 1- 2, 26)	1,740	2,320	33,139
15	(4, 10, 9, 3, 25)	1,847	2,408	31,656
16	(4, 11, 10, 2, 26)	2,304	3,022	41,299
17	(4, 12, 10, 2, 26)	2,621	3,403	48,139

The outcomes of the computational experiments are presented in a series of tables, categorised by instance size and scenario number. Each table offers a comprehensive overview of the key financial and operational indicators, enabling a clear comparison of model behaviour and trade-offs under different levels of CII-related constraints. To make the experiment brief the result of four examples (13, 14, 15, 16) are presented in the following tables and the result of example (3, 5, 6, 2, 20) will be explained in the Section 4.3.1 under the Case Studies Section (Section 4.3.1) and the result of other examples will be evaluated in the Sensitivity Analyses Section (Section 4.5.1).

The ratings of each active vessel under various scenarios are presented alongside the percentage reduction in profit compared to the baseline scenario (when CII regulation is not applied), offering a clear view of how vessel performance and profitability evolve under regulatory pressure. Furthermore, the detailed tables show the profit and associated cost in the portfolio optimisation. Additionally, vessel-level CO_2 emissions are illustrated through scenario-based graphs, which highlight the environmental implications of different operational

strategies. The average distance sailed by each vessel is also visualised, offering insight into routing adjustments driven by CII compliance. Further, individual vessel ratings are detailed across scenarios, demonstrating shifts in vessel allocation and deployment in response to the regulation.

Collectively, these figures and tables provide a comprehensive understanding of the impact of CII on portfolio optimisation including how supplier-customer matching, vessel and speed assignment, fuel consumption, voyage distance, emissions, and overall profitability are affected. This evidence-based analysis supports strategic decision-making under environmental regulatory constraints and highlights the complexity of achieving both economic and sustainability goals in maritime logistics.

4.4.1 **CII Case Studies**

One illustrative example is the instance defined by 3 LNG providers, 5 customers, 6 vessels, at second speed level, during a planning horizon of 20 weeks. This scenario operates under fixed sailing speeds (16 knots) and rigid loading and unloading time windows, providing a realistic operational context reflective of actual LNG shipping constraints. In the baseline scenario, the optimisation focuses solely on profitability. All four vessels deployed in this case achieve acceptable environmental performance without targeted intervention, one vessel attains an 'A' rating, and the remaining three secure 'B' ratings (see Figure 4.2). However, when CII constraints are introduced in subsequent scenarios, the model begins to reprioritise vessel deployment and route allocation to minimise penalties associated with suboptimal ratings.

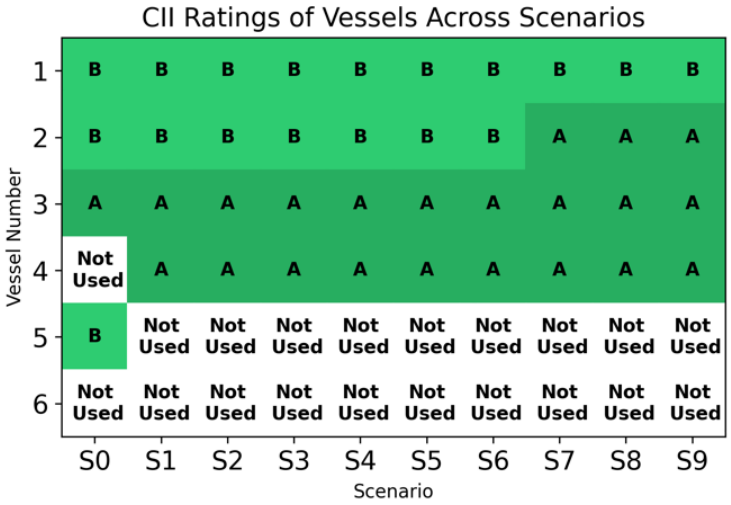

Figure 4.2: CII Ratings of Vessel Across Scenarios Example (3, 5, 6, 2, 20)

In early CII-constrained scenarios (Scenarios 1-6), the model replaces Vessel No.5 (V5) with a larger vessel (V4) offering a heavier DWT (see Table 3.5). Although this substitution results in a lower profit due to reduced loading and unloading cargo volume (stemming from lower capacity and loading factor of the selected vessel). The newly allocated vessel demonstrates superior fuel efficiency, particularly in low-speed operations. This efficiency and with higher DWT result in an upgraded CII rating ('A' rating), validating the trade-off between profit and compliance. By the fifth scenario, as observed in Table 4.6, the model initially attempts to maintain consistent cargo matching across scenarios (evidenced by relatively stable port costs from S0 to S6). However, as CII penalties become more severe, the model begins to exhibit more pronounced shifts in strategic behaviour. Notably, for the first time, a provider-customer relationship is altered, and the supplier-cargo pairing is adjusted in pursuit of improved CII ratings. In this scenario, the model opts for a longer route and selects a different LNG provider, resulting in an upgrade of the CII rating from 'B' to 'A'. Although this reallocation leads to higher fuel consumption (as shown in Table 4.6), it also significantly increases sailing time relative to idle time (see Figure 4.3), thereby improving operational efficiency under the CII framework. Despite these operational improvements, the total CO_2 emissions in scenarios 7, 8, and 9 are higher than in scenarios 1 to 6 (see Figure 4.4). Nevertheless, as illustrated in Figure 4.2and Figure 4.5, the vessel ratings in the final three scenarios are better, with more vessels achieving an 'A' rating.

This shift underscores the nonlinear and, at times, counterintuitive impacts of environmental performance measures. Specifically, increased vessel activity under more efficient operating conditions can lead to better CII ratings compared to scenarios involving inefficiencies during idling or shorter routes. By the final scenario, the model successfully achieves a fleet configuration comprising three vessels rated ‘A’ and one rated ‘B’, reflecting a substantial strategic transition towards environmental optimisation under regulatory pressure.

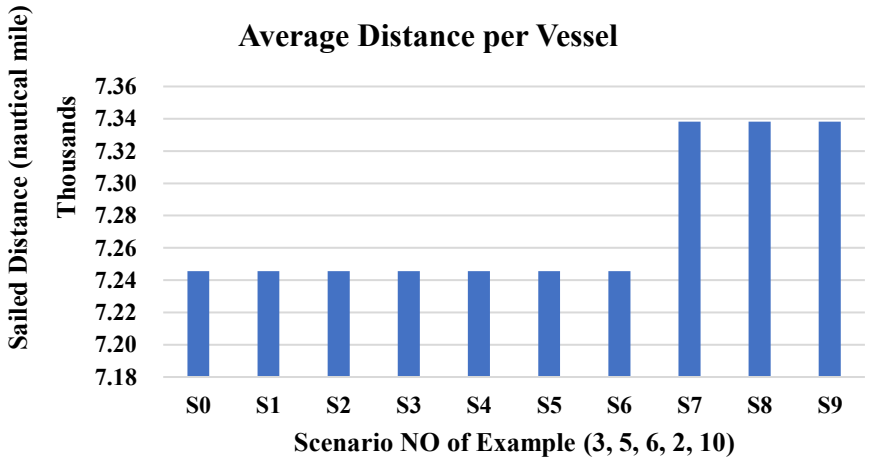

Figure 4.3 Ave. Sailed Distance per vessel for (3, 5, 6, 2, 20)

Table 4.6: Detailed Profit & Cost ($) of example (3, 5, 6, 2, 20)

Scenario	Total Profit	Revenue - Expenditure	Shipping Cost	Fuel Cost	Idle Cost	Port Cost	Total Profit excluding CII Cost	CII Cost	Rating A	Rating B	Rating C	Rating D	Rating E	Active Vessels	Active Vessels Numbers
S0	117,508,344	162,398,255	33,868,449	2,577,008	6,567,728	1,876,727	117,508,344	-	1	3	0	0	0	4	1, 2, 3, 5
S1	116,235,478	162,158,456	33,868,449	2,510,074	6,567,728	1,876,727	117,335,478	1,100,000	2	2	0	0	0	4	1, 2, 3, 4
S2	115,935,478	162,158,456	33,868,449	2,510,074	6,567,728	1,876,727	117,335,478	1,400,000	2	2	0	0	0	4	1, 2, 3, 4
S3	115,435,478	162,158,456	33,868,449	2,510,074	6,567,728	1,876,727	117,335,478	1,900,000	2	2	0	0	0	4	1, 2, 3, 4
S4	114,735,478	162,158,456	33,868,449	2,510,074	6,567,728	1,876,727	117,335,478	2,600,000	2	2	0	0	0	4	1, 2, 3, 4
S5	113,835,478	162,158,456	33,868,449	2,510,074	6,567,728	1,876,727	117,335,478	3,500,000	2	2	0	0	0	4	1, 2, 3, 4
S6	112,735,478	162,158,456	33,868,449	2,510,074	6,567,728	1,876,727	117,335,478	4,600,000	2	2	0	0	0	4	1, 2, 3, 4
S7	111,474,749	159,403,727	34,109,984	2,531,713	6,421,244	1,916,037	114,424,749	2,950,000	3	1	0	0	0	4	1, 2, 3, 4
S8	110,724,749	159,403,727	34,109,984	2,531,713	6,421,244	1,916,037	114,424,749	3,700,000	3	1	0	0	0	4	1, 2, 3, 4
S9	109,874,749	159,403,727	34,109,984	2,531,713	6,421,244	1,916,037	114,424,749	4,550,000	3	1	0	0	0	4	1, 2, 3, 4

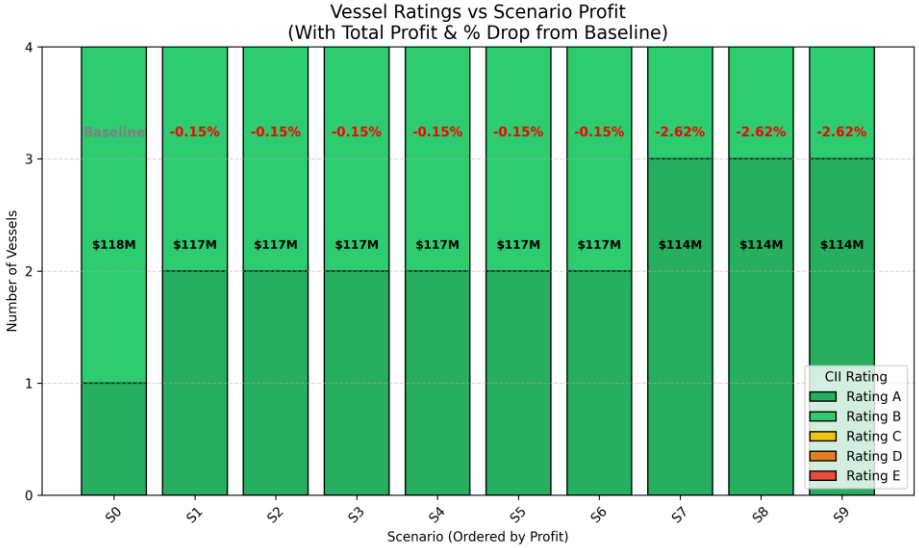

Figure 4.5: Vessel Rating and Scenario Profit for (3, 5, 6, 2, 20)

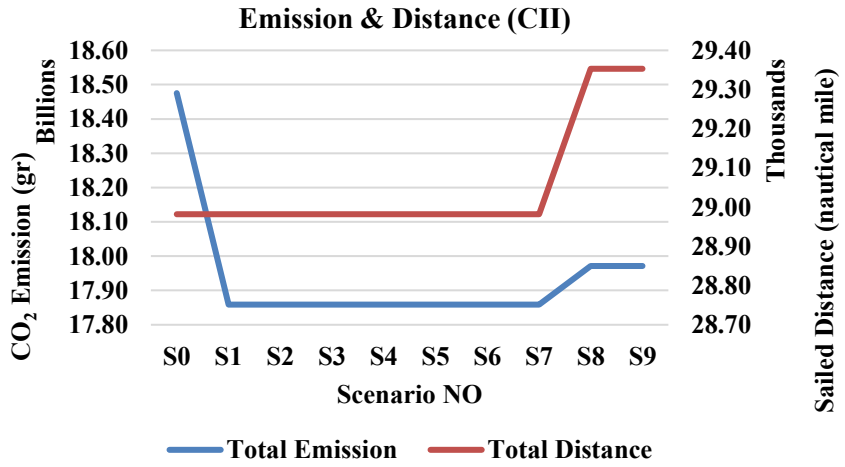

Figure 4.4: CO_2 Emission & Sailed Distance Example (3, 5, 6, 2, 20)

For the two additional case studies (4, 9, 10, 2, 26) and (4, 9, 10, 1-2, 26) which represent the same number of cargo delivery (9-cargo) under different speed configurations (16 knots and 14 & 16 knots), further insights can be drawn from Table 4.7 and Table 4.8. In both examples, the portfolio achieves its highest profit in the baseline scenario (S0), where CII constraints are not applied. As the CII regulation is introduced and penalties increase, the portfolio profit consistently decreases across scenarios.

The model attempts to preserve the original cargo matching established in the baseline scenario as much as possible. Where preserving these matches is not feasible due to rating penalties, the model strategically reallocates vessels and, when necessary, alters supplier-customer pairings to maintain optimal profit while improving the fleet's CII ratings. However, analysis of emission trends (visible in Figure 4.8 and Figure 4.13) demonstrates that the presence of CII constraints does not necessarily guarantee a reduction in CO_2 emissions. Despite the earlier case (Figure 4.4), the emissions in the baseline scenario (S0) are lower than those observed in the CII-constrained scenarios.

This observation is further supported by the increased average sailing distances across scenarios (Figure 4.6 and Figure 4.11), and by a comparison of detailed cost components including fuel, shipping, and idle costs. These costs reflect the model's strategy of mitigating penalties for lower-rated vessels by increasing sailing time, reallocating vessels, and shifting supplier-customer pairings. This approach results in reduced idle time and increased fuel consumption, yet vessels attain better CII ratings.

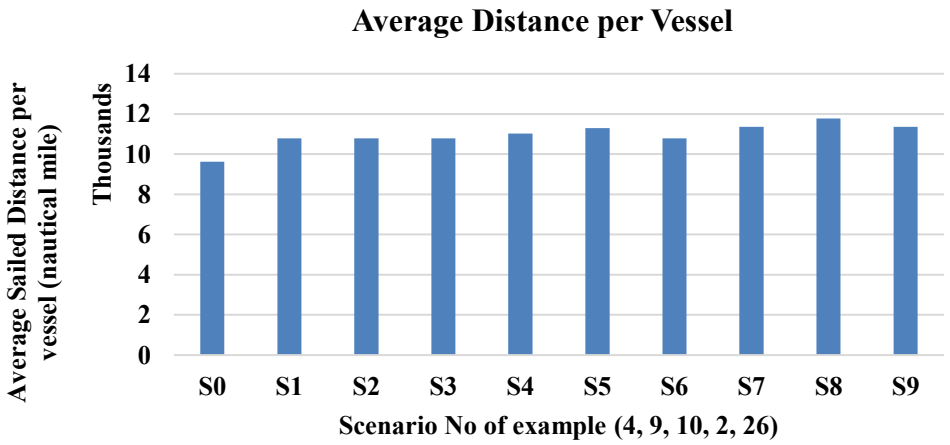

Figure 4.6: Ave. Sailed Distance per vessel for (4, 9, 10, 2, 26)

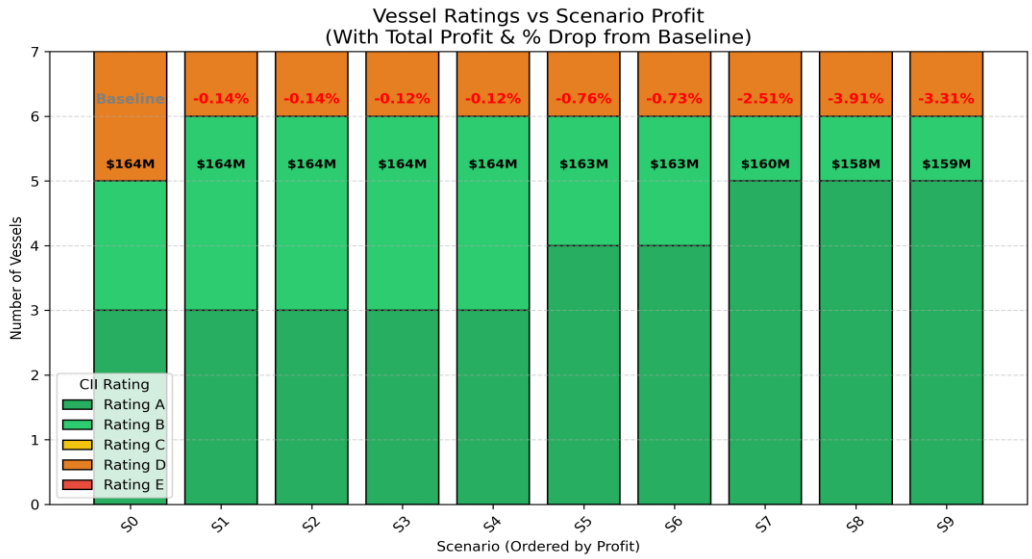

Figure 4.7: Vessel Rating & Profit per Scenario for (4, 9, 10, 2, 26)

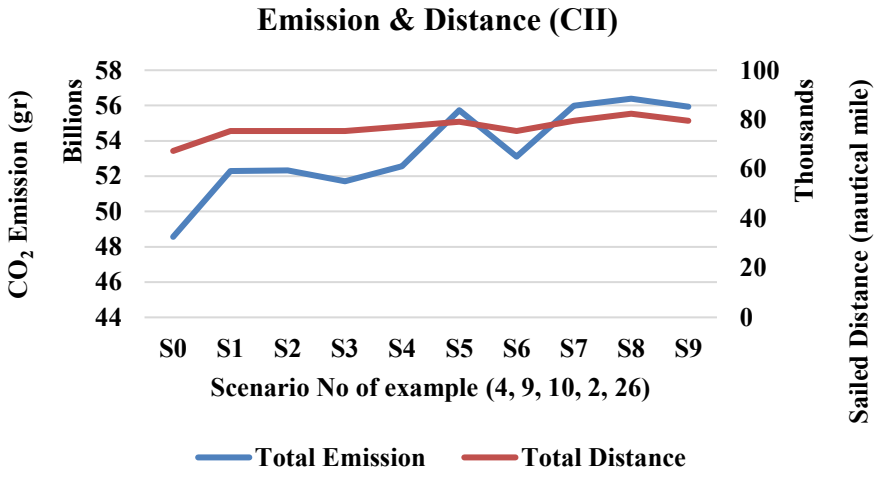

Figure 4.8: CO_2 Emission & Sailed Distance for (4, 9, 10, 2, 26)

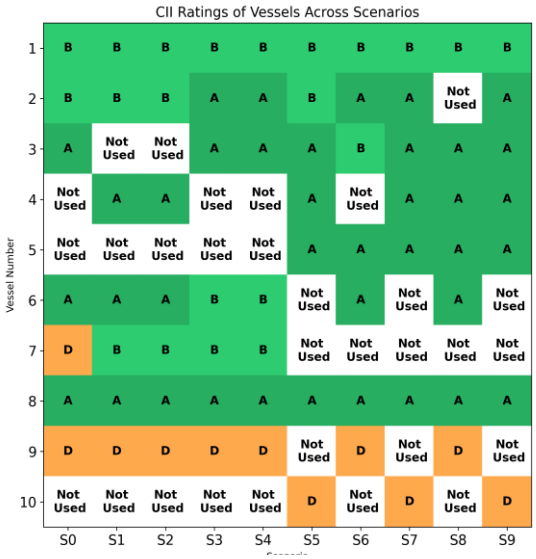

Figure 4.9: CII Rating of each vessel per scenario for (4, 9, 10, 2, 26)

Table 4.7: Detailed Profit & Cost ($) of example (4, 9, 10, 2, 26)

Scenario	Total Profit	Revenue - Expenditure	Shipping Cost	Fuel Cost	Idle Cost	Port Cost	Total Profit excluding CII Cost	CII Cost	Rating A	Rating B	Rating C	Rating D	Rating E	Active Vessels	Active Vessels Numbers
S0	165,019,115	270,716,097	70,094,016	6,983,563	25,460,111	3,159,292	165,019,115	-	3	2	0	2	0	7	1, 2, 3, 6, 7, 8, 9
S1	159,804,888	269,479,942	75,372,650	7,484,387	19,900,234	3,067,783	163,654,888	3,850,000	4	2	0	1	0	7	1, 2, 3, 4, 6, 8, 9
S2	158,579,507	270,245,674	75,372,650	7,485,377	20,140,357	3,067,783	164,179,507	5,600,000	3	3	0	1	0	7	1, 2, 4, 6, 7, 8, 9
S3	156,615,939	270,233,906	75,372,650	7,405,158	20,172,376	3,067,783	164,215,939	7,600,000	3	3	0	1	0	7	1, 2, 3, 6, 7, 8, 9
S4	151,757,803	269,442,558	76,476,163	7,525,580	20,215,229	3,067,783	162,157,803	10,400,000	3	3	0	1	0	7	1, 2, 3, 4, 6, 8, 9
S5	150,925,661	269,400,864	77,749,298	7,976,044	17,523,586	2,976,275	163,175,661	12,250,000	4	2	0	1	0	7	1, 2, 3, 4, 5, 8, 10
S6	147,119,812	269,688,972	75,372,650	7,616,227	20,412,500	3,067,783	163,219,812	16,100,000	4	2	0	1	0	7	1, 2, 3, 5, 6, 8, 9
S7	142,584,401	266,676,088	77,990,834	8,008,166	17,377,102	3,015,585	160,284,401	17,700,000	5	1	0	1	0	7	1, 2, 3, 4, 5, 8, 10
S8	135,782,297	266,055,634	79,896,729	8,088,290	16,889,716	3,198,602	157,982,297	22,200,000	5	1	0	1	0	7	1, 3, 4, 5, 6, 8, 9
S9	131,672,372	266,548,347	77,990,834	9,192,454	17,377,102	3,015,585	158,972,372	27,300,000	5	1	0	1	0	7	1, 2, 3, 4, 5, 8, 10

Table 4.8: Detailed Profit & Cost ($) of example (4, 9, 10, 1-2, 26)

Scenario	Total Profit	Revenue - Expenditure	Shipping Cost	Fuel Cost	Idle Cost	Port Cost	Total Profit excluding CII Cost	CII Cost	Rating A	Rating B	Rating C	Rating D	Rating E	Active Vessels	Active Vessels Numbers
S0	165,025,022	270,706,400	71,183,940	6,843,010	24,495,137	3,159,292	165,025,022	-	2	2	0	2	1	7	1, 2, 4, 5, 7, 8, 9
S1	161,660,867	269,954,328	79,664,891	7,294,302	15,607,993	2,976,275	164,410,867	2,750,000	4	2	1	0	0	7	1, 2, 3, 4, 7, 8, 9
S2	160,950,798	269,994,441	79,664,891	7,294,484	15,607,993	2,976,275	164,450,798	3,500,000	4	2	1	0	0	7	1, 2, 3, 4, 7, 8, 9
S3	159,871,947	269,382,699	79,664,891	7,461,593	15,607,993	2,976,275	163,671,947	3,800,000	5	1	1	0	0	7	1, 2, 3, 4, 5, 8, 9
S4	158,522,108	269,403,348	79,664,891	7,432,082	15,607,993	2,976,275	163,722,108	5,200,000	5	1	1	0	0	7	1, 2, 3, 4, 5, 8, 9
S5	156,696,970	269,410,967	79,664,891	7,464,838	15,607,993	2,976,275	163,696,970	7,000,000	5	1	1	0	0	7	1, 3, 4, 5, 6, 8, 9
S6	154,459,198	269,423,624	79,664,891	7,515,267	15,607,993	2,976,275	163,659,198	9,200,000	5	1	1	0	0	7	1, 2, 3, 4, 5, 8, 9
S7	151,918,165	266,609,200	79,906,427	7,457,514	15,461,509	3,015,585	160,768,165	8,850,000	6	0	1	0	0	7	1, 2, 3, 4, 5, 8, 9
S8	149,661,445	266,682,774	79,906,427	7,537,807	15,461,509	3,015,585	160,761,445	11,100,000	6	0	1	0	0	7	1, 3, 4, 5, 6, 8, 9
S9	146,669,137	266,387,326	79,906,427	7,412,525	15,733,652	3,015,585	160,319,137	13,650,000	6	0	1	0	0	7	1, 2, 3, 4, 6, 8, 9

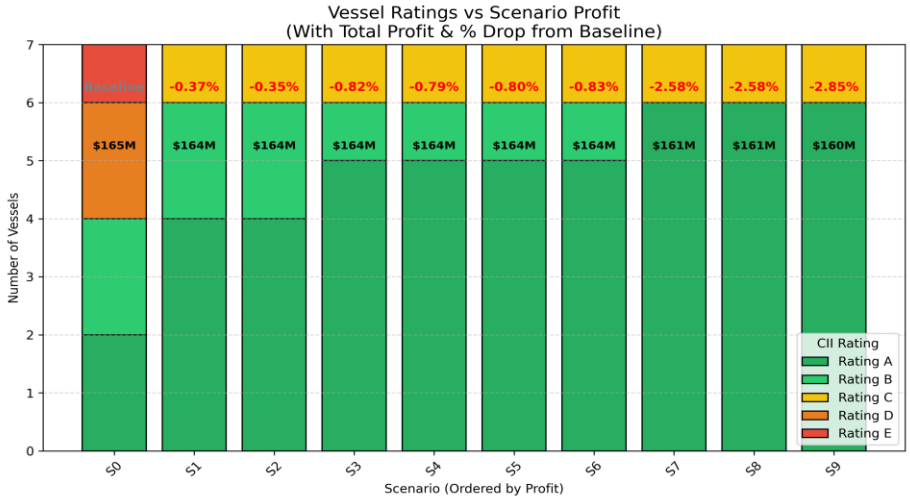

Figure 4.10: Vessel Rating & Profit per Scenario Example (4, 9, 10, 1-2, 26)

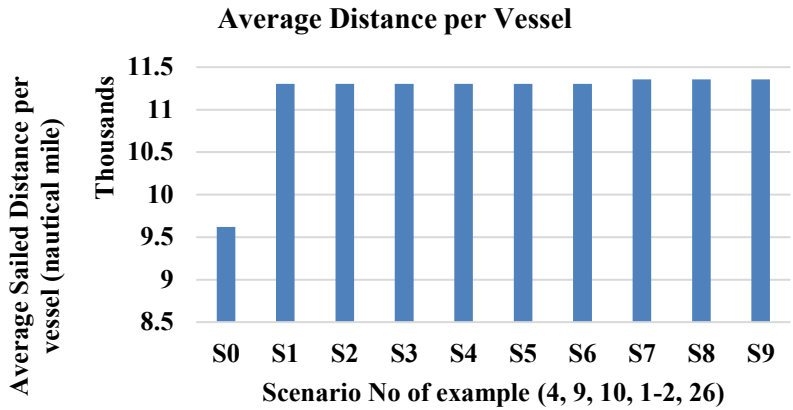

Figure 4.11: Ave. Sailed Distance per Vessel Example (4, 9, 10, 1-2, 26)

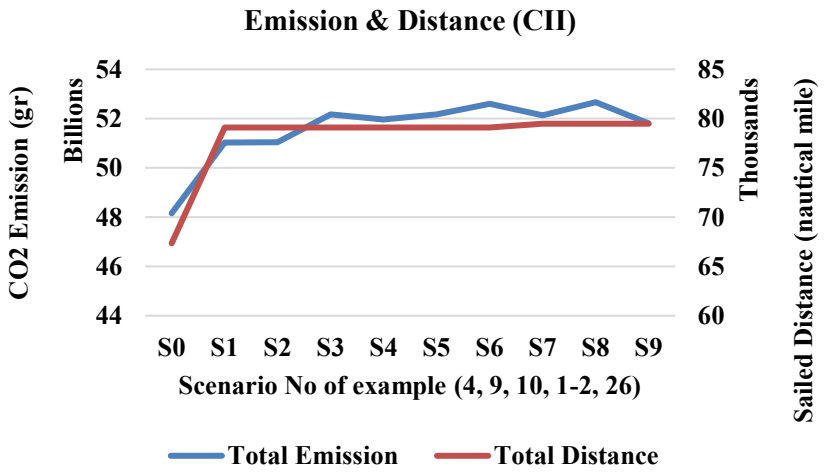

Figure 4.13: CO_2 Emission & Sailed Distance Example (4, 9, 10, 1-2, 26)

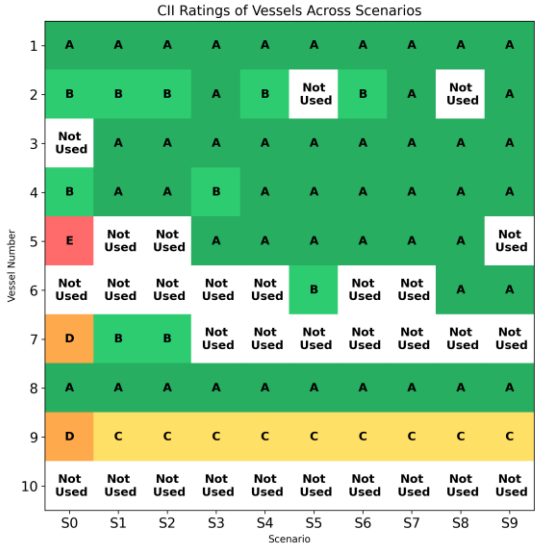

Figure 4.12: CII Rating of each vessel per scenario Example (4, 9, 10, 1-2, 26)

The results from the additional examples (4, 10, 9, 3, 25), (4, 11, 10, 2, 26), and (4, 12, 10, 2, 26) further confirm the consistent patterns observed in earlier experiments. In each case, the outcomes follow a similar trajectory in terms of portfolio profit, vessel rating, and CO_2 emissions, as detailed in the corresponding emission and profit figures. These consistent results reinforce a key finding that compliance with the CII framework and the achievement of higher vessel ratings do not necessarily correspond with reductions in CO_2 emissions.

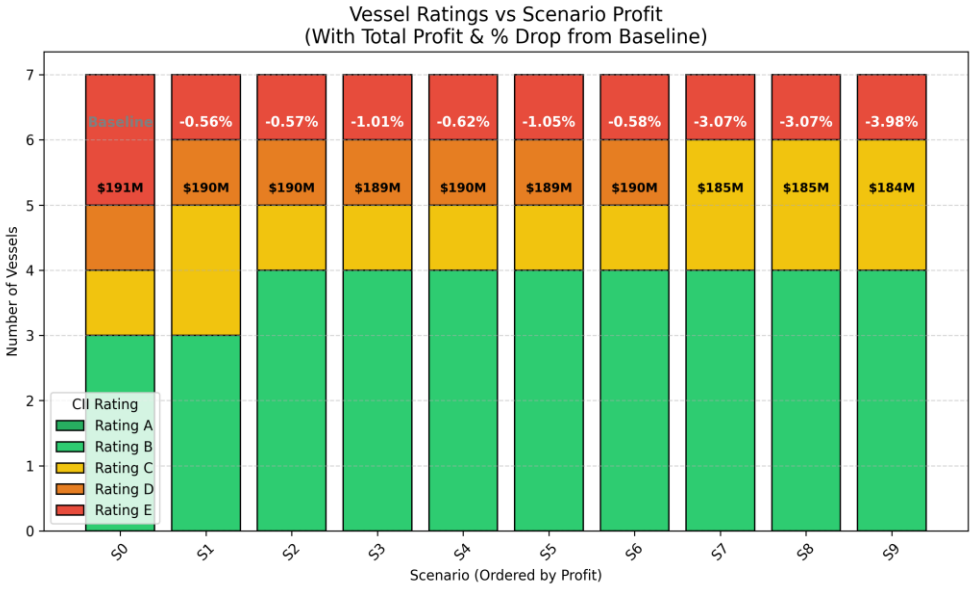

Figure 4.14: Vessel Rating & Profit per Scenario for (4, 10, 9, 3, 25)

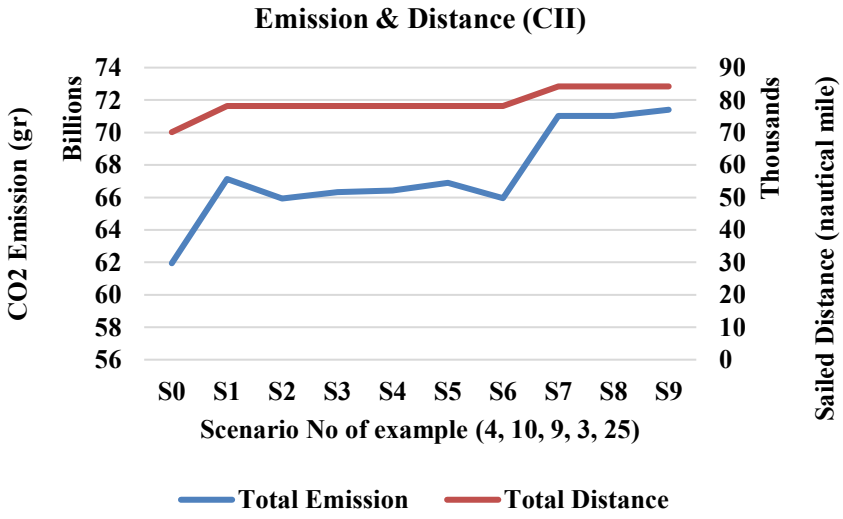

Figure 4.15 CO_2 Emission & Sailed Distance for (4, 10, 9, 3, 25)

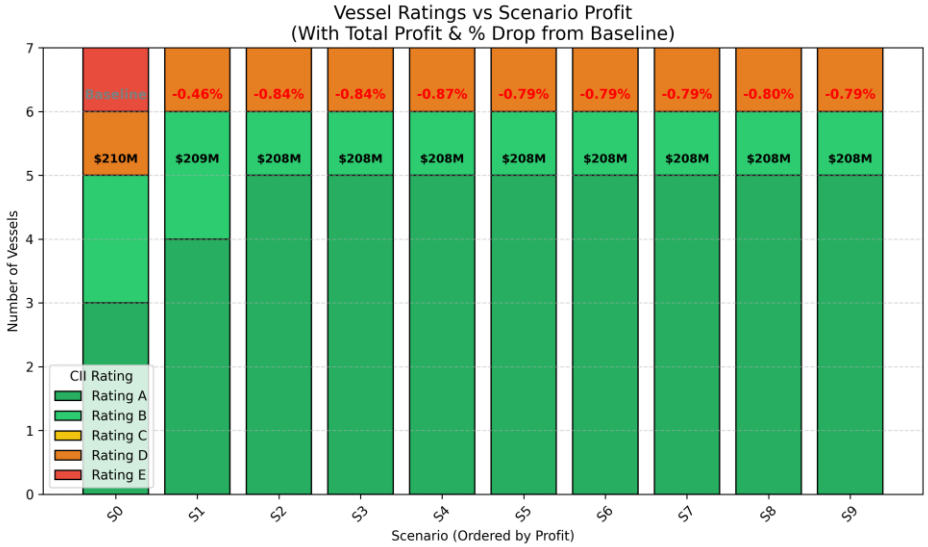

Figure 4.17: Vessel Rating & Profit per Scenario for (4, 11, 10, 2, 26)

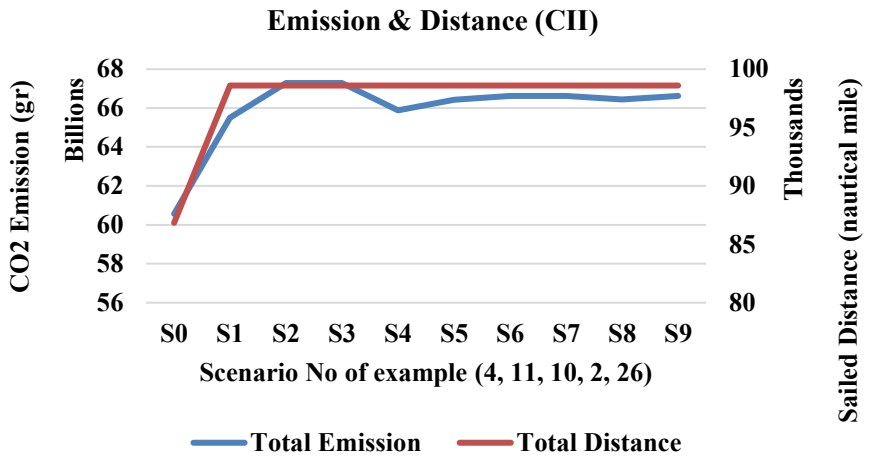

Figure 4.16: CO_2 Emission & Sailed Distance for (4, 11, 10, 2, 26)

Table 4.9: Detailed Profit & Cost of example of (4, 12, 10, 2, 26)

Scenario	Total Profit	Revenue - Expenditure	Shipping Cost	Fuel Cost	Idle Cost	Port Cost	Total Profit excluding CII Cost	CII Cost	Rating A	Rating B	Rating C	Rating D	Rating E	Active Vessels	Active Vessels Numbers
S0	213,123,961	354,604,775	89,757,393	9,266,910	38,222,515	4,233,996	213,123,961	-	3	2	1	1	1	8	1, 2, 3, 5, 6, 7, 8, 10
S1	207,869,807	353,898,403	101,753,460	10,233,291	26,049,358	4,142,487	211,719,807	3,850,000	5	2	0	1	0	8	1, 2, 3, 4, 6, 7, 8, 9
S2	206,860,841	353,956,157	101,753,460	10,250,010	26,049,358	4,142,487	211,760,841	4,900,000	5	2	0	1	0	8	1, 2, 3, 4, 6, 7, 8, 9
S3	205,386,444	353,824,189	101,753,460	10,342,440	25,549,358	4,142,487	212,036,444	6,650,000	5	2	0	1	0	8	1, 2, 3, 5, 6, 7, 8, 9
S4	202,740,080	353,128,636	104,130,108	10,838,912	23,568,557	4,050,979	210,540,080	7,800,000	6	1	0	1	0	8	1, 2, 3, 4, 5, 6, 8, 10
S5	200,110,783	353,077,341	102,848,210	10,716,914	24,850,455	4,050,979	210,610,783	10,500,000	6	1	0	1	0	8	1, 2, 3, 4, 5, 6, 8, 10
S6	196,739,922	353,128,770	104,130,108	10,839,204	23,568,557	4,050,979	210,539,922	13,800,000	6	1	0	1	0	8	1, 2, 3, 4, 5, 6, 8, 10
S7	192,839,922	353,128,770	104,130,108	10,839,204	23,568,557	4,050,979	210,539,922	17,700,000	6	1	0	1	0	8	1, 2, 3, 4, 5, 6, 8, 10
S8	188,339,922	353,128,770	104,130,108	10,839,204	23,568,557	4,050,979	210,539,922	22,200,000	6	1	0	1	0	8	1, 2, 3, 4, 5, 6, 8, 10
S9	183,243,138	353,120,463	104,130,108	10,827,681	23,568,557	4,050,979	210,543,138	27,300,000	6	1	0	1	0	8	1, 2, 3, 4, 5, 6, 8, 10

4.4.2 **Discussion and Implications**

This scenario-based analysis demonstrates that incorporating CII constraints into fleet optimisation models leads to significant changes in vessel assignment and routing strategies, even when the spatial distribution of cargo flows remains constant. Notably, these operational adjustments are not always intuitive; improved environmental performance can result from both technological interventions (e.g., enhanced vessel efficiency) and operational trade-offs (e.g., choosing longer routes to improve the sailing-to-idle ratio).

The findings also underscore the persistent economic tension between profitability and environmental compliance. While early improvements in CII ratings can often be achieved through relatively low-cost adjustments such as reallocating vessels within the existing fleet compliance under more stringent regulatory scenarios increasingly demands higher-cost decisions. These may include rerouting, extend voyage durations, or reduce cargo volumes to maintain or improve vessel ratings.

Crucially, the results reinforce a key insight: compliance with the CII framework and the attainment of higher vessel ratings do not inherently equate to lower CO_2 emissions. In several scenarios, vessels received improved ratings despite higher overall emissions, primarily due to optimisation decisions that favoured higher fuel use but improved sailing efficiency. Therefore, it cannot be assumed that a vessel achieving a better CII rating is operating with a lower environmental impact. This highlights the complexity of environmental performance measurement and the need to evaluate regulatory metrics within a broader context of fuel consumption, voyage characteristics, and carbon outcomes.

Moreover, the analysis reflects how penalty-based regulatory frameworks can prompt strategic adaptation, even in the absence of hard emission caps. As the severity of penalties increases, the model dynamically adjusts its optimisation objectives, reflecting real-world behaviours that shipping companies may adopt in response to evolving regulatory pressures.

In conclusion, the integration of CII considerations within routing and allocation optimisation models represents more than a compliance tool; it signifies a structural redefinition of maritime operational priorities. As

environmental regulations become more stringent, such optimisation models will be essential for industry stakeholders seeking to balance economic performance with decarbonisation goals. These tools offer critical insights into the cost of compliance and the strategies that can reconcile profitability with environmental responsibility.

4.5 Improved Genetic-Based Metaheuristic Algorithm (IGBMHA)

The under-study optimisation problem by a very large number of interdependent decisions is characterised an NP- hard problem, rendering it computationally intractable when approached by exact methods alone. To address this complexity, a tailored GBMH has been improved. This algorithm is designed not only to explore the solution space efficiently but also to incorporate regulatory and environmental considerations particularly, the CII. While the inclusion of CII-related criteria does not alter the boundaries of the feasible solution space, it substantially increases the computational effort required to identify optimal or near-optimal solutions. To mitigate this challenge, several enhancements have been embedded into the MH framework with the dual objective of maintaining computational efficiency while systematically steering solutions towards environmentally favourable outcomes.

The first enhancement lies in the construction of initial solutions. A green-prioritisation module has been developed, which evaluates vessels based on fuel consumption rates and loading capacities to derive CO_2 emission rankings. These rankings are subsequently used to bias the initial population towards lower-emission vessels. By embedding environmental considerations at the outset, the algorithm ensures that computational resources are directed towards promising regions of the search space, thereby improving both convergence speed and sustainability outcomes.

The second enhancement is a targeted mutation mechanism, designed to systematically improve the CII performance of solutions with poor environmental outcomes. At each generation, solutions with the highest emission profiles are identified, and within these, the vessels contributing most adversely to their CII ratings are replaced with lower-emission alternatives. This focused replacement process strengthens the evolutionary

pressure towards greener solutions, without diluting the algorithm's capacity to maintain profit maximisation as a primary objective.

A further improvement concerns the reallocation of cargoes from lower-rated vessels to those with superior CII ratings, provided such adjustments are feasible. Within this feasibility assessment, the routing of underperforming vessels may be modified by transferring their assigned supplier–customer pairings to better-rated alternatives, on the condition that this does not downgrade the rating of the receiving vessel. This form of reallocation reflects an operational rather than a technological intervention, illustrating how environmental performance gains can be achieved through enhanced efficiency and strategic planning without imposing prohibitive costs on fleet operators.

In combination, these three enhancements green-prioritised initialisation, targeted mutation of high-emission solutions, and strategic vessel reallocation have proven effective in guiding the search towards solutions that balance profitability and environmental compliance. Empirical results demonstrate that the improved GBMH can attain near-optimal solutions for large-scale, real-world problem instances while offering superior scalability compared to exact optimisation approaches. Crucially, the framework illustrates how operational strategies can be leveraged to comply with IMO's short-term environmental measures, without necessitating immediate investment in costly technological retrofits.

4.5.1 **Experimental Result of IGBMHA**

To validate the improved and extended metaheuristic algorithm, the same experimental cases presented in the mathematical model section were executed using the developed MH. The results show that the MH algorithm achieves between 97% and 99% of the optimality of the MILP solution, while requiring only a fraction of the execution time.

Given the substantial execution time gap observed in the largest MILP case (Example 12) compared with smaller-scale cases (see Table 3.10), this example is selected to illustrate the MH's performance in this section, avoiding repetitive explanations for each case. A concise summary of the results is provided in tables and figures,

with detailed visual comparisons for the largest MILP instance Example (4, 12, 10, 2, 26) to highlight the relative performance of MH against the exact method.

In both methods, profit decreases as scenarios progress and penalties increase. While MILP profits are consistently higher than those of the MH, the difference remains small, with MH optimality consistently above **97%**, indicating strong performance despite the heuristic nature of the approach. In terms of execution time, the MH method outperforms the MILP by a substantial margin (see Table 4.10 and Figure 4.18).

Regarding vessel ratings, the IGBMHA and exact method solutions are closely aligned, with both approaches assigning ratings of 'A' and 'B' to seven of the eight active vessels. However, the MILP achieves six 'A'-rated vessels compared to five in the MH results (Figure 4.19). This small difference highlights a subtle but important trade-off: in real-world decision-making, the MH provides a near-optimal profit outcome far more quickly, but in some cases may marginally reduce top-tier environmental ratings. Stakeholders therefore need to consider whether the computational efficiency and speed of the MH justify a minimal environmental rating compromise, especially when rapid decision-making is critical in dynamic markets.

The MH demonstrates exceptional consistency, with a standard deviation in optimality of just 0.42% and an optimality gap variation of 0.002%. These findings confirm that the MH delivers near-optimal solutions with minimal deviation while dramatically reducing computational time, making it particularly suitable for large-scale, real-world portfolio optimisation problems where both profitability and regulatory compliance must be balanced. Having validated the performance and scalability of the metaheuristic algorithm against the MILP formulation, the next step is to assess its applicability in large-scale, realistic operational settings.

Table 4.10: Metaheuristic and Exact Method Approaches Comparison Example (4, 12 ,10, 2, 26)

(4, 12, 10, 2, 26)	Metaheuristic Approach				MILP (Exact method Approach)				MH's optimality vs MILP	No of Active Vessels in MH & MILP
	Total Profit	'A' Rated	'B' Rated	Execution time (s)	Total Profit	'A' Rated	'B' Rated	Execution time		
S0	209,198,803	3	2	246 s	213,123,961	3	2	3 h 40 min	98%	8
S1	206,149,845	5	1	260 s	211,719,807	5	2	3h 15 min	97%	8
S2	206,149,845	5	1	254 s	211,760,841	5	2	3 h 16 min	97%	8
S3	204,415,459	5	2	233 s	212,036,444	5	2	3h 14 min	96%	8
S4	204,415,459	5	2	233s	210,540,080	6	1	2h	97%	8
S5	204,415,459	5	2	230s	210,610,783	6	1	2h	97%	8
S6	204,415,459	5	2	240s	210,539,922	6	1	2h	97%	8
S7	204,415,459	5	2	256s	210,539,922	6	1	1h 56 min	97%	8
S8	204,415,459	5	2	260s	210,539,922	6	1	1h 56 min	97%	8
S9	204,415,459	5	2	259s	210,543,138	6	1	1h 56 min	97%	8

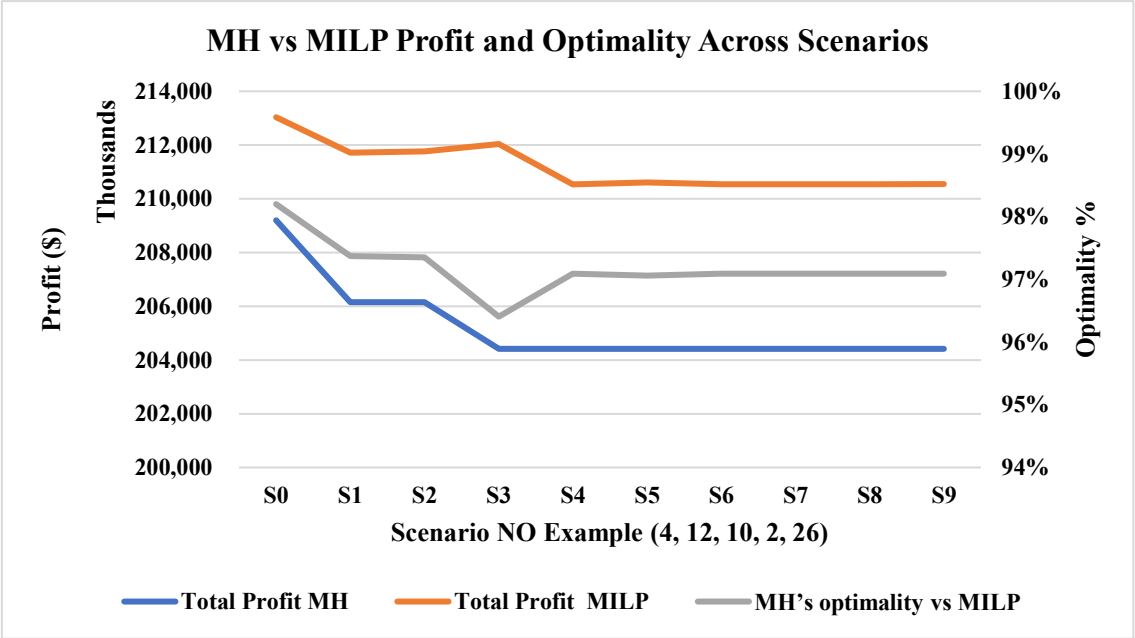

Figure 4.18: MH vs MILP Profit & Optimality Across Scenarios Example (4, 12, 10, 2, 26)

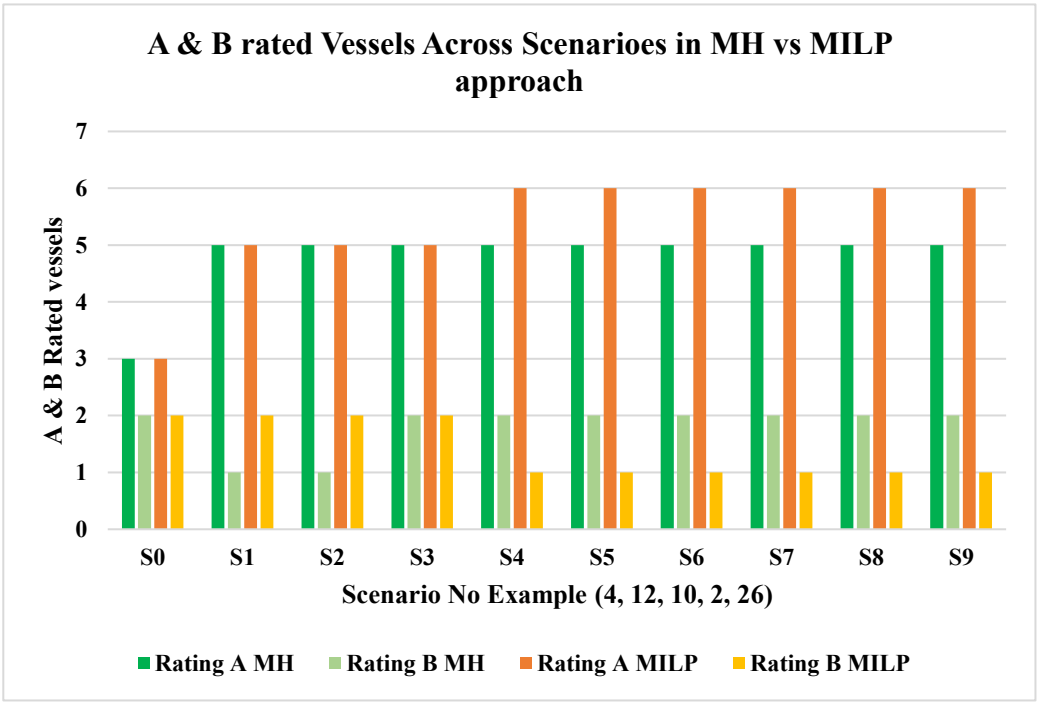

Figure 4.19: No of A & B Rated Vessels in MH vs MILP approach Example (4, 12, 10, 2, 26)

4.5.2 **Real-World Large-Scale Test Cases Experiments**

The primary motivation for developing the mathematical model and extending the metaheuristic approach is to deliver a comprehensive portfolio-planning framework that not only maximises company profits but also incorporates the International Maritime Organization's short-term environmental measures. By enabling operational adjustments such as optimising sailing speeds and modifying routing strategies without imposing substantial additional costs, the proposed framework supports businesses in maintaining competitiveness while ensuring regulatory compliance and promoting a sustainable energy supply chain.

To further evaluate the performance of the proposed optimisation framework and assess its scalability, two sets of real-world–inspired test cases were conducted. These experiments are designed to capture realistic operational complexity in terms of customer demand, fleet composition, speed variability, and planning horizon, while incorporating the CII constraint into the optimisation process.

The first set of experiments models a four-month delivery plan involving 30 customers, 5 suppliers, and a heterogeneous fleet of 15 vessels. Two operational configurations are examined:

- A single uniform speed of 16 knots (speed level 2).
- A dual-speed configuration combining 14 and 16 knots.

These 30 cargoes reflect a realistic short-term planning horizon and enable analysis of how speed flexibility influences both portfolio profit and environmental performance.

The second set of experiments extends the analysis to a full one-year planning horizon with 90 customer demands, 2 suppliers, and a fleet of 45 vessels. Two speed configurations are also tested:

- Uniform 16 knots.
- A combination of 14 and 16 knots.

This large-scale scenario provides a robust test of the model's ability to handle complex, high-volume delivery schedules over extended timeframes.

The results of the 30-cargo portfolio optimisation at a constant speed of 16 knots are presented below. As shown in Figure 4.20 and Figure 4.22, the MH approach seeks to preserve the baseline pairing and allocation established in the optimised solution, even when the CII constraint is introduced. However, as penalties for lower ratings increase, both routing and vessel allocation are adjusted to achieve improved ratings, with this revised configuration maintained thereafter with lower number of active vessels (reducing from 14 vessels to 12). This outcome indicates that achieving higher ratings requires companies to sacrifice a portion of their profit; however, such sacrifices do not necessarily translate into lower emissions. As illustrated in Figure 4.21 the baseline plan without CII yields the lowest emissions, whereas changes in routing and supplier–customer pairing

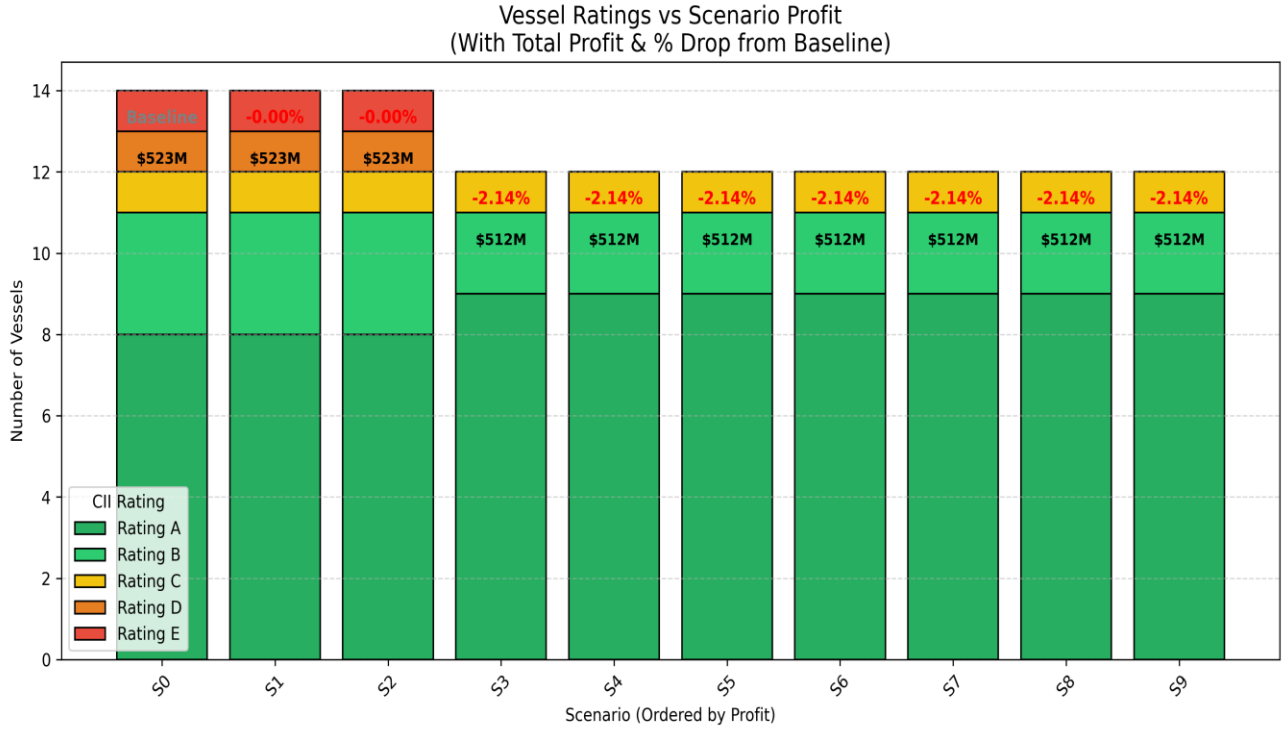

Figure 4.20: Vessel Rating & Profit per Scenario for (5, 30, 15, 2, 35)

to get the better CII rating led to increased emissions. This pattern is also reflected in the average sailing distance of vessels, which rises when routing adjustments are made (Figure 4.23).

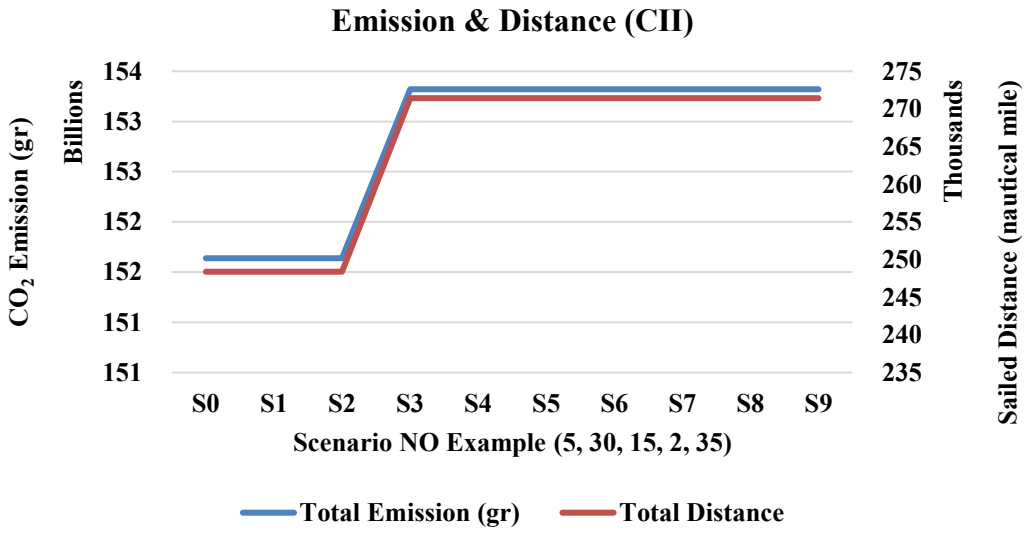

Figure 4.21:CO_2 Emission & Sailed Distance Example (5, 30, 15, 2, 35)

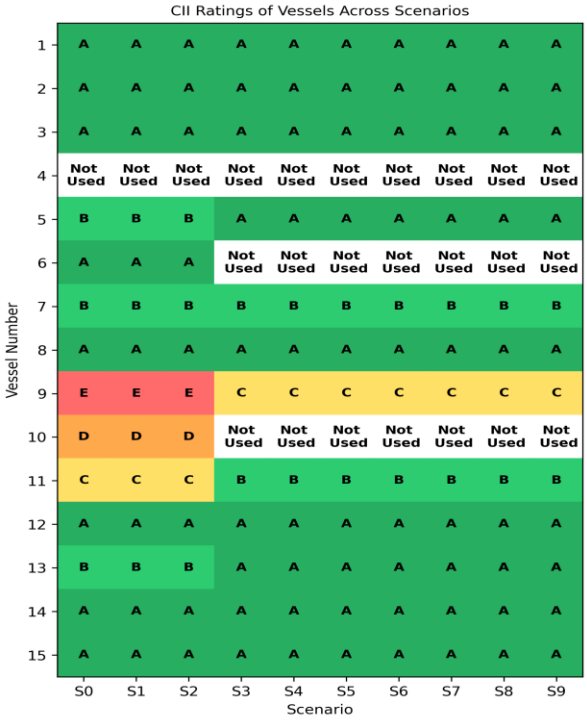

Figure 4.22: CII Ratings of Vessel Across Scenarios Example (5, 30, 15, 2,35)

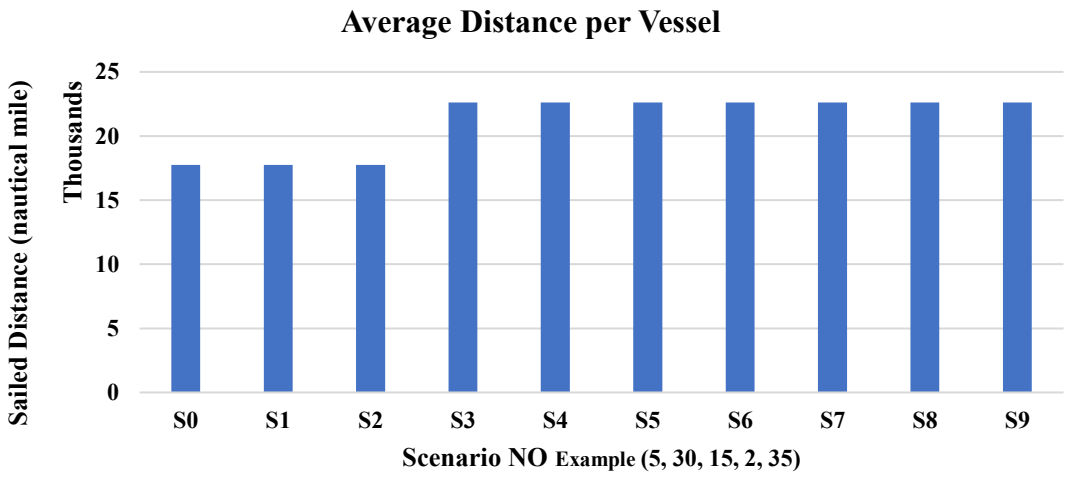

Figure 4.23: Ave. Sailed Distance per vessel for (5, 30, 15, 2, 35)

Running the same 30-cargo example with a combination of lower sailing speeds (14 and 16 knots) results in achieving a favourable rating from the outset, without substantial profit sacrifice of the portfolio (see Figure 4.24). This behaviour remains consistent until the final scenario, where penalties increase sharply. At this stage, the MH solution attains 10 'A'-rated vessels, 1 'B'-rated vessel, and 1 'C'-rated vessel, at the cost of a 4.48% reduction in profit. Notably, even in the initial baseline scenario, ratings were already strong where fleet receives 8 'A'-rated vessels, 1 'B'-rated vessel, and 3 'C'-rated vessels, demonstrating the significant role of lower sailing speeds in securing high ratings while minimising profit loss.

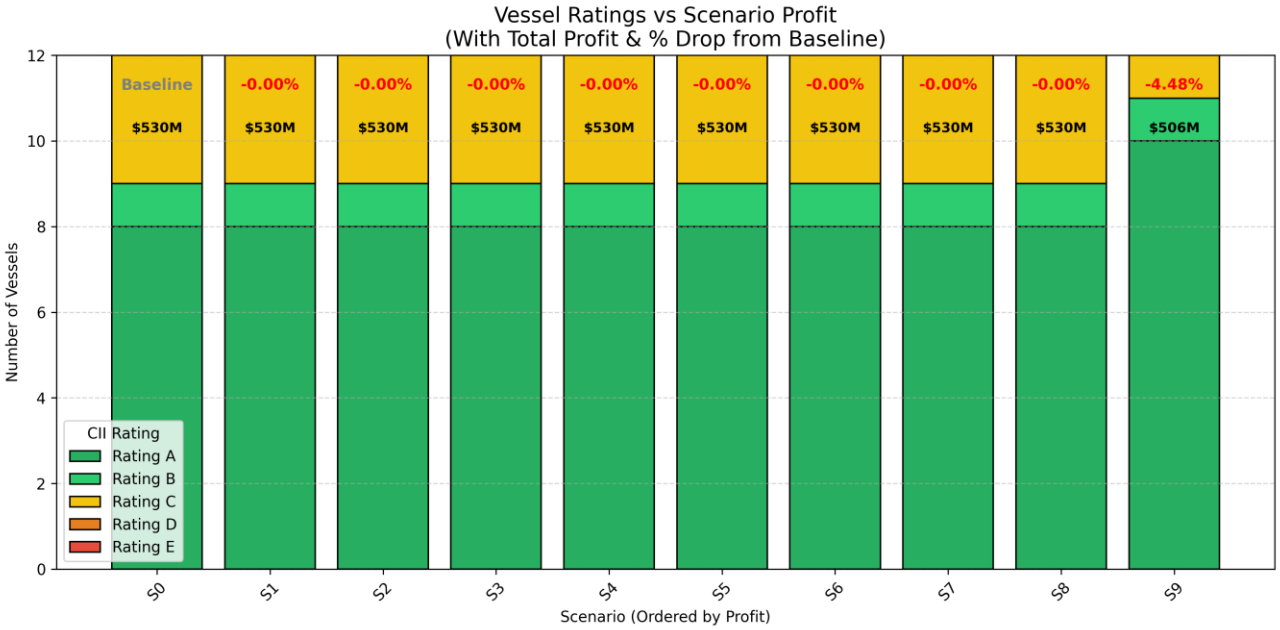

Figure 4.24: Vessel Rating & Profit per Scenario for (5, 30, 15, 1-2, 35)

As mentioned earlier, the CII is a short-term regulatory measure derived from a vessel's annual fuel consumption and total distance sailed. In this study, the delivery schedule of 90 cargoes representing one year of operations based on industry-provided data and is used as the modelling horizon. To examine the impact of CII compliance on vessel ratings and to understand how CII influences portfolio optimisation outcomes in a year, two experiments were designed and executed under different sailing speeds. The results of these experiments, including their effects on vessel ratings and portfolio profitability, are presented in the following figures. It is important to note that operating at lower speeds contributes significantly to achieving a better CII rating, even at the early stages of the planning horizon. Figure 4.25 shows the profit of each scenario and vessel rating when the portfolio optimisation has been conducted under the second speed level (16 knots). Figure 4.26 shows where two speed levels (14 and 16 knots respectively) are involved in the optimisation. As can be seen from these two figures, when lower speeds are involved in the optimisation, the model can get a good CII rating even in the early stage and by not losing that much profit.

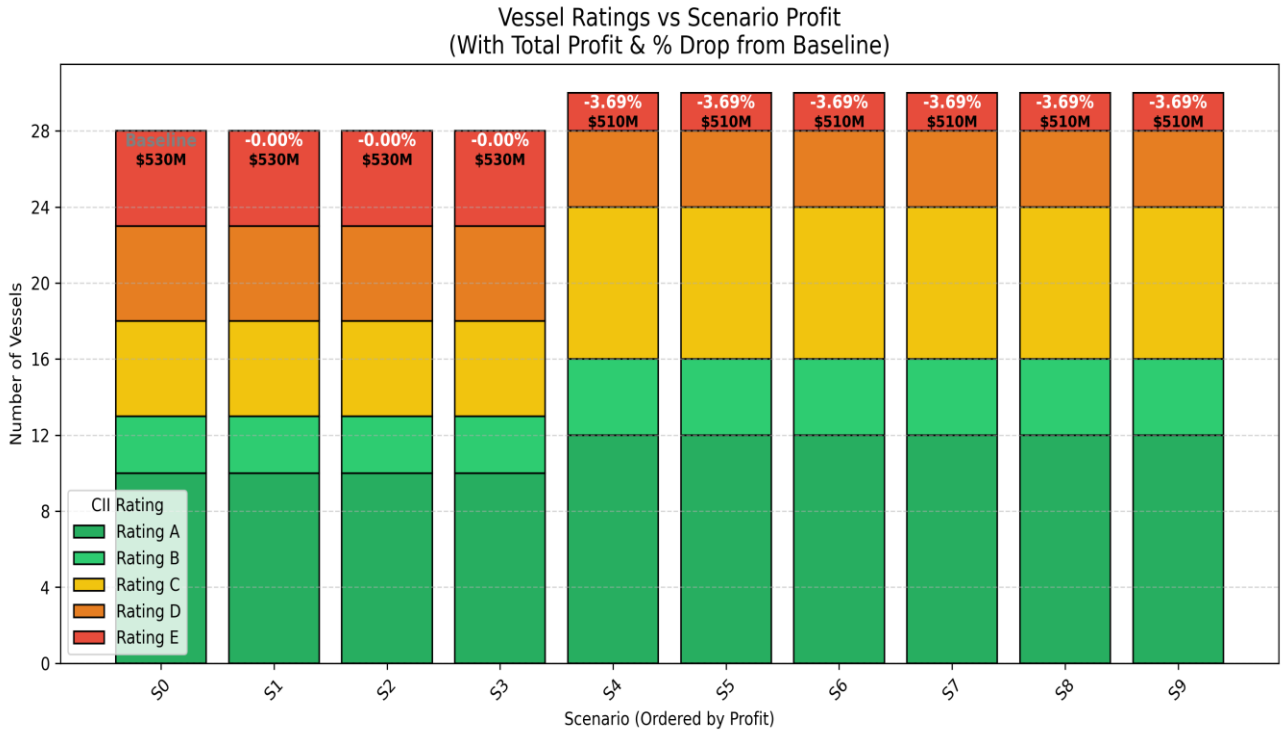

Figure 4.25: Vessel Rating & Profit per Scenario for (2, 90, 45, 2, 52)

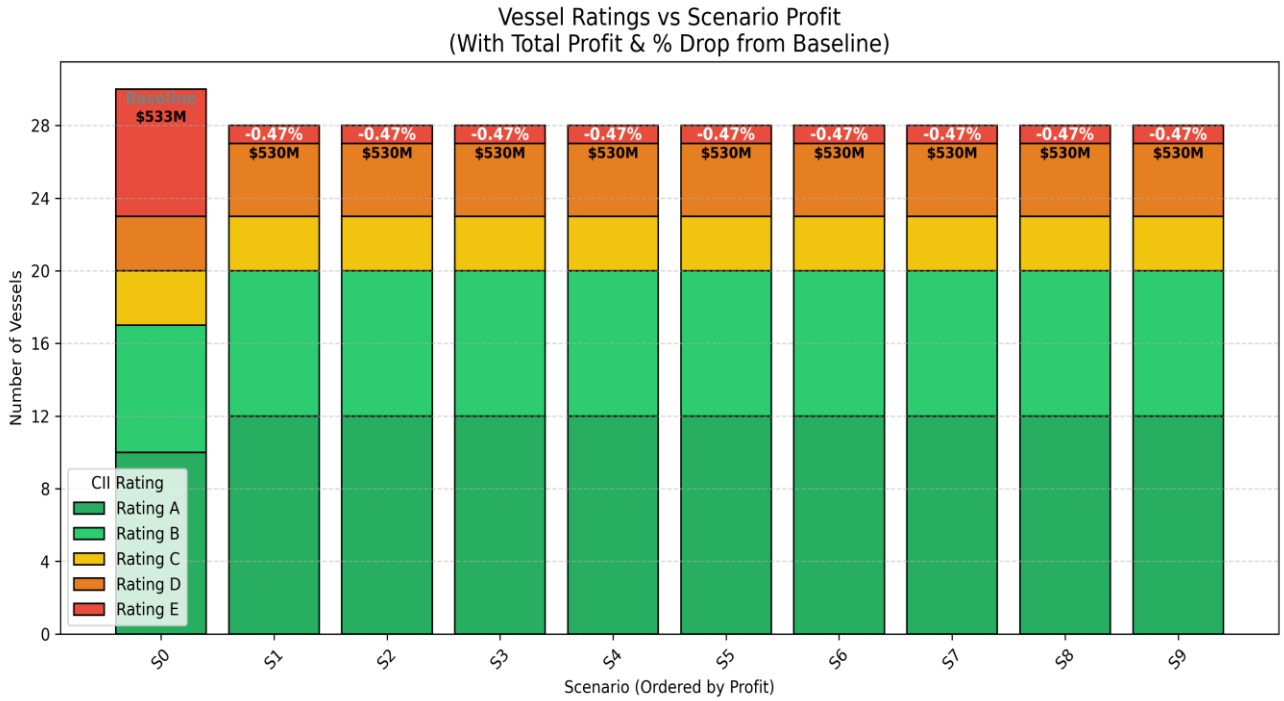

Figure 4.26: Vessel Rating & Profit per Scenario for (2, 90, 45, 1-2, 52)

For both sets, the results demonstrate that introducing the CII penalty directly alters vessel allocation and routing decisions, even when the original cargo assignments remain largely intact. As observed in the smaller-scale experiments, compliance with CII often necessitates vessel reassignments to improve ratings, sometimes resulting in reduced portfolio profit due to mismatched capacities or longer routes. Importantly, these reassignments do not consistently lead to lower CO_2 emissions confirming the earlier finding that better ratings under CII do not guarantee improved environmental outcomes.

The one-year scenarios highlight in particular, the trade-off between economic and environmental objectives: while penalty avoidance drives operational changes such as increased sailing time and reduced idle time, these adjustments can increase fuel consumption and emissions in certain cases. Nevertheless, the optimised plans reveal that a well-calibrated combination of speed adjustment, vessel reassignment, and route modification can deliver acceptable ratings with minimal profit loss, offering a practical pathway for shipping companies to maintain competitiveness while meeting regulatory requirements.

4.6 Sensitivity Analyses

To evaluate the robustness and practical implications of the proposed optimisation model, a series of sensitivity analyses are conducted. These analyses examine how variations in vessel sailing speeds and time window flexibility affect three critical performance dimensions: overall portfolio profit, fleet-level CII ratings, and total CO_2 emissions. By systematically varying these operational parameters across multiple scenarios, the analysis aims to explore the trade-offs between environmental compliance and economic performance, and to identify strategies that yield optimal outcomes under evolving regulatory constraints.

4.6.1 Impact of Vessel Speed on Portfolio Optimisation and CII Performance

To investigate the sensitivity of the proposed portfolio optimisation model to variations in vessel speed, a comprehensive analysis is conducted using a representative case study. Six distinct speed scenarios are defined to capture the operational effects of both fixed and mixed-speed policies:

- **SAS1**: All vessels operate exclusively at 16 knots.
- **SAS2**: All vessels operate exclusively at 18 knots.
- **SAS3**: Vessels may operate at either 16 or 18 knots.
- **SAS4**: Vessels may operate at either 14 or 16 knots.
- **SAS5**: Vessels may operate at either 14 or 18 knots.
- **SAS6**: Vessels are permitted to operate at all three speed levels 14, 16, and 18 knots.

To evaluate the operational and environmental implications of these scenarios, two case studies are selected: (3, 5, 6, SL, 20), comprising 3 LNG providers, 5 customers, and 6 vessels over a 20-week planning horizon; and (4, 8, 9, SL, 25), involving 4 LNG providers, 8 customers, and 9 vessels across 25 weeks.

Each speed scenario was further analysed under ten CII compliance scenarios, in which progressively increasing penalty costs are imposed on vessels failing to achieve an 'A' rating. This dual-layered design enabled a detailed

examination of the interactions between sailing speed, vessel allocation, carbon emissions, and portfolio profitability under escalating regulatory pressure.

In SAS1 and SAS2, vessels operate at fixed speeds of 16 and 18 knots, respectively, under rigid loading and unloading time windows. In contrast, SAS3 through SAS6 introduce speed flexibility, allowing the model to optimise sailing speeds and routing strategies dynamically. This enables a more nuanced trade-off between fuel efficiency, emissions, and scheduling feasibility.

The resulting analysis offers valuable insights into how speed variability, particularly when aligned with decarbonisation regulations, can influence operational decisions, fleet-wide environmental performance, and economic outcomes in maritime logistics.

The CO_2 emissions resulting from each Sensitivity Analysis Scenario (SAS) across the ten CII penalty settings are illustrated in Figure 4.27. The figure clearly demonstrates the substantial influence of vessel speed on emissions performance. The highest level of CO_2 emissions consistently occurs under SAS2, where vessels operate solely at 18 knots. This is followed by SAS5, where vessels sail at either 14 or 18 knots. In contrast, SAS4, which allows vessels to operate at 14 or 16 knots, yields the lowest emissions across all CII scenarios. Notably, SAS6, which permits operation at all three speed levels (14, 16, and 18 knots), also aligns with this low-emission category but only when CII constraints are active. This suggests that the model prioritises lower speeds when penalised for suboptimal ratings.

Profitability outcomes under the various speed settings are presented in Figure 4.28. In the absence of CII penalties (scenario S0), the highest profit is achieved under SAS6, due to the model's flexibility to use higher speeds when economically advantageous. However, once CII compliance becomes relevant, the profit margin under SAS6 declines, and it converges with SAS4 indicating that in regulatory contexts, both scenarios tend to rely on slower, more efficient speeds.

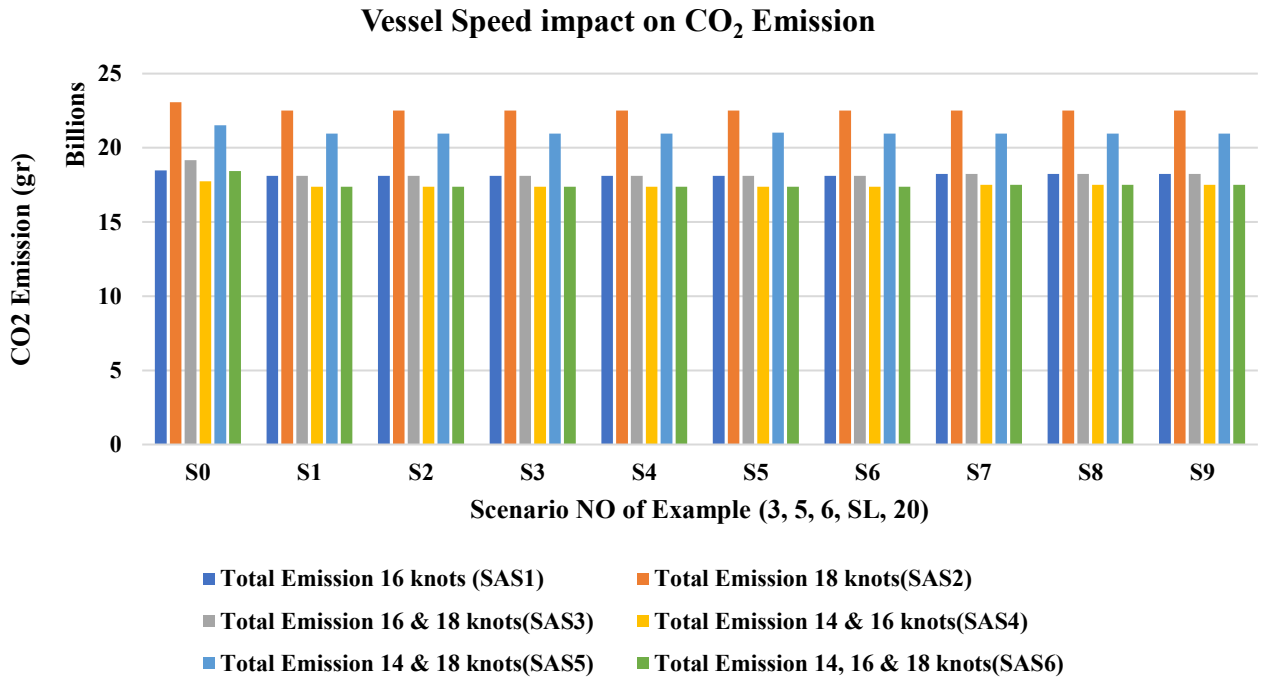

Figure 4.27: Different Speed Level impact on CO_2 emission example (3, 5, 6, SL, 20)

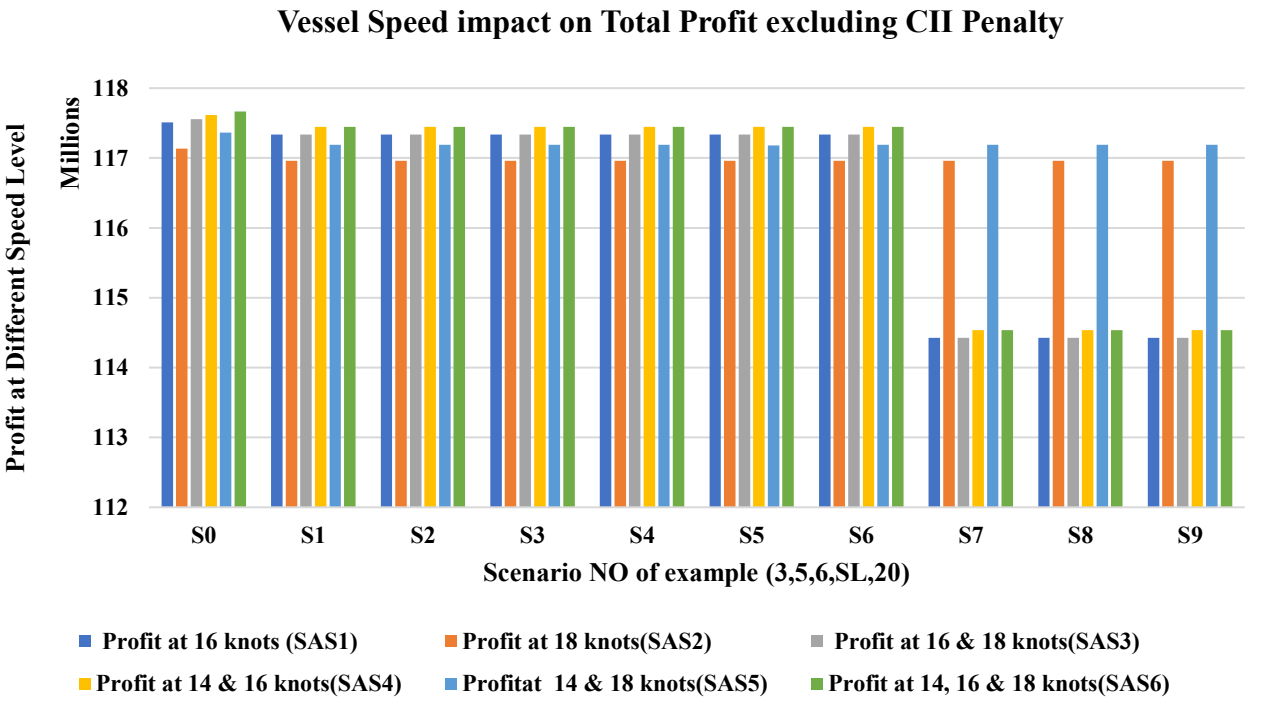

Figure 4.28: Different Speed Level impact on Portfolio Profit example (3, 5, 6, SL, 20)

Further insights can be drawn from Figure 4.29, which detail the distribution of A rated vessel per scenario. In SAS2 and SAS5, the time window constraints at both loading and discharging ports prevent vessels from obtaining an ‘A’ rating at solo high speed and lower speed; instead, these scenarios predominantly result in ‘B’ and ‘C’ ratings (Figure 4.30 & Figure 4.31). Despite this, both scenarios deliver relatively high profits in the final three CII penalty scenarios (Figure 4.28), when penalty costs are steep. This outcome reflects a trade-off strategy where the model accepts lower environmental ratings in exchange for higher profit, particularly when the cost of full compliance outweighs the economic benefit.

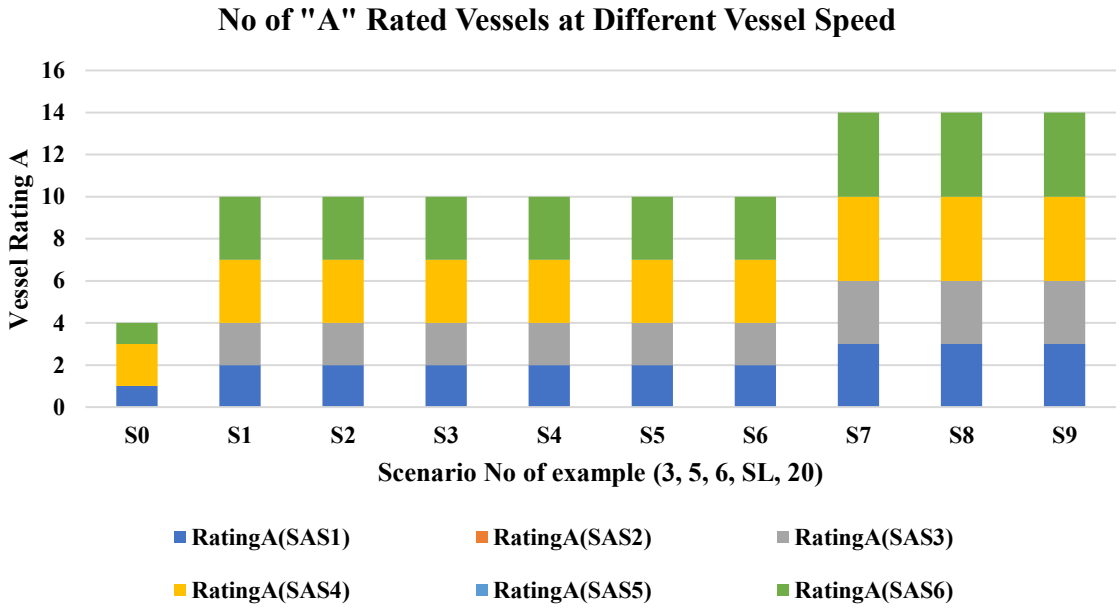

Figure 4.29: No of “A” Rated Vessel at Different Vessel Speed example (3, 5, 6, SL, 20)

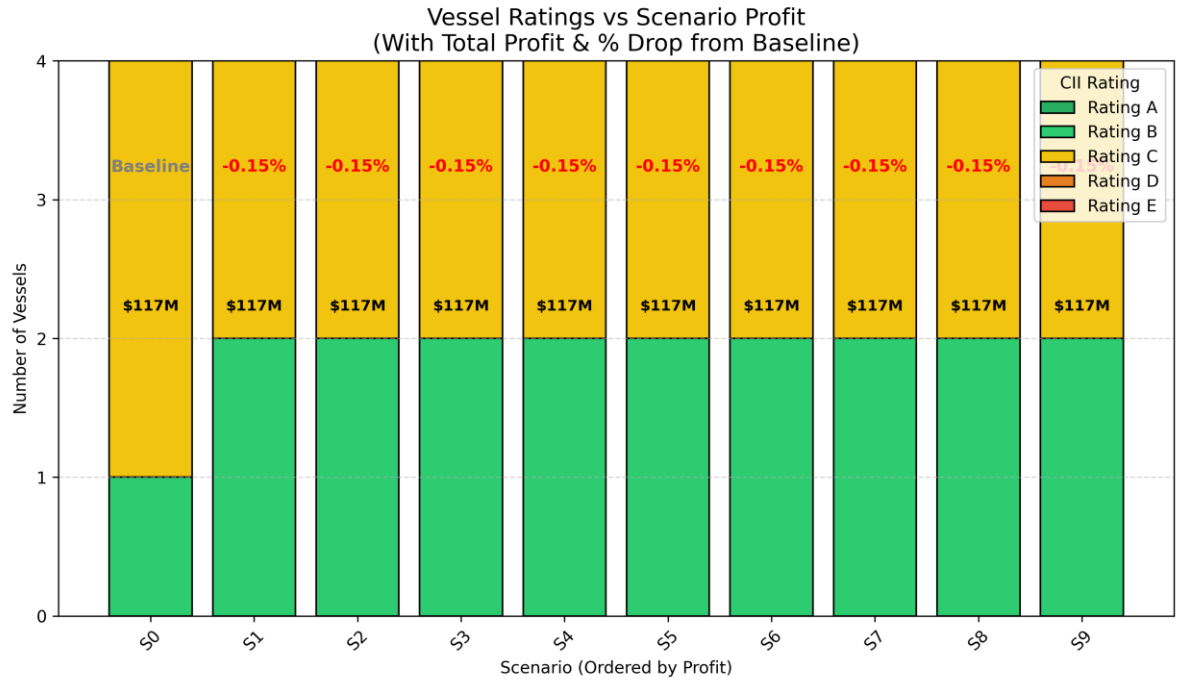

Figure 4.30: SAS2 Profit & Vessel Ratings example (3, 5, 6, 3, 20)

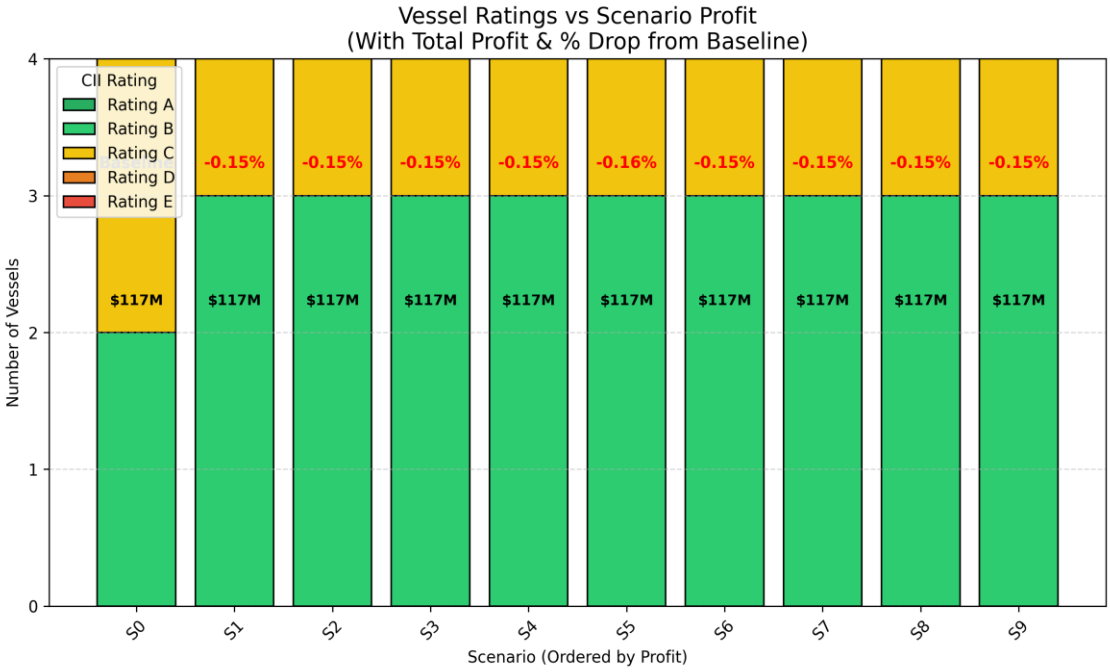

Figure 4.31: SAS5 Profit &Vessel Rating (3, 5, 6, 1-3, 10)

In the second case study, (4, 8, 9, SL, 25), an interesting pattern emerges: when CII is not enforced (scenario S0), the overall CO_2 emissions are lower compared to most scenarios where CII penalties are applied. This counterintuitive result, also observed in earlier examples within the Mathematical Experiment section (Section 4.3), highlights how emission reductions are not guaranteed simply by introducing CII constraints, particularly if other operational factors such as time windows or penalty weights limit flexibility.

Once CII penalties are introduced (scenarios S1–S9), the highest emissions are consistently observed in SAS2 (fixed 18 knots) and SAS5 (14 & 18 knots), both of which involve high-speed operation either entirely or partially. These configurations lead to greater fuel consumption and consequently higher CO_2 emissions, despite regulatory pressure (Figure 4.32). In contrast, the lowest CO_2 emissions (excluding the baseline S0) occur under SAS6, where the model is allowed to optimise vessel deployment using a combination of all three speeds (14, 16, and 18 knots). This flexibility enables the model to dynamically allocate lower speeds when possible (particularly for longer hauls or when time windows permit) while still allowing occasional use of higher speeds where operationally justified. The results underscore the environmental advantage of incorporating a broader range of speed options in the optimisation framework, especially under tightening regulatory conditions.

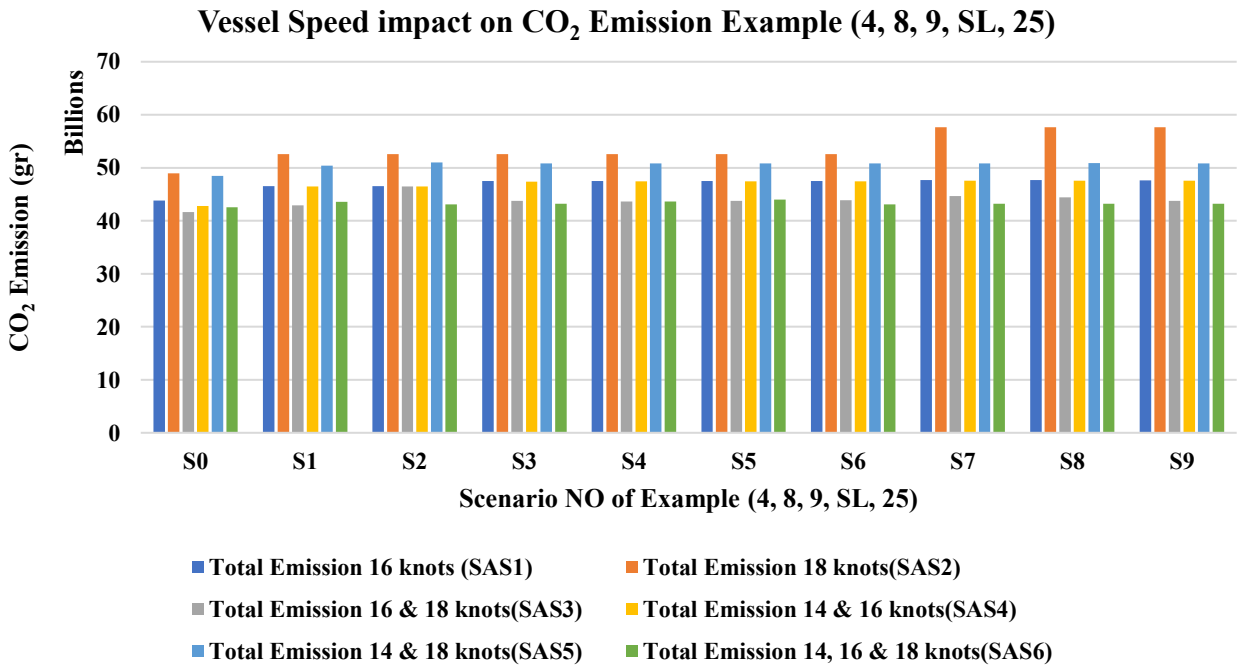

Figure 4.32: Different Speed Level impact on CO2 emission example (4, 8, 9, SL, 25)

As illustrated in Figure 4.33, higher portfolio profits are generally achieved in scenarios where vessels have access to higher sailing speeds, particularly in SAS5 (14 & 18 knots) and SAS6 (14, 16, & 18 knots). This is largely due to the model's ability to leverage faster transit times, allowing more efficient scheduling and reduced idle time, especially under tighter time window constraints.

In contrast, the lowest profit levels are observed in SAS1 (fixed 16 knots) and SAS4 (14 & 16 knots). These scenarios limit the vessels' ability to meet tight loading and discharging schedules efficiently, often forcing suboptimal supplier-customer pairings and reducing the model's flexibility in optimising vessel allocation. The lack of flexibility to deviate from strict time windows combined with the exclusion of higher speeds constrains the system's economic performance, even if environmental outcomes are improved.

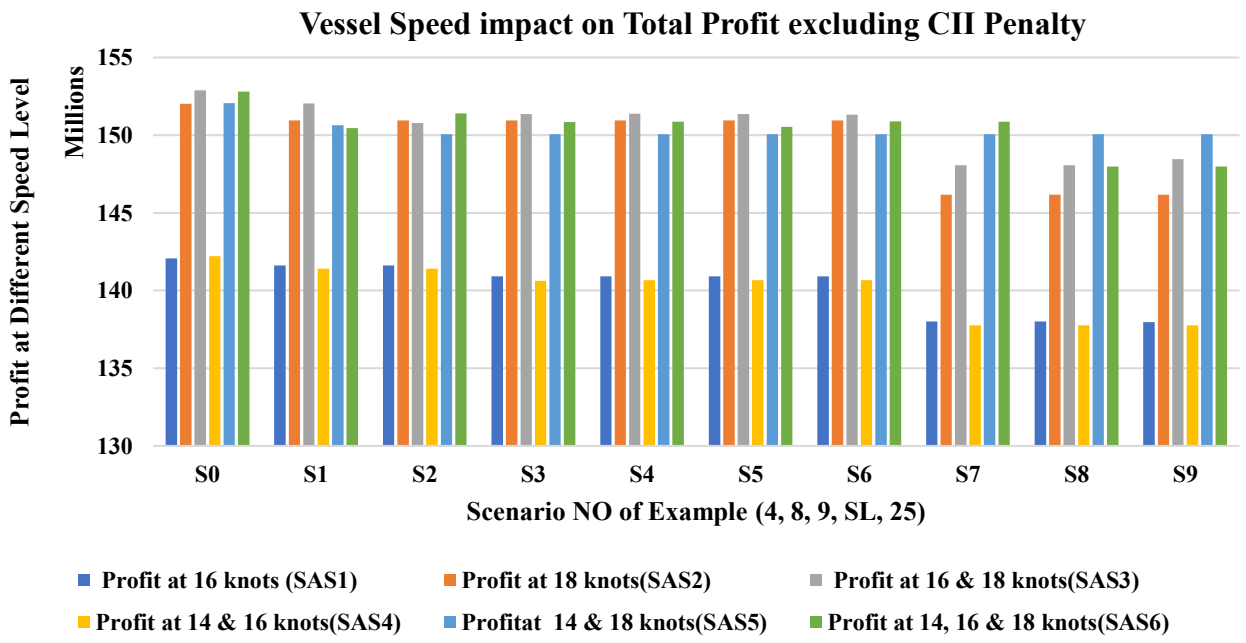

Figure 4.33: Different Speed Level impact on Portfolio Profit example (4, 8, 9, SL, 25)

Further insights can be drawn from Figure 4.34, which illustrates the distribution of vessels achieving an 'A' rating across different sensitivity analysis scenarios (SAS). In SAS2, where vessels operate exclusively at a constant speed of 18 knots throughout the planning horizon, the model fails to achieve any 'A' ratings.

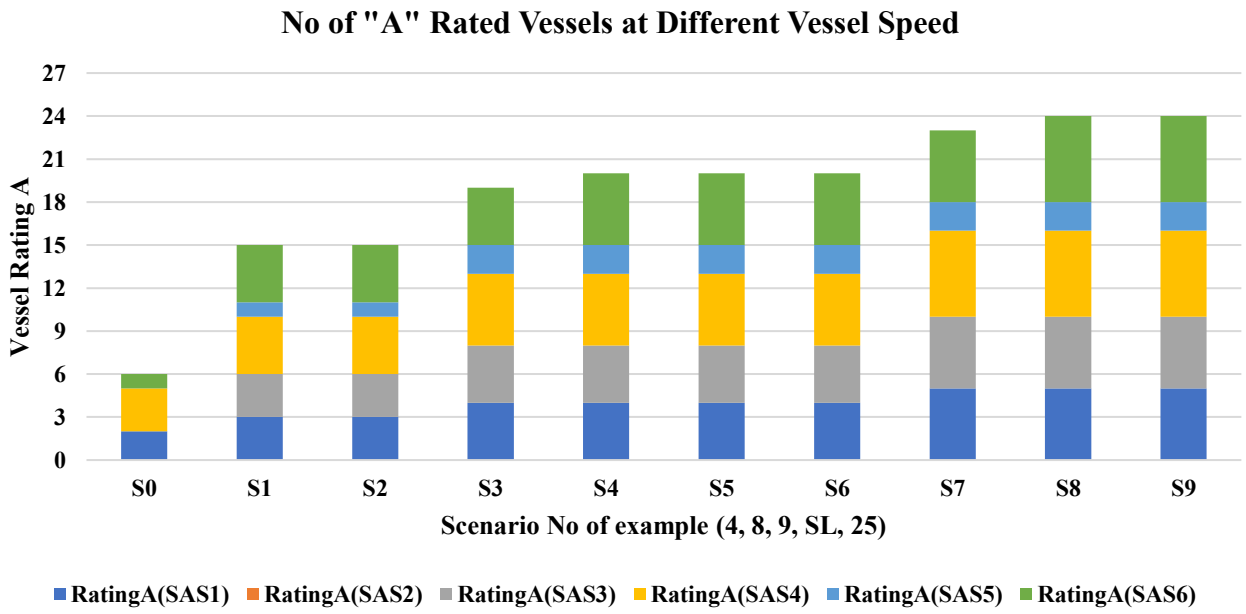

Figure 4.34: No of "A" Rated Vessel at Different Vessel Speed example (4, 8, 9, SL, 25)

This is primarily due to the high fuel consumption and elevated CO_2 emissions associated with this higher fixed speed. Consequently, vessels in this scenario predominantly receive lower ratings, such as 'B', 'C', or even 'D', as shown in Figure 4.35.

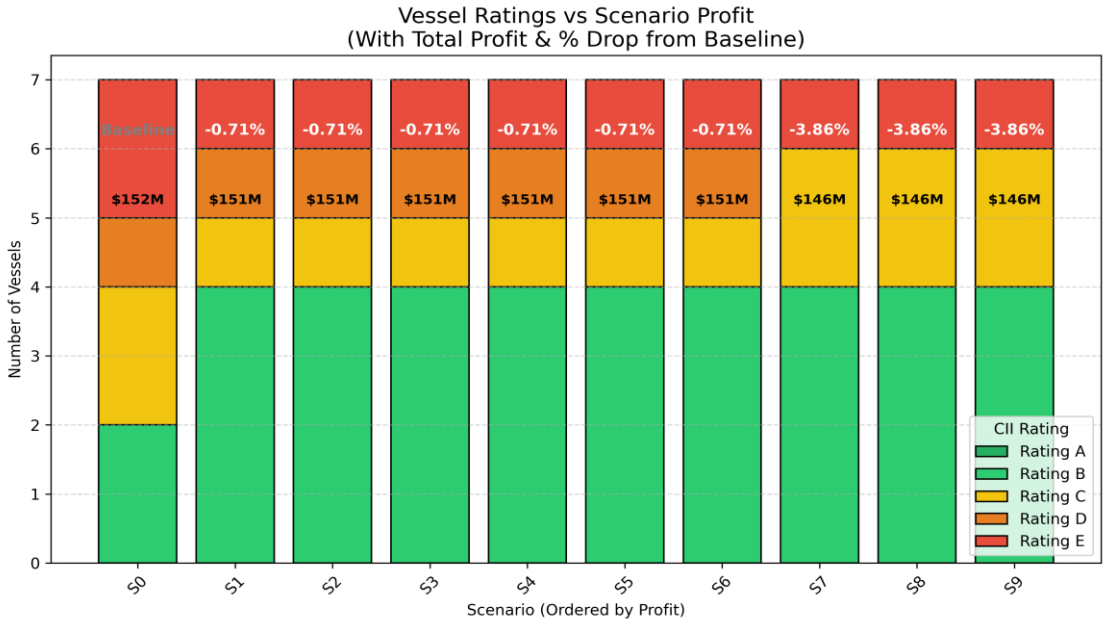

Figure 4.35:SAS2 Profit & Vessel Ratings example (4, 8, 9, 3, 25)

Nevertheless, across all scenarios in the demonstrated experiments, there is a consistent and gradual increase in the number of 'A'-rated vessels as the CII penalty intensifies**.** This demonstrates the model's adaptive behaviour under stricter regulatory environments; wherein higher penalties incentivise the selection of slower speeds and more environmentally compliant vessel operations.

4.6.2 **Impact of Time Window Flexibility on Profitability, Emissions, and CII Ratings**

Operational flexibility in the form of extended loading and discharging time windows can significantly influence vessel scheduling, speed selection, and idle time management. To investigate the impact of time window thresholds on portfolio profit, vessel-level CII ratings, and total carbon emissions, two sensitivity scenarios are developed. These aim to assess whether looser time constraints can enable better optimisation of environmental and economic outcomes.

First scenario: Expanded Time Windows by Two-Day.

In this scenario, one day is added to both the start and end of the loading and discharging time windows, effectively extending the window from 2 days to 4 days.

To evaluate the effects, three representative examples (3,5,6,1-2,20), (3,5,6,1-2-3,20), and (4,8,9,1-2,25) are selected to execute. These configurations are solved to optimality (zero optimality gap), providing a consistent basis for comparison with baseline scenarios using the original, tighter time windows.

The results demonstrate that, this increased flexibility allows vessels to better align their arrival and departure schedules, potentially reducing idle time and enabling the use of lower sailing speeds without compromising feasibility and results in both higher portfolio profit and improved vessel CII ratings, even in the initial planning scenarios. With greater flexibility, the model could allocate vessels more effectively and operate them at lower speeds, thus reducing fuel consumption and emissions. Despite minor reductions in profit (ranging between 0.5% and 1.7%), the trade-off is economically justified given the substantial improvement in environmental compliance. The fleet consistently achieved more favourable CII outcomes with minimal financial compromise.

The detailed breakdown of profit and vessel CII ratings for each of the evaluated examples is presented in Figure 4.36, Figure 4.37and Figure 4.38, confirming that even modest extensions to operational time windows can yield substantial sustainability and compliance benefits.

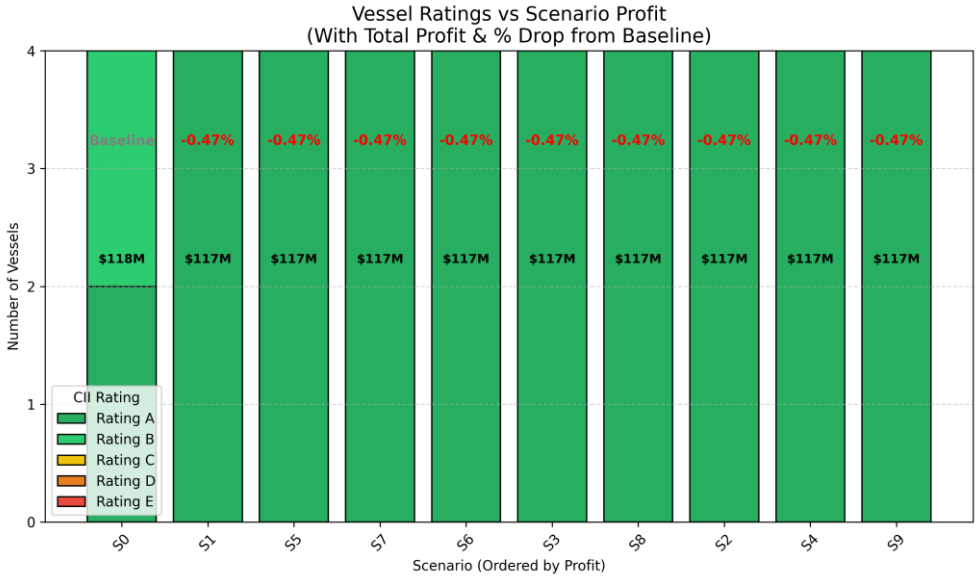

Figure 4.36: Sensitivity Analyses Vessel Rating TW 1st Scenario example (3, 5, 6, 1-2, 20)

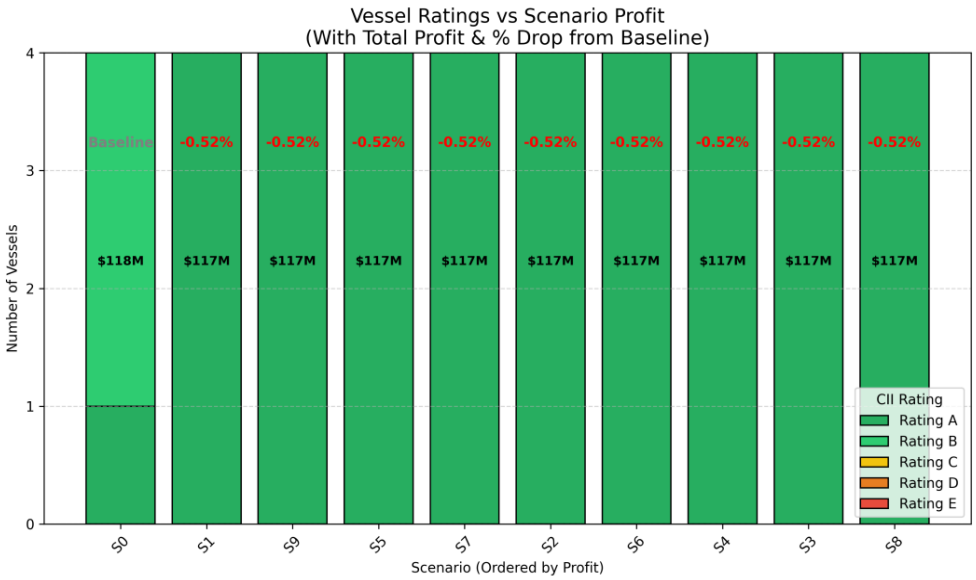

Figure 4.37: Sensitivity Analyses Vessel Rating TW 1st Scenario example (3, 5, 6, 1-2-3, 20)

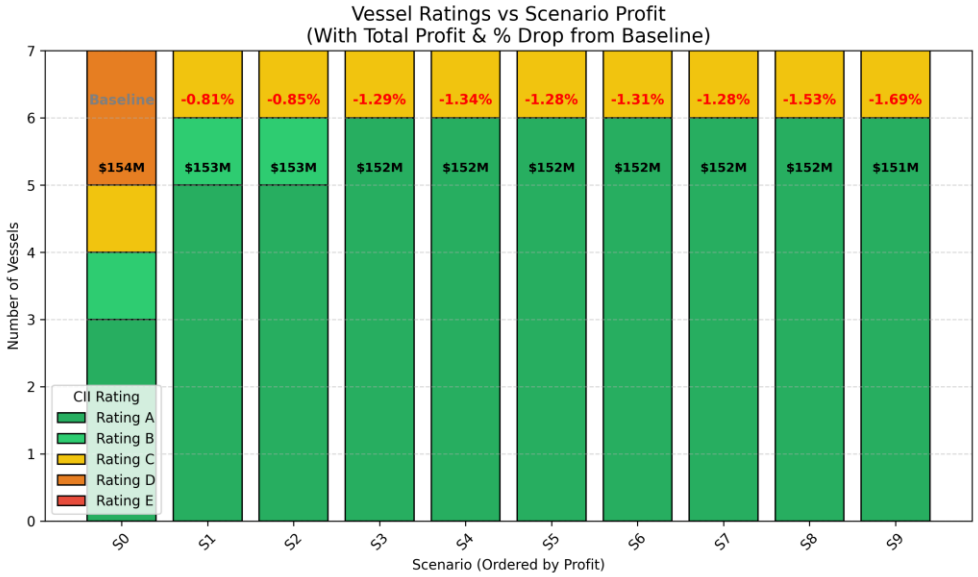

Figure 4.38: Sensitivity Analyses Vessel Rating TW 1st Scenario example (4, 8, 9, 1-2, 25)

Second Scenario: Expanded Time Windows by One-Day.

In the second time window flexibility scenario, a more moderate adjustment was tested: a one-day extension only to the end of the loading and discharging time windows is added. Unlike the first scenario, which offered a symmetric increase at both ends, this configuration provides limited but still meaningful scheduling flexibility. The model effectively leveraged this extended window to optimise vessel allocation and speed decisions. It favoured lower operational speeds, resulting in reduced fuel consumption and lower CO_2 emissions, while keeping the original provider-customer pairings and routing structure. This consistency indicates that the additional day allowed more efficient use of vessel time without disrupting the logistical integrity of the supply chain.

The results showed notable improvements in CII ratings across the fleet, with most vessels reaching a rating of A or B (see Figure 4.39, Figure 4.40 and Figure 4.41). Additionally, portfolio profit remained very close to the baseline, indicating that the environmental gains are achieved without significant economic sacrifice. The model's preference for allocating more fuel-efficient vessels under this relaxed constraint further highlights the synergy between environmental performance and fleet-level optimisation.

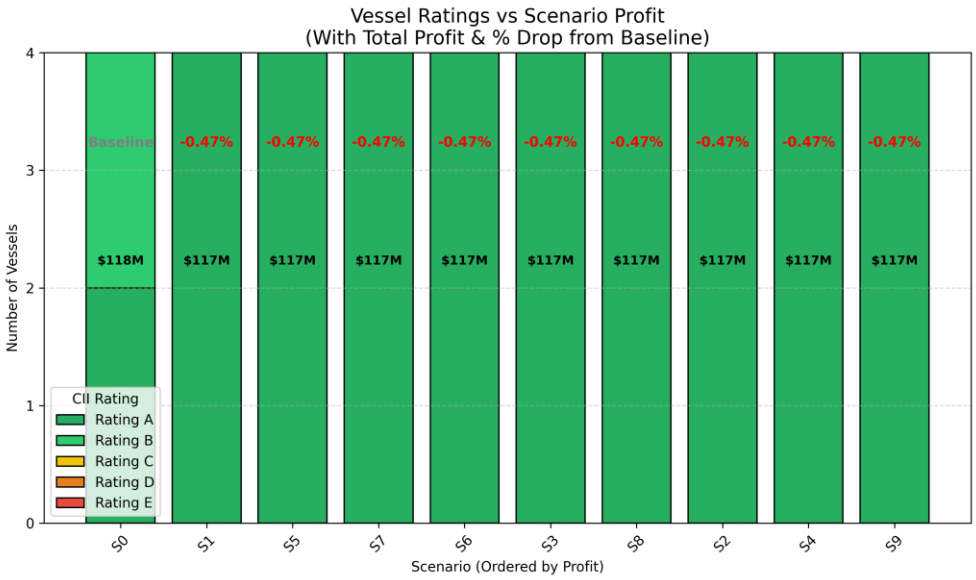

Figure 4.39: Sensitivity Analyses Vessel Rating TW 2nd Scenario example (3, 5, 6, 1-2, 20)

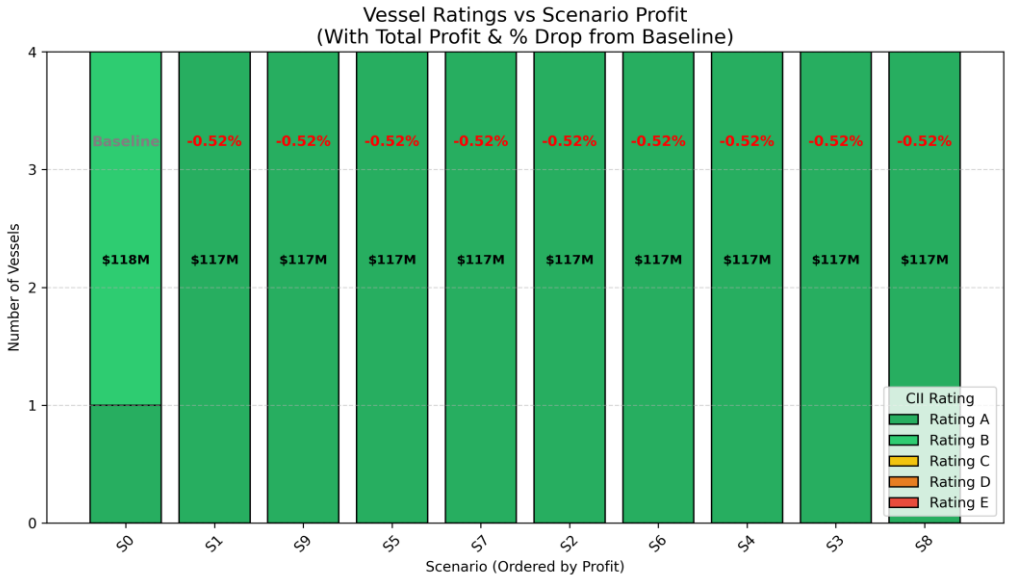

Figure 4.40: Sensitivity Analyses Vessel Rating TW 2nd Scenario example (3, 5, 6, 1-2-3, 20)

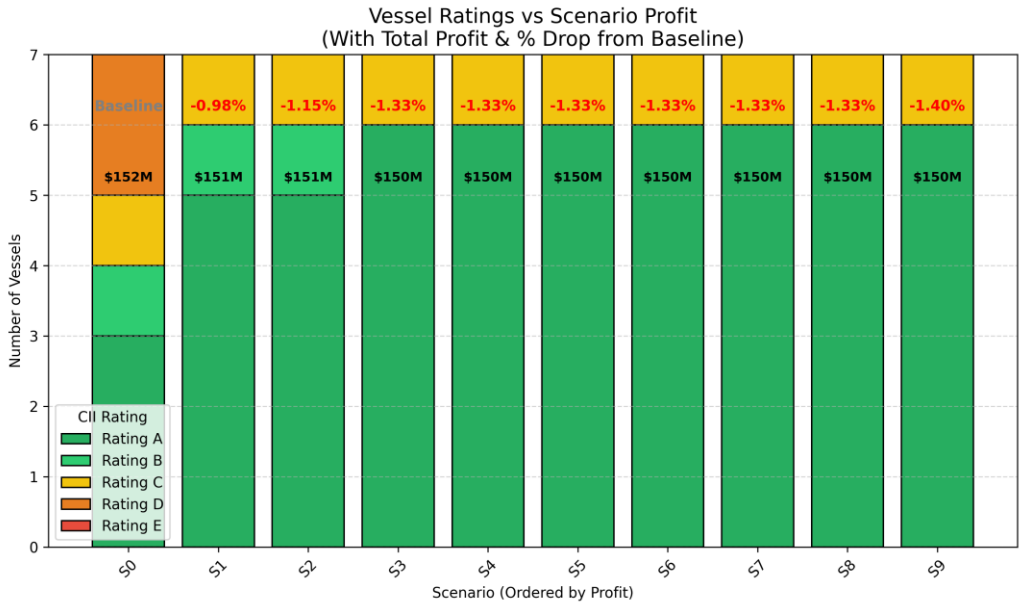

Figure 4.41: Sensitivity Analyses Vessel Rating TW 2nd Scenario example (4, 8, 9, 1-2, 25)

The results indicate that extending the delivery time window by one or two days yields higher profits and lower CO_2 emissions compared with the no-extension scenario. This outcome is primarily attributable to reduced vessel idle time and lower fuel consumption under the extended time window scenarios. Moreover, between the two extension options, the two-day extension outperforms two-day extension in terms of profitability, fuel consumption, and vessel utilisation. These findings underscore the importance of carefully selecting delivery time window thresholds to achieve improved economic performance while simultaneously reducing environmental impacts. To better illustrate the benefits of increased time window flexibility and the corresponding use of lower sailing speed**s**, the emission results of example (4,8,9,1-2,25) across no extension, one day extension and two-day extension in time window has been provided in Figure 4.42. The figure clearly demonstrates a substantial reduction in CO_2 emissions. When comparing the case with no time extension to those with extended windows, the results show a significant drop in emissions due to the model's increased reliance on lower speeds. Moreover, even between the one-day and two-day extension scenarios, the one more day flexibility allows the model to capitalise more effectively on low-speed operation without compromising fulfilment of demand or logistical feasibility.

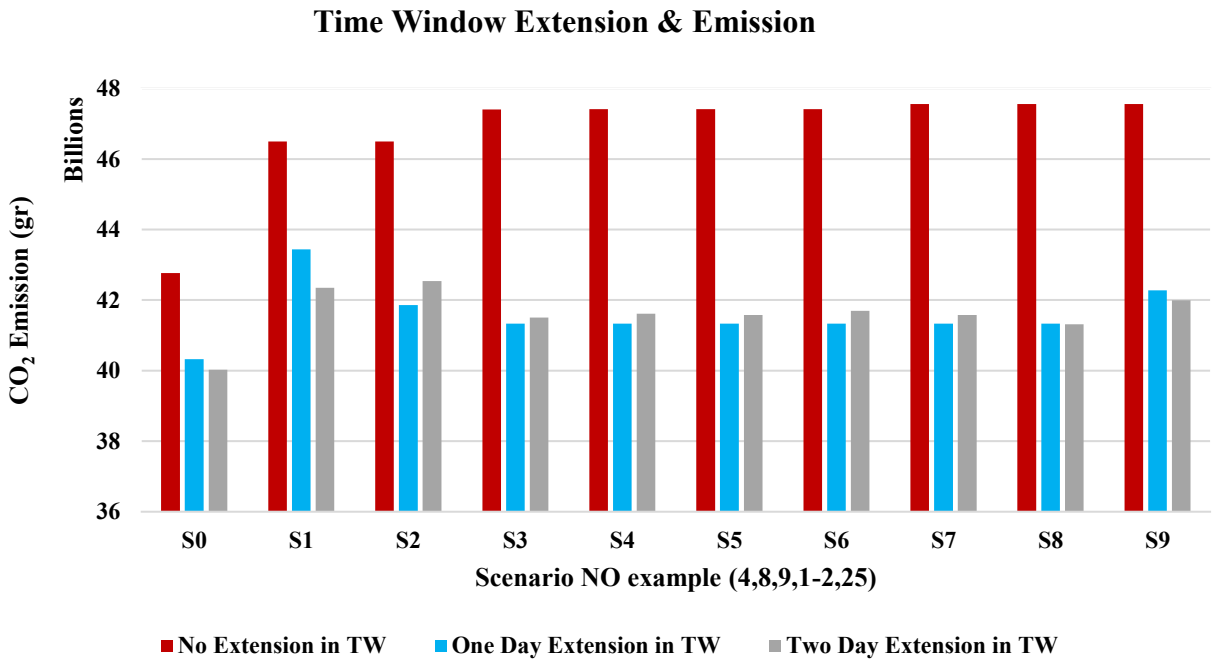

Figure 4.42: TW flexibility impact on Emission example (4, 8, 9, 1-2, 25)

In terms of profitability, the portfolio profit is highest in the scenario with the two-day extension (Figure 4.38) as the system can optimise vessel deployment more efficiently balancing slower speeds with better CII ratings and reduced fuel consumption. This outcome confirms the dual advantage of extended time windows, enhanced environmental performance and improved economic returns, highlighting the critical role of port time flexibility in sustainable maritime logistics.

4.7 Conclusion

In this chapter, 400 experiments were conducted to evaluate the validity and robustness of the proposed mathematical model, particularly in relation to how it responds when the CII regulation is incorporated into portfolio optimisation. To ensure scalability and applicability to real-world scenarios, a genetic-based metaheuristic algorithm was enhanced and successfully applied to manage a one-year delivery planning horizon, effectively accounting for CII constraints.

One of the key findings of this study is the critical role of speed variation, particularly the inclusion of lower sailing speeds, in supporting optimal delivery planning. Lower speeds contribute significantly to achieving acceptable CII ratings while still meeting customer demand requirements. This highlights that speed is not only an operational parameter but also a key decision variable influencing supplier–customer pairing, routing, and vessel allocation.

However, as highlighted in the emissions results, compliance with CII regulations does not necessarily lead to a reduction in total CO_2 emissions. In several scenarios, emissions were observed to increase even when vessels achieved improved CII ratings. This indicates that the CII metric reflects a trade-off between fuel consumption, sailed distance, and vessel deadweight tonnage, where operational decisions such as speed selection, route changes, and vessel allocation can improve CII ratings without necessarily reducing absolute emissions.

In this context, the modelling of speed becomes particularly important. While vessel speed is represented using discrete levels in this study to maintain computational tractability, this simplification is not expected to significantly affect the overall routing or emission outcomes, as the selected speed levels capture the main operational regimes and their associated trade-offs. However, this approach may limit the precision of fine-grained speed adjustments. Future work could explore continuous or piecewise linear speed modelling to further improve solution accuracy and better capture detailed operational behaviour.

The sensitivity analyses further revealed that flexibility in the loading and discharging time windows, enables better scheduling outcomes. This flexibility allows the model to select more efficient vessel-speed combinations, resulting in improved CII ratings while incurring only marginal profit losses.

Additionally, vessel-port compatibility emerged as a significant constraint. In scenarios where an inefficient vessel is the only compatible option, the model is limited in its ability to reduce emissions or improve ratings, emphasising the importance of having a diversified and efficient fleet.

Collectively, these findings suggest that the use of low-carbon fuels may be essential in achieving genuine emission reductions. While the CII regulation pushes for operational optimisation, it does not always lead to lower emissions. The model ultimately balances trade-offs among distance sailed, fuel consumption, DWT, and profit, often without a corresponding drop in emissions despite regulatory compliance.

CHAPTER 5 CONCLUSION AND FUTURE RESEARCH

Summary

This chapter concludes the thesis by reflecting on the achievement of the research objectives outlined in Section 1.2. It highlights the key contributions from both theoretical and practical perspectives in Section 1.4, demonstrating the study's relevance to sustainable maritime logistics and decision-making under regulatory constraints. Section 5.2 discusses the limitations of the current work and outlines potential directions for future research to build upon the findings and further enhance the applicability of the proposed modelling framework.

5.1 New Contributions and Implications

The global transition towards sustainable energy has cemented LNG as a critical bridge fuel, placing unprecedented operational demands on maritime logistics. As international regulatory bodies, particularly the IMO, enforce stringent decarbonisation mandates, shipping operators are forced to rethink traditional supply chain strategies. Historically, academic literature and industrial practices have approached LNG delivery planning in a fragmented manner, isolating vessel routing, inventory management, and time-varying market prices from the compounding complexities of environmental compliance. Specifically, there has been a notable absence of unified, portfolio-level modelling capable of balancing the commercial imperative of profit maximisation with the rigid, cumulative constraints of operational metrics such as the CII.

To bridge this critical gap, this research introduced an integrated optimisation framework designed to serve as a comprehensive decision-support tool for commercial LNG distributors. By developing a robust MILP formulation and a highly efficient Genetic-Based Metaheuristic Algorithm, this study successfully united dynamic cargo pairing, heterogeneous fleet scheduling, variable speed selection, and onboard inventory and boil-off management within a strict, carbon-constrained environment.

The objectives of this thesis, as outlined in Section 1.2, are comprehensively addressed through a structured progression across previous chapters, with each corresponding research question from Section 1.3 answered in turn. This is demonstrated by the following list of applied methodologies and research outcomes:

1) Conducting a systematic literature review was conducted (Chapter 2), which successfully identified critical methodological gaps in current operations research specifically, the lack of integrated, portfolio-level models capable of balancing complex LNG logistics with emerging environmental regulations like the CII.
2) Developing a robust Mixed-Integer Linear Programming model was successfully formulated. It embeds practical constraints including vessel-port compatibility, , commercial time windows, time-varying energy prices, heterogeneous vessel speeds, ballast/laden differentiation, and capacity variations tied to calorific values (Chapter 3).
3) Developing a genetic-based metaheuristic algorithm to address the NP-hard nature of the MILP model. Benchmarking against empirical data demonstrated that this approach is highly effective for large-scale applications, achieving approximately 96% of the exact model's optimality while requiring only one-twentieth of its execution time (Chapter 3).
4) Incorporating the IMO's CII regulations and analyse the operational and economic impacts. The baseline MILP model was successfully extended to internalise CII metrics (CO_2 emissions, fuel consumption, and distance sailed). The analysis quantified the trade-offs, demonstrating that achieving higher CII ratings significantly alters fleet average sailing distances, vessel allocation, and overall profitability (Chapter 4).
5) Enhancing the metaheuristic algorithm for CII compliance and evaluate strategic trade-offs. The metaheuristic algorithm was enhanced to generate CII-compliant, year-long delivery portfolios on a scenario-by-scenario basis. The evaluation yielded critical insights, proving that lower sailing speeds and flexible time windows can improve emissions ratings without catastrophic profit losses. Furthermore, it identified that for vessels with inherent structural or port compatibility limitations, operational optimisation is insufficient, making the adoption of alternative low-carbon fuels necessary (Chapter 4).

The findings of this research extend beyond the immediate mathematical results, offering significant implications for industry practitioners, policymakers, and the academic community:

1) Managerial and Commercial Implications:

For LNG distributors, fleet operators, and portfolio managers, this thesis provides a highly actionable, strategic decision-support framework. By quantifying the exact trade-offs between profit maximisation and CII compliance, the model empowers operators to transition from reactive regulatory reporting to proactive, environmentally constrained fleet management. The research explicitly demonstrates that negotiating flexible delivery time windows and implementing strategic slow steaming can safeguard profitability while preventing severe regulatory penalties. Consequently, this framework serves as a vital tool for commercial stakeholders to optimize asset utilisation and protect their current fleets from becoming commercially stranded in an increasingly regulated market.

2) Regulatory and Policy Implications:

The findings offer crucial feedback to international regulatory bodies, such as the IMO, regarding the practical realities of the CII framework. The sensitivity analysis reveals a critical structural limitation within the industry: for certain vessels restricted by rigid port compatibility or older technical designs, operational optimisation even using advanced metaheuristic yields only marginal improvements in emissions ratings (e.g., shifting from a D to a C rating). This implies that while the CII successfully forces operational discipline, policymakers must recognize that regulatory compliance cannot be achieved through logistical optimisation alone. This finding provides empirical backing for the urgent, parallel need to incentivise massive capital investment in alternative low-carbon fuels and infrastructure.

3) Methodological and Academic Implications:

From an Operations Research perspective, this study establishes a new methodological benchmark for large-scale maritime routing under cumulative environmental constraints. Historically, the literature has struggled to balance the NP-hard nature of multi-vessel routing with the complex, year-long mathematical coupling required by emissions tracking. By successfully integrating dynamic boil-off, variable calorific values, and cumulative CII penalties into both an exact MILP formulation and a highly efficient genetic metaheuristic, this research proves that massive, environmentally constrained industrial datasets are computationally

solvable. This hybrid approach equips the academic community with a robust, foundational blueprint for modelling future environmental policies and mapping emerging zero-carbon supply chains.

Finally, to demonstrate the tangible results of the proposed framework, an illustrative delivery plan for five cargoes is provided in Appendix A. This appendix presents the comprehensive final output of the model, detailing the successful integration of portfolio optimisation, supplier-customer pairing, routing, scheduling, and on-board inventory management. The breakdown of vessel activities includes expected arrival and departure times, loading and discharging operations, and highly granular data on dynamic boil-off and heel quantities. By translating complex mathematical results into accessible operational schedules, such outputs empower logistics managers with a clear understanding of both current fleet performance and forthcoming strategic actions, ultimately enhancing the decision-making process across the modern LNG supply chain.

5.2 Limitations and Future Research

Although this thesis offers a comprehensive approach to portfolio optimisation within the energy shipping sector, providing valuable insights into the trade-offs between profitability, operational cost, and environmental performance, there remain several limitations that open avenues for future research.

The mathematical framework and metaheuristic algorithm developed in this thesis operate under deterministic assumptions, meaning that parameters such as time-varying fuel price, customer demand volumes, and port time windows are assumed to be known with certainty across the planning horizon. While this deterministic baseline is absolutely necessary to establish the foundational integration of operational and CII regulatory constraints, real-world LNG supply chains are subject to significant volatility. Future research should therefore seek to extend this framework into the realm of stochastic or robust optimisation. By incorporating uncertainty on both the supplier side (e.g., unexpected supply disruptions, price shocks, or berth unavailability) and the customer side (e.g., fluctuating demand volumes or shifting delivery windows), future models could evaluate the resilience of the delivery portfolio. Developing predictive or adaptive algorithms to handle such dynamic disruptions would further elevate the practical applicability of the decision-support tool in highly volatile market conditions.

In the planning framework developed in this research, it has been assumed that the entire fleet remains available throughout the considered time horizons. This assumption broadly reflects industry practice, particularly in contexts where a substantial number of cargoes must be transported globally. Nonetheless, in practice there are periods during which vessels remain idle for extended durations, still incurring operational and opportunity costs for the company. To mitigate these costs, chartering out idle vessels represents a viable strategy. By temporarily reallocating underutilised assets, companies can offset the financial burden associated with inactivity while simultaneously recovering part of the fixed costs, thereby enhancing overall portfolio efficiency. The analysis also reveals a critical insight that compliance with CII regulations does not necessarily lead to reduced CO_2 emissions. In several instances, scenarios without CII enforcement exhibited lower emissions despite achieving lower ratings. This paradox highlights the need for further empirical investigation into the effectiveness of CII as an operational regulatory mechanism. As this thesis represents one of the first attempts to study CII within a portfolio optimisation context, it lays the groundwork for extending this analysis to include other IMO measures such as the EEXI, EU ETS and Fuel EU Maritime.

Incorporating the option for fuel switching where vessels can change onboard fuel types based on economic and environmental conditions could enhance both profitability and CII performance. This extension would require integrating the cost of alternative fuels and their carbon intensity directly into the optimisation process, enabling dynamic adjustments that improve ratings without sacrificing financial outcomes if applicable.

Another area for further exploration is the inclusion of weather-related disruptions and ocean currents. Adverse weather conditions can cause delays in loading and discharging operations, potentially affecting time window feasibility, vessel allocation, and overall supply chain efficiency. Incorporating stochastic or scenario-based modelling of weather events could provide a more realistic representation of operational uncertainty.

Lastly, the current model assumes that all cargoes are transported via the shortest possible sailing paths. While this assumption ensures computational tractability, it limits the model's adaptability to real-world routing constraints, such as geopolitical disruptions, piracy zones, or port congestion. Future research could consider multiple route alternatives and allow the model to endogenously select paths based on cost, emissions, and regulatory compliance.

In summary, while this research provides a robust and novel foundation, its extension to incorporate uncertainty in the portfolio, fuel flexibility, weather variability, ocean currents, boil off gas management, alternative routing, and broader regulatory instruments will help create even more realistic and practical optimisation tools for sustainable maritime logistics. Although the inclusion of all these features would substantially increase model complexity and computational difficulty, integrating a limited subset of such elements would bring the proposed framework closer to real-world fuel supply chain operations.

REFERENCES

Al-Breiki, M., & Bicer, Y. (2020). Technical assessment of liquefied natural gas, ammonia and methanol for overseas energy transport based on energy and exergy analyses. *International journal of hydrogen energy, 45*, 34927–34937. https://doi.org/10.1016/j.ijhydene.2020.04.181

Al-Haidous, S., Govindan, R., Elomri, A., & Al-Ansari, T. (2022). An optimization approach to increasing sustainability and enhancing resilience against environmental constraints in LNG supply chains: A Qatar case study. *Energy Reports, 8*, 9742–9756. https://doi.org/10.1016/j.egyr.2022.07.120

Al-Haidous, S., Msakni, M. K., & Haouari, M. (2016). Optimal planning of liquefied natural gas deliveries. *Transportation Research Part C: Emerging Technologies, 69*, 79–90. https://doi.org/10.1016/j.trc.2016.05.017

Ali Pitchay, S. & Shorman, S., 2015. Significance of parameters in genetic algorithm, the strengths, its limitations and challenges in image recovery. *Journal of Engineering and Applied Science*, February, Volume 10, pp. 585-593.

Andersson, H., Christiansen, M., Desaulniers, G., & Rakke, J. G. (2017). Creating annual delivery programs of liquefied natural gas. *Optimization and Engineering, 18*, 299–316. https://doi.org/10.1007/s11081-015-9305-y

Balcombe, P., Brierley, J., Lewis, C., Skatvedt, L., Speirs, J., Hawkes, A., & Staffell, I. (2019). How to decarbonise international shipping: Options for fuels, technologies and policies. *Energy conversion and management, 182*, 72–88. https://doi.org/10.1016/j.enconman.2018.12.080

Barreiro, J., Zaragoza, S., & Diaz-Casas, V. (2022). Review of ship energy efficiency. *Ocean Engineering, 257*, 111594. https://doi.org/10.1016/j.oceaneng.2022.111594

Bartlett, P. (2023, January). *Clarksons expects 30% of ships to be rated D or E in CII assessments.* Retrieved from https://www.seatrade-maritime.com/green-shipping/clarksons-expects-30-of-ships-to-be-rated-d-or-e-in-cii-assessments

Bayraktar, M., & Yuksel, O. (2023). A scenario-based assessment of the energy efficiency existing ship index (EEXI) and carbon intensity indicator (CII) regulations. *Ocean Engineering, 278*, 114295. https://doi.org/10.1016/j.oceaneng.2023.114295

Bilgili, L. (2021). Comparative assessment of alternative marine fuels in life cycle perspective. *Renewable and Sustainable Energy Reviews, 144*, 110985. https://doi.org/10.1016/j.rser.2021.110985

Biresselioglu, M. E., Demir, M. H., & Kandemir, C. (2012). Modeling Turkey's future LNG supply security strategy. *Energy Policy, 46*, 144–152. https://doi.org/10.1016/j.enpol.2012.03.045

Bittante, A., Pettersson, F., & Saxén, H. (2018). Optimization of a small-scale LNG supply chain. *Energy, 148*, 79–89. https://doi.org/10.1016/j.energy.2018.01.120

Calvert, S., Deakins, E., & Motte, R. (1991). A Dynamic System for Fuel Optimization Trans-Ocean. *Journal of Navigation, 44*, 233–265. doi:10.1017/S0373463300009978

Chen, Y., Zhou, X., Chen, S., & Mi, J. J. (2024). LNG freight rate and LNG price, carbon price, geopolitical risk: A dynamic connectedness analysis. *Energy, 302*, 131517. https://doi.org/10.1016/j.energy.2024.131517

Cheng, L., Xu, L., & Bai, X. (2025). Cargo selection, route planning, and speed optimization in tramp shipping under carbon intensity indicator (CII) regulations. *Transportation Research Part E: Logistics and Transportation Review, 194*, 103948. https://doi.org/10.1016/j.tre.2024.103948

Cho, J., Lim, G. J., Biobaku, T., Bora, S., & Parsaei, H. (2014). Liquefied natural gas ship route planning model considering market trend change. *Transactions on Maritime Science, 3*, 119–130. https://doi.org/10.7225/toms.v03.n02.003

Cho, J., Lim, G. J., Kim, S. J., & Biobaku, T. (2018). Liquefied natural gas inventory routing problem under uncertain weather conditions. *International Journal of Production Economics, 204*, 18–29. https://doi.org/10.1016/j.ijpe.2018.07.014

Chuah, L. F., Mokhtar, K., Ruslan, S. M., Bakar, A. A., Abdullah, M. A., Osman, N. H., . . . Show, P. L. (2023). Implementation of the energy efficiency existing ship index and carbon intensity indicator on domestic ship for marine environmental protection. *Environmental Research, 222*, 115348. https://doi.org/10.1016/j.envres.2023.115348

Clark, D., Barahona, S., & Queljoe, M. D. (2023, June). *New estimates provide insights on CO2 emissions from global shipping.* Retrieved from https://oecdstatistics.blog/2023/06/15/new-estimates-provide-insights-on-co2-emissions-from-global-shipping/

ClassNK. (2022, February). *Outlines of EEXI regulation.* ClassNK. https://www.classnk.or.jp/hp/pdf/activities/statutory/eexi/eexi_rev5e.pdf

ClassNK. (2023). *CII (Carbon Intensity Indicator).* Green Certification Department. Tokyo: ClassNK. https://www.classnk.or.jp/hp/pdf/activities/statutory/seemp/CII_en.pdf

de Oliveira, M. A., Szklo, A., & Branco, D. A. (2022). Implementation of Maritime Transport Mitigation Measures according to their marginal abatement costs and their mitigation potentials. *Energy Policy, 160*, 112699. https://doi.org/10.1016/j.enpol.2021.112699

Deshpande, D., Shahrukh, M., Srinivasan, R., & Karimi, I. A. (2022). *Optimal Liquefied Natural Gas (LNG) Annual Delivery Program Reflecting both Supplier and Customer Perspectives* (Vol. 49). Elsevier. https://doi.org/10.1016/B978-0-323-85159-6.50101-9

DNV. (2019, June). *Assessment of selected alternative fuels and technologies in shipping.* https://www.dnv.com/maritime/publications/alternative-fuel-assessment-download/

DNV. (2022, January). *"No room for complacency" despite advancement in shipping safety.* https://www.dnv.com/expert-story/maritime-impact/Navigating-new-safety-challenges-after-a-decade-of-progress/

DNV. (2022, February). *Maritime Forecast 2050: Energy transition outlook 2022.* https://www.dnv.com/Publications

dos Santos, V. A., Pereira da Silva, P. & Serrano, L. M. V., 2022. The Maritime Sector and Its Problematic Decarbonization: A Systematic Review of the Contribution of Alternative Fuels. *Energies*, Volume 15. https://doi.org/10.3390/en15103571

Ejder, E., Dinçer, S., & Arslanoglu, Y. (2024). Decarbonization strategies in the maritime industry: An analysis of dual-fuel engine performance and the carbon intensity indicator. *Renewable and Sustainable Energy Reviews, 200*, 114587. https://doi.org/10.1016/j.rser.2024.114587

Eriksen, U., Kristiansen, J., Fagerholt, K., & Pantuso, G. (2022). Planning a maritime supply chain for liquefied natural gas under uncertainty. *Maritime Transport Research, 3*, 100061. https://doi.org/10.1016/j.martra.2022.100061

Ersoy, A. E., Çelebi, U. B., Yuksel, O., & Bayraktar, M. (2025, February). Predictive analysis of engine power

limitations for fuel reduction in a tanker ship using a rule-based machine learning technique. *Journal of Cleaner Production, 200*, 145535. https://doi.org/10.1016/j.jclepro.2025.145535

Faber, J., Hanayama, S., Zhang, S., Pereda, P., Comer, B., Hauerhof, E., . . . others. (2020). Fourth IMO GHG Study. London, *UK*. https://wwwcdn.imo.org/localresources/en/OurWork/Environment/Documents/Fourth%20IMO%20GHG%20Study%202020%20-%20Full%20report%20and%20annexes.pdf

Ghafri, S. Z., Revell, C., Lorenzo, M. D., Xiao, G., Buckley, C. E., May, E. F., & Johns, M. (2023). Techno-economic and environmental assessment of LNG export for hydrogen production. *International Journal of Hydrogen Energy, 48*, 8343–8369. https://doi.org/10.1016/j.ijhydene.2022.11.160

Ghiami, Y., Woensel, T. V., Christiansen, M., & Laporte, G. (2015). A combined liquefied natural gas routing and deteriorating inventory management problem. *Computational Logistics: 6th International Conference, ICCL 2015, Delft, The Netherlands, September 23-25, 2015, Proceedings 6. 144*, pp. 91–104. MIT press. https://doi.org/10.1007/978-3-319-24264-4_7

Goel, V., Furman, K. C., Song, J.-H., & El-Bakry, A. S. (2012). Large neighbourhood search for LNG inventory routing. *Journal of Heuristics, 18*, 821–848. https://doi.org/10.1007/s10732-012-9206-6

Goel, V., Slusky, M., van Hoeve, W.-J., Furman, K. C., & Shao, Y. (2015). Constraint programming for LNG ship scheduling and inventory management. *European Journal of Operational Research, 241*, 662–673. https://doi.org/10.1016/j.ejor.2014.09.048

Grønhaug, R., & Christiansen, M. (2009). *Supply chain optimization for the liquefied natural gas business* (Vol. 241). Springer. https://doi.org/10.1007/978-3-540-92944-4_10

Grønhaug, R., Christiansen, M., Desaulniers, G., & Desrosiers, J. (2010). A branch-and-price method for a liquefied natural gas inventory routing problem. *Transportation Science, 44*, 400–415. https://doi.org/10.1287/trsc.1100.0317

Gu, Y., & Wallace, S. W. (2017). Scrubber: A potentially overestimated compliance method for the Emission Control Areas: The importance of involving a ship's sailing pattern in the evaluation. *Transportation Research Part D: Transport and Environment, 55*, 51–66. https://doi.org/10.1016/j.trd.2017.06.024

Halvorsen-Weare, E. E., & Fagerholt, K. (2013). Routing and scheduling in a liquefied natural gas shipping problem with inventory and berth constraints. *Annals of Operations Research, 203*, 167–186. https://doi.org/10.1007/s10479-010-0794-y

Halvorsen-Weare, E. E., Fagerholt, K., & Rönnqvist, M. (2013). Vessel routing and scheduling under uncertainty in the liquefied natural gas business. *Computers & Industrial Engineering, 64*, 290–301. https://doi.org/10.1016/j.cie.2012.10.011

Haug, H. V., Solum, S. H., Warholm, S. B., Fagerholt, K., Li, M., & Norstad, I. (2023). Planning LNG Annual Delivery Programs with Speed Optimization and Multiple Loading Ports. *International Conference on Computational Logistics. 3*, pp. 170–184. Elsevier. https://doi.org/10.1007/978-3-031-43612-3_10

Hua, R., Yin, J., Wang, S., Han, Y., & Wang, X. (2024). Speed optimization for maximizing the ship's economic benefits considering the Carbon Intensity Indicator (CII). *Ocean Engineering, 293*, 116712. https://doi.org/10.1016/j.oceaneng.2024.116712

IMO. (2011). *Marine Environment.* International Maritime Organization London, UK.

https://www.imo.org/en/ourwork/environment/pages/default.aspx

IMO. (2018). Initial IMO strategy on reduction of GHG emissions from ships. *Initial IMO strategy on reduction of GHG emissions from ships*.

IMO. (2021a, June). *guidelines on operational carbon intensity indicators and the calculation methods (CII GUIDELINES, G1).* International Maritime Organization London, UK.

IMO. (2021b, February). *EEXI and CII - ship carbon intensity and rating system.* International Maritime Organization London, UK. https://www.imo.org/en/mediacentre/hottopics/pages/eexi-cii-faq.aspx

IMO (2022a, June). *guidelines on the preference lines for use with operational carbon intensity indicators (CII REFERECES LINES GUIDELINES, G2).* International Maritime Organization London, UK.

IMO. (2022b, June). *guidelines on the operational carbon intensity reduction factors relative to reference lines (CII REDUCTION FACTORS GUIDELINES, G3).* International Maritime Organization London, UK

IMO. (2022c, June). *guidelines on the operational carbon intensity rating of ships (CII RATING GUIDELINES, G4).* International Maritime Organization London, UK.

IMO. (2022d, June). *2022 interim guidelines on correction factors and voyage adjustments for CII calculation (CII GUIDELINES, G5).* International Maritime Organization London, UK.

IMO. (2023). Amendments to the Annex of the Protocol of 1997 to Amend the International Convention for the Prevention of Pollution from Ships.

Inal, O. B., Zincir, B., Dere, C., & Charpentier, J.-F. (2024). Hydrogen fuel cell as an electric generator: a case study for a general cargo ship. *Journal of Marine Science and Engineering, 12*, 432. https://doi.org/10.3390/jmse12030432

IRENA. (2019, September). *Navigating to a renewable future: Solutions for decarbonising shipping, Preliminary findings, International Renewable Energy Agency, Abu Dhabi.* https://www.irena.org/publications/2019/Sep/Navigating-the-way-to-a-renewable-future

Jia, H., Adland, R., Prakash, V., & Smith, T. (2017). Energy efficiency with the application of Virtual Arrival policy. *Transportation Research Part D: Transport and Environment, 54*, 50–60. https://doi.org/10.1016/j.trd.2017.04.037

Jokinen, R., Pettersson, F., & Saxén, H. (2015). A MILP model for optimization of a small-scale LNG supply chain along a coastline. *Applied Energy, 138*, 423–431. https://doi.org/10.1016/j.apenergy.2014.10.039

Khalilpour, R., & Karimi, I. A. (2012). *Contract selection under uncertainty: LNG buyers' perspective* (Vol. 31). Elsevier. https://doi.org/10.1016/B978-0-444-59506-5.50128-0

Kim, H., Yeo, S., Lee, J., & Lee, W.-J. (2023). Proposal and analysis for effective implementation of new measures to reduce the operational carbon intensity of ships. *Ocean Engineering, 280*, 114827. https://doi.org/10.1016/j.oceaneng.2023.114827

Li, X., Armagan, E., Tomasgard, A., & Barton, P. I. (2011). Stochastic pooling problem for natural gas production network design and operation under uncertainty. *AIChE Journal, 57*, 2120–2135. https://doi.org/10.1002/aic.12419

Lu, B., Ming, X., Lu, H., Chen, D., & Duan, H. (2023). Challenges of decarbonizing global maritime container shipping toward net-zero emissions. *npj Ocean Sustainability, 2*, 11. https://doi.org/10.1038/s44183-023-00018-6

Mandal, A., Biswas, J., Farooqui, Z., & Roychowdhury, S. (2021). A detailed perspective of marine emissions and their environmental impact in a representative Indian port. *Atmospheric Pollution Research, 12*, 101194. https://doi.org/10.1016/j.apr.2021.101194

Mitchell, M. (1998). *An introduction to genetic algorithms* (Vol. 31). MIT press.

Mokhatab, S., Mak, J. Y., Valappil, J., & Wood, D. A. (2013). *Handbook of liquefied natural gas* (Vol. 148). Gulf Professional Publishing.

Moraes, L. A., & Faria, L. F. (2016). A stochastic programming approach to liquified natural gas planning. *Pesquisa Operacional, 36*, 151–165. https://doi.org/10.1590/0101-7438.2016.036.01.0151

Mosayebi, M. and Sodhi, M., 2020, July. Tuning genetic algorithm parameters using design of experiments. *In Proceedings of the 2020 genetic and evolutionary computation conference companion*. 1937-1944. https://doi.org/10.1145/3377929.3398136

Msakni, M. K., & Haouari, M. (2018). Short-term planning of liquefied natural gas deliveries. *Transportation Research Part C: Emerging Technologies, 90*, 393–410. https://doi.org/10.1016/j.trc.2018.03.013

Mutlu, F., Msakni, M. K., Yildiz, H., Sönmez, E., & Pokharel, S. (2016). A comprehensive annual delivery program for upstream liquefied natural gas supply chain. *European Journal of Operational Research, 250*, 120–130. https://doi.org/10.1016/j.ejor.2015.10.031

Prasetyo, D. W., Herawati, S., & Hananto, T. (2023). Carbon Reduction Program Implementation Strategy on Product Tanker Fleet Against the Carbon Intensity Indicator (CII) Decreasing Target. *International Journal of Advanced Multidisciplinary, 2*, 349–358. http://dx.doi.org/10.38035/ijam.v2i2.299

Qi, J., Wang, S., & Psaraftis, H. (2021, February). Bi-level optimization model applications in managing air emissions from ships: A review. *Communications in Transportation Research, 1*, 100020. https://doi.org/10.1016/j.commtr.2021.100020

Rakke, J. G., Andersson, H., Christiansen, M., & Desaulniers, G. (2015). A new formulation based on customer delivery patterns for a maritime inventory routing problem. *Transportation Science, 49*, 384–401. https://doi.org/10.1287/trsc.2013.0503

Rakke, J. G., Stålhane, M., Moe, C. R., Christiansen, M., Andersson, H., Fagerholt, K., & Norstad, I. (2011). A rolling horizon heuristic for creating a liquefied natural gas annual delivery program. *Transportation Research Part C: Emerging Technologies, 19*, 896–911. https://doi.org/10.1016/j.trc.2010.09.006

Saldarriaga-Cortés, C., Salazar, H., Moreno, R., & Jiménez-Estévez, G. (2019). Stochastic planning of electricity and gas networks: An asynchronous column generation approach. *Applied energy, 233*, 1065–1077. https://doi.org/10.1016/j.apenergy.2018.09.148

Sangaiah, A. K., Tirkolaee, E. B., Goli, A., & Dehnavi-Arani, S. (2020). Robust optimization and mixed-integer linear programming model for LNG supply chain planning problem. *Soft computing, 24*, 7885–7905. https://doi.org/10.1007/s00500-019-04010-6

Sardar, A., Anantharaman, M., Islam, T. M., & Garaniya, V. (2024). Data collection framework for enhanced carbon intensity indicator (CII) in the oil tankers. *The Canadian Journal of Chemical Engineering*. https://doi.org/10.1002/cjce.25384

Schroer, M., Panagakos, G., & Barfod, M. B. (2022). An evidence-based assessment of IMO's short-term measures for decarbonizing container shipping. *Journal of Cleaner Production, 363*, 132441. https://doi.org/10.1016/j.jclepro.2022.132441

Sell. (2025, February). *Shell LNG Outlook 2025*. https://www.shell.com/what-we-do/oil-and-natural-gas/liquefied-

natural-gas-lng/lng-outlook-2025.html

Shao, Y., Furman, K. C., Goel, V., & Hoda, S. (2015). A hybrid heuristic strategy for liquefied natural gas inventory routing. *Transportation Research Part C: Emerging Technologies, 53*, 151–171. https://doi.org/10.1016/j.trc.2015.02.001

Sheikhtajian, S., Nazemi, A., & Feshari, M. (2020). Marine inventory-routing problem for liquefied natural gas under travel time uncertainty. *International Journal of Supply and Operations Management, 7, 1*.

Shell. (2023). *Shell LNG outlook 2023.* https://www.shell.com/what-we-do/oil-and-natural-gas/liquefied-natural-gas-lng/lng-outlook-2023.html#iframe=L3dlYmFwcHMvTE5HX291dGxvb2tfMjAyMy8=

Sheng, D., Meng, Q., & Li, Z.-C. (2019). Optimal vessel speed and fleet size for industrial shipping services under the emission control area regulation. *Transportation Research Part C: Emerging Technologies, 105*, 37–53. https://doi.org/10.1016/j.trc.2019.05.038

Stålhane, M., Rakke, J. G., Moe, C. R., Andersson, H., Christiansen, M., & Fagerholt, K. (2012). A construction and improvement heuristic for a liquefied natural gas inventory routing problem. *Computers & Industrial Engineering, 62*, 245–255. https://doi.org/10.1016/j.cie.2011.09.011

Sui, C., de Vos, P., Stapersma, D., Visser, K., & Ding, Y. (2020). Fuel consumption and emissions of ocean-going cargo ship with hybrid propulsion and different fuels over voyage. *Journal of Marine Science and Engineering, 8*, 588. https://doi.org/10.3390/jmse8080588

Tadros, M., Ventura, M., & Soares, C. G. (2023). Review of current regulations, available technologies, and future trends in the green shipping industry. *Ocean Engineering, 280*, 114670. https://doi.org/10.1016/j.oceaneng.2023.114670

Ten, K. H., Kang, H.-S., Siow, C.-L., Goh, P. S., Lee, K.-Q., Huspi, S. H., & Soares, C. G. (2023). Automatic identification system in accelerating decarbonization of maritime transportation: The state-of-the-art and opportunities. *Ocean Engineering, 289*, 116232. https://doi.org/10.1016/j.oceaneng.2023.116232

Tran, T. T., Browne, T., Veitch, B., Musharraf, M., & Peters, D. (2023). Route optimization for vessels in ice: Investigating operational implications of the carbon intensity indicator regulation. *Marine Policy, 158*, 105858. https://doi.org/10.1016/j.marpol.2023.105858

UNCTAD. (2023, September). *Bold global action needed to decarbonize shipping and ensure a just transition: UNCTAD report.* https://unctad.org/news/bold-global-action-needed-decarbonize-shipping-and-ensure-just-transition-unctad-report

Utku, D. H. (2023). An application: A multi-mode natural gas and liquefied natural gas supply chain management problem. *Journal of Engineering Research, 11*, 384–401. https://doi.org/10.36909/jer.17465

Utku, D. H., & Soyöz, B. (2020). A mathematical model on liquefied natural gas supply chain with uncertain demand. *SN Applied Sciences, 2*, 1–15. https://doi.org/10.1007/s42452-020-03297-7

Venkataramanan, V. S., & Srinivasan, R. (2024). Agent-Based Dynamic Simulation for Supply Chain Management of LNG Import Terminals. *Industrial & Engineering Chemistry Research, 63*, 2750–2768. https://doi.org/10.1021/acs.iecr.3c03375

Wang, S., Psaraftis, H. N., & Qi, J. (2021, February). Paradox of international maritime organization's carbon intensity indicator. *Communications in Transportation Research, 1*, 100005. https://doi.org/10.1016/j.commtr.2021.100005

Werner, A., Uggen, K. T., Fodstad, M., Lium, A.-G., & Egging, R. (2014). Stochastic mixed-integer programming for integrated portfolio planning in the LNG supply chain. *The Energy Journal, 35*, 299–316. https://doi.org/10.5547/01956574.35.1.5

Xiaozhi, F. E. (2020). *LNG inventory routing problem under uncertain weather.* Master thesis

Yazdi, A. K., Kaviani, M. A., Emrouznejad, A., & Sahebi, H. (2020). A binary particle swarm optimization algorithm for ship routing and scheduling of liquefied natural gas transportation. *Transportation Letters, 12*, 223–232. https://doi.org/10.1080/19427867.2019.1581485

Yazdi, A. K., Komijan, A. R., Raissi, S., & Modiri, M. (2021). A robust model for supplying LNG from different contracts considering overall and incremental discount options. *Energy Sources, Part A: Recovery, Utilization, and Environmental Effects, 43*, 1805–1824. https://doi.org/10.1080/15567036.2019.1663310

Yu, H., Fang, Z., Fu, X., Liu, J., & Chen, J. (2021). Literature review on emission control-based ship voyage optimization. *Transportation Research Part D: Transport and Environment, 93*, 102768. https://doi.org/10.1016/j.trd.2021.102768

Yuan, Q., Wang, S., & Peng, J. (2023). Operational efficiency optimization method for ship fleet to comply with the carbon intensity indicator (CII) regulation. *Ocean Engineering, 286*, 115487. https://doi.org/10.1016/j.oceaneng.2023.115487

Zarrinkolah, M. T., & Hosseini, V. (2023). Methane slip reduction of conventional dual-fuel natural gas diesel engine using direct fuel injection management and alternative combustion modes. *Fuel, 331*, 125775. https://doi.org/10.1016/j.fuel.2022.125775

Zhang, H., Liang, Y., Liao, Q., Yan, X., Shen, Y., & Zhao, Y. (2017). A three-stage stochastic programming method for LNG supply system infrastructure development and inventory routing in demanding countries. *Energy, 133*, 424–442. https://doi.org/10.1016/j.energy.2017.05.090

Zhang, H., Wu, Y., Zhen, L., Jin, Y., & Wang, S. (2024). Optimization problems in liquefied natural gas transport and storage for multimodal transport companies. *Electronic Research Archive, 32*, 4828–4844. https://doi.org/10.3934/era.2024221

Zhang, L., Zhang, S., & Yu, C. (2021). Network optimisation for transporting liquefied natural gas from stations to end customers. *International Journal of Production Research, 59*, 1791–1813. https://doi.org/10.1080/00207543.2020.1725682

Zhang, Q., Guan, H., Chen, S., & Wan, Z. (2024). Towards decarbonization: How EEXI and CII regulations affect container liner fleet deployment. *Transportation Research Part D: Transport and Environment, 133*, 104277. https://doi.org/10.1016/j.trd.2024.104277

Zincir, B. (2023). Slow steaming application for short-sea shipping to comply with the CII regulation. *Brodogradnja: An International Journal of Naval Architecture and Ocean Engineering for Research and Development, 74*, 21–38. https://doi.org/10.21278/brod74202

APPENDICES

Appendix A. Full View of the Portfolio Optimisation Planning

A detailed overview of the portfolio planning process for LNG deliveries is provided in Appendix A, offering greater clarity on how the planning framework operates for each cargo. The planning integrates routing, scheduling, and inventory management of the tankers, outlining the quantity of LNG loaded, the volume discharged, and the heel retained on board. It further captures boil-off gas losses across different voyage segments, including during laden and ballast legs, as well as cumulative boil-off over the full journey. The timing of each of these processes is also documented, thereby illustrating how operations are coordinated and how they may be adjusted or refined by companies to suit specific commercial or operational requirements. A concise summary of the final portfolio report and planning outcomes is presented in the table below.

Table 5.1: Portfolio Planning for example (3, 5, 6, 2, 20)

Cargo ID	1	2	3	4	5
Loading Port	1st Supplier	1st Supplier	3rd Supplier	1st Supplier	3rd Supplier
Unloading Port	Gate LNG Terminal	Barcelona	Dahej LNG	Grain LNG	Izmir Aliaga
Loading Amount	3,451,584	3,479,604	3,711,993	2,702,443	3,854,413
Unloading Amount	3,748,317	3,774,108	4,000,000	3,000,000	3,800,000
Loading Time	2023-07-01 00:00:00	2023-07-05 00:00:00	2023-07-11 00:00:00	2023-07-13 00:00:00	2023-07-19 00:00:00
Unloading Time	2023-07-15 09:52:28	2023-07-20 02:59:57	2023-07-14 13:18:45	2023-07-27 04:59:58	2023-08-05 00:00:00
Vessel No	3	5	1	2	1
CII Rating Report	A	B	B	B	B
Boil-off before Loading	-	278	140	856	62
Boil-off Laden Leg	42,914	45,225	7,213	42,178	28,532
Boil-off idle Laden	-	-	-	-	25,881
Boil-off Ballast leg	20,700	21,282	3,394	20,344	27,275
Boil-off idle Ballast	-	-	62	-	-
idle Time before Loading	0 days 00:00:00	4 days 00:00:00	2 days 00:11:00	12 days 00:00:00	0 days 21:23:00
Arrival Time Loading	2023-07-01 00:00:00	2023-07-01 00:00:00	2023-07-08 23:48:40	2023-07-01 00:00:00	2023-07-18 02:37:29
Loading Service Time	1 days 12:00:00	1 days 12:00:00	1 days 12:00:00	1 days 12:00:00	1 days 12:00:00
Laden Leg Time	12 days 21:52:00	13 days 15:00:00	2 days 01:19:00	12 days 17:00:00	8 days 03:04:00
Arrival Time Unloading	2023-07-15 09:52:28	2023-07-20 02:59:57	2023-07-14 13:18:45	2023-07-27 04:59:58	2023-07-28 15:03:43

Laden idle Time	0 days 00:00:00	0 days 00:00:00	0 days 00:00:00	0 days 00:00:00	7 days 08:56:00
Unloading Service Time	1 days 12:00:00	1 days 12:00:00	1 days 12:00:00	1 days 12:00:00	1 days 12:00:00
Ballast Leg Time	12 days 21:52:00	13 days 15:00:00	2 days 01:19:00	12 days 17:00:00	16 days 12:15:00
Ballast idle Time	0 days 00:00:00	0 days 00:00:00	0 days 21:23:00	0 days 00:00:00	0 days 00:00:00
Loading Amount	3,451,584	3,479,604	3,711,993	2,702,443	3,854,413
Heel on board at the start of Laden	3,851,584	3,879,604	4,072,358	3,102,443	3,914,692
Heel on board at the end of Laden	3,808,670	3,834,379	4,065,145	3,060,265	3,886,160
Heel on board at the start of idle Laden	3,808,670	3,834,379	4,065,145	3,060,265	3,886,160
Heel on board at the end of idle Laden	3,808,670	3,834,379	4,065,145	3,060,265	3,860,279
Unloading Amount	3,748,317	3,774,108	4,000,000	3,000,000	3,800,000
Heel on board at the start of Ballast	60,353	60,271	65,145	60,265	60,279
Heel on board at the end of Ballast	39,653	38,989	61,751	39,921	33,004
Heel on board at the start of idle Ballast	39,653	38,989	61,751	39,921	33,004
Heel on board at the end of idle Ballast	39,653	38,989	61,689	39,921	33,004
Time at the start of idle before Loading	2023-07-01 00:00:00	2023-07-01 00:00:00	2023-07-08 23:48:40	2023-07-01 00:00:00	2023-07-18 02:37:29
Time at the end of idle before Loading	2023-07-01 00:00:00	2023-07-05 00:00:00	2023-07-11 00:00:00	2023-07-13 00:00:00	2023-07-19 00:00:00
Loading Time	2023-07-01 00:00:00	2023-07-05 00:00:00	2023-07-11 00:00:00	2023-07-13 00:00:00	2023-07-19 00:00:00
Time at the start of Laden	2023-07-02 12:00:00	2023-07-06 12:00:00	2023-07-12 12:00:00	2023-07-14 12:00:00	2023-07-20 12:00:00
Time at the end of Laden	2023-07-15 09:52:28	2023-07-20 02:59:57	2023-07-14 13:18:45	2023-07-27 04:59:58	2023-07-28 15:03:43
Time at the start of idle Laden	2023-07-15 09:52:28	2023-07-20 02:59:57	2023-07-14 13:18:45	2023-07-27 04:59:58	2023-07-28 15:03:43
Time at the end of idle Laden	2023-07-15 09:52:28	2023-07-20 02:59:57	2023-07-14 13:18:45	2023-07-27 04:59:58	2023-08-05 00:00:00
Unloading Time	2023-07-15 09:52:28	2023-07-20 02:59:57	2023-07-14 13:18:45	2023-07-27 04:59:58	2023-08-05 00:00:00
Time at the start of Ballast	2023-07-16 21:52:28	2023-07-21 14:59:57	2023-07-16 01:18:45	2023-07-28 16:59:58	2023-08-06 12:00:00
Time at the end of Ballast	2023-07-29 19:44:55	2023-08-04 05:59:55	2023-07-18 02:37:29	2023-08-10 09:59:55	2023-08-23 00:14:57
Time at the start of idle Ballast	2023-07-29 19:44:55	2023-08-04 05:59:55	2023-07-18 02:37:29	2023-08-10 09:59:55	2023-08-23 00:14:57
Time at the end of idle Ballast	2023-07-29 19:44:55	2023-08-04 05:59:55	2023-07-19 00:00:00	2023-08-10 09:59:55	2023-08-23 00:14:57

Appendix B: Publications Arising from This Thesis

Mostafazadeh, P., Kavakeb, Sh., Pakzad Moghaddam, S.H., Matellini, D.B., Nguyen, T.T, 2025. *"Optimising LNG Supply Chain Portfolio for ADP Using a Hybrid Genetic Algorithm and Mathematical Modelling"*.

Mostafazadeh, P., Kavakeb, Sh., Pakzad Moghaddam, S.H., Matellini, D.B., Nguyen, T.T, 2026. *"Operational Trade-offs in LNG Shipping under Carbon Intensity Regulation: A Data-Driven Evaluation of Portfolio and Routing Strategies"*.